https://doi.org/10.15388/vu.thesis.480
https://orcid.org/0000-0001-8506-422X

VILNIUS UNIVERSITY
UNIVERSITY OF TRENTO

Erna Marija Meškytė

Identification of the Role of Transcription Factor ETV7 in Breast Cancer Aggressiveness

DOCTORAL DISSERTATION

Natural Sciences,
Biochemistry (N 004)

VILNIUS 2023

The dissertation was prepared between 2018 and 2023 at Institute of Biochemistry, Life Sciences Center, Vilnius University and Department of Cellular, Computational and Integrative Biology, University of Trento.

Academic supervisor – Dr. Daiva Baltriukienė (Vilnius University, Natural Sciences, Biochemistry – N 004).
Academic supervisor – dr. Yari Ciribilli (University of Trento, Natural Sciences, Biochemistry - N004).

This doctoral dissertation will be defended in a public meeting of the Dissertation Defence Panel:

Chairman – Prof. Dr. Daumantas Matulis (Vilnius University, Lithuania, Natural Sciences, Biochemistry – N 004).

Members:

Dr. Paola Campomenosi (Insubria University, Italy, Natural Sciences, Biochemistry – N 004),
Prof. Dr. Alessio Nencioni (University of Genoa, Italy, Natural Sciences, Biochemistry – N 004),
Dr. Colinda Scheele (VIB Leuven, Belgium, Natural Sciences, Biochemistry – N 004),
Prof. Dr. Vytautė Starkuvienė-Erfle (Heidelberg University, Germany, Natural Sciences, Biochemistry – N 004).

The dissertation shall be defended at a public meeting of the Dissertation Defence Panel at 15:00 on the 22nd June 2023 in Room R401 of the Life Sciences Center, Vilnius University. Address: Saulėtekio Ave. 7, LT-10257, Vilnius, Lithuania, Tel.: +370 5 223 4420; e-mail: info@gmc.vu.lt.

The text of this dissertation can be accessed at the libraries of Vilnius University, as well as on the website of Vilnius University:
www.vu.lt/lt/naujienos/ivykiu-kalendorius

https://doi.org/10.15388/vu.thesis.480
https://orcid.org/0000-0001-8506-422X

VILNIAUS UNIVERSITETAS
TRENTO UNIVERSITETAS

Erna Marija Meškytė

ETV7 transkripcijos veiksnio vaidmuo krūties vėžio agresyvumo vystymesi

DAKTARO DISERTACIJA

Gamtos mokslai,
Biochemija (N 004)

VILNIUS 2023

Disertacija rengta 2018–2023 metais Vilniaus universitete ir Trento universitete.

Mokslinė vadovė – dr. Daiva Baltriukienė (Vilniaus universitetas, gamtos mokslai, biochemija – N 004);
Mokslinis vadovas – dr. Yari Ciribilli (Trento universitetas, gamtos mokslai, biochemija – N 004).

Gynimo taryba:
Pirmininkas – prof. dr. Daumantas Matulis (Vilniaus universitetas, Lietuva, gamtos mokslai, biochemija – N 004).
Nariai:
Dr. Paola Campomenosi (Insubrijos universitetas, Italija, gamtos mokslai, biochemija – N 004),
Prof. dr. Alessio Nencioni (Genujos universitetas, Italijs gamtos mokslai, biochemija – N 004),
Dr. Colinda Scheele (VIB Leuven, Belgija, gamtos mokslai, biochemija – N 004),
Prof. dr. Vytautė Starkuvienė-Erfle (Heidelbergo universitetas, Vokietija, gamtos mokslai, biochemija – N 004).

Disertacija ginama viešame Gynimo tarybos posėdyje 2023 m. birželio mėn. 22 d. 15:00 val. Vilniaus universiteto Gyvybės mokslų centro R401 auditorijoje. Adresas: Saulėtekio alėja 7, LT-10257, Vilnius, Lietuva, tel. +370 5 223 4420; el. paštas info@gmc.vu.lt.

Disertaciją galima peržiūrėti Vilniaus universiteto bibliotekoje ir VU interneto svetainėje adresu: *https://www.vu.lt/naujienos/ivykiu-kalendorius*

ABBREVIATIONS

5-FU	5-fluorouracil
ALDH	aldehyde dehydrogenase
b_2M/B2M	b_2-microglobulin
BC	breast cancer
BCA	bicinchoninic acid assay
BCL-2	B-cell lymphoma 2
bFGF	basic fibroblast growth factor
BS	binding site
BSA	bovine serum albumin
CAFs	cancer-associated fibroblasts
CAR	chimeric antigen receptor
ChIP	chromatin immunoprecipitation
CRI	cancer-related inflammation
CSCs	cancer stem cells
CXCL	chemokine (C-X-C motif) ligand
DEGs	differentialy expressed genes
DMSO	dimethylsulfoxide
DNMT3A	DNA methyltransferase 3 alpha
dTMP	deoxythymidine monophosphate
ECM	extracellular matrix
EGF	epidermal growth factor
ELISA	enzyme-linked immunoSorbent assay
EMT	epithelial-mesenchymal transition
EpCAM	epithelial cell adhesion molecule
ER	estrogen receptor
ER	endoplasmic reticulum
ETS	E26 transformation-specific
FBS	fetal bovine serum
GAS	gamma-activated sequence
GSEA	gene set enrichment analysis
H&E	hematoxylin and eosin
H3ac	acetylation of H3
H3K4me3	tri-methylation of lysine 4 on histone 3
H3K9me3	tri-methylation of lysine 9 on histone 3
HDAC	histone deacetylation

HER2	Human Epidermal Growth Factor Receptor 2
HLA	human leukocyte antigens
HSCs	hematopoietic stem cells
IF-F	immunofluorescent staining of frozen tissue
IFN	interferon
IFNAR	interferon-α/β receptor
IgG	immunoglobulin G
IKK	IκB kinase
IL	interleukin
IRDS	IFN-related DNA damage-resistance signature
IRF	interferon regulatory factor
ISG	interferon-stimulated gene
ISG3	ISG factor 3
ISREs	interferon-stimulated response element
IκBα	nuclear factor of kappa light polypeptide gene enhancer in B-cells inhibitor, alpha
KO	kock-out
LMP	lysosomal membrane
LOH	loss of heterozygosity
LPS	lipopolysaccharide
MAPK	mitogen-activated protein kinase
MDSCs	myeloid-derived suppressor cells
MFE	mammosphere formation efficiency
MHC	major histocompatibility complex
NF-κB	nuclear factor kappa-light-chain-enhancer of activated B cells
NLRC5	NLR Family CARD Domain Containing 5
NSB	nuclear separation buffer
PBS	phosphate-buffered saline
PDGF	platelet-derived growth factor
PFA	paraformaldehyde
PI	protease inhibitors
PI	propidium iodide
PNT	pointed domain
PR	progesteron receptor
PRRs	pattern Recognition Receptors

s/c	subcutaneous
SERMs	selective estrogen receptor modulators
STAT	signal transducer activator of transcription
TAAs	tumor-associated antigens
TAMs	tumor-associated macrophages
TAPs	transporters of antigen processing
TCGA	the cancer genome atlas
TE	tris-EDTA
TGF-β	transforming growth factor beta
TLR	toll-like receptor
TME	tumor microenvironment
TNFR1	tumor necrosis factor receptor 1
TNFR2	tumor necrosis factor receptor 2
TNF-α	tumor necrosis factor α
Tregs	regulatory T cells
TS	thymidylate synthase
VEGF	vascular endothelial growth factor

CONTENT

INTRODUCTION

In 2020, female breast cancer was the most frequently diagnosed cancer worldwide (11.7% of total cases, 2.3 million new cases in 2020) and surpassed lung cancer as the leading cause of global cancer incidence. Among females, breast cancer has the highest incidence rate and the highest mortality rate[1]. Despite the advances in early diagnostics and treatment and relatively high survival rates, metastases, and relapses due to resistance are the major concerns for clinicians and breast cancer patients. Hence, there is a never-ending need to gain a better understanding of breast cancer biology and find novel therapeutic strategies[2,3]. In this study, we are focusing on ETV7, a poorly studied transcriptional repressor, known to be up-regulated in different types of cancer[4–8]. In breast cancer (BC), increased expression of ETV7 correlates with the aggressiveness of cancer[8]. Previously, we demonstrated that in BC, ETV7 is up-regulated upon the treatment with various DNA-damaging drugs and that this increased expression promotes resistance to chemotherapy[9,10]. Interestingly, ETV7 is also an interferon-stimulated gene (ISG)[11]. Recently, it has been demonstrated that ETV7 represses several ISGs and hence negatively regulates the IFN-mediated control of influenza viruses, confirming that ETV7 is a suppressor of the type I IFN response in mammalian cells[12]. Type I interferons are critical regulators of tumor-immune system interaction[13,14]. Published and our preliminary data suggest that ETV7 is involved in breast cancer aggressiveness and could be a novel regulator of breast cancer immunity.

AIM AND TASKS

This work aims to identify the role of ETV7 transcription factor in breast cancer aggressiveness and breast cancer immunity. To achieve this aim we focused on the following tasks:

1. To identify the involvement of ETV7 in the resistance to 5-FU and regulation of plasticity in breast cancer cells.
2. To investigate the role of ETV7 in breast cancer inflammation.
3. To study the importance of ETV7 in breast cancer immunity.
4. To evaluate the effect of ETV7 silencing in cancer cells.
5. To confirm the pro-tumorigenic potential of ETV7 *in vivo*.

RELEVANCE OF THIS STUDY

Even though the involvement of ETV7 in the tumorigenesis of various cancer types is confirmed by multiple studies, the exact role of ETV7 in cancer aggressiveness is still poorly characterized. This is the first study that investigates the role of ETV7 in the breast cancer stem cell population. Moreover, the role of ETV7 in breast cancer immunity has not been previously

studied, hence it is also the first study that tries to decipher the involvement of ETV7 in immune evasion. Importantly, as ETV7 is not conserved in most rodents, *in vivo* studies related to ETV7 are practically non-existent, this would be the first study which investigates the pro-tumorigenic potential of ETV7 in the formation of solid tumors in mice.

1. LITERATURE REVIEW

1.1 Breast cancer

Breast cancer is a very heterogeneous disease both at histological and molecular levels, as well as, clinically[15,16]. The initiation of breast cancer starts with transforming events in a single cell. These events can be both genetic and epigenetic. The progression of the tumor is then facilitated by the accumulation of additional genetic changes, clonal expansion, and selection[17].

1.1.1 Epidemiology

In 2020, female breast cancer was the most frequently diagnosed cancer worldwide (11.7% of total cases, 2.3 million new cases in 2020) and surpassed lung cancer as the leading cause of global cancer incidence. Among females, breast cancer has the highest incidence rate and the highest mortality rate. It is worth mentioning, that the mortality rate in highly-developed countries is significantly lower (17% higher mortality in the transitioning countries)[1]. There is a significant variation in breast cancer survival rates worldwide, in developed countries the expected 5-year survival rate can reach up to 88% whereas in developing countries it could be as low as 40%[1,18].

Despite the advances in early diagnostics and treatment and the relatively high survival rates, metastases and relapses due to resistance to therapies are the major concerns for clinicians and breast cancer patients. Hence, there is a never-ending need to gain a better understanding of breast cancer biology and find novel therapeutic strategies[2,3].

1.1.2 Breast anatomy

Firstly, to be able to better study breast cancer tumorigenesis, we need to understand breast anatomy and physiology. The mammary gland (breast in humans) is an organ, specialized in the production and secretion of milk and is unique to mammals. The female breast contains 12-20 milk-producing lobes which are connected to the nipple via ducts[19].

The mammary gland is composed of two tissue compartments – the epithelium, which consists of ductal and alveolar cells, which produce milk (glandular tissue), and the stroma – a connective tissue, also known as

mammary fat pad [19,20]. In the mammary gland, there are two types of epithelial cells – luminal and basal cells. Both types of cells are collectively organized in a series of ducts that drain lobuloalveolar structures during lactation[21]. The luminal epithelium forms the inner layer of laticiferous ducts. Instead, the basal epithelium consists of myoepithelial cells that form the outer layer of mature mammary ducts. It also harbors stem and progenitor cells, which form both luminal and myoepithelial cells/layer[22]. The adipose tissue of breast cancer, also known as the mammary fat pad, has a network of nerves, blood vessels, lymph nodes and, fibrous connective tissue, which supports the correct function of the breast[23,24].

1.1.3. Breast cancer initiation

Breast cancer develops through a sequence of defined pathological and clinical stages, starting with ductal hyperproliferation, and progressing to in situ, invasive and metastatic carcinomas[17,25]. Although the steps of breast cancer progression are quite well-defined, the most challenging question remains the transition from a normal cell to a malignant cell and understanding how the cell of origin can modulate breast cancer heterogeneity and the development of different subtypes of breast tumors. Several studies demonstrated that in solid tumors the intrinsic differentiation programs of cellular precursors contributed to the heterogeneity and behaviors of tumor cells and thus it was speculated that luminal-type breast cancers may be derived from luminal progenitor cells, whereas basal-like breast cancers may be derived from basal/myoepithelial progenitor cells[17,26]. However, this hypothesis was not fully confirmed, as several studies demonstrated that human luminal progenitor cells have overlapping gene- and surface marker-expression profiles with basal-like tumors and cell lines, proposing that basal-like tumors can derive from luminal-linage cells[27–30]. Moreover, other studies observed that there was an increase in lineage infidelity and/or imbalace at the earliest stage of breast cancer initiation. Furthermore, the lineage imbalance was also observed in the precancerous breast lesions. These disruptions of lineage homeostasis can cause differentiated cells to lose their identity and gain plasticity, promoting the malignant transformation of breast tumors and increasing their hetrogeneity[31–33].

1.1.4 Breast cancer classification

As already mentioned, breast cancer is a heterogeneous disease, and this heterogeneity significantly affects behaviour, aggressiveness, and responsiveness to therapy of breast cancer cells, hence influencing the prognosis of the patient. This diversity resulted in trying to classify breast

cancer patients using different methods. Breast cancer classification aims to determine the best treatment plan based on the biology and responsiveness to the treatment associated with each type of breast cancer. At the moment the most common classifications are histopathological and molecular[34–36].

1.1.4.1 Histopathological classification

The histopathological classification categorizes breast carcinomas based on the morphological features of the tumor. Breast cancer can be broadly divided into in situ carcinomas and invasive or infiltrating carcinomas. Breast carcinoma in situ is further subdivided into the more frequent ductal or lobular carcinoma in situ and these two subtypes together encompass a heterogeneous group of tumors. Then both subtypes according to the structural features of the tumor can be divided into smaller groups[36,37].

Like in situ carcinomas, invasive carcinomas form a heterogeneous group of tumors divided into histological subtypes. The principal invasive tumor types are infiltrating ductal, invasive lobular, ductal/lobular, mucinous, tubular, medullary and, papillary carcinomas[37].

Even though this classification was a valuable tool for several decades, it is based only on histology and not taking the molecular markers into the consideration. Furthermore, in case of the invasive breast carcinomas, about 70-80% of the tumors belong to invasive ductal carcinomas indicating that there is a need to use an additional classification system to better stratify this cancer subtype[36].

1.1.4.2 Molecular classification

Large-scale gene expression profile studies demonstrated that breast cancer is not a single disease and according to the intrinsic molecular features could be classified into several groups. In 2000, Perou and colleagues. presented the classification of breast cancer based on hierarchical clustering of gene expression profiles and identified the major subtypes: luminal A, luminal B, HER2-positive, triple negative/basal, and normal breast-like (Fig. 1). Later on, this classification was further confirmed by additional studies[38,39]. More recently, a new subtype, called claudin-low has been identified[40].

In the Western world, the luminal subtype is the most common and accounts for approximately 70% of all breast cancer cases. The luminal subtype is estrogen receptor (ER) and progesterone receptor (PR) positive and normally has a good prognosis. The luminal B subtype can be PR-negative and, in some cases, HER2 positive and show high levels of Ki67 proliferation marker. Tumors belonging to the luminal B subtype are usually poorly differentiated and the patients bearing this type of tumor have a worse prognosis compared to luminal A[38,41,42].

Normal-like tumors account for 7.8% of all breast cancer cases in a lymph node negative cohort and share a similar immunohistochemistry status with luminal A subtype with a normal breast tissue profiling [38,41].

The subtype overexpressing HER2 accounts for approximately 15% of all invasive breast cancers. This subtype is usually estrogen receptor and progesterone receptor negative with strong HER2 positivity. HER2-positive subtype has a high level of Ki67 and TP53 mutations are common. This subtype is highly aggressive, however, because of the advancement in the targeted therapies, the patient having this subtype of breast cancer usually responds well to anti-HER2 targeted treatment [37,43].

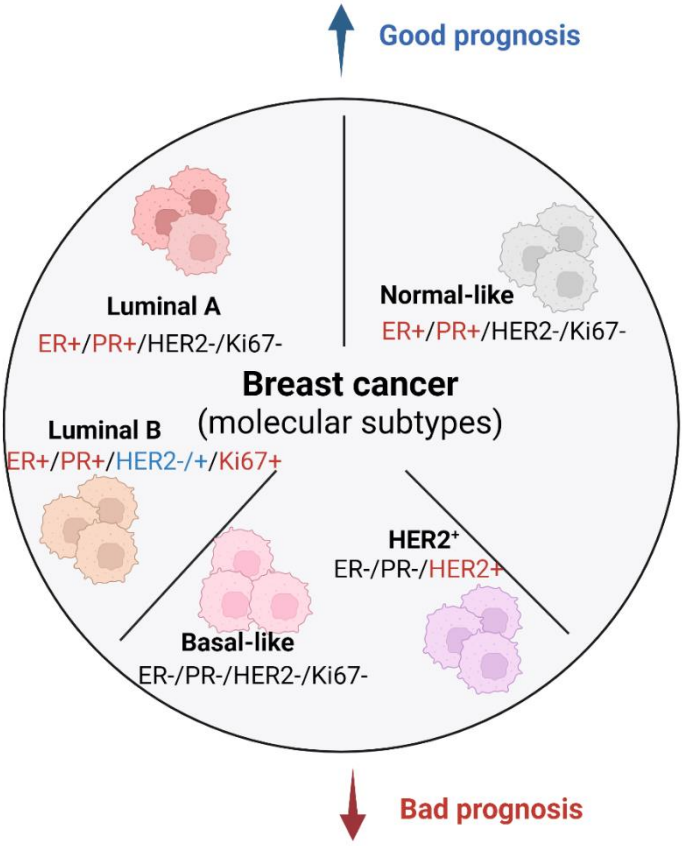

Figure 1. **Different molecular subtypes of breast cancer and their most important molecular features**[44]. Breast cancer is divided into five molecular subtypes depending on differential gene expression: Luminal A, luminal B, basal-like, HER2 positive, and normal-like (differentially expressed genes are indicated in the figure, below the breast cancer subtype). Different molecular subtypes have not only different expression markers but also are associated with better or worse prognoses. For each breast subtype the level of the proliferation marker Ki67 is indicated. Created in Biorender.com.

The basal-like subtype is the most aggressive molecular subtype of breast cancer and comprises approximately 15% of all invasive breast carcinomas. It is called basal-like due to its pattern of gene expression similar to basal epithelial cells[45]. The basal-like subtype is a heterogeneous group of cancers

and the unanimously accepted description of this subtype is still lacking[46]. Most of the time basal-like breast tumors are represented by a triple-negative profile. The triple-negative profile is defined by low or absent expression of estrogen (ER) and progesterone (PR) receptors and the lack of expression of human epidermal growth factor (EGF) receptor-2 (HER2) and is often associated with mutations in *BRCA1* gene[47]. Triple-negative breast cancers grow and spread fast and a have high incidence of brain and lung metastasis. Relapses and reduced sensitivity to standard therapies are common features of triple-negative breast cancer and patients bearing this type of tumor have the poorest survival outcome among all breast cancer subtypes[47–49].

Claudin-low breast cancer subtype is defined by low expression of the cell-cell adhesion genes, high expression of epithelial-mesenchymal transition (EMT) genes, and stem cell-like/less differentiated gene expression patterns. Claudin-low tumors are also known to be infiltrated by immune and stromal cells[50,51].

1.1.5 Cancer stem cells (CSCs)

Cancer stem cells, an evolving field of cancer research, provides the "functional classification" for breast cancer based on the hypotheses that the heterogeneity of breast cancer is either due to the oncogenic transformation of a single mammary stem cell or due to transformation of mammary stem cells at various levels[52].

At the moment there are two widely accepted models for the origin of cancer: hierarchical cancer stem cell models and stochastic, also known as the clonal evolution, model[53]. The clonal evolution model proposes that every cell within the tumor has tumorigenic potential. According to this model, a normal somatic cell with time accumulates genetic mutations (at least five), which lead to the acquisition of the hallmarks of cancer and thus propagation of a tumor[53,54]. Cancer stem cell theory describes a hierarchical organization of tumors with the tumorigenic CSC subpopulation ranked at the top level[53,55].

The origins of CSCs are not conclusive and there are several hypotheses[56]. Cancer stem cells could originate from normal stem cells, which became malignant due to random mutations during DNA replication[57]. Furthermore, the dysregulated stoma signaling and pro-inflammatory conditions force normal stem cells to become malignant[53]. As an alternative, CSCs can derive from differentiated cells via genomic instability of tumor cells, microenvironment signals, or horizontal genetic transfer[58].

The amount of cancer stem cells is difficult to estimate, and it depends on the type of cancer. In solid tumors, CSCs rates are in the range from below 1% to 80% [59–62]. Cancer stem cells share several similar traits with normal stem cells, including the most important one – self-renewal and the ability to give rise to more differentiated cancer cells. There is no universal marker for

cancer stem cells, however, there are some cell surface markers associated with stem cells that are used for the identification, isolation, and enrichment of cancer stem cells *in vivo* and *in vitro*. Importantly, the expression of CSC surface markers is tissue- and tumor-specific[53,58,63]. For example, $CD44^{+}/CD24^{-/low}$ and $ALDH^{+}$, $EpCAM^{+}$ markers are used in breast cancer, $CD133^{+}$ - for colon, brain, and lung cancer, $CD90^{+}$ for liver, etc[63–66] (Fig. 2).

Another important trait of cancer stem cells is the intrinsic resistance to both chemotherapy and radiotherapy[53,65,67]. There are several molecular mechanisms responsible for the reduced sensibility of cancer stem cells to the treatment, including cell cycle kinetics, asymmetric cell division, DNA replication and repair mechanisms, anti-apoptotic proteins, and transporter proteins[65].

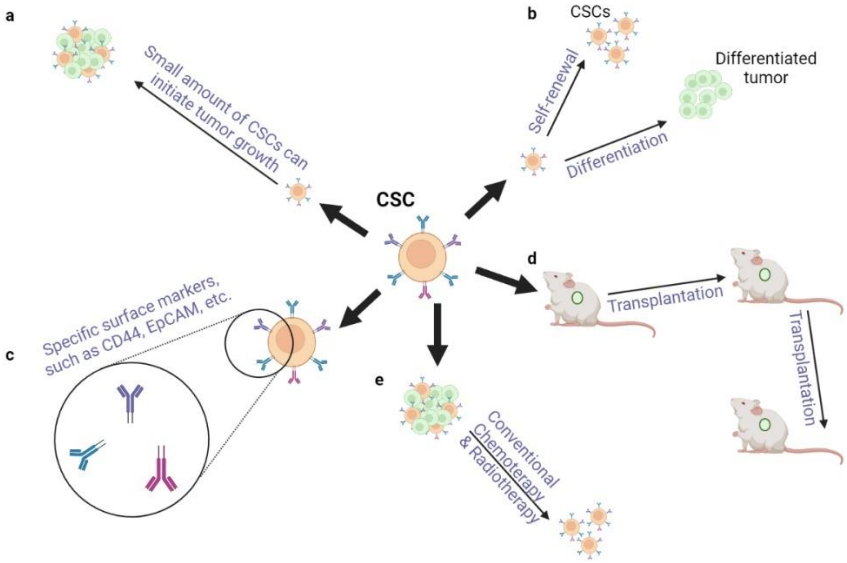

Figure 2. Principal features of cancer stem cells[68]. A) Only a small number of CSCs is sufficient for tumor initiation; B) Self-renewal and differentiation properties; C) CSCs have specific surface markers; D) Ability to be transplanted; E) Resistance to chemotherapy and radiotherapy. Created in Biorender.com.

1.1.5.1 Cancer stem cell plasticity

As mentioned previously, there are several different theories, regarding the origins of CSCs – one theory suggests that CSCs emerge from normal stem/progenitor cells, which encounter a special genetic mutation or environmental alteration; however, the second theory suggests that CSCs arise from normal somatic cells that gain some stem-like traits and malignant behaviors through heterotypic or/and genetic change[63,69]. For example, cancer cells can become more stem-like due to epithelial-mesenchymal transition (EMT)[63]. Mani and colleagues demonstrated that the induction of EMT led to

the acquisition of mesenchymal characteristics and an increase in the expression of stem-cell markers in immortalized human mammary epithelial cells[70].

Interestingly, an alternative, the CSC plasticity model, has recently been proposed[71,72]. Several studies show that there is a bidirectional conversion between self-renewing and non-self-renewing cells, suggesting that CSCs can arise from the transition of non-stem cells to stem-like cells[71–73].

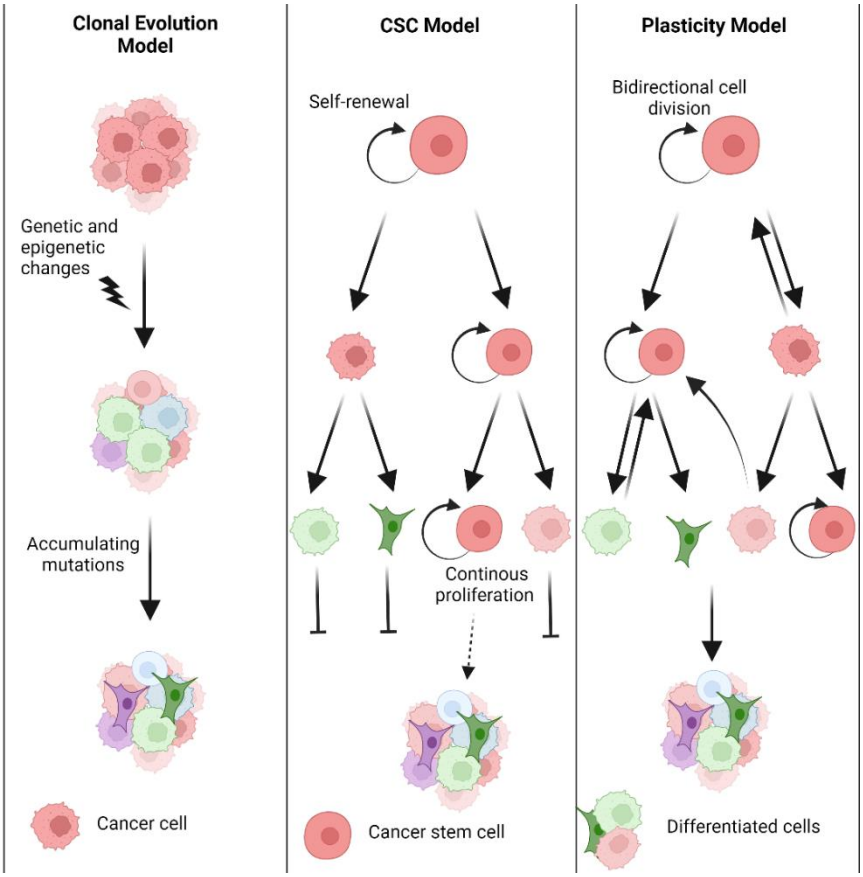

Figure 3. Models of tumor heterogeneity[72]**.** According to the clonal evolution model, normal somatic cells with time accumulate genetic mutations, leading to the acquisition of cancer hallmarks and the formation of tumor; the CSCs model propose that small subpopulation of cells within tumors self-renew and differentiate into different cell types found in tumors; the plasticity model, which suggests the ability of cancer cells to transition between several cellular states. Created in Biorender.com.

This dynamic change from a non-CSC state to a CSC-like state is called cancer stem cell plasticity and is determined by a variety of intrinsic and extrinsic signals[71,73,74]. Importantly, the CSC plasticity model proposes that stochastic

and CSC models are not mutually exclusive and suggest a higher level of complexity and heterogeneity within a tumor (Fig.3)[71,72,75].

1.1.5.2 Breast cancer stem cells (BCSCs)

In 2003, Al-Hall and colleagues first time isolated CSCs in breast cancer, using cell surface markers CD44 and CD24. This $CD44^{+}/CD24^{-}$ cell population had the potential to form tumors *in vivo*[76]. BCSCs are identified or isolated by using surface markers. Now it is known that several different BCSC populations express distinct surface markers, moreover, the functions of BCSCs are determined by the markers they contain[69,77].

Several markers are documented to be specific for BCSCs, such as CD44, CD24, ADLH1, EpCAM, ABCG2, CD133, CD49f, LGR5, SSEA-3, CD70, and PROCR[69,77,78]. The most commonly used markers for BCSCs are CD44, CD24, EpCAM, and ALDH1 will be described more in detail.

CD44 is a transmembrane receptor for hyaluronan acid[69,77–79]. CD44 is important for breast cancer adhesion, motility, migration, and invasion[80]. Moreover, CD44 is involved in cell proliferation and tumor angiogenesis[81]. CD24 is a surface glycoprotein, known to be low expressed or absent in BCSCs. Low expression of CD24 increases the ability of a tumor to grow and to form metastasis[69].

EpCAM is a type I transmembrane glycoprotein, which is known to be overexpressed in BCSCs and can promote the survival of these cells via activation of the Wnt/β-catenin signaling pathway. Moreover, EpCAM is important for migration and metastasis formation, as it promotes the adhesion between epithelial cells[77,82].

Another important marker for BCSCs is the aldehyde dehydrogenase 1 (ALDH1), which is a NAD(P)+ dependent enzyme that mediates the oxidation of intracellular aldehydes into a carboxylic acid. ALDH1 is also involved in the oxidation of the retinol to retinoic acid, a process important for stem cell differentiation. Importantly, ALDH1-high activity is a marker for tumor progression and poor survival of breast cancer patients[77,78,83,84].

Interestingly, different populations of BCSCs can have different surface markers, for example, it was recently demonstrated that BCSCs exist in a mesenchymal-like and epithelial-like state[85,86]. The BCSC population characterized by $CD44^{+}/CD24^{low/-}$ markers belong to the mesenchymal-like BCSCs that are more quiescent, highly invasive, and present at the tumor invasive front. Instead, the $ALDH^{+}$ population belongs to epithelial-like BCSCs and has a high proliferation rate and is localized more centrally in the tumor[86].

1.1.5.3 Methods for the Identification and Isolation of BCSCs

BCSCs can be identified using several techniques, depending on the expression of cell surface markers or on the functional aspects of BCSCs[78].

The most commonly used method of BCSCs detection is based on the specific cell surface markers or their combination and the cells expressing these specific markers are identified using fluorescence-activated cell sorting or magnetic cell sorting[78,87]. The advantage of using cellular markers for the identification of BCSCs is the fact that the isolation specificity is higher compared to functional assays, however, the expression of various markers is highly affected by cell type, cell culture conditions, and the microenvironment and there is no universal marker for the determination of BCSCs[78]. Hence, the assays based on surface markers should be supplemented by functional assays, based on specific BCSCs traits. For example, BCSCs can be isolated using side population cell isolation with Hoechst 33342, which is based on the unique trait of stem cells to express high levels of ABC transporter protein family members, ALDEFLUOR assay, based on high expression of ALDH1 or mammosphere formation assay, showing the self-renewal and proliferation potential of BCSCs[75,78,88,89].

Moreover, the golden standard for evalutation of BCSC functionality *in vivo* is xenotransplantation into immunodeficient mice. This assay permits to test BCSCs` ability to generate serially transplantable tumors, which demonstrates the self-renewal potential. However, even used as the gold standard, this assay has some serious concerns, as murine microenvironment differs from humans and the immune response is inappropriate[90,91].

1.1.6 Breast cancer treatment

Advances in diagnostics, subtyping, and therapies allow clinicians to take the heterogeneity of breast cancer into the consideration while choosing the optimal treatment strategy for each patient. The choice of treatment depends on various factors like mass localization, tumor stage, grade and expression of estrogen, progesterone, and HER2 receptors, and the time of the diagnosis[92]. The two main approaches in breast cancer treatment are local and systemic therapy. Surgery and radiotherapy are the most common local treatments, whereas systemic treatments include chemotherapy, hormonal therapy, immunotherapy, and targeted therapy[93].

The first-line approach for early breast cancer without metastasis is surgery. However, most patients will additionally need some form of systemic therapy. Systemic therapy can be given before the surgery – neoadjuvant therapy, which is needed to shrink large tumors, or after the surgery – adjuvant therapy – if the surgical outcomes and biomarker analysis indicate an increased risk of relapses[93].

The decision of which systemic therapy to use is based on many validated biomarkers. For example, hormonal therapy, which aims to balance or block

hormones, should be given to all patients with detectable ER and/or PR expression and hence it is the most used therapy for the treatment of luminal subtype breast cancer[93]. Anti-estrogenic drugs are divided into the three most used groups – selective estrogen receptor modulators (SERMs), selective estrogen receptor degraders, and aromatase inhibitors[94]. Tamoxifen is the most used selective estrogen receptor modulator. SERM binds to the ER, and induces conformational changes in the receptor, leading to the dimerization of the receptor and blockage of expression of estrogen-dependent genes[95]. Fulvestrant is a selective estrogen receptor degrader. Fulvestrant binds to ER and inhibits receptor dimerization and hence blocks the localization of the receptor to the nucleus[96]. Aromatase inhibitors are another class of anti-estrogenic drugs. Aromatase is an enzyme, involved in the synthesis of estrogen from androgens. Aromatase inhibitors block the activity of aromatase leading to disrupted estrogen biosynthesis[94].

The overexpression of HER2 makes it a favorable therapeutic target and there are several anti-HER2 agents (e.g. trastuzumab, pertuzumab), which could be used for the treatment of HER2-positive breast cancer[43]. Trastuzumab is a monoclonal antibody that targets the extracellular domain of the HER2 protein and prevents the activation of its kinase domain[97,98].

Due to the lack of ER, PR, and HER2 expression, standard chemotherapy remains the main treatment for triple-negative breast cancer. Standard chemotherapy is also used for the treatment of HER2-positive and high-risk luminal breast cancers[92]. The biggest drawback of standard chemotherapy is the lack of selectivity, meaning that chemotherapeutical drugs eliminate not only cancer cells but also normal healthy cells, especially the ones that have high division rates like immune cells[99]. Chemotherapeutical drugs are divided into groups according to their mechanism of action and the most common are the following – antimetabolites (e.g. 5-fluorouracil (5-FU)), alkylating agents (e.g. carboplatin, cisplatin, oxaliplatin, lomustine), antimicrotubular agents (taxanes such as paclitaxel), Topoisomerase I and II inhibitors (doxorubicin), antibiotics (e.g. actinomycin D)[100].

Furthemrore, tumors and their metastases often develop various immunosuppression mechanisms that prevent cancer from being detected by the immune system. Hence, cancer immunotherapy aims to activate the immune system against these malignant cells[23,101].

1.1.6.1 5-fluorouracil (5-FU)

5-fluorouracil is widely used to treat a variety of cancer, including colorectal and breast cancer. 5-FU is an analog of uracil with a fluorine atom at the C-5 position instead of hydrogen[102,103]. Fluorouracil enters the cell using the same facilitated transport mechanisms as uracil. In the cell, 5-fluorouracil is converted into several active metabolites, such as fluorodeoxyuridine monophosphate, fluorodeoxyuridine triphosphate, and fluorouridine triphosphate. These active metabolites disrupt RNA synthesis and thymidylate

synthetase activity[103–105]. One of the 5-FU metabolites, fluorodeoxyurdine monophosphate forms a stable complex with thymidylate synthase (TS) and hence inhibits the production of deoxythymidine monophosphate (dTMP) dTMPs are crucial for DNA replication and repair, therefore its depletion leads to cytotoxicity[104]. Furthermore, fluorodeoxyuridine triphosphate can also directly damage DNA by misincorporation into it[106].

1.1.6.2 Immunotherapy

Cancer immunotherapy is one of the most significant advances in oncology in recent years[107,108]. Although breast cancer is not the most immunogenic tumor, the successful application of immunotherapy in the breast cancer is growing[108–110]. The success of immunotherapy in breast cancer field can be illustrated by the increased number of immunotherapy-based clinical trials. In January 2022, 745 immunotherapy-based trials enrolling patients with solid tumors, including BC, were identified on clinicaltrials.gov, with 450 (60.4%) exclusively dedicated to BC[108]. The most commonly used immunotherapies utilize immune checkpoint inhibitors, chimeric antigen receptor (CAR) T-cell therapy and cancer vaccines for the treatment of cancer[111].

1.2 Tumor microenvironment and immune response

Breast cancer consists not only of neoplastic cells but also of the tumor microenvironment (TME). The tumor microenvironment is formed of different types of cells, including endothelial cells, stromal cells, and immune cells (Fig. 4). TME-forming cells and cancer cells interact in several ways. There could be direct communication through cell-cell contact or indirect communication by releasing various soluble molecules that shape tumor microenvironment[107,112].

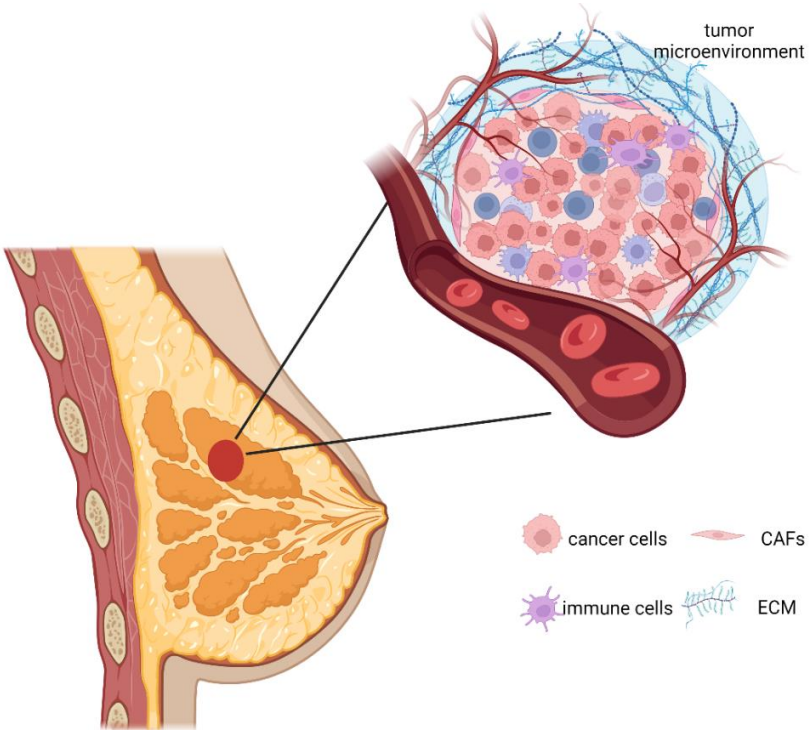

Figure 4. Breast tumor microenvironment (TME). The TME of the breast consists of cancer cells, surrounded by neo-vasculature, stromal cells such as cancer-associated fibroblast, tumor-associated macrophages, and other immune cells and extracellular matrix (ECM). All of these components collaborate to promote breast cancer progression, resistance to therapies, and metastasis[113]. Created in Biorender.

The tumor microenvironment can either promote or reduce tumor progression. This is particularly valid for the immune component of the tumor microenvironment, as on one hand, tumor-infiltrating immune cells help to fight tumors by eliminating immunogenic neoplastic cells, on the other hand, TME immune cells can contribute to developing the resistance to anti-cancer treatments, can modulate tumor immunogenicity and help to escape immune response[112]. Furthermore, the responsiveness to cancer immunotherapy highly depends on the tumor microenvironment. An in-depth understanding of the tumor microenvironment could help better understand tumor-immune cell interactions, which could lead to increased efficacy in immunotherapy[114,115].

1.2.1 Interferon and interferon response

1.2.1.1 Interferons

Interferons (IFNs) are a broad class of cytokines, responsible for the host defense and are crucial for mobilizing an immune response to pathogens. Interferons are divided into three classes: type I (mainly IFN-α/β), type II (IFN-γ), and type III (IFN-λs), all three classes of IFNs share the ability to

activate antiviral immune response by the interaction with their receptors[116,117].

Type I interferons are secreted by infected cells and can act in an autocrine, paracrine, or systemic fashion[118]. Upon ligation to its receptor, type I IFN upregulates approximately 300 Interferon-stimulated genes (ISGs). 51 of these genes play role in host defense, while other genes contribute to inflammation, signaling, transcription, and immunomodulation[118]. Type I IFNs not only induces antiviral ISGs, but they can also regulate the innate immune response by promoting antiviral functions of dendritic cells, monocytes, and natural killers[118,119]. Type I IFNs can significantly upregulate MHC class I-dependent antigen presentation, therefore infected cells display more antigens on the surface and are recognized and subsequently eliminated by $CD8^+$ T cells. Additionally to MHC molecules, other ISGs related to antigen processing are lysosomal membrane permeabilization (LMP) components of proteasome and transporters of antigen processing (TAPs), both of which are important for transporting and loading peptides onto MHC class proteins.

Interferon-γ (IFN- γ) is the only member of the type II interferon class. IFN-γ is a pleiotropic cytokine with immunomodulatory, antiviral, and antitumor functions. It is known to be involved both in innate and adaptive immune response[120]. During an innate immune response, the production of IFN-γ is mainly regulated by natural killer cells, whereas during an adaptive immune response – $CD8^+$ and $CD4^+$ T cells are the main sources of IFN-γ[121]. IFN-γ can recruit immune cells to recognize and eliminate pathogens. IFN-γ can also act on stromal cells, such as macrophages, myeloid-derived suppressor cells, dendritic cells, and B cells. As already mentioned previously, the effect of IFN-γ is mediated via the activation of many ISGs, which define the function of immune cells[120].

Type III interferon is the most recently discovered class of IFNs. The known members of the type III IFN class are IFN-λ1, IFN-λ2, IFN-λ3, and IFN-λ4 [122]. This class of interferons has a similar functionality as type I IFN and regulates a similar set of genes, however, type IFNs act globally, instead IFN-λs act primarily in the mucosal epithelial cells[117].

1.2.1.2 IFN signaling pathway

Following IFN binding to cell surface receptors, a signal is transmitted through the membrane and into the cells, causing a significant change in cellular properties. All IFNs signal through the JAK-STAT signaling pathway[123]. Type I IFNs signal through the same receptor, the type I IFN receptor (IFNAR). IFNAR is formed by two subunits – IFNAR1 and IFNAR2 – which after being bound by IFN I are endocytosed and activate their associated tyrosine kinase, TYK2, and JAK. Once activated, JAKs phosphorylate IFN receptor chains on highly conserved tyrosine residues,

which leads to the repositioning or binding of STAT proteins[118,123]. Consequently, conserved tyrosine residues of STATs are phosphorylated, and STAT proteins are released from the receptor, where conformational changes lead to homo-or heterodimerization. A nuclear localization signal is exposed, leading to facilitated translocation to the nucleus. After entering the nucleus, STATs function as transcriptional activators that drive ISG expression[123].

The proteins of the STAT family are normally found in the cytoplasm and as already mentioned previously, they are downstream targets of JAKs. STATs are some of the most important cytokine-activated transcription factors in the process of immune response[124]. The STAT family consists of seven members: STAT1, STAT2, STAT3, STAT4, STAT5a, STAT5b, and STAT6[125]. All members of the STAT family regulate some processes in immune signaling, however, for IFN signaling STAT1 and STAT2 are the most important[123].

During type I and type III interferon signaling both STAT1 and STAT2 are phosphorylated, leading to heterodimerization and interaction with IFN regulatory factor (IRF) 9 – formation of ISG factor 3 (ISG3) complex. This complex is then translocated to the nucleus and binds IFN-stimulated regulatory elements (ISREs) in DNA upstream of ISGs and induces the transcription of hundreds of type I and type III ISGs[123,126]. Meanwhile, type II IFN signaling drives STAT1 phosphorylation on tyrosine 701, which leads to homodimerization, nuclear translocation, and DNA binding at gamma-activated sequence (GAS) elements upstream of IFN-γ induced genes, hence inducing the transcription of IFN-γ-activated genes (Fig. 5)[123].

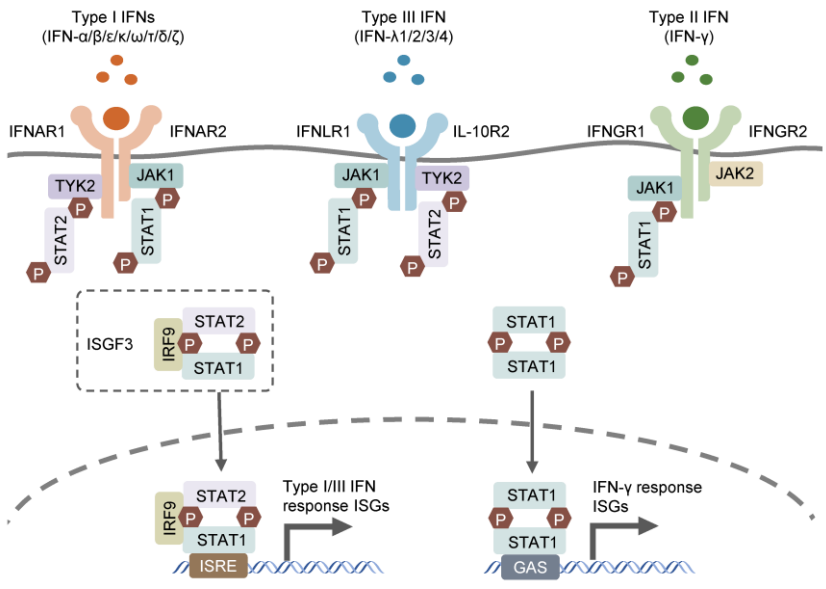

Figure 5. Type I, type II, and type III IFN signaling pathways[127]. Different types of interferons bind to their specific receptors, present on the cell surface and

subsequently activate JAK-STAT signaling pathways, leading to induced expression of their related ISGs.

Interferon-stimulated genes are a diverse group of more than 300 genes, responsible for mediating the biological and therapeutical effects of IFN stimulation[119]. Many ISGs are responsible for controlling viral, bacterial, and parasite infection by directly targeting pathways that are crucial for the pathogen's life cycle. Other ISGs are important for reinforcing the IFN response. For example, pattern recognition receptros (PRRs) and many interferon regulatory factors (IRFs) are normally present in cells at baseline, but upon stimulation with IFN, their gene expression is upregulated. The upregulation of this set of ISGs reinforces IFN signaling and enhances pathogen detection[123]. After activation, IRFs can directly induce several subsets of ISGs in a JAK-STAT-independent manner, this alternative ISG induction pathway is probably an evolutionary mechanism to counteract pathogen-mediated innate immune evasion[128].

1.2.1.3 IFN roles in cancer

Several studies demonstrated that interferons are involved in a wide range of anti-tumoral activities, such as induction of apoptosis, inhibition of angiogenesis and proliferation, cell differentiation, and immune regulation[129].

Data from years of studies demonstrate that type I IFNs can change the expression of proto-oncogenes and tumor suppressor genes involved in cell proliferation[130]. For instance, Einat et al. demonstrated that in lymphoma cells, IFN-α inhibited the transcription of the *c-MYC* gene, which regulates the progression of cells from the G0 phase to the S phase, leading to reduced proliferation of tumor cells[131]. Type I and type II IFNs can also upregulate the expression of p53 with leads to cell cycle arrest[132]. Furthermore, IFNs can induce tumor cell apoptosis through various mechanisms, such as the TRAIL pathway[133,134], the activation of pro-apoptotic members of the Bcl-2 family[129], or via CD95/Fas[135]. IFNs are also involved in the inhibition of angiogenesis by downregulating key angiogenic factors in endothelial cells and stroma, such as IL-8, platelet-derived growth factor (PDGF), and vascular endothelial growth factor (VEGF)[119,129,130].

As already mentioned previously, IFNs are key regulators of the anti-tumor immune response. All three, IFN-α, -β, and -γ, can directly upregulate the expression of surface tumor-associated antigens (TAAs) by increasing MHC I class and MHC II class molecules. The increase of TAAs on the cancer cell surface renders tumor cells more immunogenic and more vulnerable to identification and subsequent destruction by the immune system[129,136]. Furthermore, recent studies demonstrate that defective IFN signaling is involved in the resistance to checkpoint blockage[137]. Indirectly, IFNs modulate the immune system by activating dendritic cells to cross-present tumor antigens to T cells and by enhancing complete CD8+ maturation, which

is necessary for becoming cytotoxic T cells[138,139]. IFNs also inhibit the proliferation of T regulatory cells, stimulate T helper cell function, and promote macrophages to polarize toward M1-like proinflammatory macrophages instead of M2-pro-tumoral macrophages – all of these actions of IFNs reduce the development of immunosuppressive tumor microenvironment[13,129].

On the contrary, some studies demonstrated that in specifc situations IFNs can have pro-tumoral effects[129]. For example, it was reported, that a low dose of IFN-λ produced at the tumor site by host-infiltrating cells could facilitate the survival of tumor cells in the circulation and promote their metastatic potential[120]. Another prometastatic role of IFN-γ was identified in prostate cancer cells, where it enhanced epithelial-to-mesenchymal transition via activation of JAK/STAT1 signaling and induction of IFIT5[120]. One of the most important pro-tumor activities of IFNs is the upregulation of a subset of ISGs, known as IFN-related DNA damage-resistance signature (IRDS), which helps cancer cells to develop resistance to the treatment[140].

1.3 Inflammation and cancer

The first hint of the cross-talk between inflammation and cancer was noticed already in the 19th century by Rudolf Virchow, as he detected the presence of leukocytes within tumors[141]. It took some decades to confirm this observation, however nowadays cancer-related inflammation is recognized as a hallmark of cancer, with a well-established link between chronic inflammation and tumor development[142].

Several molecular and cellular pathways linked with cancer-related inflammation have been unveiled[143]. These pathways roughly can be divided into two groups: extrinsic pathway and intrinsic pathway. The extrinsic pathway is driven by inflammatory leukocytes and soluble pro-inflammatory mediators, which increase cancer risks[144]. The clear link between chronic inflammation and cancer is demonstrated in colorectal cancer, which develops in patients with inflammatory bowel disease. Patients bearing this disease are five-to seven-fold more likely to develop colorectal cancer[145,146]. A similar example could be represented by lung cancer, where chronic airway inflammatory conditions due to tobacco smoke inhalation (or other irritating substances) are the main risk factor to develop lung cancer[147]. The intrinsic pathway is related to genetic events that cause neoplastic transformation and launche the expression of inflammation-related programs, which add to the construction of an inflammatory tumor microenvironment. The most widely known molecular player in cancer-related inflammation (CRI) include the transcription factor NF-κB, the signal transducer activator of transcription-3 (STAT3), and primary inflammatory cytokines such as IL-1β, IL-4, MCP-1, IL-10, IL-11, IL-12, IL-6, IL-23, TGF-β, and TNF-α[143,144,147].

1.3.1 TNF-a/NF-κB axis in cancer

TNF-α/TNFR1/NF-κB axis is one of the major signaling routes regulating inflammatory and immune processes in tumors[148,149]. Tumor necrosis factor (TNF) is a cytokine, which is involved in the regulation of various cellular processes spanning from the pro-inflammatory response to cell differentiation and cell death [150,151]. TNF-α binds to two different receptors, TNFR1 and TNRF2, initiating the signal transduction cascades. TNFR1 is expressed by all types of human cells and is the key receptor for TNF-α, meanwhile, TNFR2 is mainly expressed in immune cells and mediates a narrower spectrum of biological responses[152]. One of the main functions of TNF-α/TNFR1 is to activate NF-κB signaling[149]. More specifically, TNF-α binds to TNFR1 and stimulates the recruitment of the death domain-containing proteins RIP1 and TRADD. Then, TRAF2-cIAP1/2 complexes are recruited to TNFR1-bound TRADD. The cIAP1 and 2 proteins promote auto-ubiquitination and also the ubiquitination of other downstream signaling proteins, e.g. RIP1. This allows the LUBAC complex to ubiquitinate NEMO, a subunit of the IKK complex. Phosphorylation and activation of the IKK complex lead to the phosphorylation of the NF-κB inhibitory protein IκBα, resulting in proteasomal degradation[153,154]. Now NF-κB can translocate to the nucleus and initiate transcription[154] (Fig.6). The family of NF-κB transcription factors consists of five proteins - RelA, RelB, c-Rel, p100, and p150. All of them have the rel homology domain, which is crucial for dimerization, DNA binding, and interaction with IκB inhibitors. NF-κB proteins are regulating the expression of hundreds of genes, involved in inflammation, immunity, proliferation, and cell death[155,156]. The main function of NF-κB is to control the immune response at various levels.

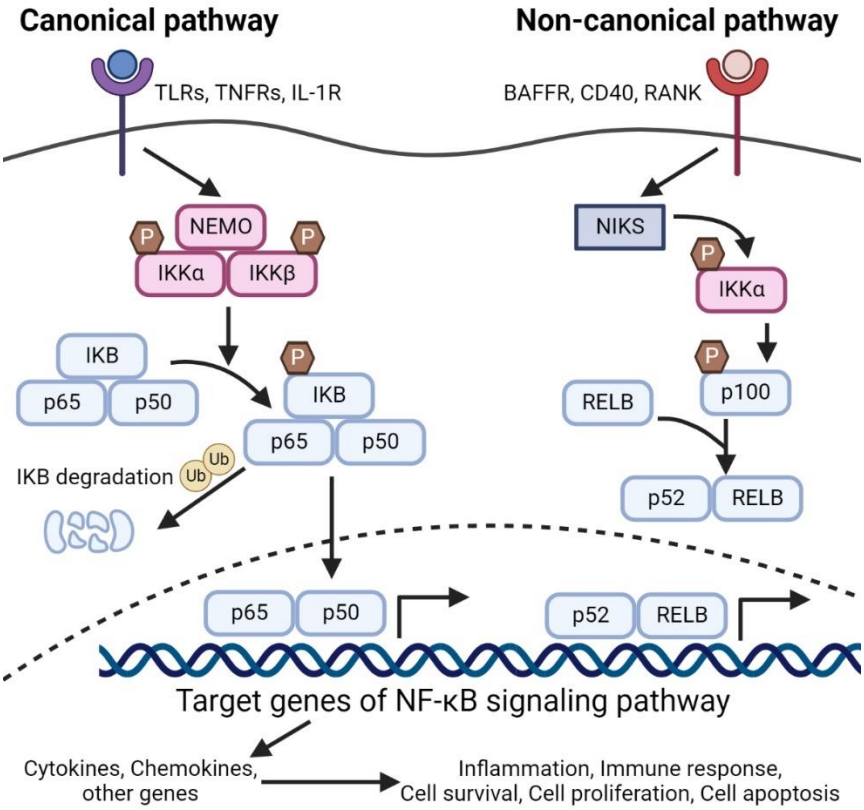

Figure 6. The canonical and non-canonical NF-κB signaling pathway[157]**.** The canonical NF- κB pathway is mediated via TLRs, TNFRs, and IL-1R. The activation of the pathway leads to the phosphorylation and degradation of inhibitory protein IκB. After the degradation of IκB, the members of NF- κB are released and translocate into the nucleus. Instead, the non-canonical NF- κB pathway depends on the activation of p100/RelB complex by CD40, RANK and BAFFR. The activation of NF-κB regulates a wide range of cellular processes by modulating the expression of chemokines and cytokines. Created in Biorender.com.

Depending on the context, TNF-α/TNFR1/NF-κB regulatory axis can promote or suppress tumor progression. In some situations, the constitutive activation of NF-κB could lead to chronic inflammation and tumor progression due to enhanced cell proliferation, survival, invasion, and angiogenesis[158,159]. Instead in another contexts, a disrupted activation of NF-κB signaling helps cancer cells to evade host immune responses[141,158,160,161].

1.4 Immune Surveillance and immunoediting model

Various studies in humans and mice demonstrate that the immune system can monitor, recognize and eliminate nascent tumor cells. This process is called immune surveillance or immunoediting and consists of three essential phases: elimination, equilibrium, and escape[162,163]. Initially, innate and

adaptive immune systems collaborate to detect, control, and destroy transformed cells. The acute inflammatory response is an important part of this phase. Immune cells start to secrete proinflammatory cytokines like interleukin-12, and interferon-γ and innate immune cells (such as natural killer cells, dendritic cells, and macrophages) proceed to kill cancer cells. After maturation, some innate immune cells migrate to lymph nodes and activate tumor-specific $CD4^+$ and $CD8^+$ T cells, which then migrate to the tumor site and facilitate the killing of cancer cells[162]. At this point, the tumor cells are eliminated, or some resistance clonal variants develop. It is possbile that immune response enters into an equilibrium phase – cancer cells are not eliminated, however, the immune system controls tumor cell outgrowth. If the immune system is not able to eliminate cancer cells during the equilibrium phase, then the phase of immune evasion is reached which eventually leads to the clinical manifestation of cancer[163,164]. Importantly, immune escape is now recognized as a cancer hallmark[165]. The main known immune evasion mechanisms include co-opting immune checkpoint pathways, repressing the antigen-presenting machinery and recruiting immunosuppressive cells in the microenvironment[166].

1.4.1 Mechanisms of immune evasion

Understanding immune evasion mechanisms is crucial for the development of more efficient cancer therapies.

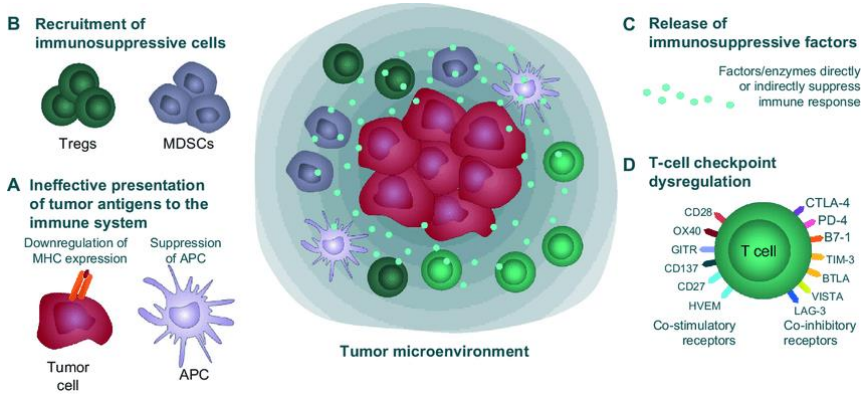

Figure 7. Immune evasion or immunosuppressive strategies employed by tumor cells[167]. There are several immune evasion mechanisms used by tumors. A) Tumors can downregulate the presentation of tumor antigens and hence avoid the recognition by T cells. B) Tumors can create an immunosupressive microenvironment by recruiting various immunosuppressive cells, such as T regulatory cells (Tregs) or myeloid-derived suppressor cells (MDSCs). C) Tumors can evade the host immune system by secreting immuno-modulating or immunosuppressive cytokines, chemokines and other mediators. D) Tumors can evade the immune system by dysregulating T-cell checkpoint pathways.

The most well-studied tumor immune evasion mechanisms are the following: the downregulation of tumor antigen presentation, the expression of immune inhibitory co-stimulatory receptors (e.g. PD-1, CTLA-4), the immunosuppressive tumor microenvironment (e.g. the secretion of IL-10, TGF-β by cancer cells), infiltration of suppressive immune cells (e.g. T regulatory cells, tumor-associated macrophages (TAMs)[162,168,169] (Fig.7). The immune evasion mechanisms relative to this project, will be described more in detail later in this chapter.

1.4.1.1 Antigen presenting

To understand how tumor cells adapt to evade immune surveillance, it is important first to understand the physiologic MHC pathway of antigen presentation[136]. In normal cellular physiology, proteins are mostly degraded by one of the two major proteolytic pathways: the lysosomal pathways and the ubiquitin-proteosome pathway[170]. The lysosomal pathway mainly degrades proteins taken up by endocytosis or autophagy, meanwhile, the ubiquitin-protease pathway is involved in the degradation of cytosolic proteins, misfolded and damaged proteins, mutated proteins in cancer cells, and viral proteins[170]. In both pathways, proteins are cleaved into oligopeptides that are presented to T cells by the major histocompatibility complex (MHC) molecules. The difference is that peptides derived from the proteins degraded by the lysosomal pathway are mainly presented on the MHC class II molecules whereas peptides created during the ubiquitin-proteosome pathway are presented on the MHC class I molecules[170]. MHC class I molecules are expressed on the plasma membrane of most cells and their main function is to present these peptides to cytotoxic T $CD8^+$ cells[136,170]. Antigen processing machinery consists of several cellular components[168]. It starts with continuous protein degradation into oligopeptides by the ubiquitin-proteaseome pathway. Polyubiquinated proteins are cleaved and the resulting peptides are processed in the antigen presentation machinery, which consists of proteasome/immunoproteasome, peptide transporters (TAP1 and TAP2), endoplasmic reticulum chaperons and the Golgi apparatus[171]. There are several types of proteosomes, known as proteosomes, immunoproteasomes, and thymoproteasosmes[172]. Immunoproteasome generates a wider variety of peptides and it is known from the literature that peptides produced by immunoproteasomes are more suitable for the presentation on MHC I molecules[136,173]. Immunoproteasome assembly is induced by inflammatory cytokines such as IFN-γ and TNF-α. During the generation of the immunoproteasome, the β1, β2, and β5 subunits of the constitutive proteasome are substituted with more efficient immunoproteasome subunits – β1i (LMP2, gene *PSMB9*), β2i (LMP10, gene *PSMB10*) and β5i (LMP7, gene *PSMB8*)[174–176]. Peptide transporter called TAP transfers peptides produced by immunoproteasome into the lumen of the endoplasmic reticulum (ER). TAP consists of two subunits – TAP1 and TAP2- both needed for the transportation of the peptides[177]. After the transportation to the endoplasmic reticulum, the peptides are further trimmed and afterward are fitted into the grooves of MHC

I molecules[136,170,177] (Fig. 8). MHC class I heterodimer consists of a heavy chain, which could vary between HLA-A, HLA-B and HLA-C and an invariant light chain called b_2-microglobulin (b_2M).

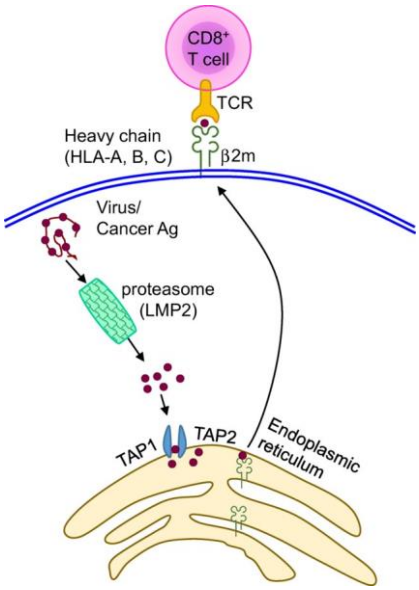

Figure 8. The MHC class I dependent antigen-presentation pathway[178]. Antigens of cancer or viral origins are processed by the immunoproteasome which consists of LMP2, LMP7 and other components. Immunoproteosome cuts these antigens into peptides that are transported into the endoplasmic reticulum through TAP1 and TAP2 transporters. The processed peptides are loaded onto the MHC class I molecules, composed of heavy chain and beta-2-microglubulin. Then. MHC class I molecule with peptide is exposed to the cell surface and can be recognized by the cytotoxic T cells.

To be functional, the heterodimer has to be stabilized which happens when a peptide is loaded into the peptide-binding groove of MHC I[161]. After assembly, peptide-MHC class I complex migrates to the cell membrane, fuses with it, and the bound peptides are exposed extracellularly, where the complex can be recognized by $CD8^+$T cells[170].

The regulation of MHC I antigen presentation is also important for tumors, as the downregulation or loss of effective antigen presentation is a key immune escape mechanism in cancer[136,179]. By impairing MHC I antigen presentation, cancer cells become undetectable and avoid being killed by cytotoxic T cells[179]. The downregulation of MHC I antigen presentation has been reported in 40-90% of human tumors and often is a marker for poor diagnosis[161,170].

Several different alterations can cause an abnormal MHC I display on the cell surface – genetic, epigenetic, transcriptional, and post-transcriptional[161]. MHC I aberration can be also divided into, reversible and irreversible,

depending on the possibility to restore MHC I expression following the cytokine or pharmacological treatment[161,168]. The most common genetic alteration (irreversible) is the loss of heterozygosity (LOH) of the HLA-ABC gene[168]. Another important irreversible defect is the loss of β2M protein expression due to LOH or mutation. The loss of β2M protein results in the complete loss of antigen presentation, as β2M is responsible for the MHC I complex stability[180]. HLA-I expression is strongly induced by type I and type II interferons, therefore, during immune evasion tumor cells target IFN-related pathways. HLA heavy chains and antigen-presenting machinery element promoters contain interferon-stimulated response element (ISRE) region, the binding site for the interferon regulatory factor-1 (IRF1). Following the IFN-γ binding to IFNGR1 extracellular domain, IRF1 is induced by JAK/STAT pathway. In cancer cells functional mutation in JAK/STAT and IRF1 reduces the responsiveness to IFN-γ, hence the antigen-presenting is not upregulated. These mutations are also associated with poor prognosis and resistance to immunotherapies. Other genetic changes are related to genes involved in antigen-presenting machinery, such as LMP2, LPM9, and TAP1/TAP2, resulting in reduced antigen presentation[168].

Loss of MHC class I in cancer cells is often a result of epigenetic silencing, transcriptional and post-transcriptional/translational modifications of HLA genes, or other genes crucial for antigen processing and presentation. In this case, the alterations are reversible, and the antigen-presenting could be restored upon the pharmacological treatment, which is a very important point for the more efficient immunotherapies[161,168].

The transcription of MHC-I heavy chain and other antigen presentation pathway genes is controlled via three major transcription binding sites: an Enhancer A region, which is recognized by NF-κB, an interferon-stimulated response element (ISRE), which can be bound by IRF1, and an SXY-module, which is recognized NLRC5[136,161,168]. In many cancers NF-κB is constitutively active, however, some tumors can downregulate NF-κB signaling and hence impair MHC I expression[181]. Furthermore, the expression of NF-κB is associated with a better response to immunotherapy in melanoma patients[182]. In addition to NF-κB, interferons play an important role in the induction of MHC I expression[161]. The downregulation of interferon pathways has been documented in some cancers such as melanoma, lung cancer, and breast cancer and is involved in the development of the resistance to immune-checkpoint inhibitors and adoptive cell therapy via the impairment of the antigen presentation pathway[137,161,183–186]. NLRC5, as a third major regulator of the MHC-I transcription, was discovered only recently[187]. NLRC5 is expressed upon the stimulation with IFN-γ. In several types of cancers, such as colorectal, ovarian, breast, and uterine cancers, the downregulation of the NLRC5 expression has been observed as an immune evasion mechanism. Furthermore, in melanoma, NLRC5 is known to induce anti-tumor immunity by upregulating antigen processing and presentation. Additionally, the

expression of NLRC5 correlates with the response to immune-checkpoint inhibitors in melanoma[161,188,189]. MHC I expression on the cell surface can be also modulated by the activation of various oncogenes, including MAPK, EGFR, HER2, c-MYC, n-MYC, and PI3K/AKT[161,168,190–192].

Epigenetic silencing is another common reversible defect in MHC class I antigen presentation. Epigenetic modulations can impair the transcription of HLA heavy chains, β2M, antigen-presenting machinery, or MHC-I regulatory proteins[161]. It has been demonstrated that histone deacetylation (HDAC) reduces the expression of key components of the antigen-presenting pathway, such as LMP2, LMP9, TAP1/TAP2 in neuroblastoma, cervical cancer, and melanoma[193–195]. DNA hypermethylation is another epigenetic modulation that cause the reduced expression of MHC-I and related genes[136,161,168,196].

1.4.1.2 Tumor-associated macrophages (TAMs)

A variety of stromal cells in the tumor microenvironment play an important role in tumor progression and immune evasion[197,198]. In solid tumors, tumor-associated macrophages are the most represented population[199,200]. In breast cancer, TAMs can be very abundant and may represent 50% of the number of cells within the tumor[201]. Macrophages are very plastic cells that can adapt and respond to external stimuli. Although the macrophage activation statuses are very complex, the most accepted model of macrophage classification simplifies polarization statuses in two extreme populations: the M1-like or pro-inflammatory and M2-like or anti-inflammatory. In the presence of the stimuli like lipopolysaccharide (LPS), IFN-γ, or TNF-γ, macrophages can polarize into M1 status, which is described by the expression of CD68, CD86, and CD80. M1 macrophages adopt a pro-inflammatory phenotype, with high antigen-presenting capacity and production and secretion of cytokines and chemokines like TNF-α, IL-1β, IL-12, CXCL9, and CXCL10, which promote pro-inflammatory Th1 response. Conversaly, IL-4, IL-13, IL-10, or glucocorticoids push macrophages to polarize to M2 status. M2 macrophages produce anti-inflammatory cytokines, particularly IL-10 and TGF-β [202]. M2 macrophages are also described by high expression of CD163, CD204, and CD206 and have immunomodulatory effects, and play a crucial role in inhibiting endogenous antitumor immunity. Importantly, tumor-associated macrophages are known to adopt phenotype common to M2-like macrophages, secrete inhibitory cytokines, and modulate immune cells by creating an immunosuppressive tumor microenvironment that is favorable to tumor progression and resistance to immunotherapies.

1.5 The ETS family of transcription factors

In this project we are focusing on ETV7, also called TEL2 – a member of the large ETS family[4,203]. The members of the ETS family can regulate the expression of genes involved in various fundamental cellular processes, such as cell cycle control, differentiation, proliferation, apoptosis, development,

tissue remodeling, and angiogenesis. Hence, it is not surprising, that dysregulation of ETS factor activity results in tumor initiation, progression, and metastatic spread[204–206]. Members of the ETS family are mainly involved in tumor progression, however, several members act as tumor suppressors[205,207,208].

There are several ways how ETS family members can be activated in cancer. In hematological cancers, chromosomal translocation is one of the most common activations of ETS factors[205]. It often involves the fusion of ETV6 with different partners, such as JAK2, ABL, EVI1, TRKc, and AML1[209]. However, chromosomal translocation is rarely found in solid tumors, a part from prostate cancer, which often have a rearrangement in ERG and ETV1[205,210]. Tumorigenesis can be also caused by ETS hyper-activation due to overexpression or gene amplification, this type of oncogenic activation is more common in breast, prostate, and hematological cancers[209]. A wide range of ETS factors, including ESA-1, ETS-1, ETS-2, PEA3, ERM, and ER81 are known to be upregulated in breast cancer and their upregulation correlates with poor prognosis[211]. Another way how some ETS factors can initiate transformation is by cytoplasmic localization. Even though it has been thought that the ETS factors function only in the nucleus as a transcription factor, for the ETS member ESE-1 a cytoplasmic role was also identified[212].

Moreover, ETS factors often undergo post-translational modifications[205]. Particularly, it is known that phosphorylation increases the interaction of ETS factors with transcription co-activators or co-repressors. This might be a main mechanism for ETS family activation due to the dysregulated upstream signaling in cancer cells[206].

1.5.1 ETV7 structure and physiological function

The ETS family of transcription factors consists of 28 members, all containing highly conserved DNA-binding domains[211,213]. This DNA-binding domain is formed from approximately 85-90 amino acids and is called the ETS domain, which recognizes unique purine-rich DNA sequences containing GGAA/T (ETS binding site). A subgroup of ETS factors also has the pointed domain (PNT), which is important for protein-protein interaction (Fig. 9)[206,214].

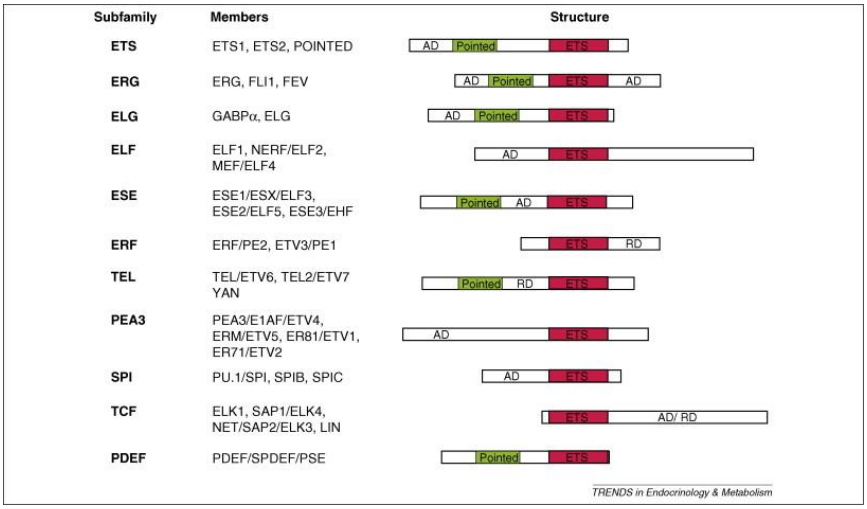

Figure 9. ETS family members and their structure[213]**.** ETS family members are divided into eleven subfamilies, according to their structural features. In the figure, every subfamily is presented by listing the members of the subfamily and by demonstrating the main functional domains, characteristic for each subfamily. Domains: AD (transcriptional activation domain); ETS (DNA binding domain); Pointed (basic helix–loop–helix pointed domain) ; RD (transcriptional repressor domain).

ETV7, the protein that we are focusing on in this study, is known to be closely related to ETV6. Although they both act as transcriptional repressors, bind similar DNA motifs, and can directly interact, they play opposite biological functions[4,215].

ETV7 and ETV6 structurally are very similar. *ETV6* has 8 coding exons, which all, apart from exon 5, have a very similar size to *ETV7*, which also has an additional alternatively spliced exon[203]. Both *ETV6* and *ETV7* genes encode a transcriptional repressor containing these key domains: N-terminal pointed domain, a less-conserved central domain, an ETS domain, and a smaller C-terminal inhibitory domain, which is missing in some isoforms of ETV7[4,203,215–217]. The pointed domains of ETV7 and ETV6 show >60% identity and are responsible for homodimerization and heterodimerization, e. g. ETV6 with ETV7. The pointed domain is also important for the repression of the target genes[203,215]. The central domains of ETV7 and ETV6 are crucial for the strong repression activity of these proteins[218]. Both ETV6 and ETV7 have highly conserved ETS domains, which show >85% identity between these two proteins. The structure of this domain facilitates ETV6 and ETV7 binding to target genes' regulatory regions containing ccGGAAgt sequence (Fig.10)[203,215].

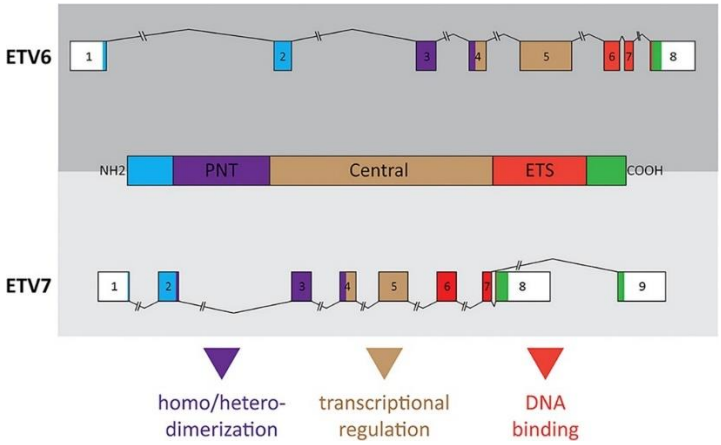

Figure 10. Structure of genes and encoded proteins of ETV6 and ETV7[215]. A schematic representation of the ETV6 and the ETV7 genes. Numbered boxes correspond to exons, which are colored according to the corresponding domain on the encoded protein. PNT – pointed domain. The function of each domain is summarized at the bottom.

Even though these two proteins are highly similar, they conduct different biological effects. ETV6 is highly ubiquitously expressed, meanwhile the expression of ETV7 is low in a wide range of tissues but markedly higher in hematopoietic tissues, such as the bone marrow or fetal liver[203,216,218]. Several studies identified multiple roles of ETV7 in hematopoiesis. One study demonstrated that the overexpression of ETV7 in human and mice hematopoietic stem cells (HSCs) increases the proliferation, leading to the exhaust of HSCs in mice[219]. Moreover, Quintana and co-workers. investigated the role of ETV7 in zebrafish erythropoiesis and demonstrated that ETV7 is crucial for the normal development of red blood cells, via the regulation of the lanosterol synthase gene and the cholesterol synthesis pathway[220].

ETV6 is known to inhibit colony formation in NIH3T3 fibroblasts, while ETV7 stimulates colony formation[221]. In the pro-monocytic cell line U937 during the induced differentiation with vitamin D3, ETV7 but not ETV6 is downregulated and the forced overexpression of ETV7 in these cells inhibited differentiation[221].

Still, the information regarding the regulation of ETV7 is limited. Since ETV7 is similar to ETV6, it is thought that control of nuclear localization could be a key regulatory mechanism, as it is in the case of ETV6 regulation. ETV6 is delocalized from the nucleus to cytoplasm via its N-terminal domain, containing several putative MAP kinase phosphorylation sites, which are not present in shorter isoforms, the same phenomenon was also observed for ETV7[216,222,223]. Moreover, a previous study conducted in our laboratory demonstrated that ETV7 was upregulated in cancer cells upon the combined treatment with Doxorubicin and TNF-α[224].

Interestingly, ETV7 is also an Interferon-stimulated gene (ISG), and its expression was induced by type I, type II, and type III interferon treatment in several cell lines[11,225–227]. Furthermore, ETV7 was upregulated in hESCs-derived hepatocytes infected with the Hepatitis C virus and upon infection with SARS-Cov-2 and influenza viruses[12,228,229]. In case of infection with the influenza virus, ETV7 represses a subset of interferon-stimulated genes, important for host immune response, suggesting a possible role of ETV7 in antiviral immunity[12].

1.5.2 ETV7 in cancer

In humans, the *ETV7* gene is located within the MHC cluster region at chromosome 6p21. This region is known to be involved in a wide range of cancers, such as cervical cancer, non-small cell lung carcinomas, ovarian and breast carcinomas, and B-cell non-Hodgkin's lymphomas[230]. Unfortunately, the role of ETV7 in cancer has been poorly investigated, partially because of the absence of ETV7 in most rodent species, including mice[220,231]. Only recently, in 2019, a transgenic mouse model carrying a single copy of the human ETV7 genes has been established. Crossing these ETV7-expressing mice with leukemia-prone mice (Ptenfl/fl; Mxl-Cre) accelerates PtenΔ/Δ leukemogenesis. Furthermore, it was demonstrated that ETV7 enhances self-renewal and colony-forming activity in Pten-/- cells, suggesting thatETV7 is a positive regulator of tumorigenesis in the absence of the tumor suppressor gene Pten[231].

Elevated expression of ETV7 has been associated with several types of cancer. Particularly, the analysis of the expression of ETV7 in various cancers demonstrated that it is upregulated in 70% of acute lymphoblastic leukemia and acute myeloid leukemia samples and 48% of pediatric solid tumor xenografts[4,232]. Moreover, ETV7 was found to be up-regulated in 85% of medulloblastoma cases, while another study identified ETV7 as one of the top 10 up-regulated proteins in hepatocellular carcinoma[6,10]. Another study identified ETV7 as a novel prognostic factor in bladder cancer[5]. In 2016, Piggin and colleagues reported an increase in the expression of ETV7 in all types of breast cancer compared to healthy tissue. Interestingly, the levels of ETV7 correlated with the aggressiveness of the tumor, meaning that the highest levels of ETV7 were detected in the most aggressive subtypes of breast cancer (Fig. 11)[8].

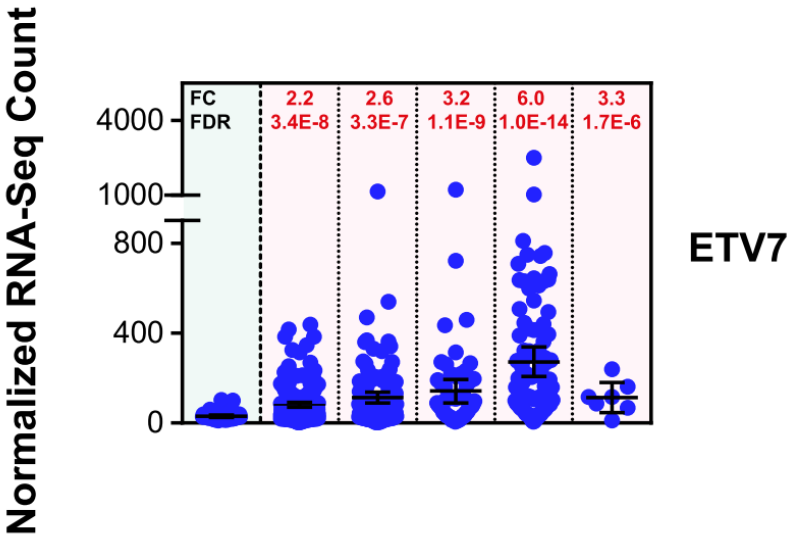

Figure 11. The expression of ETV7 for normal breast and breast cancer subtypes[8]. The expression of ETV7 for normal breast (green background, first column) and breast cancer subtypes (pink background). Plotted values are for individual samples (normalized counts), and error bars represent the mean with a 95 % confidence interval. Fold change (FC) and FDR from unpaired Limma voom differential expression analysis are shown, with red indicating a significant upregulation compared with normal (FDR < 0.05).

It has been demonstrated that ETV7 cooperated with Eμ-MYC and promoted the proliferation and survival of normal mouse B cells, hence accelerating the development of lymphoma[233]. Moreover, forced expression of ETV7 in mouse bone marrow cells causes a non-transplantable myeloproliferative disease, which accelerates tumorigenesis upon the treatment with DNA-damaging drugs[4].

Further evidence supporting the pro-tumorigenic function of ETV7 is coming from the studies related to chemoresistance. A recent study identified a transcription-independent activity of ETV7, that allowed ETV7 to physically interact with mTOR in the cytoplasm and generate a novel complex called mTORC3, which promoted resistance to rapamycin, an mTOR-targeting drug[10]. Additionally, a recent study in our laboratory demonstrated that ETV7 can mediate the development of resistance to doxorubicin in MCF7 and MDA-MD-231 breast cancer cells. It was observed that the expression of ETV7 was upregulated upon the treatment with DNA-damaging drugs, including Doxorubicin. Elevated ETV7 led to repressed DNAJC15, a co-chaperon member of the HSP40 family, which is also known as an inhibitor of ABCB1, one of the most important ABC transporters involved in drug resistance. In particular, ETV7 can directly bind the *DNAJC15* promoter and recruit the DNA methyltransferase DNMT3A. This cooperation leads to the

hypermethylation of the *DNAJC15* promoter and the repression of this gene, leading to increased levels of ABCB1 and enhanced levels of drug efflux (Fig.12)[9].

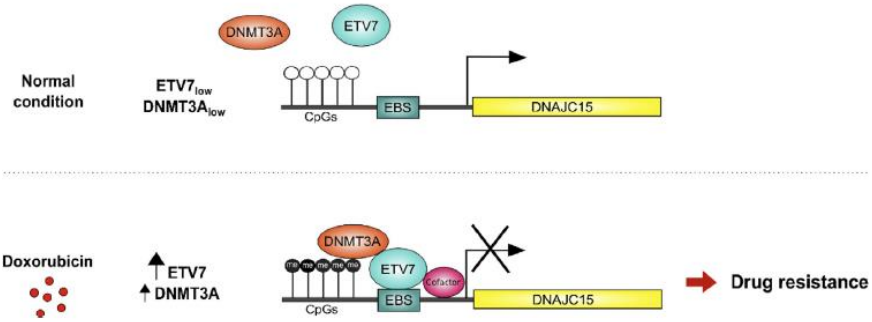

Figure 12. A graphical model for ETV7-dependent Doxorubicin resistance in breast cancer cells[9]. In normal conditions, the levels of ETV7 and DNMT3A are low and DNAJC15 is normally expressed. Upon the treatment with doxorubicin, the expression of ETV7 and DNMT3A is induced. Hence, ETV7 binds the DNAJC15 promoter and recruits DNMT3A, leading to the methylation of CpGs. This results in the repression of DNAJC15 and thus the resistance to doxorubicin. EBS: ETV7 Binding Site. Methylated CpGs are shown as black-filled circles, whereas unmethylated CpGs are marked as white-empty circles.

On the contrary, in a few tumor types, ETV7 can act as a tumor suppressor. For example, in nasopharyngeal carcinoma ETV7 represses the *SERPINE1* gene, reducing metastatic spreading[208]. Furthermore, it is reported that ETV7 is downregulated in drug-resistant gastric cancer[234].

2. MATERIALS AND METHODS

2.1 Cell culture conditions

MCF7 cells were obtained from the Interlab Cell Line Collection bank (IRCCS Ospedale Policlinico San Martino, Genoa, Italy), T47D and BT-549 cells were received from Dr. U. Pfeffer (IRCCS Ospedale Policlinico San Martino); HEK293T and HUH-7 cells were a gift from Prof. J. Borlak (Hanover Medical School, Germany), HCC70 from Dr. M.R. Maiello (INT-Fondazione G. Pascale, Naples, Italy), while MDA-MB-231 and SK-BR-3 cells were a gift from Prof. A. Provenzani (CIBIO Department, University of Trento, Italy), while ZR-75-1 cell line was a gift from Prof. A. Zippo (CIBIO Department, University of Trento, Italy). H1299 cells were obtained from Dr. D. Menendez (National Institute for Environmental Health Center, NIEHS, NIH, Research Triangle Park, NC, USA), while H460 and H1975 cells from Dr. A. Alama (Ospedale Policlinico San Martino, Genova, Italy). U2OS, SJSA1, and HCT116 (both parental and p53-/-) cells were received from Prof. A. Inga (CIBIO Department, University of Trento, Italy).

MCF7, T47D, SK-BR-3, HUH-7, and HEK293T cells were grown in DMEM medium (Gibco, Life Technologies, ThermoFisher Scientific, Milan, Italy) supplemented with 10% FBS (Gibco), 2mM L-Glutamine (Gibco) and a mixture of 100U/ml Penicillin / 100µg/ml Streptomycin (Gibco). MDA-MB-231 cells were cultured in the same medium with the addition of 1% Non-Essential Amino acids (Gibco). 4T1, A549, HCT166, HCC70, HCT116 $p53^{-/-}$, H460, SJSA1, U2OS, H1975, H1299, BT-549, and ZR-75-1 were grown in RPMI medium (Gibco) supplemented with 10% FBS (Gibco), 2mM L-Glutamine (Gibco), and a mixture of 100U/ml Penicillin / 100µg/ml Streptomycin (Gibco); BT-549 cells were also supplemented with 1% of the Insulin-Transferrin-Selenium supplement (Gibco) and ZR-75-1 cells were additionally supplemented with 1% of Sodium Pyruvate (Gibco).

Cells were grown at 37°C with 5% CO_2 in a humidified atmosphere. Cell lines were monthly checked for mycoplasma contaminations and have recently been authenticated by PCR-single-locus-technology (Eurofins Genomics, Ebersberg, Germany or DDC Medical, Fairfield, OH, USA).

Cell line	Species	Tissue	Tumor subtype	p53 status
4T1	Mouse	Mammary gland tumor	basal-like	mutated
BT-549	Human	Breast cancer	basal-like	mutated
HCC70	Human	Breast cancer	basal-like	mutated
MCF7	Human	Breast cancer	luminal A	wild-type
MDA-MB-231	Human	Breast cancer	basal-like	mutated
SK-BR-3	Human	Breast cancer	HER2-positive	mutated
T47D	Human	Breast cancer	luminal A	mutated
ZR-75-1	Human	Breast cancer	luminal A/HER2-positive	wild-type

Table 1. Breast cancer lines used in this PhD thesis[41,235]**.** This table summarizes breast cancer cell lines used in this thesis, according to the tumor subtype and p53-status (according to TP53 database, p53.fr).

Cell line	Species	Tissue	p53 status
A549	Human	Lung carcinoma	wild-type
H1299	Human	Lung carcinoma	null
H1975	Human	Lung adenocarcinoma	mutated
H460	Human	Lung carcinoma	wild-type
HCT116	Human	Colorectal carcinoma	wild-type
HEK293T	Human	Embryonic kidney	wild-type
HUH-7	Human	Hepatocellular carcinoma	mutated
SJSA1	Human	Osteosarcoma	wild-type
U2OS	Human	Osteosarcoma	wild-type

Table 2. Cell ines used in this PhD thesis. This table summarizes other cell lines used in this thesis, describing tissue of origin and p53-status (according to TP53 database, p53.fr).

2.2 Treatments and cytokine stimulation

Based on the experimental design, 5-fluorouracil (5-FU) (Sigma Aldrich, Milan, Italy) was used at different concentrations and for different time points. Navitoclax and Elacridar were obtained from MedChemExpress and Selleckchem (Aurogene, Rome, Italy), respectively. MCF7, T47D, MDA-MB-231, and SK-BR-3 cells were treated with 1.5 μM Doxorubicin (MedChemExpress) for 24 hours for mRNA analysis and Chromatin Immunoprecipitation.

MCF7 and T47D cells were treated with 20 ng/ml IL-6 (PeproTech, London, UK), and 10 ng/ml or 20 ng/ml TNF-α (PeproTech), respectively. Cells were stimulated for 1 hour for protein analysis and immunofluorescence, 4 hours for Chromatin ImmunoPrecipitation, a luciferase reporter assay, and mRNA analyses and, 24 hours for enzyme-linked immunosorbent assay. Cells

were treated with 20 ng/ml recombinant human IFN-γ (Peprotech) for different periods based on the experiment.

2.3 Plasmids and cloning

The expression plasmids pCMV6-Entry-Empty and pCMV6-Entry-ETV7 C-terminally tagged with DDK-Myc were purchased from Origene (Tema Ricerca, Bologna, Italy). pGL3-NF-κb reporter, containing *Photinus pyralis* (Firefly) luciferase gene under the control of an NF-κB responsive element was a gift from Dr. Alessio Nencioni (University of Genoa, Italy). 4xM67 pTATA TK-Luc, containing four copies of the sequence GGTTCCCGTAAATGCATCA (underlined is the STAT-binding site) was obtained from Prof. David Frank (Dana-Farber Cancer Institute, Boston, MA, USA). pRL-SV40 (Promega, Milan, Italy) plasmid constitutively expressing the *Renilla reniformis* luciferase cDNA was used as transfection efficiency control for gene reporter assay.

The pcDNA3-TNFR1 expression vector was generated by cloning with the primers indicated below to PCR amplify (using Q5 High-Fidelity PCR kit, New England Biolabs, Euroclone, Milan, Italy) the TNFR1 reference sequence from pBMNZ-neo-Flag-TNFR1 L380A (gift from Martin Kluger, Addgene plasmid # 43949; http://n2t.net/addgene:43949)[236] and inserting it into pcDNA3.1 plasmid (the tails containing the target sequences of restriction endonucleases are indicated in lowercases):

Fw: gcggtaccATGAGGGCCTGGATCTTCTTTC

Rv: tagcggccgcTCATCTGAGAAGACTGGGCGCG

The purified PCR product was inserted into the pcDNA3.1 backbone using KpnI and NotI restriction endonucleases and T4 DNA Ligase (New England Biolabs). Correct cloning was verified by diagnostic restriction and direct sequencing (Microsynth, Balgach, Switzerland).

2.4 Transient transfection

24 hours prior to transfection, 0.2 x 10^6 of SK-BR3 and MDA-MB-231 cells were seeded in 6-well plates. Cells were transfected using Lipofectamine LTX and Plus Reagent (Life Technologies) along with 1 µg of pCMV-Entry-Empty or pCMV-Entry-ETV7 plasmid (Origene and[9]). After 48 hours the cells were collected and processed accordingly.

2.5 Generation of stable pAIP-ETV7 and Empty cell lines

To obtain cell lines with stable over-expression of ETV7, cells were transduced with the lentiviral vector pAIP Empty or pAIP ETV7. After 24 hours, the medium containing lentiviral particles was replaced with the new

medium. After additional 24 hours, the cells were put in selection by adding Puromycin (Life Technologies) at a concentration ranging from 1 to 2.5 µg/ml, according to the sensitivity of the cell line to the puromycin. After 4 cycles of selection, single clones were selected according to the Corning protocol for cell cloning by serial dilution in a 96-well plate. During the single clone selection, the puromycin concentration was gradually reduced to the range from 0.75 to 1.5 µg/ml.

2.6 RNA interference

Target RNAs were silenced using small interfering RNAs (siRNAs) and the transfection reagent INTERFERin® (Polyplus-Transfection, Euroclone). Scrambled siRNA was used as a control. Scrambled siRNA and ETV7 targeting siRNA (#1 and #2) were purchased from Integrated DNA Technologies (IDT, Tema Ricerca). 24 h before transfection cells were seeded in 6-well or 96-well plates to reach 50–60% confluence. Then the cells were transfected with 20 nM siRNA and 7 µl or 0.75 µl of INTERFERin reagent per well, according to the used plate format. The transfection mix was diluted respectively in 200 µl or 50 µl of OptiMEM medium (Gibco, Life Technologies), vortexed for 10 s, incubated at room temperature for 15 min, and added to the cells. Analyses on the silenced cells were performed 72 h post-transfection.

2.7 Western blot

Total protein cell extracts were obtained by lysing the cells with RIPA buffer (150mM Sodium Chloride, 1.0% NP-40, 0.5% Sodium Deoxycholate, 0.1% SDS, and 50mM Tris-HCl pH 8.0 supplemented with protease inhibitors (PI) (Roche, Milan, Italy). Proteins were quantified using the BCA method (Pierce, ThermoFisher Scientific) and then 25-50 µg of proteins were loaded on 8%, 10%, or 12 % polyacrylamide gels for SDS-PAGE. After the separation, the proteins were transferred on a nitrocellulose membrane (Amersham, Euroclone) which was probed over-night at 4°C with specific antibodies diluted in 1-3% skimmed milk-PBS-0.1% Tween solution: TNFR1 (H-5, Santa Cruz Biotechnologies, DBA, Milan, Italy), STAT3 (124H6, Cell Signaling Technologies, Euroclone, Milan, Italy), pSTAT3 (Y705, Cell Signaling Technologies), HSP70 (C92F3A-5, Santa Cruz Biotechnologies), TEL2 (E-1, Santa Cruz Biotechnologies), GAPDH (6C5, Santa Cruz Biotechnologies), pIKBα (Ser32/36, Santa Cruz Biotechnologies), p53 (DO-I, sc-126, Santa Cruz Biotechnologies), α-actinin (H2, sc-17829, Santa Cruz Biotechnologiesm), BCL-2 (100, sc-509, Santa Cruz Biotechnologies), Survivin (D-8, sc-17779, Santa Cruz Biotechnologies), EpCAM (ab71916, Abcam, Cambridge, UK), β-Tubulin (3F3-G2, sc-53140, Santa Cruz Biotechnologies), H3 (ab18521, Abcam), B2M (BBM.1, sc-13565, Santa Cruz Biotechnologies), PARP-1 (46D11, Cell Signaling Technologies), LMP-

2 (G-3, sc-373996, Santa Cruz Biotechnologies), LMP-7 (A-12, sc-365699, Santa Cruz Biotechnologies), IRF-1 (E-4, sc-514544, Santa Cruz Biotechnologies). Detection was performed with ECL Select Reagent (GE Healthcare, Cytiva) using ChemiDoc XRS+ (BioRad) or UVITec Alliance LD2 (UVITec Cambridge, UK) imaging system.

2.8 Cytoplasmic-nuclear fractionation

The extraction of cytosolic and chromatin-enriched protein fractions was performed as recently described[237]. Briefly, cells were collected, centrifugated, and afterward resuspended in NSB buffer (10 mM HEPES, 10 mM KCl, 1.5 mM MgCl2, 0.34 M Sucrose, 10% Glycerol, 1 mM DTT, 0.1% TritonX-100 added with 1x PI and 1x Phosphatase Inhibitors (Roche) and left on ice for 8 min. Then, the samples were centrifuged at 1300 rpm at 4°C for 10 min. The supernatant, containing the cytoplasmic protein fraction, was collected. The remaining nuclei were resuspended in the NSB buffer supplemented with 1 mM CaCl2 and 2000 gel units/ml of MNase (New England Biolabs) and incubated at 37°C for 10 min. The MNase reaction was stopped by adding 2 mM EGTA (Sigma-Aldrich/Merck). Afterward, the samples were centrifuged at 13000 rpm at 4°C for 10 min and the fraction containing the nuclear soluble proteins was collected. The remaining pellet was resuspended in the NSB buffer supplemented with 600 mM NaCl and incubated rotating, at 4°C overnight. Then, the samples were centrifuged at 13000 rpm at 4°C for 10 min and chromatin-enriched protein fraction was collected. The protein samples were then loaded on the SDS-PAGE gel and the Western blot procedure was executed as described above.

2.9 RNA extraction and RT-qPCR

Total RNA was isolated using RNeasy® Mini Kit (Qiagen, Milan, Italy), RNeasy® Mini Plus Kit (Qiagen), or NucleoSpin RNA (MACHEREY-NAGEL), converted into cDNA with PrimeScriptTM RT reagent Kit (Takara, Diatech Lab Line, Ancona, Italy) and RT-qPCR was performed with 25 ng of template cDNA in 384 well-plate (BioRad, Milan, Italy) using qPCRBIO SyGreen 2X Mix (PCR Biosystems, Resnova, Ancona, Italy) with the CFX384 Real-Time detection system (BioRad) or QuantStudio™ 5 Real-Time PCR System (Applied Biosystems, Thermo Fisher Scientific). *YWHAZ*, *ACTB*, and *GAPDH* were used as reference genes to obtain the relative fold change by the ΔΔCt method as previously described[238]. Primers were designed using Primer-BLAST online tool (https://www.ncbi.nlm.nih.gov/tools/primer-blast/), and checked for specificity and efficiency. qPCR primer sequences (Eurofins Genomics) are listed in the Supplementary table 1.

2.10 Chromatin immunoprecipitation (Chip)

ChIP experiments were performed as previously described[9]. Briefly, $3x10^6$ MCF7 Empty/ETV7, T47D Empty/ETV7 or parental MCF7/T47D cells were seeded in 15 cm dishes. The day after, if necessary, the cells were treated with 1.5 µl of Doxorubicin for 16 hours and if needed with 20 ng/ml IL-6 for 4 hours before the collection of the sample. Afterward, cells were cross-linked for 8 min using 1% Formaldehyde. At the end of the incubation, 125 mM Glycine was added and left for 5 min. Then, the cells were washed twice with ice-cold 1X PBS, scraped, and collected in 1 ml of 1X PBS supplemented with protease inhibitors (PI) and in case needed, phosphatase inhibitors. Then, the pellet was lysed with lysis buffer (1% SDS) supplemented with 100 µg/ml salmon sperm single-strand DNA (ssDNA, Life Technologies) and PI. After the lysis, the samples were centrifuged at 800 g, at 14°C, for 10 min, and the supernatant was discarded. Then, the pellets were resuspended in the sonication buffer (0.25% SDS, 200 mM NaCl) supplemented with 100 µg/ml ssDNA and PI and sonicated using Bioruptor Pico sonicator (Diagenode, Denville, NJ, USA). To reach DNA fragments in the range of 200-700 bp, for the MCF7 cells we used 45 cycles (30 s On/ 30 s Off) and for T47D cells - 15 cycles (30 s On/ 30 s Off). After the sonication the size of the fragments was checked on the 2% agarose gel. Then, the samples were centrifuged and the pellets were conserved at -80°C. Before performing immunoprecipitation, samples were diluted and incubated with 2 µg the appropriate antibody ETV7 (Santa Cruz Biotechnologies, TEL2, E-1), pSTAT3 (Cell Signaling Technologies, 124H6), H3K9me3 (Cell Signaling Technologies, 13969P), H3K4me3 (Abcam, ab8580), H3ac (Abcam, ab47919) or IgG (Santa Cruz Biotechnologies, mouse or rabbit according to the antibody used) and Dynabeads with protein G or A (Life Technologies) overnight at 4°C in a rotator. The Input sample (10% of the sample volume) was incubated overnight at 4°C without dilution or addition of any antibodies or beads. The day after, the samples were washed through multiple washing steps and eluted at 65°C overnight by adding the elution buffer and 1X TE supplemented with 0.65% of SDS. Then, the samples were processed with 50 µg of Proteinase K (ThermoFisher Scientific) for 2 hours at 56°C and 50 µg of RNase A (VWR International, Radnor, PA, USA) for 30 min, at 37°C. Afterward, DNA was purified using QIAquick PCR purification kit (Qiagen). qPCR was performed using GoTaq® qPCR Master Mix (Promega) and BioRad CFX384 qPCR system. Primer sequences are listed in the Supplementary Table 1.

2.11 Protein co-immunoprecipitation

MCF7-Empty/ETV7 or T47D-Empty/ETV7 cells were seeded in 10 cm dishes. After 24 hours, cells were treated with 20 ng/ml IL-6 and 4 hours post-treatment lysed using CHAPS buffer and incubated overnight with 2 µg of an anti-ETV7 antibody (TEL2, Santa Cruz Biotechnologies) or normal mouse

IgG (Santa Cruz Biotechnologies) previously bound with Dynabeads protein G magnetic beads (Life Technologies). Then, the beads were washed, and the immunoprecipitated lysates were eluted and loaded on a polyacrylamide gel for SDS-PAGE. The following steps were performed equally to the previous Western blot procedure.

2.12 Gene reporter assay

First, 90,000 cells per well were seeded in 24-well plates and after 24 hours, when the cells reached 70-80% confluency, cells were transfected with Lipofectamine LTX and Plus Reagent (ThermoFisher Scientific) along with different combinations of the plasmids according to the experiment: 50 ng of normalizing vector pRL-SV40, 200 ng of expression vectors (pcDNA3.1-Empty/pcDNA3.1-TNFR1), and reporter vectors (350 ng 4xM67 pTATA TK-Luc and 300 ng pGL3-NF-κB). Twenty-four hours post-transfection, if necessary, cells were stimulated with appropriate concentrations of different cytokines. Then, the cells were washed once with 1X PBS and lysed in 1X PLB (Passive Lysis Buffer) buffer (Promega). Afterward, the activity of luciferase was measured using the Dual-Luciferase Reporter Assay System (Promega) following the manufacturer's procedure and using the Varioskan LUX multimode microplate reader (ThermoFisher Scientific). *Renilla reniformis* luciferase activity was used as an indicator of transfection efficiency and used to obtain the Relative Light Unit (RLU) values.

2.13 Spheroid formation

The 96-well plate was pre-coated with 1.5% agarose and let to solidify for 30 min. Meanwhile, cells were detached and counted. 5000 cells were seeded in each well resuspended in 200 µl of the medium. The medium was changed every 2 days, by removing 100 µl of the medium and adding 100 µl of the new medium. After 72-hour spheroids were formed and used for the treatment with 5-FU. The images were taken at 10X magnification and the data ware analysed using ImageJ software (National Institutes of Health, Bethesda, MD, USA).

2.14 Mammospheres culturing

Mammosphere formation assay was performed by modifying a previously publishes protocol[88]. Briefly, to form primary mammospheres, cells were firstly detached with trypsin, centrifuged, and resuspended in mammosphere medium (DMEM/F12 supplemented with 20 ng/ml recombinant human Epidermal Growth Factor (EGF), 10ng/ml recombinant human basic Fibroblast Growth Factor (bFGF) and 1x B27 supplement w/o Vitamin A, 2mM L-Glutamine, 100U/ml penicillin, and 100µg/ml streptomycin). To obtain a single-cell suspension, cells were passed several times through a 25G needle. Afterward, 1000 cells were resuspended in 800 µl of mammosphere

medium and seeded in each well of a 24-well ultra-low attachment plate (Corning, Rome, Italy). Plates were incubated at 37°C for one week and images were acquired at DM IL LED Inverted Microscope (Leica Biosystems, Wetzlar, Germany). After 1 week, mammospheres were counted and mammosphere forming efficiency (%) was calculated using this formula: MFE(%) = (# of mammospheres per well) / (# of cells seeded per well) x 100.

2.15 MTT viability assay

Cells were seeded in 96-well plates and treated (or silenced) with different concentrations of various drugs, according to the experimental design. At the end of the treatment, the medium was carefully aspirated, the cells were washed once with 1X PBS and 100 µl of the new medium was added to each well. Then, 10 µl of 5 ng/ml MTT reagent (Sigma-Aldrich) was added to each well. The plate was protected from the light and incubated for 3 hours. Afterward, the medium was removed and formed crystals dissolved in 100 µl of DMSO (Sigma-Aldrich) and a colorimetric measure was performed at the Varioskan LUX multimode microplate reader (ThermoFisher Scientific). Viability was calculated as a % ratio between untreated cells (or transfected with Scr control) and cells treated with a drug (silenced).

2.16 Cell Titer Glo Viability assay

A viability assay was performed using the Cell Titer-Glo Luminescent cell viability assay (Promega) following the manufacturer's instructions. Briefly, cells were seeded in white flat-bottomed 96-well plates, and 24 hours after the seeding the cells were treated with various drugs or siRNA, according to the experimental design. After 72 hours, the plates were equilibrated at room temperature for 30 min; then, 100 µl of Cell Titer-Glo reagent was added to 100 µl of medium and left in incubation for 2 min on an orbital shaker. Then, a luminescence measure was performed at the Infinite M200 plate reader (Tecan, Milan, Italy) or Varioskan™ LUX multimode microplate reader (ThermoFisher Scientific). Viability was calculated as a % ratio of viable cells treated with the indicated drug (or siRNA) with respect to DMSO or Scr control.

2.17 Annexin V-FITC/PI staining

Apoptosis was measured using the FITC Annexin V Apoptosis Detection Kit I (BD Biosciences, San Jose, CA, USA). Briefly, after the appropriate treatment or 72 hours post-silencing, cells were harvested, washed twice with cold 1X PBS, and re-suspended in 1× Annexin V Binding Buffer at the concentration of 1.5×10^6 cells/ml. 100 µl of the cell suspension was then incubated with 2.5 µl of FITC-Annexin V antibody and 5 µl of propidium iodide for 15 min at room temperature, in the dark. Subsequently, 400 µl of 1×

Annexin V Binding Buffer was added to each tube and then samples were analyzed. Flow cytometry analysis was conducted at the CIBIO Cell Analysis and Separation Core Facility using a FACS Canto A instrument (BD Biosciences).

2.18 CD44/CD24 staining

The localization of CD44 and CD24 on the cell membrane was analyzed by double staining with antibodies conjugated with fluorophores and flow cytometry analysis. Cells were seeded in a 6-well plate and, after the appropriate treatments or manipulations, were harvested and washed with 1X PBS. 3×10^5 cells were re-suspended in 30 µl PBS + 0.1% BSA and incubated with APC mouse anti-human CD44 (cat.no 559942, BD Bioscience) and FITC mouse anti-human CD24 (cat.no 555427, BD Bioscience) antibodies or with their isotype controls (FITC mouse IgG2a, k isotype, and APC mouse IgG2b, k isotypes, BD Bioscience) in ice for 30 min. After incubation cells were washed three times with PBS and finally re-suspended in 300 µl 1X PBS. Flow cytometry analysis was performed at the CIBIO Cell Analysis and Separation Core Facility using a FACS Canto A instrument (BD Biosciences).

2.19 Generation of ETV7 KO cells

ETV7-specific gRNA sequences targeting exon 6 for performing ETV7 knock-out with CRISP-Cas9 technology, were designed using the CRISPOR.org web tool[239] and cloned using sgRNA-ETV7-Ex6-1: caccgAGGGCTCATATCGGGTATCA and sgRNA-ETV7-Ex6-2: aaacTGATACCCGATATGAGCCCTc oligos into the pX330-SpCas9-sgRNA-Puro vector (obtained from Prof. Anna Cereseto, CIBIO Department, University of Trento, Italy) digested with BbsI restriction enzyme (ThermoFisher Scientific). The correct insertion of each gRNA into the plasmid was checked by direct sequencing (Eurofins Genomics).

To generate SK-BR-3 cells knock-out for ETV7, 50,000 cells per well were seeded in a 24-well plate and after 24 h transfected with 500 ng pX330-Puro-ETV7 gRNA plasmids using Lipofectamine LTX and Plus Reagent (Life Technologies). After 48 h post-transfection, cells were selected with 1 µg/ml of Puromycin (Life Technologies). After 3 days of selection, Puromycin was removed from the culture medium and once reached confluency, cells were split and harvested for indel analysis. Single-cell cloning was performed according to the Corning protocol for cell cloning by Serial dilution in 96-well plates. Obtained single clones were screened by performing TIDE (Tracking of Indels by DEcomposition) analysis. Genomic DNA was extracted using QuickExtract™ DNA Extraction Solution (Lucigen, Middleton, WI, USA). PCR on the edited region was performed using 5× FIREPol® Master Mix (Solis BioDyne, Tartu, Estonia) and specific primers (TIDE-ETV7-ex6-F: ATCAGATGCTCCTGTTGGGC, TIDE-ETV7-ex6-R:

GAGCCCCATTAGTGGCTGTT), and purified products analyzed with Sanger sequencing (Microsynth, Balgach, Switzerland). TIDE analysis and efficiency of the editing were performed through the TIDE online platform (http://shinyapps.datacurators.nl/tide/) using parental cells as reference control[240].

2.20 Immunofluorescence

To perform immunofluorescence, the cells after the treatment were fixed with 4% PFA and incubated for 10 min at room temperature. Afterward, the wells were washed once with 100 µl of 1X PBS. Then, the cells were blocked and permeabilized using 3%BSA-0.3%Trinton-X-100 PBS solution for 30 min at room temperature. Primary anti-p65 (NF-κB p65 (D14E12) XP, Cell Signalling Technologies) antibody was diluted 1:400 in 1% BSA solution and added to the wells, afterwards, the plate was incubated for 60 min at room temperature. Afterwards, the wells were washed once with 3% BSA solution. Then the secondary antibody Goat anti-Rabbit IgG (H+L) Cross-Adsorbed Secondary Antibody Alexa Fluor® 488 (Life Technologies) was diluted 1:500 in 1% BSA solution, added to the wells, and incubated for 60 min at room temperature, protected from the light. Afterward, the wells were washed once with 3% BSA solution. The nuclei were stained using Hoechst 33342 (1:5000) and incubated for 30 min at room temperature. The images were acquired using IMAGEXPRESS MD Micro Confocal High-Content Imaging System (Molecular Devices, San Jose, CA, USA).

2.21 Cancer cell conditioned medium collection and preparation

Cells were seeded in a 10 cm dish, and after reaching 70-80% confluency cells were washed once with 1X PBS, and a new medium containing reduced FBS (2.5%) was added. Cells were left growing for 48 h, conditioned medium was collected, filtered using a 0.45 µm syringe filter, and stored at -20°C for a maximum of 2 weeks before using for the experiment. When the cells needed to be stimulated, 10 ng/ml of TNF-α was added 24 hours before the collection of the conditioned medium.

2.22 Patient databases

Done in collaboration with profs. Silvio Bicciato and Mattia Forcato (University of Modena-Reggio Emilia, Italy): from TCGA: gene expression data (raw counts) and clinical information of 1102 primary tumors and 112 paired normal tissues from the breast cancer TCGA dataset (TCGA BRCA) were downloaded from the Genomic Data Commons Portal using functions of the TCGAbiolinks R package (version 2.22.4). Raw counts were normalized and gene expression levels were quantified as counts per million (cpm) using functions of the edgeR R package (version 3.36.0). The set of genes regulated

by NF-kB in response to TNF (TNFA_SIGNALING_VIA_NFKB) and defining inflammatory response (INFLAMMATORY_RESPONSE) have been downloaded from the Hallmark collection of the Molecular Signatures Database (MSigDB v2022.1.Hs; http://www.gsea-msigdb.org/gsea/msigdb/human/genesets.jsp?collection=H). Expression levels of genes and gene sets in paired primary tumors and normal tissues and in the molecular subtypes of primary tumors have been compared using the parametric test of the *ggwithinstats* and *ggbetweenstats* functions of the *ggstatsplot* R package (version 0.10.0), respectively. To identify two groups of tumors with either high or low levels of genes regulated by NF-κB in response to TNF and of genes defining inflammatory response, we used the classifier described by Adorno and colleagues[241], which is a classification rule based on gene expression signature scores. Briefly, the signature scores have been obtained summarizing the standardized expression levels of TNFA_SIGNALING_VIA_NFKB and INFLAMMATORY_RESPONSE genes into a combined score with zero mean. Tumors were classified as the signature 'Low' if the combined score was smaller than the median signature score and as the signature 'High' vice versa. This classification was applied to the expression values of the TCGA BRCA primary tumors with survival information (n=1100).

Additionally, data from cancer patients were obtained from available online tools; specifically, to determine the correlation between ETV7 expression levels and prognosis in breast cancer patients we used Kaplan-Meier plotter (http://kmplot.com/analysis/, [242]).

2.23 Soft agar

Firstly, the wells of 6-well plates were covered with 1 ml of base agar layer (0.7% agarose in RPMI complete medium + 20% FBS). After the solidification of the base, a single cell suspension containing $1x10^4$ 4T1 cells/well was rapidly mixed with the soft agar solution (0.35% agarose in completed RPMI medium) and put on the top of the base layer. Allow 10-20 min to completely solidify. Then, 1 ml of medium was added to each well. The plate was incubated at 37°C in a humified incubator for 3 weeks, changing the medium twice per week. The images were acquired and analysed using IMAGEXPRESS MD Micro Confocal High-Content Imaging System at the CIBIO High-throughput screening facility.

2.24 Enzyme-Linked ImmunoSorbent Assay (ELISA)

ELISA assays were performed using AuthentiKineTM kits (Proteintech®, D.B.A. Italia) for TNF-α, IL-8, and IL-6. Briefly, 100 µl of cell supernatant or standard solutions were added to wells and the plate was incubated for 2 hours at 37°C. After the incubation, wells were thoroughly washed 4 times with wash buffer. Afterward, 100 µl of the diluent antibody solution (1:100 for IL-

6 and IL-8, and 1:75 for TNF-α) was added to each well and the plate was incubated for 1 hour, at 37°C. The cycle of washes was performed again. Then, 100 µl of diluent HRP solution (1:100) was added to each well and the plate was incubated for 40 min at 37°C. The cycle of washes was performed. Afterward, 100 µl of TMB solution were added to each well and the plate was incubated for 20 min at 37°C protected from the light. The reaction was stopped by adding 100 µl of stop solution. The absorbance was measured immediately at 450 nm and 630 nm, using the Varioskan LUX multimode microplate reader (ThermoFisher Scientific).

2.25 Animal model

Female BALB/c mice (n=10; 4 weeks old), acquired from Institute of Biochemistry, Life Science Center, Vilnius University, Lithuania (Vet. Approval No. LT 59–13-001, LT 60–13-001, LT 61–13-004) were randomly assigned to each group (n=5). Animals were supervised daily and maintained under standard controlled conditions: humidity 55 ± 3%, temperature 22 ± 1°C, and a 12 h light/12 h dark cycle. For subcutaneous implantation, female BALB/c mice were inoculated with 60 µl of cell suspension ($1.2x10^5$ cells) under short anesthesia by continuous inhalation of 2% isoflurane gas for 5-10 min. The skin was tented up and the 4T1-pAIP-Empty or 4T1-pAIP-ETV7 cells were injected under the skin in the neck region. Tumor length (L) and width (W) were measured every day using calipers, and tumor volume (V) was calculated as [$V=(LxW^2)/2$]. No animals were deceased before the experiment endpoint. Animals were euthanized with a flow of 8.0 L/min of medical CO2 gas, followed by cervical dislocation.

2.26 Immunofluorescent staining of frozen tissue (IF-F)

Following the dissection, the tumor was washed with 1X PBS, embedded in an OCT cryostat sectioning medium, and immediately snap-frozen by liquid nitrogen. Samples were stored at -80°C until sectioning. Using cryostat, embedded tissues were cut into 4 µm thick sections. Then, samples were fixed with cold 4% PFA solution for 10 min. Washed twice with PBS. Then sections were washed twice with 1% goat serum in PBS-T (PBS with 0.4% Triton X-100) for 10 min. Non-specific binding was blocked by incubating sections with 5% fetal bovine serum in PBS-T for 30 min. After blocking, primary antibodies (VIM (RV202, 550513, BD Biosciences), α-SMA (1A4, MA1-06110, Thermo Fischer Scientific), CD44 (OX-49, MA5-17519, Thermo Fischer Scientific), Ki67 (NB110-89717SS, NovusBio) were diluted in 1% goat serum PBS-T and incubated at room temperature for 2 hours. Following the incubation with primary antibodies, sections were washed twice with 1% fetal bovine serum PBS-T for 10 min. Then slides were incubated with secondary Alexa Fluor™ 488 (A-11001, Thermo Fischer Scientific) antibody at room temperature for 1 hour, protected from the light. After incubation,

sections were washed twice with 1% fetal bovine serum PBS-T for 10 min. Nuclei were counterstained using DAPI (1:2000). Afterwards, slides were washed once with 1X PBS for 5 min. Excess wash was tapped off, one drop of Mowiol® 4-88 (Sigma-Aldrich) was applied to the slide, and a coverslip was placed on the tissue sections. Slides were examined under a fluorescent microscope. The acquired data were analysed using ImageJ software (National Institutes of Health, Bethesda, MD, USA).

2.27 Haematoxylin and eosin staining

The tissue sections were stained with the hematoxylin and eosin (H&E) fast staining kit (Carl Roth, Karlsruhe, Germany). Briefly, tumor sections were cut as described the previous section and fixed with methanol for 10 min. Then, slices were incubated for 6 min with Solution 1, washed for 10 s under tap water, then incubated for 10 s with 0.1% hydrochloric acid, and then washed again under tap water for 6 min. After the washing, tissue sections were incubated with Solution 2 for 30 seconds and rinsed with tap water for 30 seconds. Excess wash was tapped off and sections were sealed with Mowiol® 4-88 (Sigma-Aldrich) and coverslip and observed using bright-field at a Nikon SMZ18 microscope (Nikon, Tokyo, Japan).

2.28 Statistical analysis

If not indicated otherwise, statistical analyses were performed using GraphPad Prism version 9 software. For determining the statistical significance among two classes of samples, the unpaired t-test was used. Graphic illustrations were generated using the Affinity designer tool (Serif, West Bridgford, UK).

3. RESULTS

3.1 ETV7 stimulates the development of the resistance to 5-FU by modulating breast cancer stem cell-like plasticity.

Firstly, we analysed the endogenous levels of ETV7 among a panel of breast cancer cell lines, including luminal, HER2-enriched and basal-like breast cancer cell lines, summarized in Table 3.

Cell line	Tumor subtype	ER	PR	HER2	p53 status
BT-549	basal-like	-	-	-	mutated
HCC70	basal-like	-	-	-	mutated
MCF7	luminal A	+	+	-	wild-type
MDA-MB-231	basal-like	-	-	-	mutated
SK-BR-3	HER2-positive	-	-	+	mutated
T47D	luminal A	+	+	-	mutated
ZR-75-1	luminal A/luminal B/HER2$^+$	+	+/-	+/-	wild-type

Table 3. Characteristics of breast cancer cell lines used in this PhD thesis[41,235,243,244]**.** This table summarizes breast cancer cell lines, used in this thesis, according to the tumor subtype, the expression of estrogen receptor (ER), progesterone receptor (PR), human epidermal growth factor receptor 2 (HER2) and p53-status (according to TP53 database, p53.fr).

With few exceptions, we observed that the levels of ETV7 in luminal cell lines (MCF7 and T47D) were lower than in triple-negative or HER2+-derived cell lines (HCC70, BT-549 and SKBR3), suggesting a correlation between the expression of ETV7 and the aggressiveness of the tumor, which corresponds with the data from the patients and analysis of [8] (Fig.13). Higher levels of ETV7 in ZR-75-1 cells could be explained by the fact, that this cell line is still a bit controversial, as different studies demonstrated contrasting results regarding the expression of progesterone receptor and epithelial growth factor receptor 2, hence the classification of ZR-75-1 cell line in different studies varies from Luminal A/B to HER2$^+$subtype[45,235,243]. In this experiment, we could not appreciate higher levels of ETV7 in MDA-MB-231 cells, which are classified as basal-like. However, this could be due to the fact, that the basal-like subtype is very heterogenous, and it is possible that high levels of ETV7 are not present in all breast cancer cell lines belonging to this subtype. This hypothesis is also supported by patient data (data not shown), as some ETV7-related effects could be observed not in the whole cohort, but in a specific subpopulation of the patients. The analysis of ETV7 protein levels in different breast cancer-derived cell lines was also important for choosing the cellular systems for further experiments. To better appreciate the pro-tumorigenic potential of ETV7, for the overexpression experiment, we chose two luminal

breast cancer cells – MCF7 and T47D – which showed the lowest levels of ETV7. Furthermore, to confirm the importance of ETV7 in breast cancer patients and thus to give more translational value to this project, we analysed the differential expression of ETV7 in breast cancer patients, using TCGA (The Cancer Genome Atlas) gene expression database and we observed higher expression of ETV7 in breast cancer patient compared to healthy tissues, confirming previously the published data with private cohorts[8].

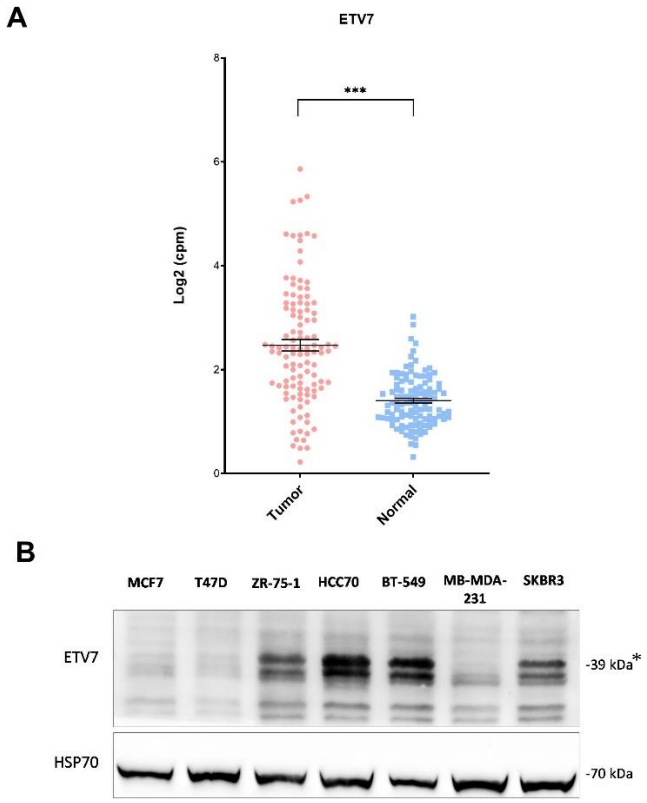

Figure 13. ETV7 expression is higher in more aggressive breast cancer cells. A) A dot plot showing the differential expression analysis for the ETV7 gene in a breast cancer matched patients' dataset from TCGA (The Cancer Genome Atlas) database. Tumor (light red), normal (light blue). *** $p \leq 0.001$. B) Western blot analysis of the different expression of ETV7 among various breast cancer-derived cell lines. On the right of each blot is indicated the approximate observed molecular weight. *The antibody againts ETV7 recognizes several ETV7 isoforms, hence multiple bands are detected in Western blot.

3.1.1 Increased ETV7 expression decreases the sensitivity of breast cancer cells to 5-FU

It has been previously demonstrated that the expression of ETV7 is induced upon the treatment with DNA-damaging drugs and this ETV7 over-expression in breast cancer cell lines reduces the sensitivity to Doxorubicin[9], thus, we decided to test if the increased ETV7 expression could also affect the cytotoxicity of other chemotherapeutic drugs. We first evaluated the sensitivity of cells to 5-Fluorouracil (5-FU), a commonly used breast cancer chemotherapeutic drug, which is also known to induce the expression of ETV7 in breast cancer cells[9,103]. Firstly, to understand if higher levels of ETV7 lead to the development of resistance to 5-FU, we treated MCF7 and T47D cells lines stably overexpressing ETV7 or Empty vector with different concentrations of 5-fluorouracil and then evaluated the viability of cells by performing CellTiter Glo assay. The analysis showed that cells with high levels of ETV7 (Fig. 14 A and C) had a significantly increased viability upon the treatment with 5-FU (Laura Pezzè data) (Fig.14 B and D).

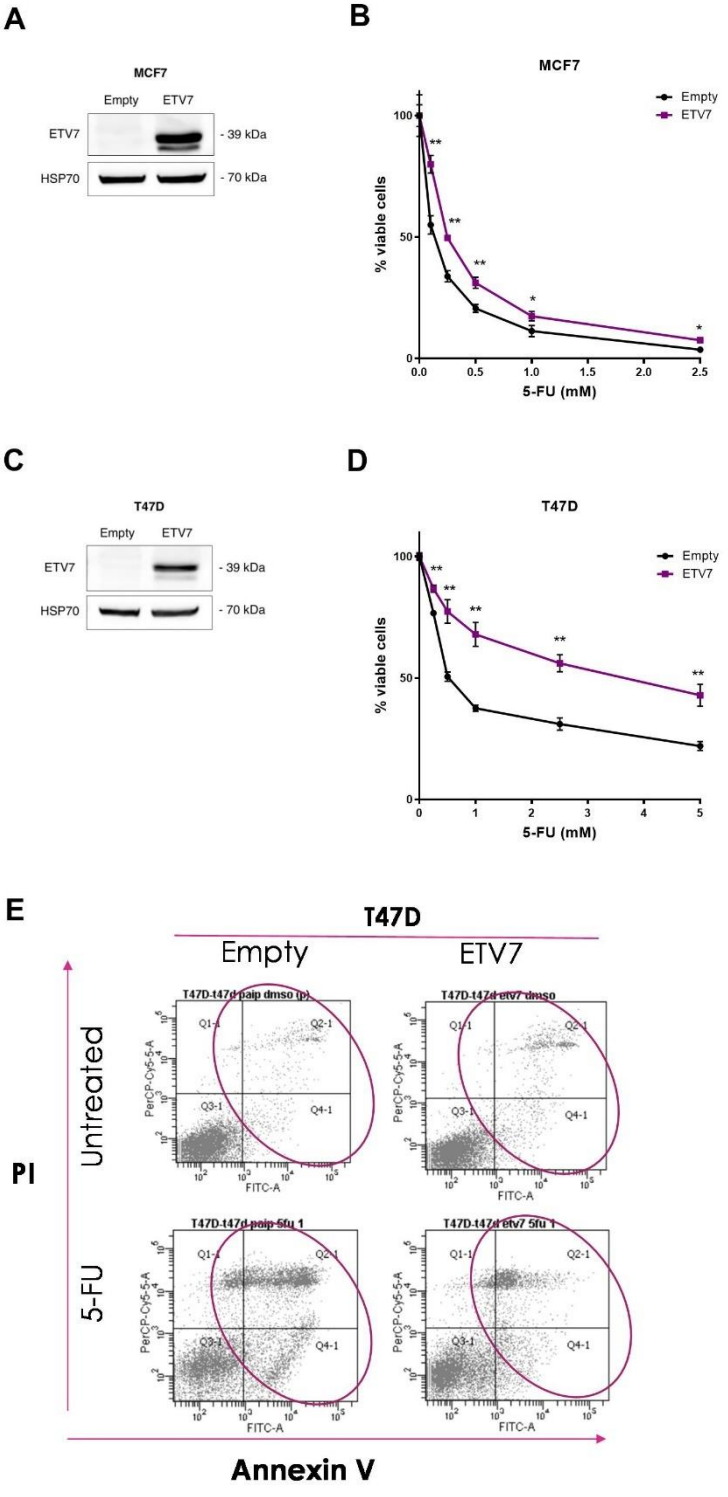
A
MCF7
Empty
ETV7
ETV7
- 39 kDa
HSP70
- 70 kDa
B
MCF7
Empty
ETV7
% viable cells
5-FU (mM)
C
T47D
Empty
ETV7
ETV7
- 39 kDa
HSP70
- 70 kDa
D
T47D
Empty
ETV7
% viable cells
5-FU (mM)
E
T47D
Empty
ETV7
Untreated
5-FU
PI
Annexin V
FITC-A
PerCP-Cy5-5-A

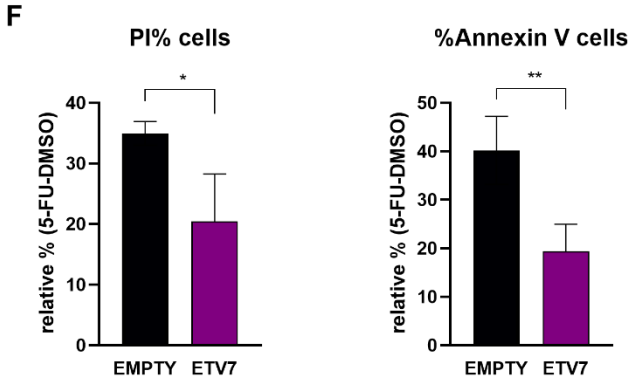

Figure 14. **The overexpression of ETV7 modulates the sensitivity to 5-FU treatment in MCF7 and T47D breast cancer cells.** A and C) Western blot analysis of ETV7, to confirm its overexpression in MCF7 (A) and T47D (C) cells. HSP70 was used as a loading control. B and D) Cell Titer Glo survival assay upon the treatment with 5-FU in MCF7 (B) and T47D (D) cells overexpressing ETV7 or harboring Empty vector. DMSO treated group was used as a control for data normalization (Laura Pezzè data). E) A representative dot-plot of the flow cytometry analysis performed on T47D Empty and T47D ETV7 cells treated with 5-FU 1 mM for 72 hours. Magenta circles indicates cells which were considered apoptotic. F) Relative percentage of PI-positive cells (on the left) or Annexin V positive cells (on the right) calculated as a difference of 5-FU treated cells and DMSO treated cells measured by Annexin V-FITC/PI staining of T47D Empty and T47D ETV7 cells treated with 5-FU 1 mM for 72 hours. *p-value < 0.05; **p-value < 0.01.

To further confirm the increased resistance of ETV7 overexpressing cells, we analysed cell death upon the treatment with 5-FU by staining treated and untreated cells with Annexin V-FITC/PI and performing flow cytometry analysis. We observed that the rate of cell death and apoptosis was decreased in T47D cells overexpressing ETV7 compared to empty control, meaning that higher levels of ETV7 can reduce the sensitivity of breast cancer cells to 5-FU treatment (Fig.14 E-F).

As cell monolayers lack some features important for drug resistance, e.g. drug penetration, we chose to test if ETV7-mediated resistance is also observed in a 3D environment[245]. Spheroids are simple models, resembling tumor architecture, hence we decided to use spheroids to further validate ETV7-mediated resistance to 5-FU[246]. Firstly, we formed spheroids using T47D Empty and T47D EVT7 cells and after 3 days, when the spheroids were formed, we treated them with different concentrations of 5-FU and observed the changes in the spheroid's size. We determined that the size of the spheroids, formed from cells overexpressing ETV7, was less affected by the treatment with 5-FU, confirming that ETV7 could increase the resistance to 5-FU treatment also in a 3D environment. (Fig. 15).

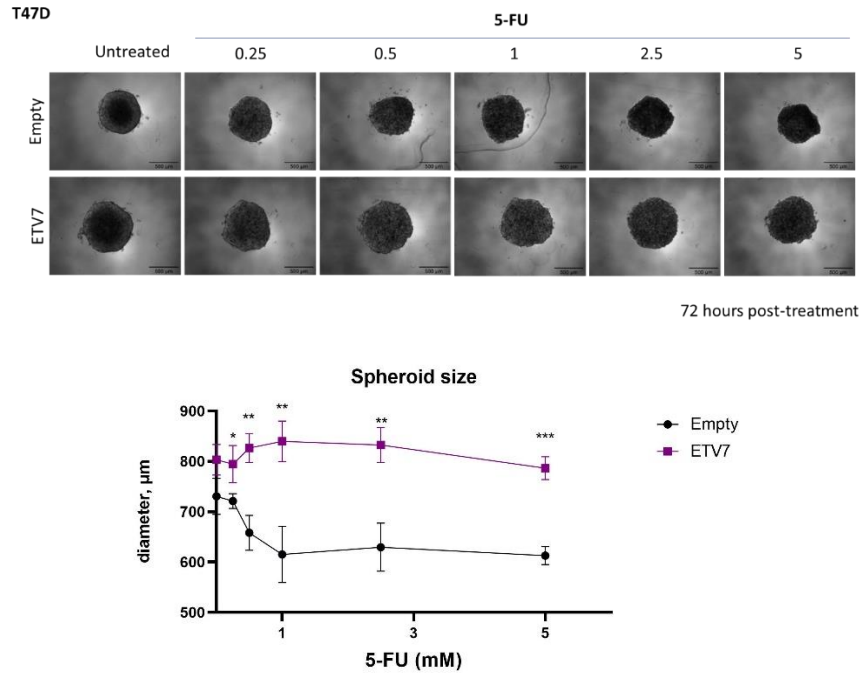

Figure 15. Overexpression of ETV7 modulates sensitivity to 5-FU treatment in T47D cell line-derived spheroids. Representative image of spheroids formed from T47D Empty and T47D ETV7 cells and treated with 5-FU 72 hours post-treatment. Below, the quantification of spheroid size (n=30) upon the treatment with 5-FU in T47D overexpressing ETV7 or empty control. *p-value < 0.05; **p-value < 0.01; *** p-value.

Moreover, to verify if the knock-down of ETV7 could increase the sensibility of breast cancer cells to the treatment with 5-FU, we silenced ETV7, using two ETV7 targeting siRNAs. The efficiency of knock-down was validated using Western blot (Fig. 16 B and C). After the silencing, we treated cells with 0.25 mM and 0.5 mM 5-FU for 72 hours and then analized cell viability by performing a CellTiter Glo assay. We demonstrated that upon ETV7 knock-down, the sensitivity to the treatment with 5-FU significantly increased in T47D and MDA-MB-231 (Fig.14A). Slightly less evident sensitization was observed also in the SK-BR-3 cell line (Suppl.Fig.1A). Interestingly, we observed slightly reduced viability of T47D and MDA-MB-231 upon the silencing of ETV7, even before the treatment with 5-FU, which could suggest that knocking down of ETV7 could affect the viability of breast cancer cells (further explained in chapter 3.4).

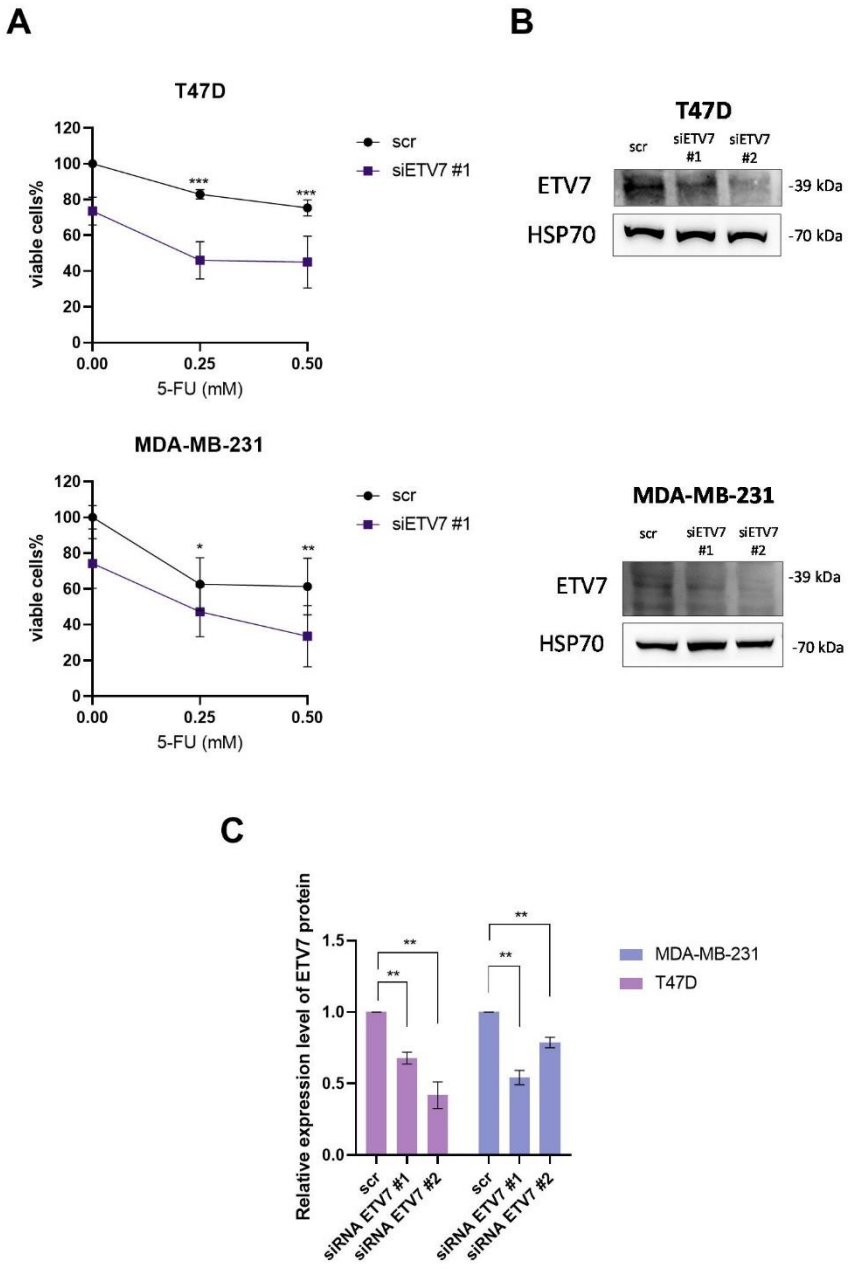

Figure 16. Knock-down of ETV7 sensitizes T47D to 5-FU treatment. A) Cell Titer Glo assay for survival analysis upon treatment with 5-FU in T47D and MDA-MB-231 cells transfected with siETV7 #1 or the scrambled control. Bars represent the averages and standard deviations of at least three independent experiments. *** $p \leq 0.001$; ** $p \leq 0.01$; * $p \leq 0.05$. B) Western blot analysis of ETV7 levels in T47D and MDA-MB-231 cells transfected with siRNA #1 and siRNA # 2 against ETV7 or the

relative scrambled control for 72 h. HSP70 was used as a loading control. C) Quantification of Western blot analysis of ETV7in T47D and MDA-MB-231 cells silenced with siETV7 #1 and siETV7 #2. Bars represent the averages and standard deviations of at least three biological replicates. Data is normalized to the signal of HSP70, which was used as a loading control; ** $p \leq 0.01$.

It has been previously demonstrated that ETV7-induced resistance to Doxorubicin involved drug efflux mediated by the ABC transporter ABCB1[9]. To understand if high levels of ABC transporters also played a role in the ETV7-mediated resistance to 5-FU in breast cancer cells, we used Elacridar, a dual inhibitor able to block ABCB1 and ABCG2. We treated cells with 5-FU alone or in combination with Elacridar and validated cell viability. The viability assay showed an increased sensitivity of MCF7 ETV7 cells to 5-FU when combined with Elacridar (Fig. 17).

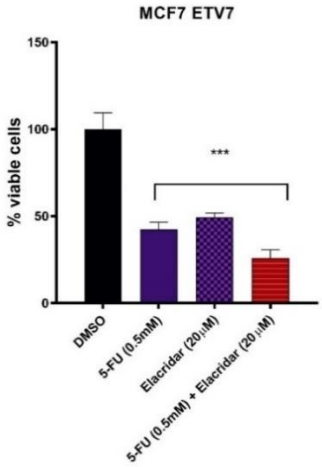

Figure 17. Inhibition of ABC transponders sensitizes MCF7 cells to 5-FU treatment. Cell Titer Glo assays for survival analysis upon treatment with 5-FU alone or in combination with ABC transporter inhibitor (Elacridar). *** $p \leq 0.001$

Moreover, we also observed that ETV7-overexpressing cells had elevated levels of two anti-apoptotic proteins – BCL-2 and Survivin (Fig. 18), which could explain the decreased percentage of apoptotic cells in flow cytometry analysis upon the treatment with 5-FU. Based on these results, we pre-treated ETV7 overexpressing cells with Navitoclax, a potent BCL-2 inhibitor, and then treated them with 5-FU. This combination of drugs led to a slight sensitization of MCF7 cells over-expressing ETV7 (Fig. 18). The same effect could not be observed in T47D cells where neither BCL-2 nor Survivin (already high at the baseline) was influenced by the over-expression of ETV7 (Supplementary Fig.1B).

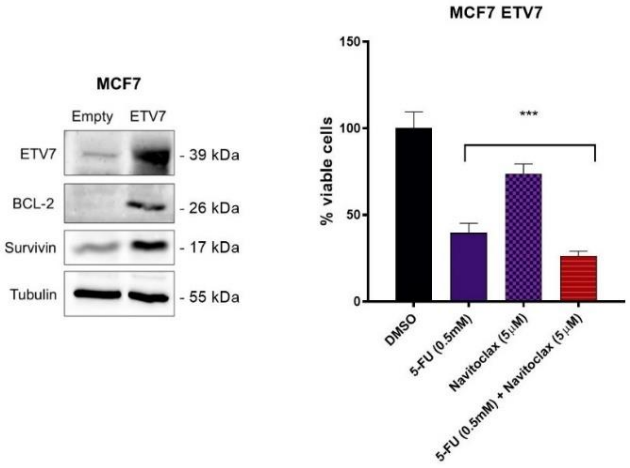

Figure 18. Inhibition of BCL-2 sensitizes MCF7 ETV7 cells to the treatment with 5-FU. On the left, Western blot analysis of BCL-2 and Survivin proteins in MCF7 Empty and MCF7 ETV7 cells. On the right, Cell Titer Glo assays for survival analysis upon treatment with 5-FU alone or in combination with a BCL-2 inhibitor (Navitoclax) (I) in MCF7 ETV7 cells. *** $p \leq 0.001$.

3.1.2 ETV7 affects breast cancer stem cell-like plasticity

Given the observed increased resistance to 5-FU, which is complemented by an increase in ABC transporter expression and higher anti-apoptotic protein levels, as well as, considering the data from the literature reporting the involvement of ETV7 in cell differentiation [221], we hypothesized that ETV7 might regulate the breast cancer stem-like cell plasticity. To test this hypothesis, we first analysed some of the most commonly accepted markers for breast cancer stem cells, including CD44 and CD24 expression and EpCAM. Firstly, using flow cytometry we measured the percentage of $CD44^+$ and $CD24^-$ cells, which represent the breast cancer stem cell population. In basal conditions, both MCF7 and T47D had a very low percentage of cancer stem cells, however, upon the overexpression of ETV7 there was a remarkable increase in $CD44^+/CD24^-$ cell population (Fig. 19 A-B and C-D). Importantly, the over-expression of ETV7 could stimulate both the increase in CD44 levels and the decrease in CD24 levels on the plasma membrane of the cells. Furthermore, we wanted to understand if ETV7 affects the expression of CD44 and CD24 at the transcriptional level, hence we performed RT-qPCR and observed that among the CD44 and CD24, only CD24 expression was regulated by ETV7 at the transcript level in both cell lines (Fig. 19 E and F).

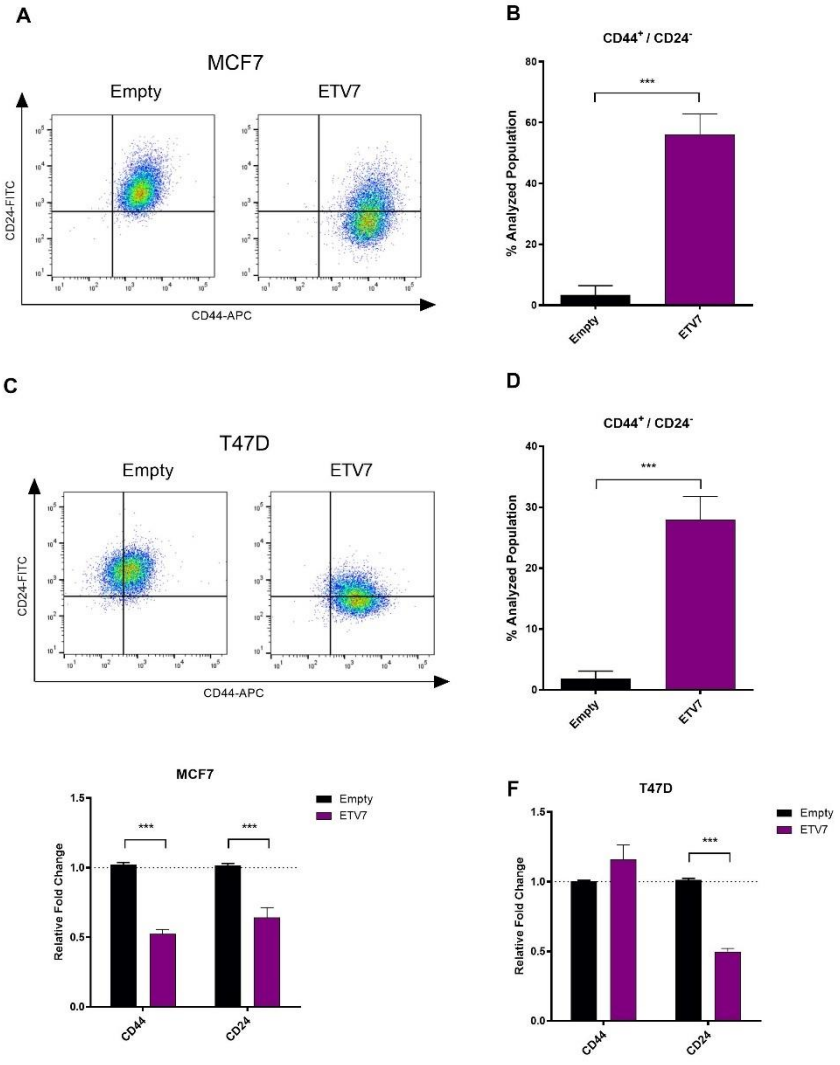

Figure 19. The over-expression of ETV7 regulates the expression of breast cancer stem cell markers. A) and C) CD44-APC and CD24-FITC staining and flow cytometry analysis in MCF7 (A) and T47D (C) Empty and ETV7 cells - a representative dot-plot of the results obtained at FACS Canto A. B and D) Quantification of the percentage of CD44+/CD24- cells in MCF7 (B) and T47D (D) Empty and ETV7 over-expressing cells. E) and F) RT-qPCR analysis of CD44 and CD24 expression in MCF7 Empty and MCF7 ETV7 (E) and T47D Empty and T47D ETV7 (F) cells. *** = p-value < 0.001.

To verify whether modulating the expression of ETV7 in the opposite direction could also affect the population of $CD44^{+}/CD24^{-}$ cells, using CRISPR/Cas9 technology, we knocked out ETV7 in SK-BR-3 cells. We chose this particular cell line because it expresses high levels of ETV7 and is characterized by a high percentage of $CD44^{+}/CD24^{-}$ cells. Notably, in a clone

of SK-BR-3 cells knocked-out for ETV7 we were able to observe a strong increase in CD24 expression, with a consequent reduction in the $CD44^{+}/CD24^{-}$ population, confirming the role of ETV7 in the modulation of cancer stem cell population (Fig. 20).

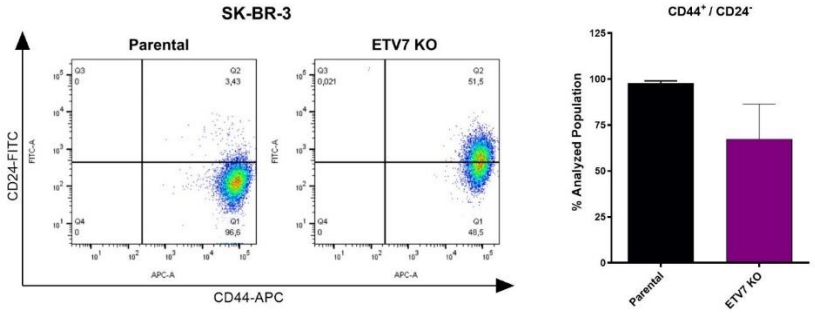

Figure 20. The knock-out of ETV7 reduces the breast cancer stem cell population in SK-BR-3 cells. CD44-APC and CD24-FITC staining and flow cytometry analysis in SK-BR-3 parental and ETV7 knock-out cells. On the right the histogram summarizing the percentage of CD44+/CD24- in parental and ETV7 knock-out cells; on the left, a representative dot plot of the results obtained at FACS Canto A.

Furthermore, to confirm our findings, we analysed the expression of a an established additional marker for breast cancer stemness, the adhesion molecule EpCAM. Noteworthy, we could appreciate a strong increase in EpCAM protein expression in ETV7 over-expressing cells (Fig. 21).

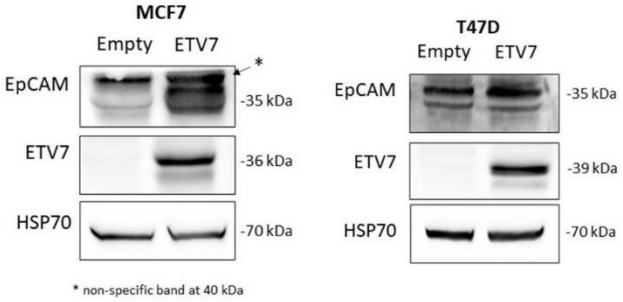

Figure 21. The overexpression of ETV7 increases the expression of EpCAM protein (BCSC marker) in MCF7 and T47D cells. Western blot analysis of EpCAM expression in MCF7 and T47D Empty and ETV7-overexpressing cells. The correct band is indicated with an arrow. HSP70 was used as a loading control. On the right of each blot is indicated the approximate observed molecular weight.

To confirm that cells overexpressing ETV7 had not only upregulated stemness marker but also acquired features related to cancer stem cells, such as self-renewal or ability to form spheres, we performed a mammosphere

formation assay. This assay consists of growing cells in non-differentiating and non-adherent conditions and evaluating their potential to form spheres.

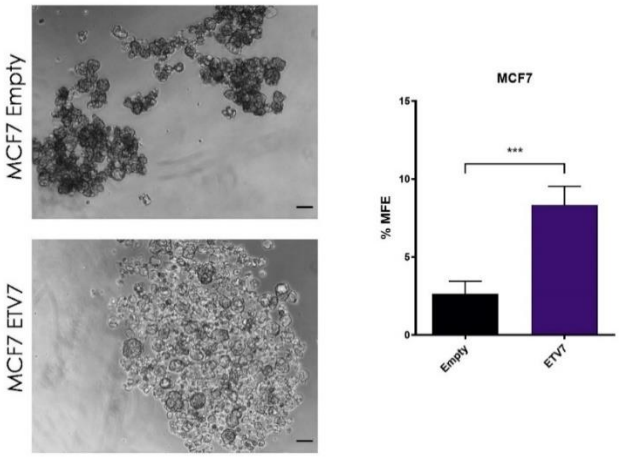

Figure 22. ETV7 promotes the mammosphere formation potential in MCF7 cells. On the left, an image representing the first generation of mammospheres formed by MCF7 Empty and MCF7 ETV7 cells. On the right, the quantification of mammosphere formation efficiency (MFE) in MCF7 Empty and MCF7 ETV7 cells. The percentage of mammosphere formation efficiency (%MFE) in MCF7 Empty and ETV7 calculated as number of mammospheres per well/number of cells seeded per well X 100.***p ≤0.001.

We measured the mammosphere formation efficiency (MFE) in MCF7 overexpressing ETV7 or harboring empty vector and we were able to observe a significant increase in mammosphere formation efficiency in MCF7 ETV7 cells with respect to control, demonstrating that ETV7 can modulate breast cancer cell plasticity and push them to be more stem-like (Fig. 22).

3.1.3 ETV7 represses interferon-stimulated genes (ISGs)

To identify the molecular mediators of the biological effects caused by the over-expression of ETV7, previously in our laboratory a transcriptome analysis on MCF7 and T47D cells over-expressing ETV7 or the relative empty plasmid by RNA-seq was performed. Gene set enrichment analysis (GSEA) highlighted “Interferon_alpha_response” and “Interferon_gamma_response”, as genes involved in the cellular response to type I or type II Interferons, respectively, as the only common significantly repressed gene sets enriched in both cellular systems over-expressing ETV7. Firstly, we analyzed a set of ISGs and we were able to demonstrate that the overexpression of ETV7 represses these genes (Laura Pezzè data) (Fig. 23).

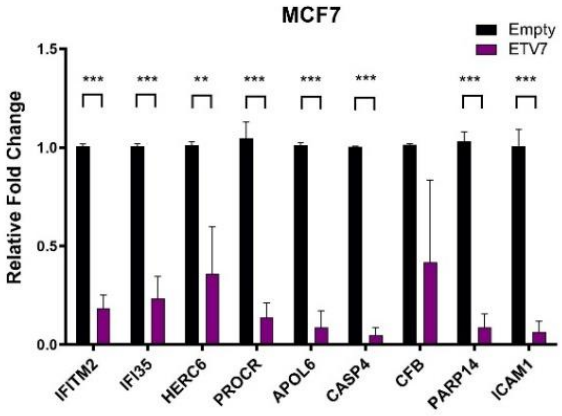

Figure 23. The over-expression of ETV7 downregulates a signature of IFN-response genes. RT-qPCR experiments analysing the expression of a set of IFN-response genes in MCF7 Empty and ETV7 cells. ** = p-value < 0.01; *** = p-value < 0.001. (Laura Pezzè data)

Furthermore, we wanted to demonstrate that this repression is specifically related to ETV7 overexpression and can be bi-directionally regulated by ETV7. We silenced ETV7 both in MCF7 and T47D parental cells using siRNAs and analysed the expression of some of the studied IFN-responsive genes (i.e., APOL6, IFI35, and IFITM2). Notably, we showed a significant upregulation of the three genes in response to ETV7 knock-down strengthening the role of ETV7 in their regulation at the transcript level in MCF7 cells (Fig. 24). The same analysis was further expanded to other BC cell lines (i.e., MDA-MB-231, SK-BR-3, and HCC-70, BT-549), confirming also in these additional cellular models the role of ETV7 in the negative regulation of interferon signaling (Fig.24).

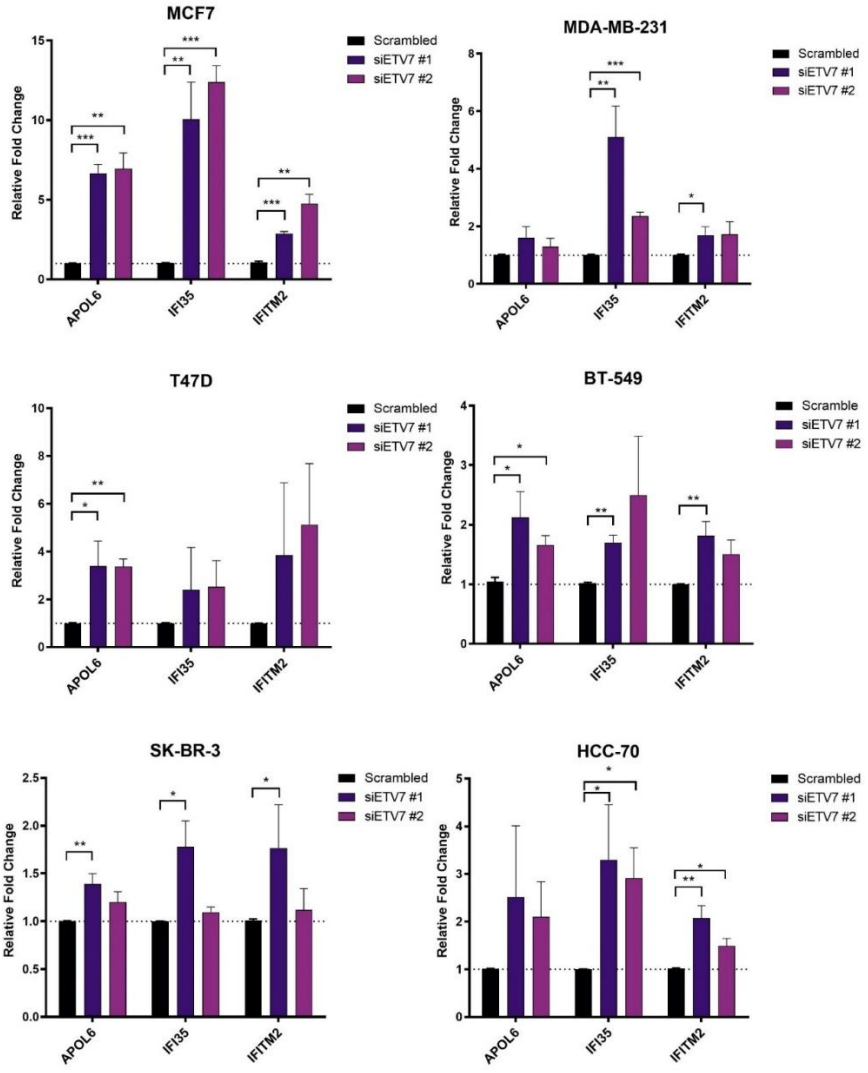

Figure 24. The knock-down of ETV7 rescues the expression of several ISGs in breast cancer-derived cells. RT-qPCR analysis of the expression of a group of IFN-responsive genes in MCF7, MDA-MB-231, BT-549, SKBR3, T47D, HCC70 cells transfected with ETV7 targeting siRNA #1 and siRNA #2 or the scrambled control. **p-value < 0.01; ***p-value < 0.001.

The results presented in this chapter suggest that ETV7 is involved in the development of the resistance to 5-FU by repressing ISGs and by increasing the BCSC population.

3.2 ETV7 reduces inflammatory responses in breast cancer cells by repressing TNFR1/NF-κB axis

3.2.1 ETV7 is involved in inflammatory and immune responses

To unveil some novel ETV7-regulated transcriptional networks, in our previous study[247] transcriptome analyses were performed in two breast cancer-derived cell lines MCF7 and T47D stably overexpressing ETV7 or harboring empty vector. Interestingly, the most significant terms identified by gene ontology analysis of commonly down-regulated DEGs involved innate immune response and inflammatory response. Furthermore, gene set enrichment analysis (GSEA) highlighted "Inflammatory response" (Fig.25A) and "TNFA_signaling_via_NF-κB" (Fig.25B) in MCF7 cells (the same tendency was observed also in T47D cells, however without reaching the statistical significance), confirming the involvement of ETV7 in these processes.

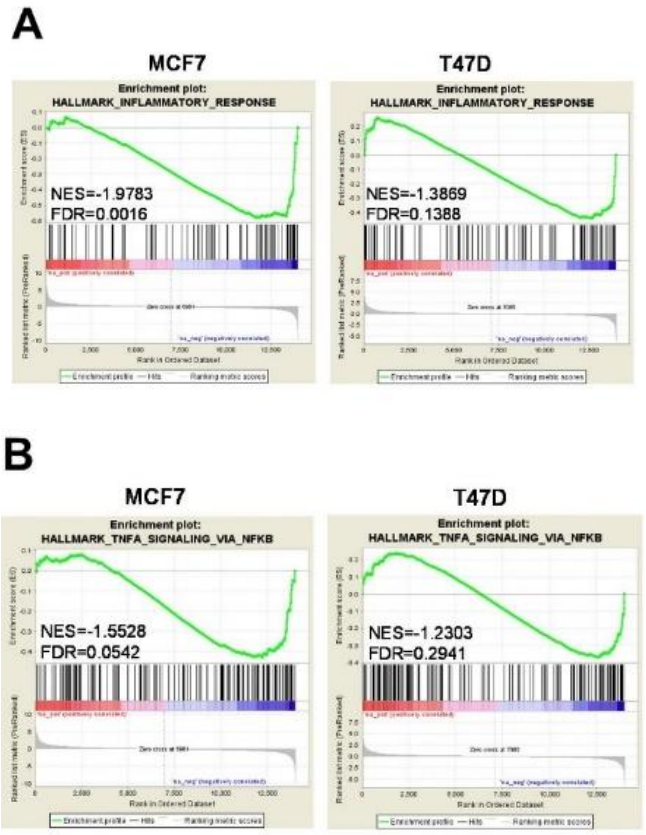

Figure 25. ETV7 modulates the inflammatory and immune responses in breast cancer. A-B) Gene Set Enrichment Analysis of MCF7 and T47D cells over-

expressing ETV7 or its Empty counterpart. Enrichment plot for the inflammatory response in MCF7 and T47D cells (A) and TNFA signaling via NFKB in MCF7 and T47D cells (B) gene sets of the Hallmark Collection. The Normalized Enrichment Score (NES) shows the degree of the enrichment of the gene set; the negative sign indicates that the gene set is down-regulated in cells over-expressing ETV7. FDR = False Discovery Rate.

After performing these analyses, we selected a list of repressed genes, known to be involved in inflammatory response pathways. For further validation *in vitro*, we chose a set of genes with a Fold Change lower than -1.2 in both MCF7 and T47D cell lines. Using RT-qPCR, we demonstrated the downregulation of all selected targets (*TNFRSF1A, IL10RB, IL1R1*, and *TLR-2*) in MCF7 and T47D (Fig.26) cells, with the only exception of *IL1R1*, which was significantly repressed only in MCF7 cells.

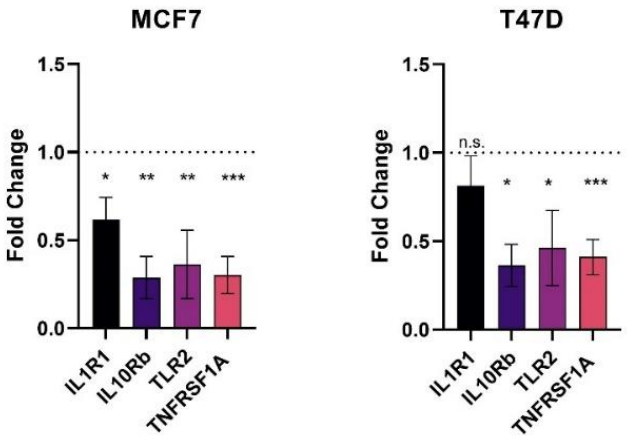

Figure 26. ETV7 represses genes involved in inflammatory and immune responses. RT-qPCR analysis for the validation of genes involved in inflammation and immune response in MCF7 and T47D cells over-expressing ETV7 or Empty vector. Bars represent the averages and standard deviations of at least three biological replicates. Whole panel: * $p \leq 0.05$; ** $p \leq 0.01$; *** $p \leq 0.001$; n.s. – not significant. Dotted line indicates the Empty control, which was used to calculate the relative fold change.

3.2.2 ETV7 represses *TNFRSF1A*

We focused our further studies on the *TNFRSF1A* gene, encoding for the TNFR1 receptor, which is the main receptor for TNF-α signaling. We showed that the expression of *TNFRSF1A* is significantly down-regulated in both MCF7 and T47D cells over-expressing ETV7 (Fig. 27A). Furthermore, we confirmed the down-regulation of *TNFRSF1A* also in SK-BR-3 and MDA-MB-231, two other breast cancer-derived cell lines, upon the transient over-expression of ETV7 (Fig. 27C). To understand if this transcriptional

repression was also detectable at the protein level, we performed Western blot analysis, demonstrating that ETV7 reduced the levels of TNFR1 protein in both MCF7 and T47D cells (Fig. 27B). A slight downregulation of TNFR1 was also detected in MDA-MB-231 cells, instead in SK-BR-3 cells the difference was not observed (Fig. 27D).

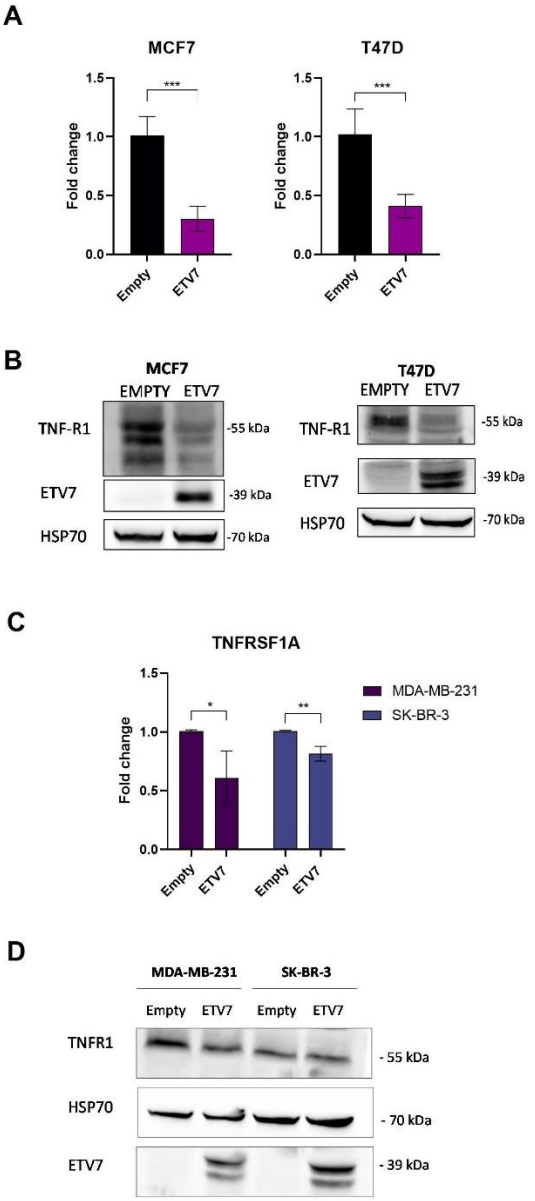

Figure 27. ETV7 downregulates TNFR1 in breast cancer cells A) RT-qPCR analysis of the normalized expression of the TNFRSF1A gene in MCF7 and T47D cells over-expressing ETV7 or harboring its Empty counterpart. Bars demonstrate the averages and standard deviations of at least three biological replicates B) The amount

of TNFR1 in MCF7 and T47D cells over-expressing ETV7 or harbouring its empty counterpart. On the right of each blot is indicated the approximate observed molecular weight. HSP70 was used as a loading control. C) RT-qPCR analysis of the normalized expression of the TNFRSF1A gene in MDA-MB-231 and SK-BR-3 cells transiently over-expressing ETV7 or harboring its Empty counterpart. Bars demonstrate the averages and standard deviations of at least three biological replicates. D) Western blot analysis on ETV7 in SK-BR-3 and MDA-MB-231 cells transiently overexpressing ETV7. On the right side of each blot is indicated the approximate observed molecular weight. HSP70 was used as a loading control. Whole panel: * $p \leq 0.05$; ** $p \leq 0.01$; *** $p \leq 0.001$.

Moreover, to understand if the regulation of *TNFRSF1A* by ETV7 is bi-directional, we knock-down ETV7 in MCF7, T47D, ZR-75-1, and MDA-MB-231 cells, using two ETV7 targeting siRNAs (siRNA#1 and siRNA#2). The level of knock-down of ETV7 was validated by performing Western blot analysis (Fig. 28B). The silencing of ETV7 reverted the repression of *TNFRSF1A* in all analysed cell lines, supporting the role of ETV7 in the regulation of *TNFRSF1A* in different cellular systems (Fig. 28A).

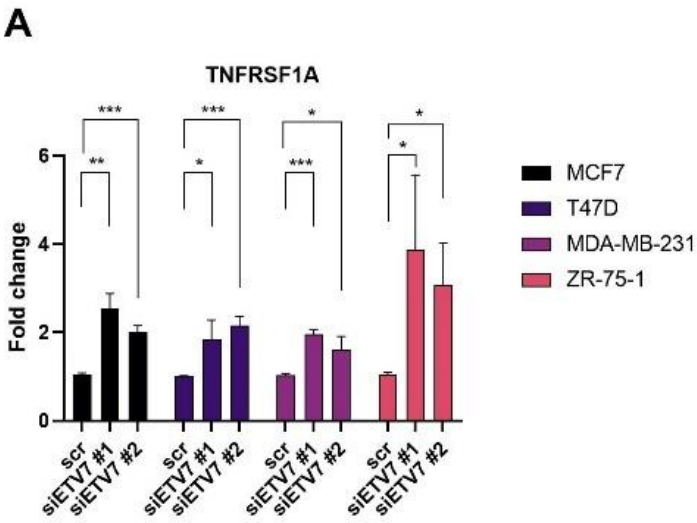

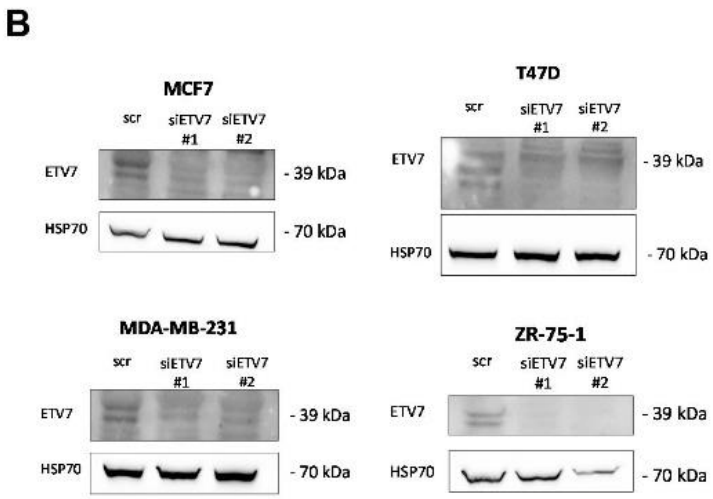

Figure 28. The knock-down of ETV7 rescues the expression of TNFRSF1A. A) RT-qPCR analysis of the normalized expression of the *TNFRSF1A* gene in MCF7, T47D, MDA-MB-231 and ZR-75-1 cells upon the silencing of ETV7, with two targeting siRNAs. Bars demonstrate the averages and standard deviations of at least three biological replicates. Whole panel: * $p \leq 0.05$; ** $p \leq 0.01$; *** $p \leq 0.001$. B) Western blot analysis of ETV7 levels in MCF7, T47D, MDA-MB-231, and ZR-75-1 cells transfected with siRNA #1 and siRNA # 2 against ETV7 or the relative scrambled control for 72 h. HSP70 was used as a loading control.

From previous studies[9,247], it is known that the expression of ETV7 is induced upon the treatment with DNA-damaging drugs. Hence, to verify if the downregulation of *TNFRSF1A* could be also observed upon the modulation of the endogenous levels of ETV7, MCF7, T47D, MDA-MB-231 and SK-BR-3 parental cell lines were treated with DNA-damaging drugs (5-FU and Doxorubicin). After confirming the induction of ETV7 (Fig. 29A-B), we analysed the expression of *TNFRSF1A* in these cell lines. Remarkably, after the treatment with 5-FU and Doxorubicin, we detected a significant downregulation of *TNFRSF1A* in all studied cell lines (Fig. 29B).

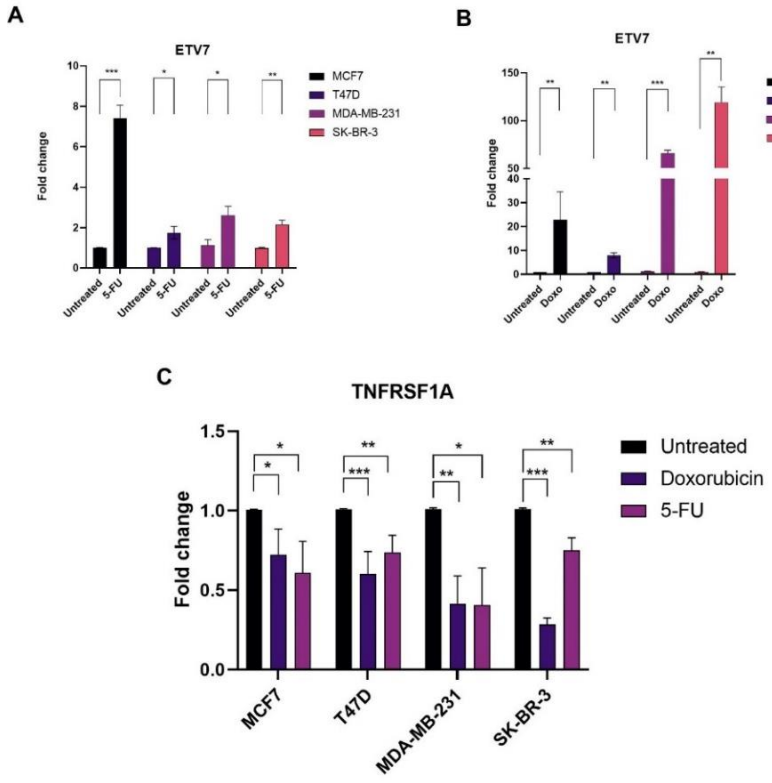

Figure 29. *TNFRSF1A* is repressed upon the induction of ETV7 with DNA-damaging drugs. A-B) RT-qPCR analysis of the normalized expression of ETV7 in MCF7, T47D, MDA-MB-231 and SK-BR-3 cells upon the treatment with 375 mM 5-FU (A) or 1.5µM of Doxorubicin for 24 hours. C) RT-qPCR analysis of the normalized expression of the *TNFRSF1A* gene in MCF7, T47D, MDA-MB-231 and SK-BR-3 cells upon the silencing of ETV7, upon the treatment with 375 mM 5-FU (A) or 1.5µM of Doxorubicin for 24 hours. Whole panel: bars demonstrate the averages and standard deviations of at least three biological replicates. * $p \leq 0.05$; ** $p \leq 0.01$; *** $p \leq 0.001$.

Knowing that the increased expression of ETV7 has been detected in breast cancer patients and correlated with breast cancer aggressiveness[8], we analysed the expression of *TNFRSF1A* in breast cancer patients compared to normal breast tissue. We performed a gene expression analysis using the TCGA database and observed a decrease in the expression of *TNFRSF1A* in breast cancer tumor tissue (BRCA dataset) compared to normal tissue (Fig. 3A). Furthermore, we analysed the expression of *TNFRSF1A* in different molecular breast cancer types and we observed that *TNFRSF1A* was significantly lower in all molecular types of breast cancer (Fig. 30B). Furthermore, to give to our findings even more translational significance, we decided to investigate if the level of *TNFRSF1A* affects the survival of breast cancer patient. We analysed the impact of the *TNFRSF1A* expression in breast cancer patients, using the

Kaplan-Meier plotter tool, and confirmed a significant correlation between lower *TNFRSF1A* levels and poor prognosis of breast cancer patients (Fig. 30C).

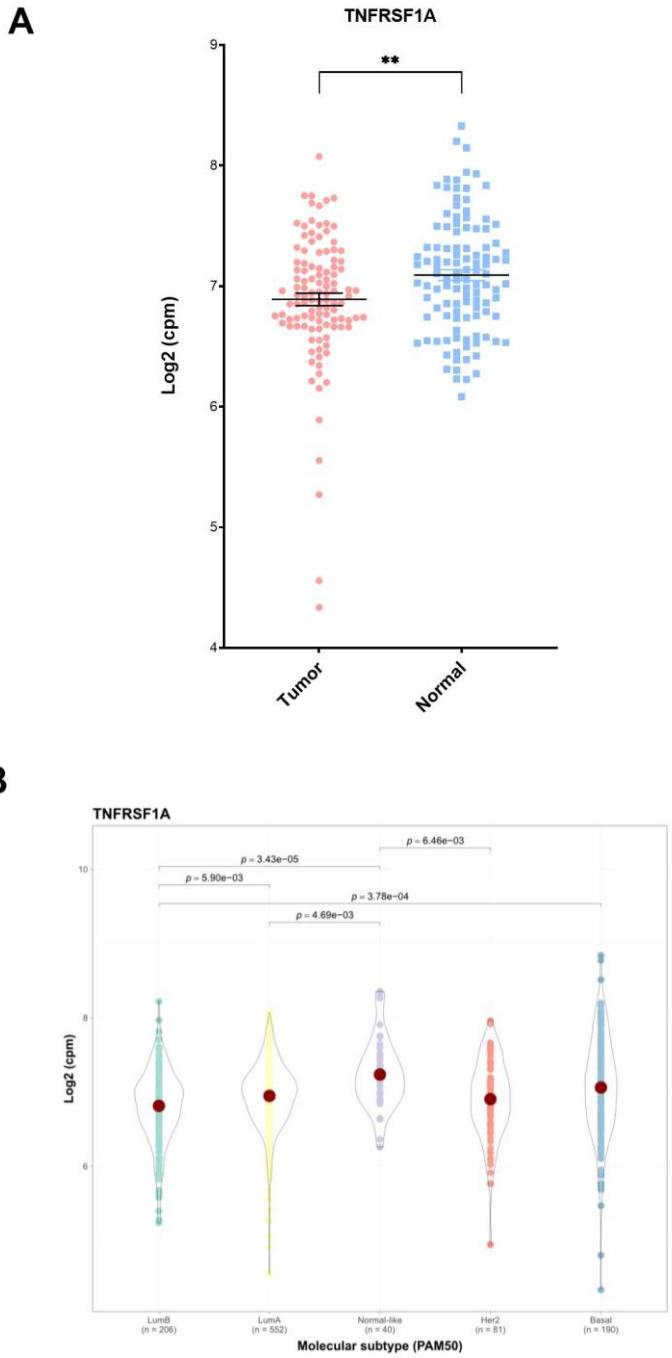

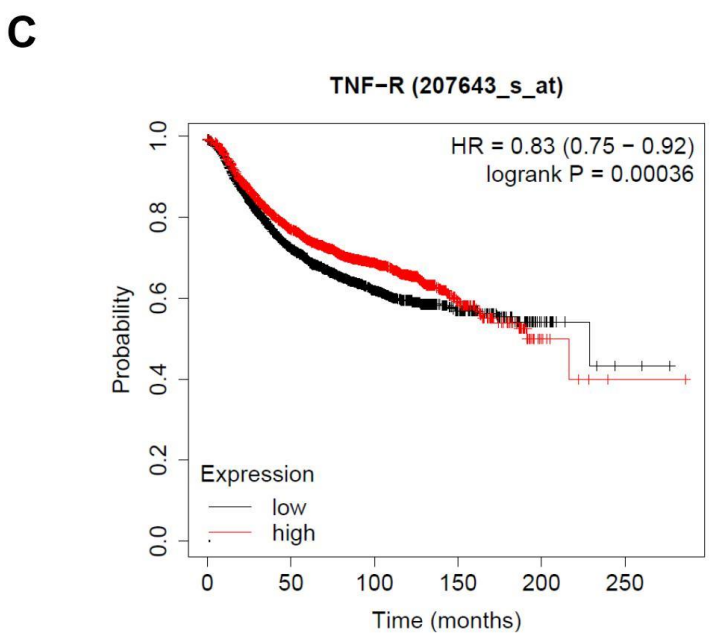

Figure 30. TNFRSF1A is downregulated in breast cancer patients. A) A box plot demonstrating the differential expression analysis for the TNFRSF1A gene in a BRCA patients' dataset from TCGA (The Cancer Genome Atlas) databases. B) The expression of TNFRSF1A in TCGA BRCA samples classified by PAM50 C) Kaplan-Meier curves for RFS from a breast cancer cohort according to the relative expression of TNFRSF1A obtained from KM plotter tool. The number of the patients are shown below the graph. HR (Hazardous Ratio) and the statistical analyses are reported in the right corner of the graph. Whole panel: ** $p \leq 0.01$.

3.2.3 ETV7 directly down-regulates *TNFRSF1A*

ETV7 is a transcriptional repressor, and hence, it was logical to understand whether it could directly regulate the expression of *TNFRSF1*A. Firstly, we analysed the regulatory region of *TNFRSF1A* and searched for putative ETV7 binding sites. Based in ETV7 consensus sequences, in the first intron of *TNFRSF1A*, we detected three potential binding sites for ETV7, containing the GGAA motive (Fig. 31A). To understand if ETV7 can bind these putative binding regions and thus directly repress *TNFRSF1A*, we performed chromatin immunoprecipitation followed by qPCR. We demonstrated the direct binding of ETV7 to the TNFRSF1A intron regions (BS#1 and BS#2) in both MCF7 and T47D cells, hence confirming that ETV7 can directly repress TNFRSF1A (Fig. 31B-C).

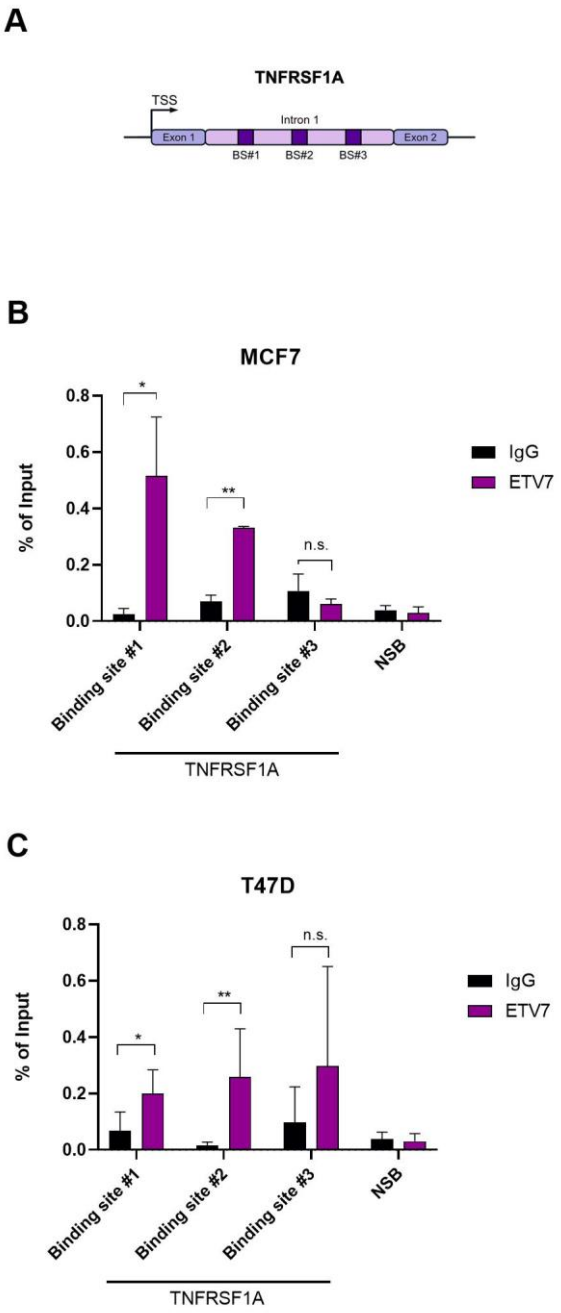

Figure 31. ETV7 directly represses the expression of TNFRSF1A in breast cancer cells. A) A schematic view of the TNFRSF1A Intron 1 and the studied ETV7 binding sites. TNFRSF1A BS#1 is located +5,483bp from the Transcription Start Site (TSS); BS#2 +5,627bp from TSS; BS#3 +6,069bp from TSS. B-C) ChIP-qPCR of TNSFRSF1A Intron 1 in MCF7 (B) or T47D (C) cells over-expressing ETV7. The

percentage of the enrichment of ETV7 or control (normal mouse IgG) bound to TNFRSF1A Intron 1 with respect to input DNA is shown. NSB=non-specific binding, the *ACTB* promoter. Bars represent the averages and standard deviations of at least three biological replicates. * p≤0.05; ** p≤0.01; *** p≤0.001, n.s. – not significant.

Following the confirmation of ETV7 binding to the regulatory region of *TNFRSF1A*, we were interested to understand the mechanistic insights of ETV7-mediated repression. We focused on analysing the activating and repressive histone marks on the first intron of *TNFRSF1A* (previously confirmed binding sites #1 and #2). We performed chromatin immunoprecipitation followed by qPCR in both MCF7 (Fig. 32A) and T47D (Fig. 32B) cells and we showed a decrease in the acetylation of lysine residues on histone H3 (H3K9ac, H3K14ac, H3K18ac, H3K23ac, H3K27ac) and in tri-methylation of lysine 4 on histone 3 (H3K4me3), which are well-known markers of open chromatin. Furthermore, in MCF7 we also observed an increase in the tri-methylation of lysine 9 on histone H3 (H3K9me3), which is a marker of closed chromatin (Fig. 32A). The observed changes in chromatin status confirm that ETV7 can directly repress *TNFRSF1A* by reducing the accessibility of chromatin.

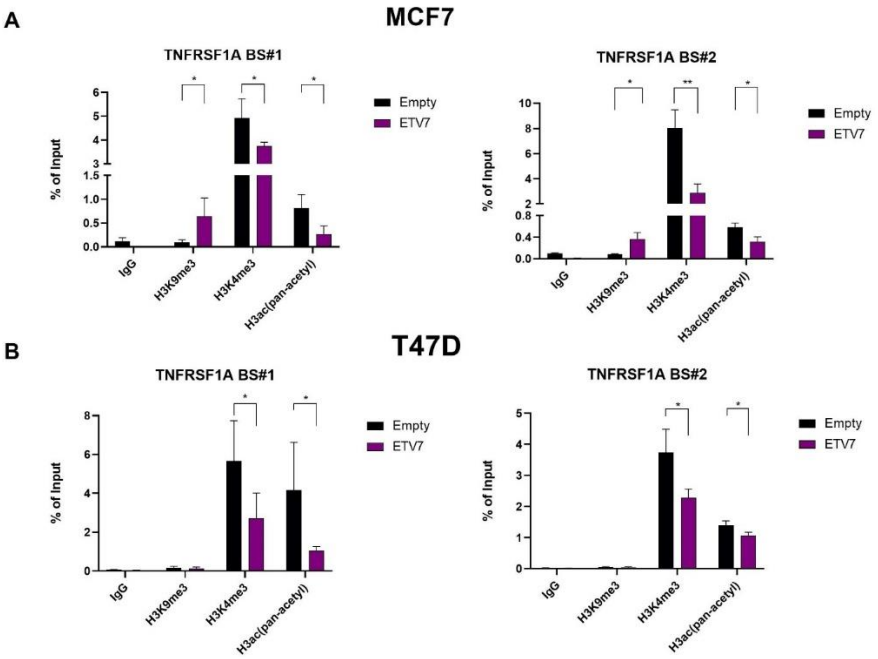

Figure 32. ETV7 represses *TNFRSF1A* by modifying chromatin accessibility. Chip-qPCR assessing H3K9me3, H3K4me3 and H3ac (pan-acetyl) deposition at the TNFRSF1A Intron 1 binding site #1 and binding site #2 in MCF7 (A) and T47D (B) overexpressing ETV7 or harboring empty vector. The percentage of the enrichment ETV7 or control (normal rabbit IgG) bound to TNFRSF1A Intron 1 with respect to

input DNA is shown. Whole panel: Bars represent the averages and standard deviations of at least three biological replicates. * p≤0.05; ** p≤0.01.

3.2.4 ETV7 reduces NF-κB activation by repressing *TNFRSF1A*

It is known that TNF-α activates NF-κB signaling by binding to the TNFR1 receptor, hence we hypothesized that the ETV7-mediated repression of *TNFRSF1A* modulates the transcriptional activity of NF-κB in MCF7 and T47D breast cancer cells. To validate our hypothesis, we executed a gene reporter assay in MCF7 and T47D cells overexpressing ETV7 or its empty counterpart, using the pGL3 reporter plasmid with NF-κB binding (Fig. 33A). Noteworthy, the over-expression of ETV7 led to significant repression of the basal NF-κB transcriptional activity in both cell lines (Fig. 33B). To evaluate if this phenomenon could also be observed upon NF-κB induction, we repeated the experiment by stimulating cells with TNF-α (the main activator of NF-κB), IL-6 (a broader pro-inflammatory cytokine), or a combination of these two cytokines to further induce the transcriptional activity. Remarkably, we observed that in ETV7-over-expressing cells NF-κB signaling was repressed even upon the stimulation (Fig. 33C-D). This effect was particularly strong in MCF7 cells, whereas T47D cells were overall less responsive to TNF-α stimulation, which could be explained by relatively high endogenous levels of NF-κB signaling in T47D cells.

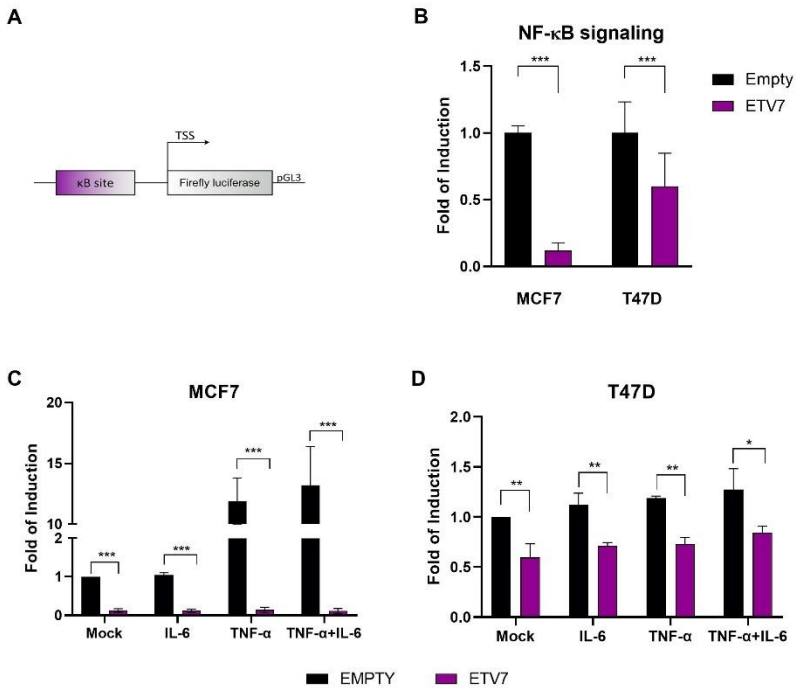

Figure 33. ETV7 reduces NF-κB activation by repressing TNFRSF1A. A) A schematic structure of the reporter plasmid used to study the NF-κB-dependent

transcriptional activity. B) Gene reporter assays in MCF7and T47D cells over-expressing ETV7, or its empty counterpart transiently transfected with pGL3-NF-κB reporter plasmid. Data is normalized using the *Renilla reniformis* luciferase reporter vector pRL-SV40 and shown as fold of induction relative to the Empty control. C-D) Gene reporter assays in MCF7 (C) and T47D (D) cells over-expressing ETV7, or its empty counterpart transfected with pGL3-NF-κB reporter plasmid and stimulated with TNF-α (10 ng/ml for MCF7 and 15 ng/ml for T47D), IL-6 (20 ng/ml) or combination of both for 4 hours. Data is normalized using the *Renilla reniformis* luciferase reporter vector pRL-SV40 and shown as a fold of induction relative to the Empty control. Whole panel: * $p \leq 0.05$; ** $p \leq 0.01$; *** $p \leq 0.001$.

Next, we decided to investigate whether the ETV7-mediated reduction in NF-κB activation reflects on the expression of NF-κB target genes. Therefore, we analysed the mRNA expression of 4 well-known NF-κB-regulated targets, such as TNF-α, IL-8, IL-6, and A20[248]. The over-expression of ETV7 significantly reduced the TNF-α-dependent expression of all these genes in both MCF7 and T47D cells, with the sole exception of IL-8, which was significantly downregulated only in MCF7 cells (Fig.34).

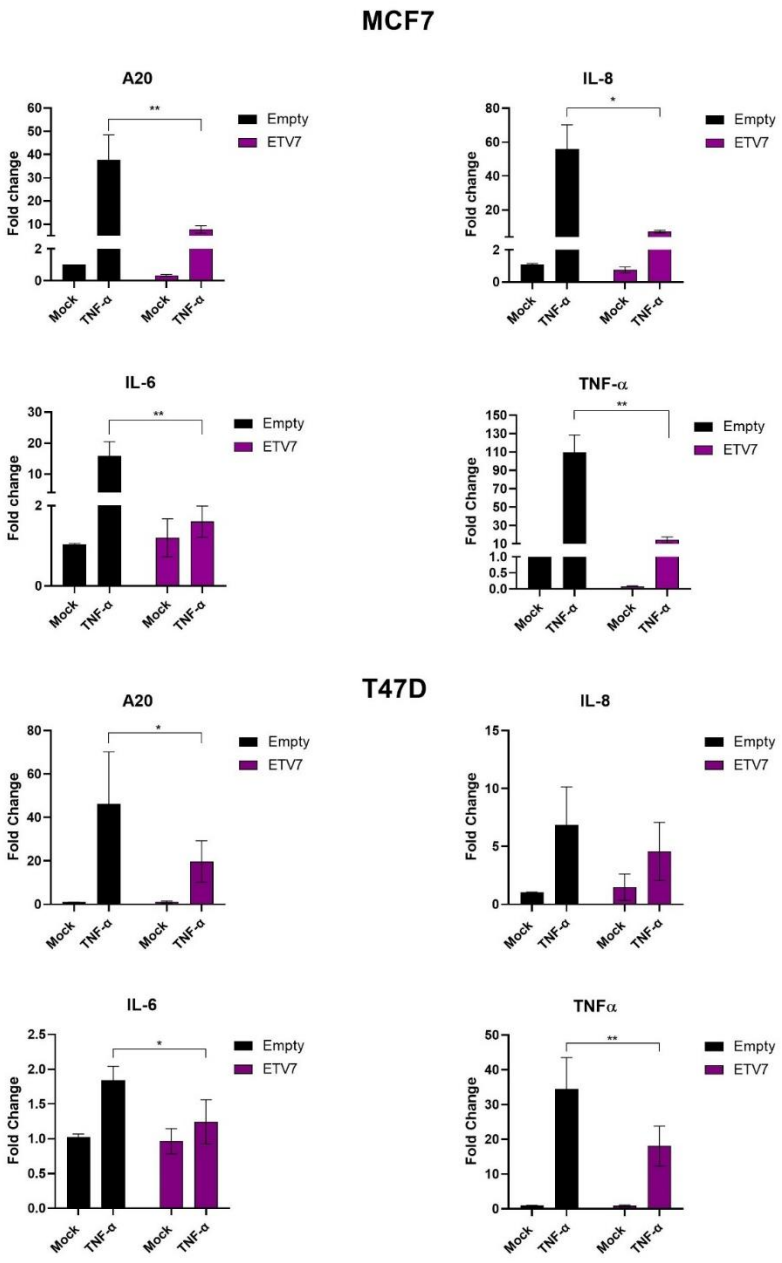

Figure 34. ETV7 downregulates NF-κB target genes in MCF7 and T47D cells. RT-qPCR analysis of known NF-κB target genes: A20, TNF-α, IL-8 and IL-6 in MCF7 and T47D ETV7 or Empty cells treated with TNF-α (10 ng/ml or 15 ng/ml, respectively) for 4 hours. Bars represent the averages and standard deviations of at least three biological replicates. * $p \leq 0.05$; ** $p \leq 0.01$; *** $p \leq 0.001$.

Furthermore, we studied the expression of these NF-κB target genes upon the knock-down of ETV7, using siRNAs in four different breast cancer-derived cell lines – MCF7, T47D, MDA-MB-231 and ZR-75-1, and we were able to demonstrate a significant up-regulation of all four target genes, which supports the role of ETV7 in the regulation of NF-κB signaling (Fig. 35A-D).

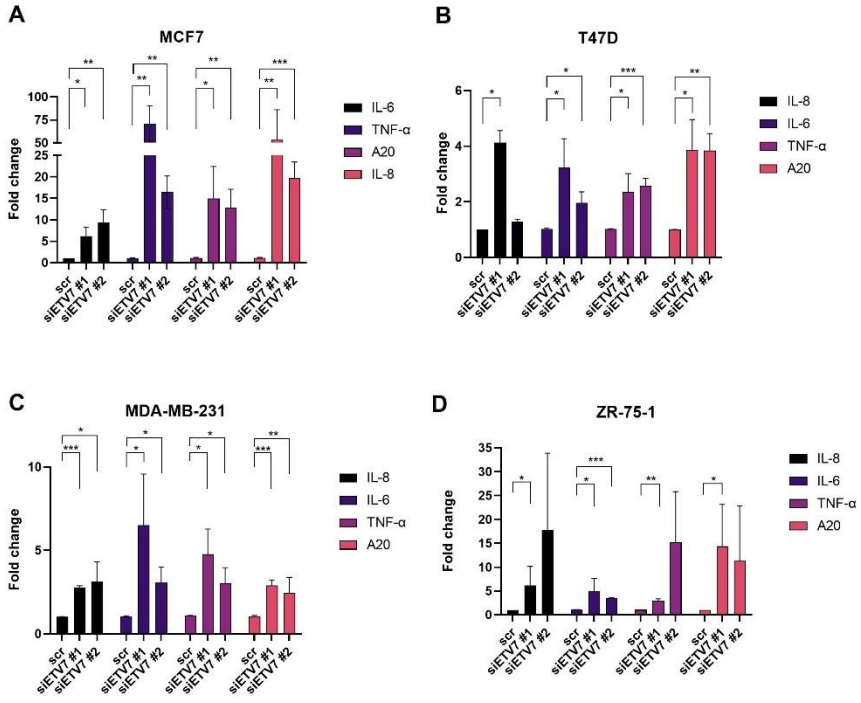

Figure 35. ETV7-mediated regulation of NF-κB target genes is bi-directional. RT-qPCR analysis of the normalized expression of NF-κB target genes (IL-8, IL-6, TNF-α and A20) in MCF7 (A), T47D (B), MDA-MB-231 (C) and ZR-75-1 (D) parental cells transfected with ETV7 targeting siRNA #1 and siRNA #2 or the scrambled control. Whole panel: Bars represent the averages and standard deviations of at least three biological replicates. * $p \leq 0.05$; ** $p \leq 0.01$; *** $p \leq 0.001$.

Moreover, the activation and translocation of NF-κB into the nucleus are initiated by the phosphorylation, ubiquitination, and proteolytic degradation of IκBα by the IKK complex. Firstly, we investigated the effect of ETV7 on the phosphorylation of IκBα. Interestingly, the over-expression of ETV7 resulted in a significant reduction in phosphorylated IκBα in both MCF7 and T47D cell lines (Fig. 36A-B).

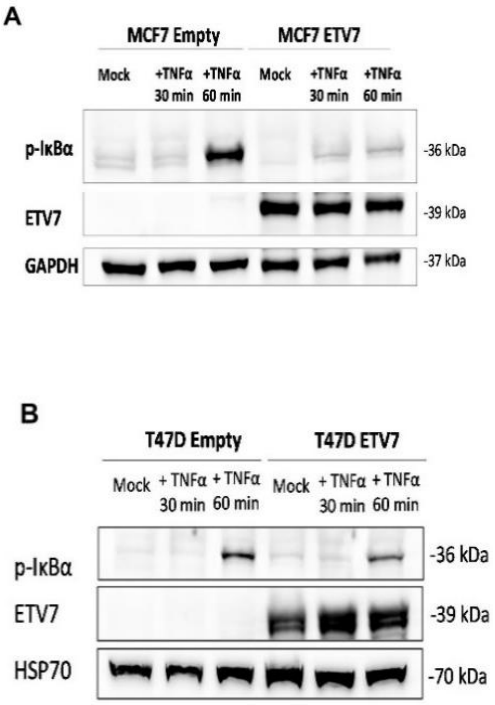

Figure 36. ETV7 reduces the phosphorylation of IκBα in MCF7 and T47D cells. Western blot analysis of phosphorylated IκBα in MCF7 (A) and T47D (B) Empty and ETV7 cells in response to 10 ng/ml or 15 ng/ml TNF-α, respectively, treatment for 1 hour. On the right of each blot is indicated the approximate observed molecular weight. GAPDH was used as a loading control.

In the NF-κB signaling pathway, phosphorylation of p65 is needed for nuclear translocation and transcription activation and since the p65 subunit is the most abundant transcriptionally active member of NF-κB in breast cancer cells[248–251], we decided to understand if the reduced phosphorylation of IκBα influences the nuclear localization of p65, we performed immunofluorescence analysis on MCF7 and T47D cells overexpressing ETV7 or its empty counterpart. In both cell lines we showed that upon the overexpression of ETV7 and NF-κB stimulation with TNF-α, p65 shuffling to the nucleus was reduced (Fig.37-38 and Suppl. Fig.1D).

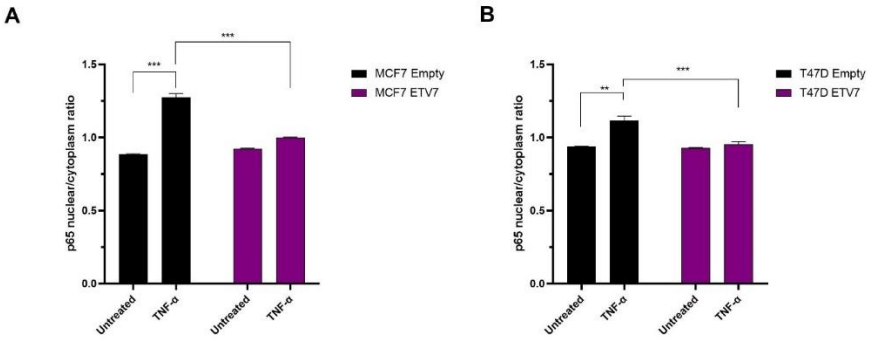

Figure 37. ETV7 reduces the nuclear translocation of p65 in breast cancer-derived cells (Part I). Quantification of nuclear:cytoplasmic ratios of p65 fluorescence intensity in T47D and MCF7 Empty and ETV7 cells untreated or treated with respectively 15 ng/ml or 10 ng/ml TNF-α for 60 min. Bars represent mean ± standard deviation from analysis of 10 (per each biological replicate; n=3) separated field images. ** p≤0.01; *** p≤0.001.

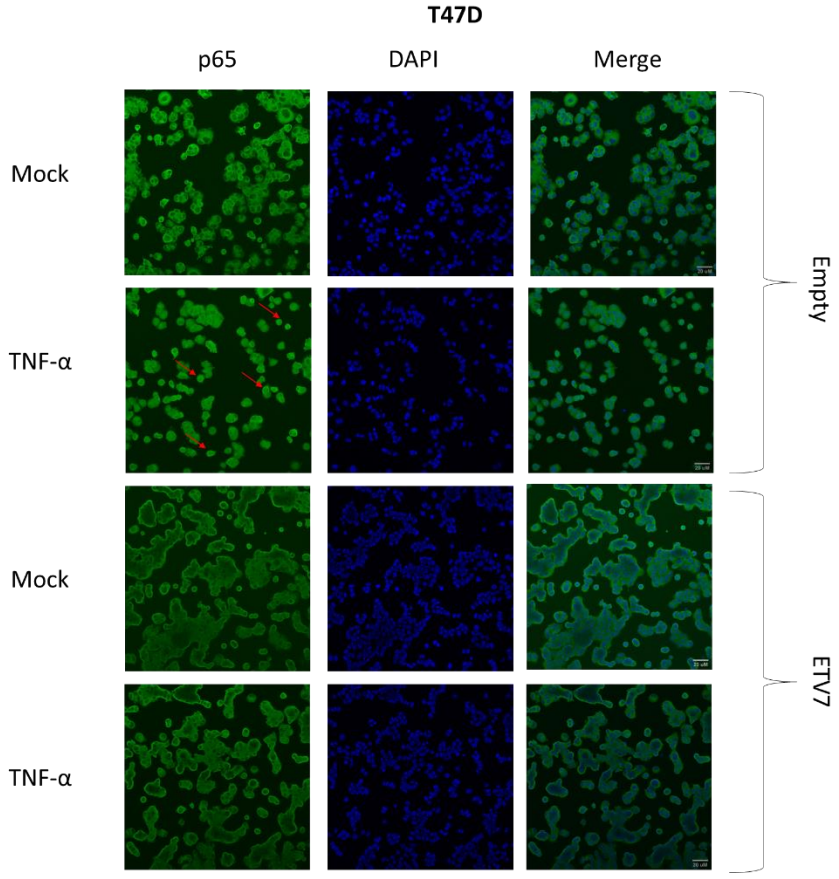

Figure 38. ETV7 reduces the nuclear translocation of p65 in breast cancer-derived cells (Part II). Immunofluorescence analysis for the p65 (green signal) nuclear translocation in T47D Empty and T47D ETV7 cells. Nuclei are stained in blue. T47D cells were untreated or treated with 15 ng/ml TNF-α for 60 min. Representative data for at least three biological replicates. 20X magnification. The arrows indicate the nuclear localization of p65.

Moreover, to confirm whether the downregulation of the NF-κB pathway, leads to the reduced inflammatory response, we analysed the secretion of several pro-inflammatory factors in MCF7 and T47D cells overexpressing ETV7 or its empty counterpart. To measure the levels of IL-8, IL-6, and TNF-α, we performed an enzyme-linked immunosorbent assay (ELISA). Remarkably, even upon the stimulation with TNF-α, we observed a significant decrease in IL-6 and IL-8 concentration in the medium from ETV7-overexpressing cells (both MCF7 and T47D) (Fig.39A-B).

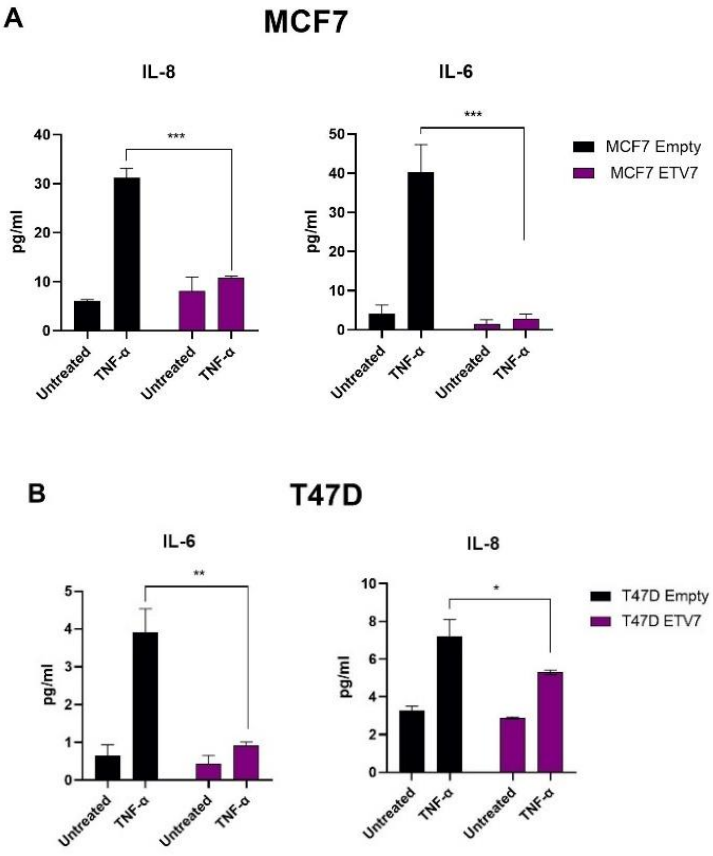

Figure 39. **ETV7 reduces the secretion of IL-8 and IL-6 in MCF7 and T47D cells**. The concentration of IL-8 and IL-6 in the supernatant of MCF-7 Empty and

MCF7 ETV7 cells without or with stimulation with TNF-α (10 ng/ml or 15 ng/ml, respectively), measured by ELISA. Bars represent the mean and the standard deviation of three biological replicates. * p≤0.05; ** p≤0.01; *** p≤0.001.

We also evaluated the basal level of TNF-α, which, as expected, was lower in the medium collected from ETV7-overexpressing MCF7 and T47D cells (Fig. 40).

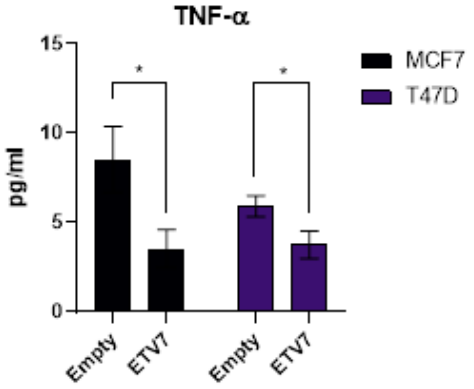

Figure 40. **ETV7 reduces secretion of TNF-α in MCF7 and T47D cells**. The concentration of TNF-α in the supernatant of MCF-7 and T47D Empty or ETV7 cells at a basal level, measured by ELISA. Bars represent the mean and the standard deviation of three biological replicates. * p≤0.05.

To confirm that the reduced NF-κB signaling depends, at least partially, on the ETV7-mediated repression of TNFRSF1A, we over-expressed TNFR1 in MCF7 ETV7 and MCF7 Empty cells and carried out a gene reporter assay using the pGL3-NF-κB reporter plasmid (Fig. 41A). The over-expression of TNFR1 was confirmed in all the conditions by Western blot analysis (Fig. 41C). Notably, upon the over-expression of TNFR1, we observed a partial but statistically significant increase in the transcriptional activity of NF-κB in MCF7 cells over-expressing ETV7 (Fig. 41B).

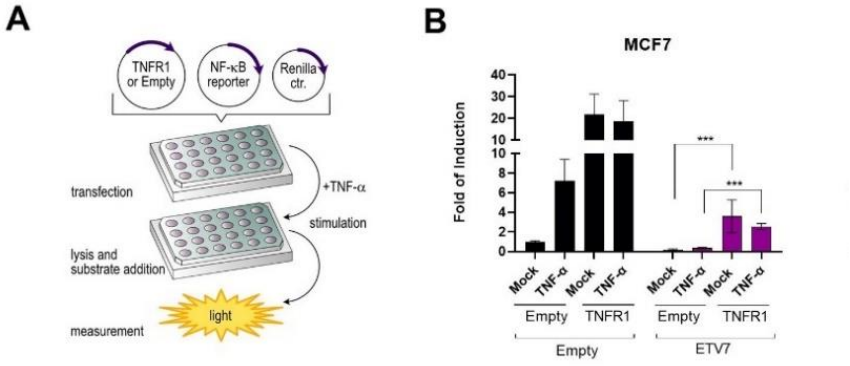

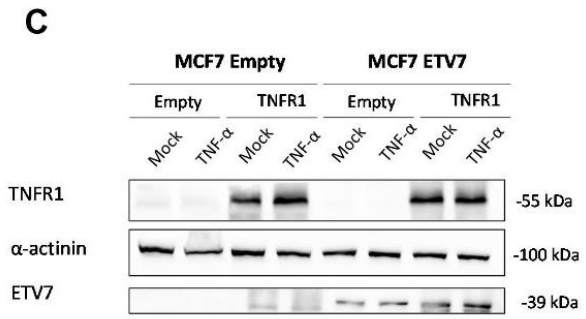

Figure 41. ETV7 downregulates NF-κB signaling in MCF7 and T47D breast cancer cells. A) A flowchart of the design of the rescue experiment. B) Gene reporter assays in MCF7 Empty or MCF7 ETV7 cells transfected with pGL3-NF-κB reporter vector and pcDNA3.1-TNFR1 or pcDNA3.1-Empty plasmids and untreated or treated with 10 ng/ml TNF-α for 4 hours. Data is normalized using the *Renilla reniformis* luciferase reporter vector pRL-SV40 and shown as a fold of induction relative to the Empty untreated control. C) Western blot analysis of the lysates obtained after performing the Luciferase assay to control the over-expression of TNFR1 in MCF7 Empty and ETV7 cells. On the right of each blot is indicated the observed molecular weight. α-actinin was used as a loading control. Whole panel: *** $p \leq 0.001$.

Finally, to put our data in a more translational context, using the TCGA database, we compared the expression of the TNF_SIGNALING_VIA_NFkB gene set in breast cancer tissues versus normal tissues and we observed a decrease in the expression of genes, belonging to TNF_SIGNALING_VIA_NFkB gene set (Fig. 42A). It was also intriguing to understand if the reduced activation of NF-κB and inflammatory response could have a prognostic value for breast cancer patients. We then executed survival analysis on samples from TCGA database and confirmed a significant correlation between reduced activation of NF-κB and lower levels of inflammatory response and a worse prognosis of breast cancer patients (Fig. 42B-C).

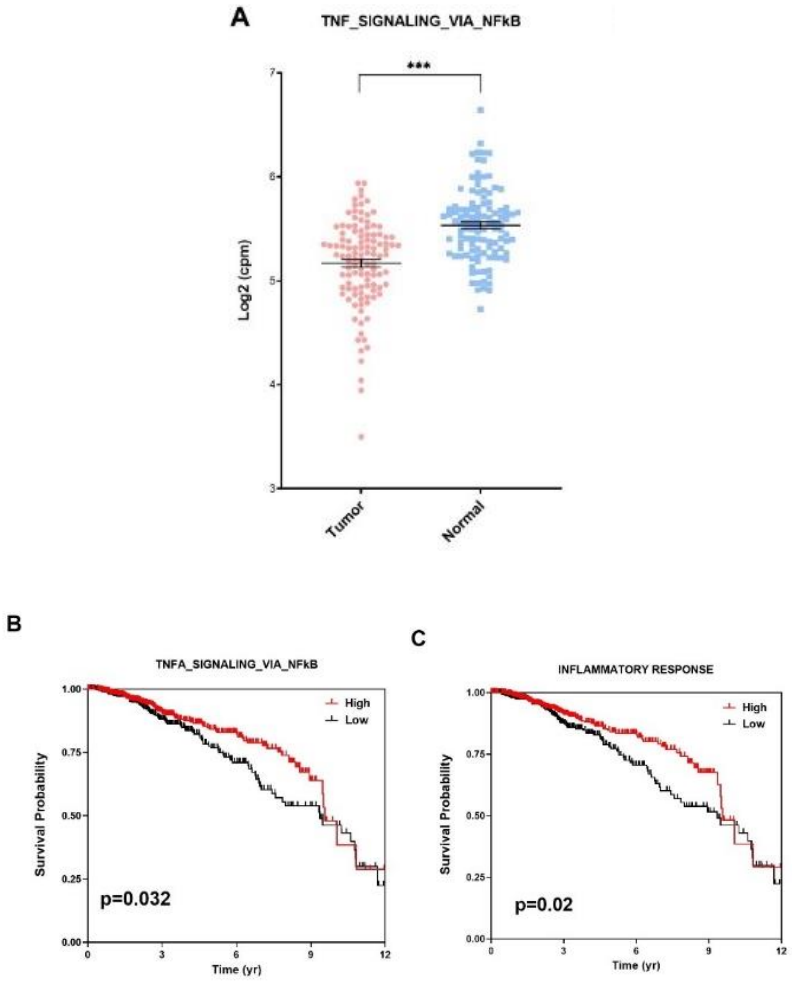

Figure 42. TNF-α signaling via NF-κB is downregulated in breast cancer patients. A) A dot plot demonstrating the differential expression analysis for the TNF_SIGNALING_VIA_NFkB gene set in a BRCA matched patients' dataset from TCGA (The Cancer Genome Atlas) database. B-C) Kaplan–Meier curves for TCGA breast cancer patients stratified according to the average expression of TNFA_SIGNALING_VIA_NFkB (B) and INFLAMMATORY_RESPONSE (C) gene signatures. Curves represent the probability of disease-specific survival (DSS). p-values are calculated with the log rank test. *** $p \leq 0.001$.

3.2.5 ETV7 competes with STAT3 in the regulation of *TNFRSF1A*

It is known that STAT3 can induce the expression of *TNFRSF1A* by binding to its first intron, which is bound also by ETV7 for the regulation of

TNFRSF1A. Moreover, the binding sites for STAT3 and ETV7 are similar (Fig. 43A). Thus, we pursued to investigate the potential cross-talk between the two transcription factors. Besides, one of our identified binding regions (ETV7 BS #2) also contains a binding site for STAT3. The potential cross-talk between STAT3 and ETV7 was also supported by the RNA-seq analysis, showing a down-regulation of the IL-6_JAK_STAT3 pathway in MCF7 and T47D cells (Fig. 43B).

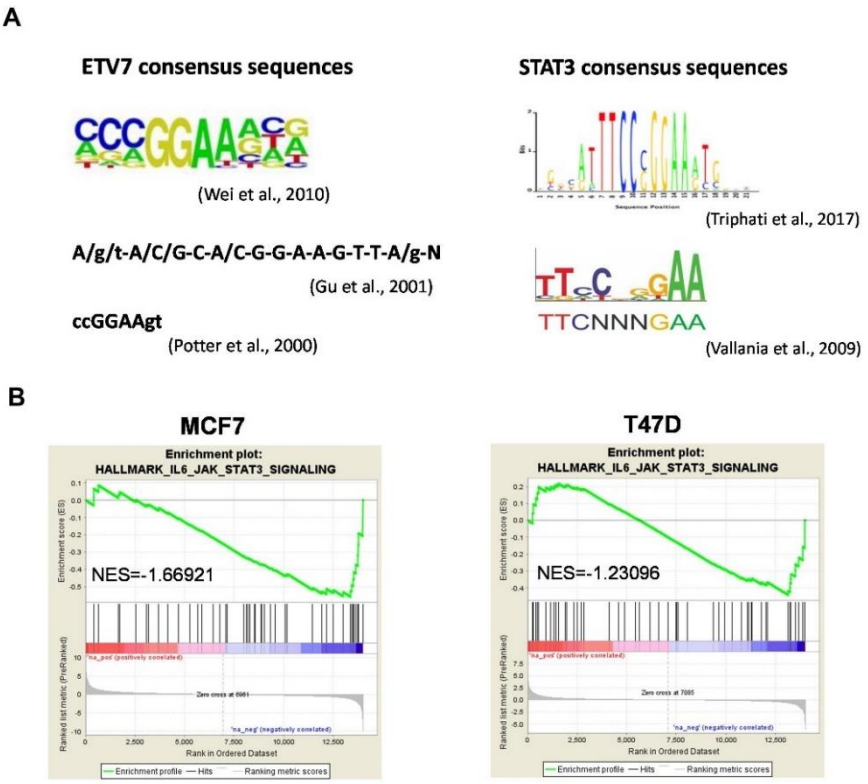

Figure 43. Potential cross-talk between ETV7 and STAT3. A) Canonical ETV7 and STAT3 binding sites known from the literature. B) Gene Set Enrichment Analysis of MCF7 and T47D cells over-expressing ETV7 or its Empty counterpart. Enrichment plot for IL6_JAK_STAT3 signalling in MCF7 and T47D cells gene sets of the Hallmark Collection. The Normalized Enrichment Score (NES) shows the degree of the enrichment of the gene set; the negative sign indicates that the gene set is down-regulated in cells over-expressing ETV7. FDR = False Discovery Rate.

Normally, STAT3 is activated by several external stimuli such as interferons, interleukins, and TNF-α. IL-6 is one of the most potent activators of STAT3; hence, we chose IL-6 for the activation of STAT3. To verify whether IL-6 can trigger the phosphorylation of STAT3 in our cellular systems and to confirm the subcellular localization of ETV7 and STAT3 endogenously at the baseline and upon the treatment with IL-6, we performed

a protein subcellular fractionation followed by Western blot analysis. The obtained data confirmed that the phosphorylated form of STAT3 is mainly located in the chromatin-associated fraction and that, as expected, the phosphorylated STAT3 increases in the chromatin compartment after the stimulation with IL-6. ETV7 protein is found both in the cytoplasmic fraction and the chromatin-associated fraction and is not affected by the stimulation with IL-6/activation of STAT3 (Fig. 44).

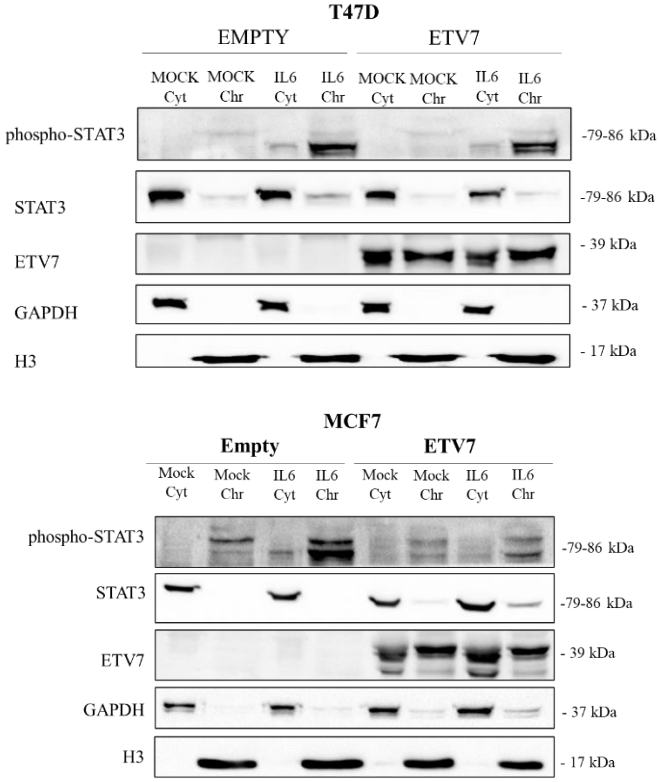

Figure 44. Localization of STAT3 and ETV7 proteins in MCF7 and T47D cells. Western blot analysis of subcellular fractionation from MCF7 and T47D Empty and ETV7 cells untreated or treated with IL-6 (20 ng/ml) for 4 hours. On the right of each blot is indicated the approximate observed molecular weight. Cyt – cytoplasmic protein fraction, Chr – chromatin-enriched protein fraction. GAPDH was used as a loading control for the cytoplasmic fraction. Histone H3 was used as a loading control for chromatin-enriched protein fraction.

Then, we analysed how the activation of STAT3 influences the expression of TNFRSF1A in MCF7 cells over-expressing ETV7 or its empty counterpart. By performing RT-qPCR, we found out that although the treatment with IL-6 induced the expression of *TNFRSF1A* in MCF7 empty cells, there was a significant reduction in the expression of *TNFRSF1A* in the cells over-expressing ETV7 (Fig. 45). These results confirm that ETV7 can down-regulate *TNFRSF1A* despite STAT3 activation.

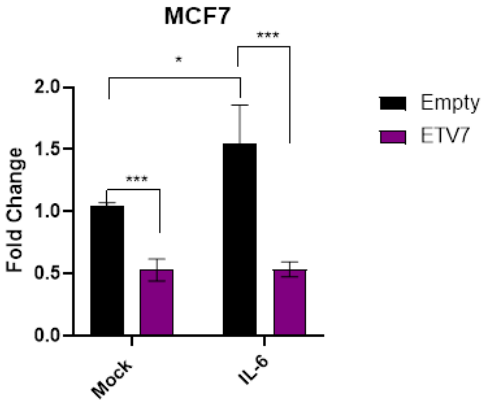

Figure 45. ETV7 competes with STAT3 in the regulation of *TNFRSF1A*. RT-qPCR analysis for the expression of TNFRSF1A after the stimulation with IL-6 (20 ng/ml) for 4 hours in MCF7 cells over-expressing ETV7 or its empty counterpart. * $p \leq 0.05$; *** $p \leq 0.001$.

As mentioned in the previous section, the ETV7 binding region is in the first intron of *TNFRSF1A*, which is also known to be a region bound by STAT3. To clarify whether ETV7 could compete with STAT3 for binding TNFRSF1A intron 1, we executed a chromatin immunoprecipitation assay followed by qPCR. We stimulated ETV7 over-expressing cells with IL-6, which activates STAT3, and performed immunoprecipitation using an antibody for phosphorylated STAT3. The activation/phosphorylation of STAT3 was confirmed by Western blot analysis for p-STAT3 (Fig. 46C). Then, using qPCR we evaluated the binding to the three regions containing binding sites for ETV7, as well as, for STAT3. Our results showed that upon the over-expression of ETV7 the ability of STAT3 to bind the 1st and the 2nd regulatory regions in TNFRSF1A was remarkably decreased in MCF7 cells (Fig. 46A-B). The tendency of the reduction in STAT3 binding to the 3rd regulatory region was also visible but not statistically significant (Suppl. Fig. 1C).

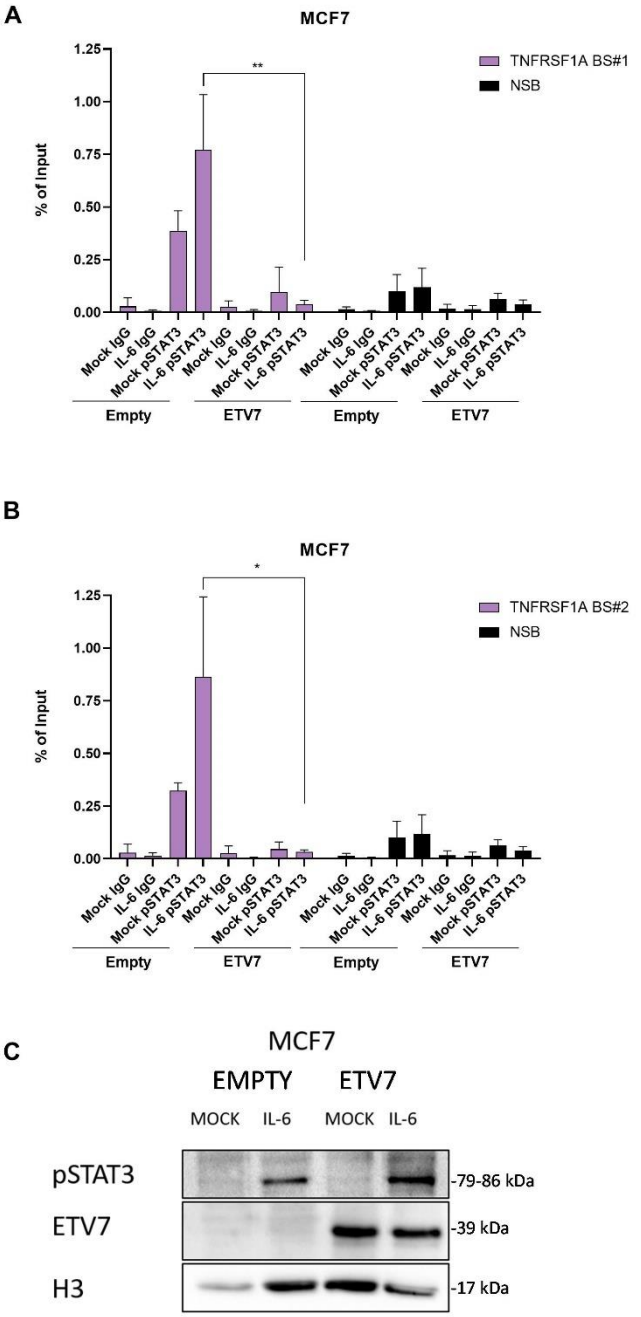

Figure 46. ETV7 downregulates *TNFRSF1A* expression even upon the activation of STAT3. A-B) ChIP-qPCR of *TNSFRSF1A* Intron 1 Binding site #1 (A); Binding site #2 (B) in MCF7 cells over-expressing ETV7 untreated or treated with IL-6 (20 ng/ml) for 4 hours. The percentage of the enrichment of pSTAT3 or control (normal rabbit IgG) bound to *TNFRSF1A* Intron 1 with respect to Input DNA is

shown. NSB=non-specific binding, a region within the *ACTB* promoter. BS = binding site. Bars represent the averages and standard deviations of at least three biological replicates. C) Western blot analysis of the lysates from ChIP assay to control the phosphorylation of STAT3. Whole panel: * $p \leq 0.05$; ** $p \leq 0.01$.

To understand the crosstalk between STAT3 and ETV7 in the regulation of *TNFRSF1A* expression, we investigated whether ETV7 could impact the STAT3 signalling. Firstly, to verify if the over-expression of ETV7 affected mRNA levels of STAT3, we analysed the expression of STAT3 in MCF7 and T47D cells over-expressing ETV7 and observed that upon the over-expression of ETV7 in both cell lines, especially in MCF7, STAT3 expression was significantly down-regulated (Fig. 47A). However, at the protein level this effect was not confirmed. Alternatively, to evaluate the effect of ETV7 on the transcriptional activity of STAT3, we executed gene reporter assays using a luciferase reporter construct containing four canonical STAT3 binding sites (4xM67 pTATA TK-Luc). Our results demonstrated that ETV7 did not affect the overall transcriptional activity of STAT3 (Fig. 47B).

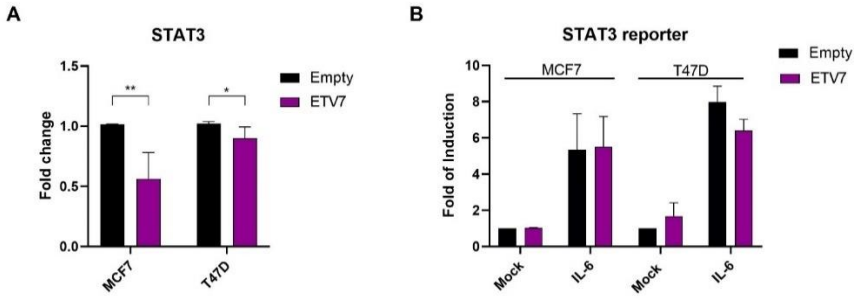

Figure 47. ETV7 does not affect the general transcriptional activity of STAT3. A) RT-qPCR analysis of STAT3 expression in MCF7 or T47D cells over-expressing ETV7 or its Empty counterpart. * $p \leq 0.05$; ** $p \leq 0.01$. B) Gene reporter assays in MCF7 Empty/ETV7 and T47D Empty/ETV7 cells transfected with M67-STAT3 reporter untreated or treated with IL-6 (20 ng/ml) for 4 hours. Data is normalized using the *Renilla reniformis* luciferase reporter vector pRL-SV40 and shown as a fold of induction relative to the Empty untreated control.

To further confirm that the displacement of STAT3 was specific to *TNFRSF1A* regulatory region and not to STAT3 targets in general, we carried out chromatin immunoprecipitation with phospho-STAT3 antibody and analyse a regulatory region of another known transcriptional target of STAT3, *MED16*[252]. We observe no statistically significant differences in STAT3's ability to bind the regulatory region of *MED16* in cells over-expressing ETV7 or empty vector, which confirmed that the ETV7-mediated displacement of STAT3 was specific for the regulatory region of *TNFRSF1A* (Fig. 48).

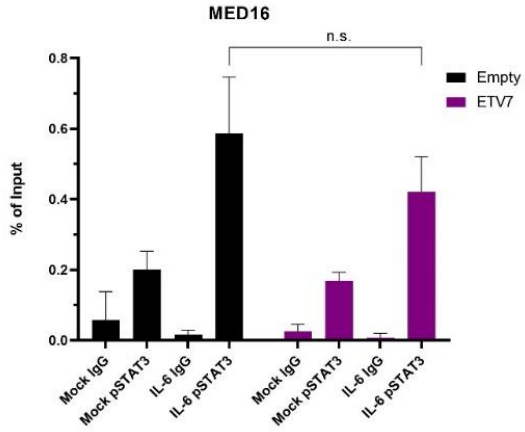

Figure 48. ETV7-mediated displacement of STAT3 is specific to the regulatory region of TNFRSF1A. ChIP-qPCR of MED16 promoter in MCF7 cells over-expressing ETV7 or its empty counterpart. The percentage of the enrichment of pSTAT3 or control (normal rabbit IgG) bound to MED16 promoter with respect to Input DNA is shown. Bars represent the averages and standard deviations of at least three biological replicates. n.s. – not significant.

Moreover, we wanted to understand if the displacement of STAT3 by ETV7 could also happen in the more physiological context, e.g., upon the endogenous modulation of ETV7 levels by DNA-damaging drugs. Hence, we performed a chromatin immunoprecipitation assay followed by qPCR on the cells treated with IL-6 (activates STAT3) and Doxorubicin (induces ETV7) and the combination of IL-6 and Doxorubicin (to create a competition between STAT3 and ETV7). Interestingly, we confirmed that the modulation of endogenous ETV7 levels with a DNA-damaging agent was sufficient for the STAT3 displacement at the binding site #2 in *TNFRSF1A* Intron I in both MCF7 cells, and in both binding sites #1 and #2 in T47D cells (Fig.49).

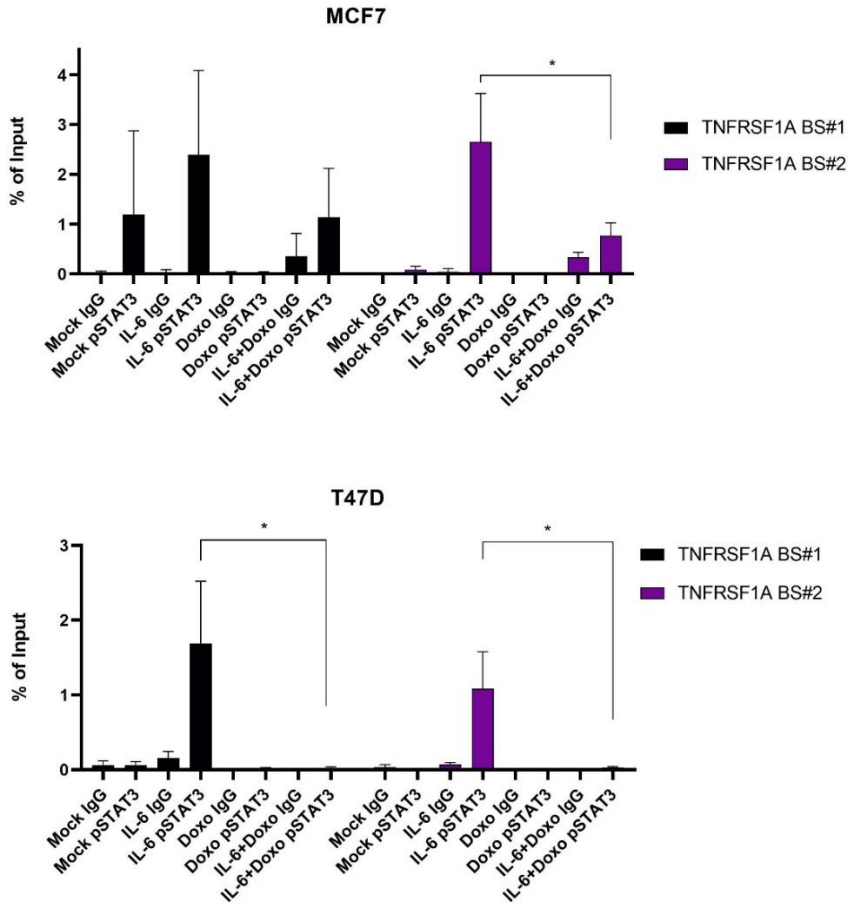

Figure 49. **ETV7 reduces the ability of STAT3 to bind the regulatory region of TNFRSF1A upon DNA-damaging treatment.** ChIP-qPCR analysis of the Intron I of TNFRSF1A binding site #1 and binding site #2 in MCF7 and T47D parental cells untreated or treated with 1.5 μM Doxorubicin (24 h), 20 ng/ml IL-6 (4 h), or the combination (IL-6+Doxo). The percentage of the enrichment of pSTAT3 or control (normal rabbit IgG) bound to TNFRSF1A Intron 1 with respect to Input DNA is shown. BS = binding site. Bars represent the averages and standard deviations of at least three biological replicates. * $p \leq 0.05$.

Furthermore, we wanted to understand whether there was a physical interaction between ETV7 and STAT3 proteins. To verify this possible interaction, we performed a protein co-immunoprecipitation (Co-IP) experiment, using antibodies against ETV7 for immunoprecipitation and probing with phosphorylated STAT3 antibodies in Western blot. Co-IP analysis did not show a direct interaction between ETV7 and STAT3 either in MCF7 or in T47D cells (Fig. 50).

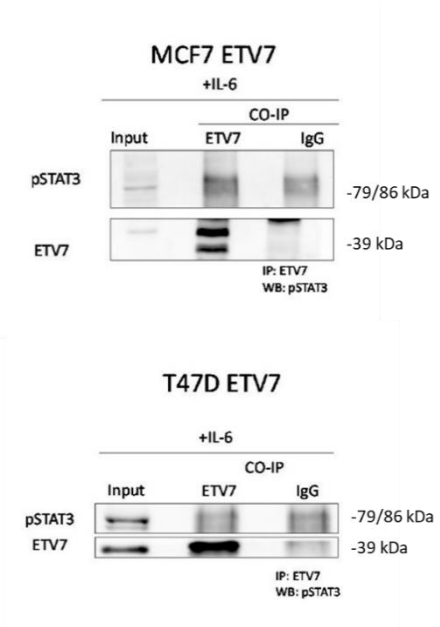

Figure 50. Direct interaction of STAT3 and ETV7 was not observed in MCF7 and T47D cells. Co-immunoprecipitation analysis of protein-protein interaction between ETV7 and pSTAT3 in MCF7 and T47D cells over-expressing ETV7. Normal IgG and INPUT were used as controls.

Overall, in this part of my PhD project, I demonstrated the ETV7-mediated repression of TNFR1/NF-κB axis, leading to reduced inflammatory response and uncovered the mechanism behind this effect, depending on the competition with STAT3 in the transcriptional regulation of the *TNFRSF1A* gene (Fig. 51)

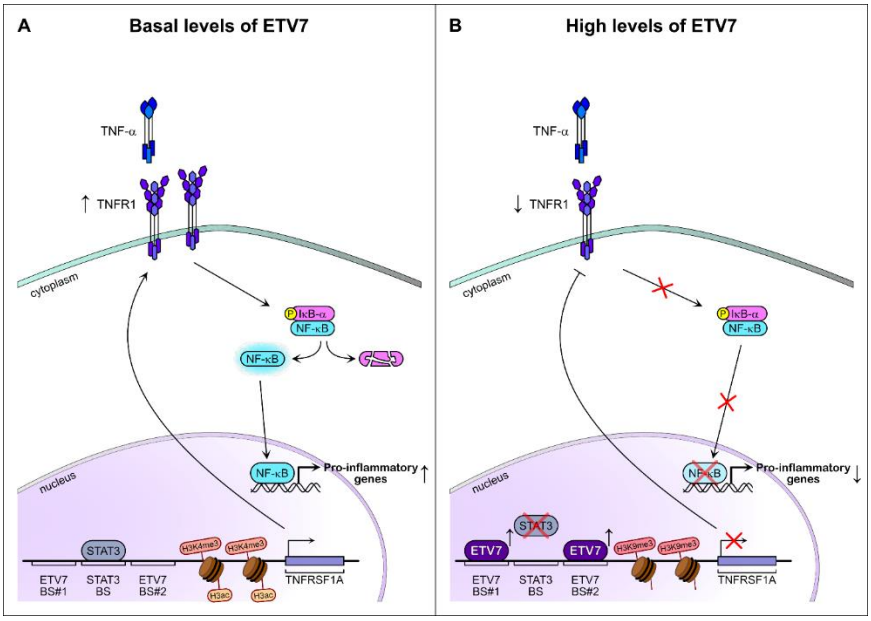

Figure 51. ETV7 can compete with STAT3 in the regulation of the *TNFRSF1A* gene influencing the NF-κB regulatory pathway. A) The canonical STAT3/TNF-α/NF-κB regulatory pathway. STAT3 binds to its regulatory element in the first intron of the *TNFRSF1A* gene and induces its expression by recruiting chromatin remodelers that result in an "active" state. Consequently, the TNF-α receptor 1 is produced. TNF-α molecules bind TNFR1 receptor and activate the NF-κB signaling pathway. B) In the context where ETV7 expression is increased, ETV7 can displace STAT3 from its binding sites on the Intron 1 of *TNFRSF1A* and directly represses its expression by altering the deposition of histone marks. This ETV7-mediated repression leads to the reduced activation of NF-κB signaling and, hence, reduces the expression of pro-inflammatory genes.

3.3. ETV7 is involved in immune evasion by repressing the antigen presentation pathway

3.3.1 ETV7 downregulates genes involved in the antigen presentation pathway

From the data presented in previous chapters, it was clear, that ETV7 is involved in cancer immunity. We demonstrated that ETV7 can repress interferon-stimulated genes and reduce pro-inflammatory responses. Logically, it was interesting for us to understand, how the impairment of these signaling pathways, could impact cancer aggressiveness. As it is known from the literature, one of the ways for cancer cells to be more aggressive and survive longer is by avoiding the host immune system[55,162]. This means, that during tumorigenesis cancer cells develop and acquire mechanisms that help to evade the immune response. One of the most important immune evasion

mechanisms is the downregulation of antigen presentation (MHC I and MHC II) which leads to reduced efficiency of cytotoxic T cells and reduced responsiveness to immunotherapy[136,161]. It is known from previous studies that the antigen-presenting pathway is mainly regulated by these three transcriptional regulators – IRF-1, NF-κB and NLRC5[136]. The data presented in previous chapters demonstrated that ETV7 can interfere with interferon signalling, as well as, with the activation of NF-κB. Based on these results, we decided to investigate if ETV7 can regulate the presentation of antigens. Firstly, we analyzed the expression of IRF-1 and NLRC5 in MCF7 and T47D overexpressing ETV7 or its empty control. After performing RT-qPCR analysis, we confirmed that in both cell lines, upon the overexpression of ETV7, *IRF-1*, *IRF-2* and *NLRC5* genes were downregulated, strengthening our hypothesis of the potential involvement of ETV7 in breast cancer immunity. The reduced levels of IRF-1 in MCF7 overexpressing cells were also confirmed in the Western blot analysis (Fig.52).

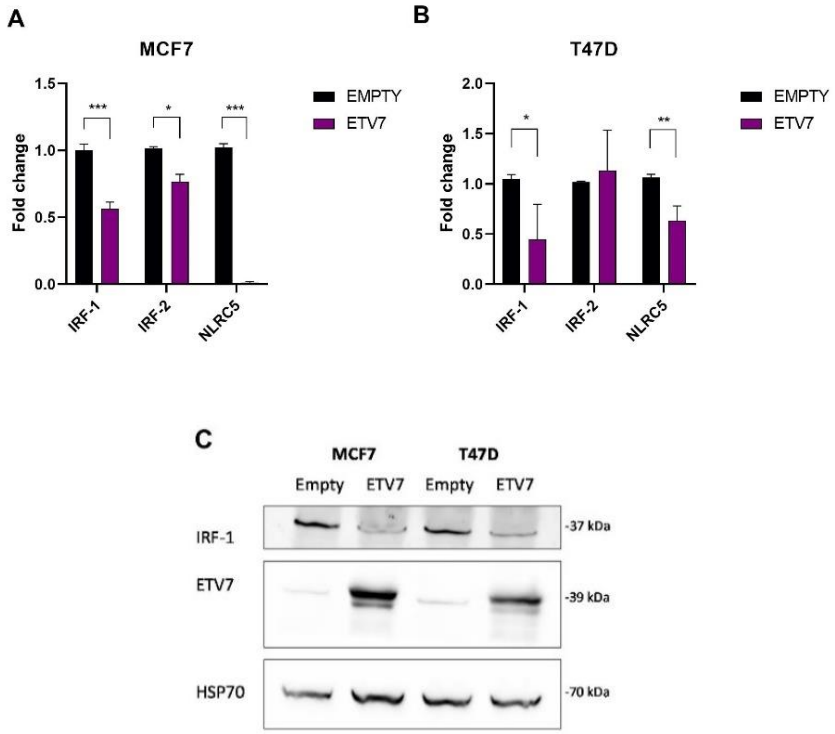

Figure 52. ETV7 downregulates transcriptional regulators of antigen presentation pathway. A-B) RT-qPCR analysis of IRF-1, IRF-2 and NLRC5 expression in MCF7 (A) or T47D (B) cells over-expressing ETV7 or its Empty counterpart. * $p \leq 0.05$; ** $p \leq 0.01$; *** $p \leq 0.01$. C) Western blot analysis of IRF-1 in MCF7 and T47D Empty and ETV7 cells. HSP70 was used as a loading control.

Following, we wanted to understand if ETV7 was regulating the antigen presentation machinery in MCF7 and T47D cells. RT-qPCR analysis revealed significant downregulation of almost all tested genes, related to antigen presentation machinery in MCF7 (Fig. 53A) and T47D (Suppl. Fig.1E) overexpressing ETV7. Furthermore, we chose several genes, which were stronger repressed by ETV7, and analysed the level of gene product in Western blot. We demonstrated, a significant decrease in the levels of LMP7 (encoded by *PSMB8*), LMP2 (encoded by *PSMB9*) and B2M upon the overexpression of ETV7 in MCF7 cells (Fig. 53B-C).

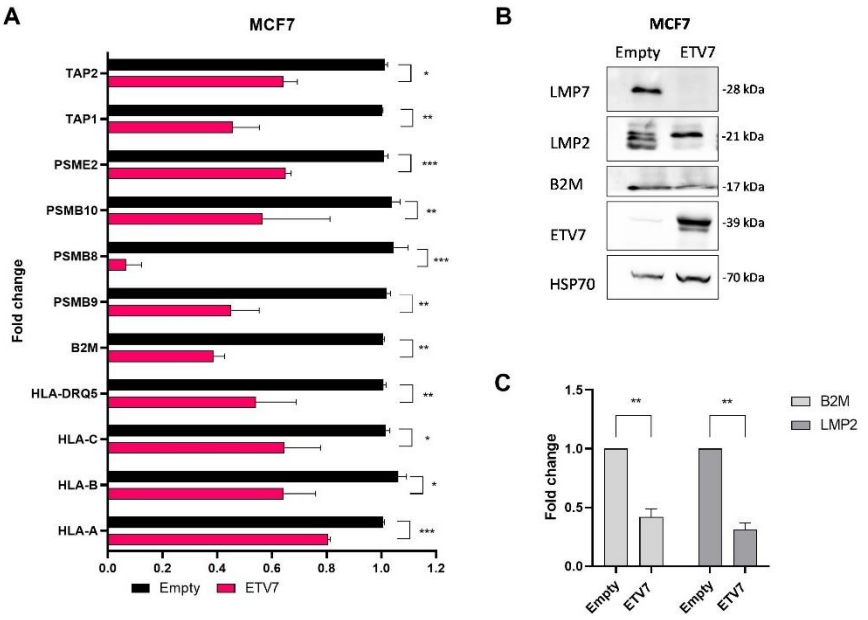

Figure 53. ETV7 represses antigen-presenting machinery in breast cancer-derived cells. A) RT-qPCR analysis of antigen-presenting in MCF7 cells over-expressing ETV7 or its Empty counterpart. * $p \leq 0.05$; ** $p \leq 0.01$; *** $p \leq 0.01$. B) Western blot analysis of LMP7, LMP2, and B2M in MCF7 Empty and ETV7 cells. HSP70 was used as a loading control. C) The quantification of Western blot analysis of LMP2 and B2M in MCF7 Empty and ETV7 cells. Bars represent the averages and standard deviations of at least three biological replicates. Data is normalized to the signal of HSP70, which was used as a loading control. ** $p \leq 0.01$.

It is known from the literature, that cancer stem cells impair the recruitment of immune cells in tumor sites and that they are masters in cancer immune evasion[253–255]. One of the mechanisms, that CSCs are employing is, the downregulation of antigen presentation and MHC molecules. Considering this knowledge and our previous data relative to modulation of cancer stem plasticity by ETV7, we decided to investigate if antigen presentation machinery is also repressed in mammospheres formed from ETV7-overexpressing cells. Gene expression analysis revealed that in ETV7-

overexpressing mammospheres, there was significant repression of several genes, related to antigen presentation machinery, confirming that ETV7 can downregulate antigen presentation also in cancer stem cell-enriched context (Fig. 54).

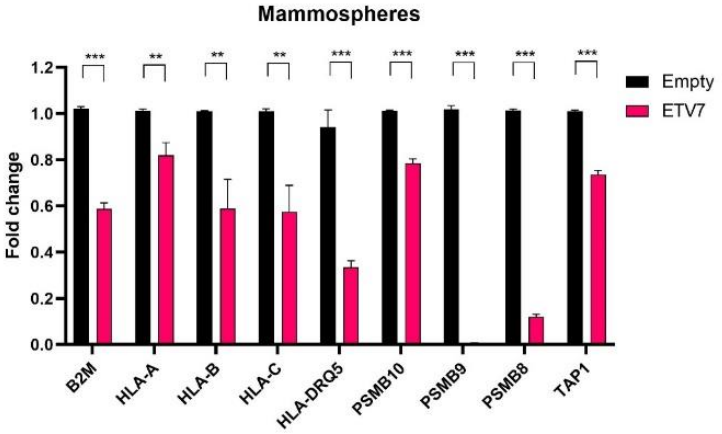

Figure 54. ETV7 represses antigen-presenting machinery in mammospheres. A) RT-qPCR analysis of antigen-presenting in mammospheres formed from MCF7 cells over-expressing ETV7 or empty control. ** $p \leq 0.01$; *** $p \leq 0.01$.

Moreover, it has been demonstrated that IFN-γ can enhance and restore the MHC I antigen processing and presentation pathway[256]. Hence, we decided to investigate if ETV7-mediated downregulation of antigen presentation machinery could be restored upon the stimulation of IFN-γ. We stimulated MCF7 cells overexpressing ETV7 or its empty control with 20 ng/ml of IFN-γ for shorter and longer periods and we could observe that in MCF7 control cells upon the stimulation there was a major enhancement of immunoproteasome-related genes and their products, meanwhile in cells overexpressing ETV7, antigen presentation pathway was induced only slightly, even when the cells were stimulated for 2 weeks, suggesting that ETV7-mediated repression cannot be restored upon the stimulation with IFN-γ, strengthening the role of ETV7 in immune evasion (Fig. 55).

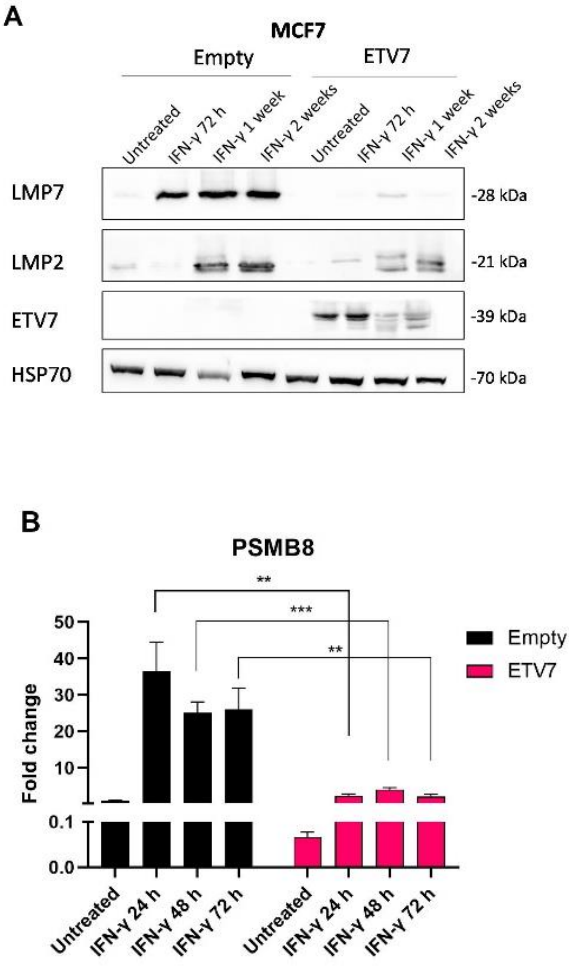

Figure 55. IFN-γ is not able to restore ETV7-mediated repression of antigen presentation. A) Western blot analysis of LMP7 and LMP2 in MCF7 Empty and ETV7 cells not stimulated or stimulated with 20 ng/ml IFN-γ for 72 hours, 1 week or 2 weeks. HSP70 was used as a loading control. B) RT-qPCR analysis of PSMB8 in MCF7 cells over-expressing ETV7 or its Empty counterpart not stimulated or stimulated with 20 ng/ml IFN-γ for 72 hours, 1 week or 2 weeks. ** $p \leq 0.01$; *** $p \leq 0.01$.

To conclude, ETV7 represses the antigen presentation pathway and this downregulation cannot be reversed by the stimulation with IFN-γ. The role of ETV7 in the regulation of antigen presentation pathway suggests, that ETV7 could be an important player in cancer immune evasion.

3.4. ETV7 knock-down induces p53-mediated apoptosis

In previous chapters, we performed various experiments after the knock-down of ETV7, as we observed the opposite effect in comparison to ETV7-overexpression. Hence, to investigate the targetability of ETV7 in breast cancer cells, in this part of the study, we analysed the effect of ETV7 knock-down on cell viability using siRNAs targeting ETV7. Firstly, we silenced ETV7 in thirteen different cancer cell lines and then evaluated cell viability. By performing a CellTiterGlo assay (Fig. 56) in eight cell lines we observed a significant decrease in cell viability, instead, in the remaining five the survival was slightly or not affected by the silencing of ETV7.

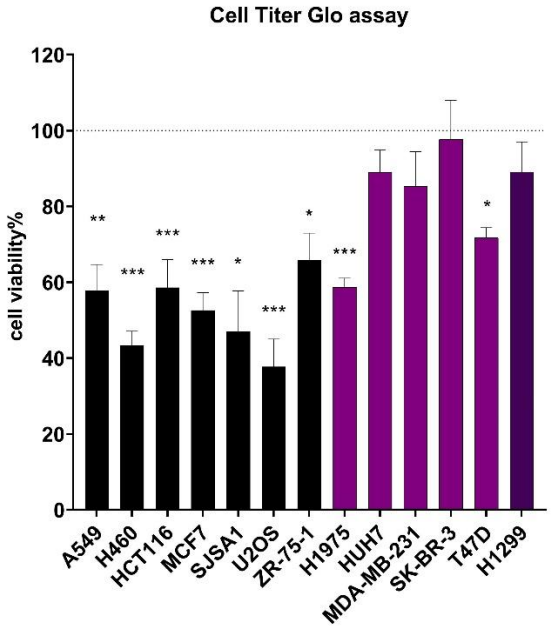

Figure 56. Silencing of ETV7 reduces viability in several cancer cell lines. CellTiterGlo cell viability assay performed in a panel of cancer cells upon the silencing with ETV7 targeting siRNA for 72 hours. *p≤0.05; ** p≤0.01; *** p≤0.01.

To understand if the reduced viability was due to apoptosis, we analysed PARP-1 cleavage by Western blot. Similarly to cell viability data, we detected cleaved PARP-1 in MCF7, ZR-75-1, and A549 cells which had lower survival upon the silencing of ETV7 (Fig. 57A-C). On the contrary, in T47D cells, which were less affected by the silencing of ETV7, apoptotic death was not observed (Fig. 57D).

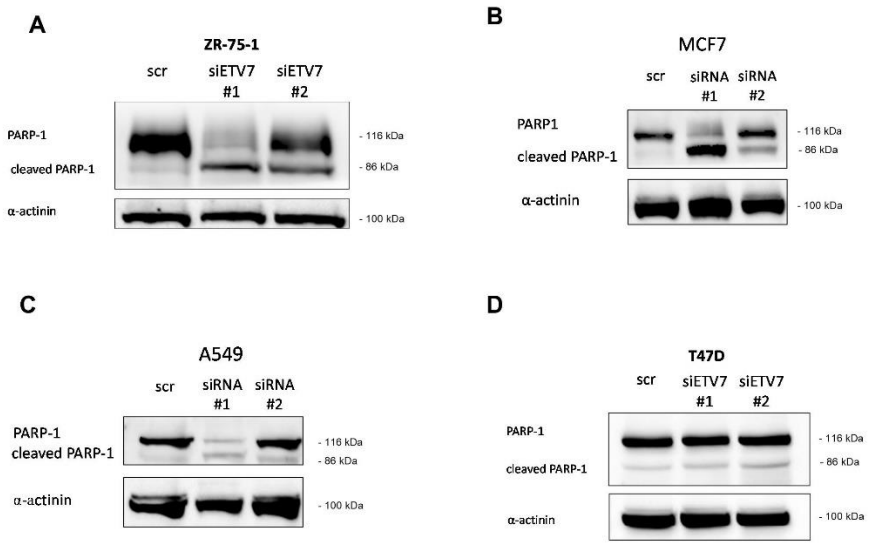

Figure 57. Silencing of ETV7 induces apoptosis in several cancer cell lines. Western blot analysis of PARP-1 cleavage in ZR-75-1 (A), MCF7 (B), A549 (C) and T47D (D) cell lines upon the knock-down of ETV7 with two ETV7 targeting siRNAs. α-actinin was used as a loading control.

To understand why some cell lines, underwent apoptosis upon the silencing of ETV7, instead, other cell lines were not affected, we looked for the genetic differences between selected cell lines. Interestingly, we observed that cells, which were not affected or less affected by ETV7 silencing, had mutated p53. (Fig. 58).

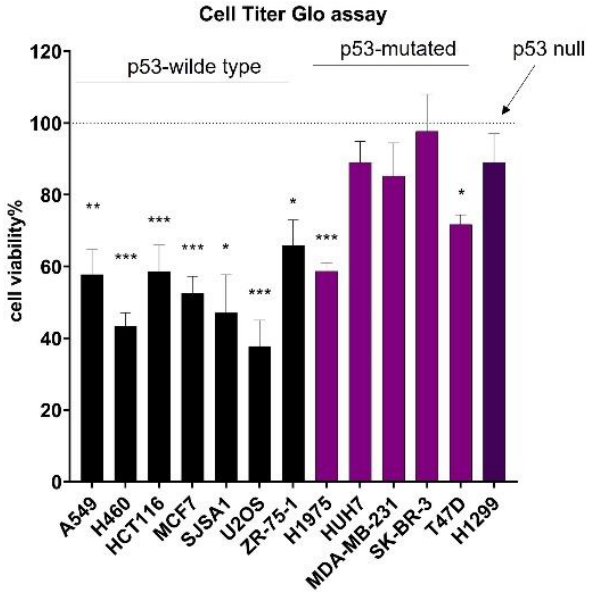

Figure 58. Silencing of ETV7 induces apoptosis in a wild-type p53 context. CellTiterGlo cell viability assay performed in a panel of p53 wild type and p53 mutant cancer cells upon the silencing with ETV7 targeting siRNA for 72 hours. *p≤0.05; ** p≤0.01; *** p≤0.01.

Hence, we hypothesized that apoptosis, observed upon the silencing of ETV7, was p53-dependent. We first analyzed the levels of p53 in Western blot and we observed a strong accumulation of p53 in response to ETV7 silencing in MCF7 cells, instead in A549 and ZR-75-3 cells the accumulation of p53 was observed only upon the silencing with siRNA #1 (Fig.59).

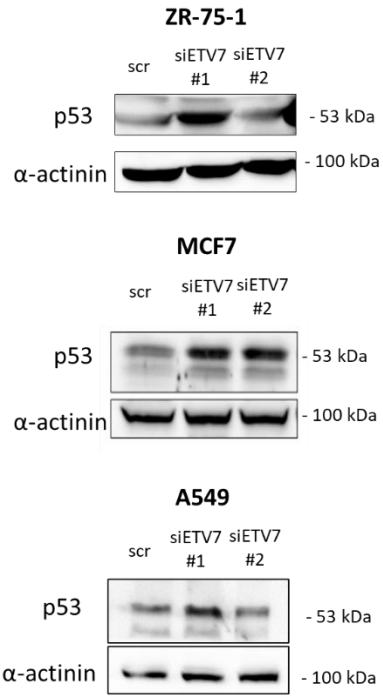

Figure 59. Silencing of ETV7 leads to the accumulation of p53 in cancer cells. Western blot analysis of p53 accumulation in ZR-75-1, MCF7 and A549 cells upon the silencing of ETV7 with two ETV7 targeting siRNAs. α-actinin was used as a loading control.

Moreover, we analysed the expression of several p53 targets – *BAX, KILLER, PUMA* - genes in the aforementioned cell lines. After performing RT-qPCR, we could observe a significantly increased expression of PUMA in all three cell lines (Fig. 60). BAX and KILLER were significantly upregulated in only ZR-75-1 cells, suggesting that PUMA could be the main mediator of p53-dependant apoptosis in MCF7, A549 and ZR-75-1 cells (Fig. 60).

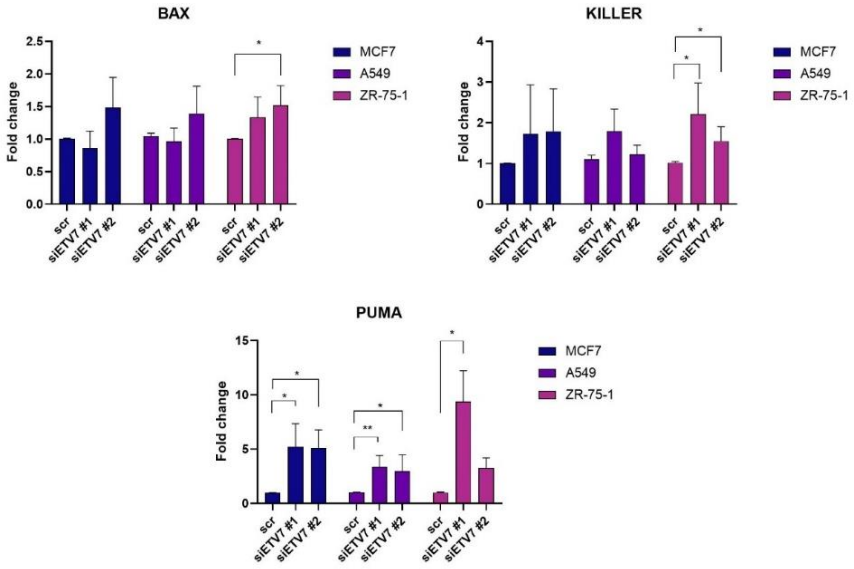

Figure 60. p53 target gene, *PUMA*, is upregulated upon the silencing of ETV7 in several cancer cell lines. RT-qPCR analysis of three p53 target genes, *BAX*, *KILLER*, *PUMA*, in ZR-75-1, MCF7 and A549 cells upon the silencing of ETV7. *p≤0.05; ** p≤0.01.

Furthermore, to confirm that p53 was responsible for the observed reduction in cell viability and apoptosis, we chose to knock-down ETV7 in HCT116 parental cell lineendogenously expressing wild-type p53 and in the available p53 knock-out HCT116 cell line. Firstly, we analyzed the cell viability upon the silencing of ETV7 in both cell lines, and we could appreciate a significant reduction in viability in the HCT116 p53 wild-type cell line, instead HCT116 $p53^{-/-}$ cells were not affected by the silencing of ETV7 (Fig. 61A). Then, to confirm that reduced viability is due to the apoptosis, we analysed the cleavage of PARP-1 in both cell lines. We detected cleaved PARP-1 only in HCT116 p53 wild-type cells (Fig. 61B), as expected, while apoptosis was not detected in HCT116 p53 $p53^{-/-}$ cells (Fig. 61C). To confirm, the involvement of p53, we analysed the accumulation of p53 in HCT116 p53 wild-type cells, which was observed upon the silencing with ETV7 targeting siRNA#1 (Fig. 61B).

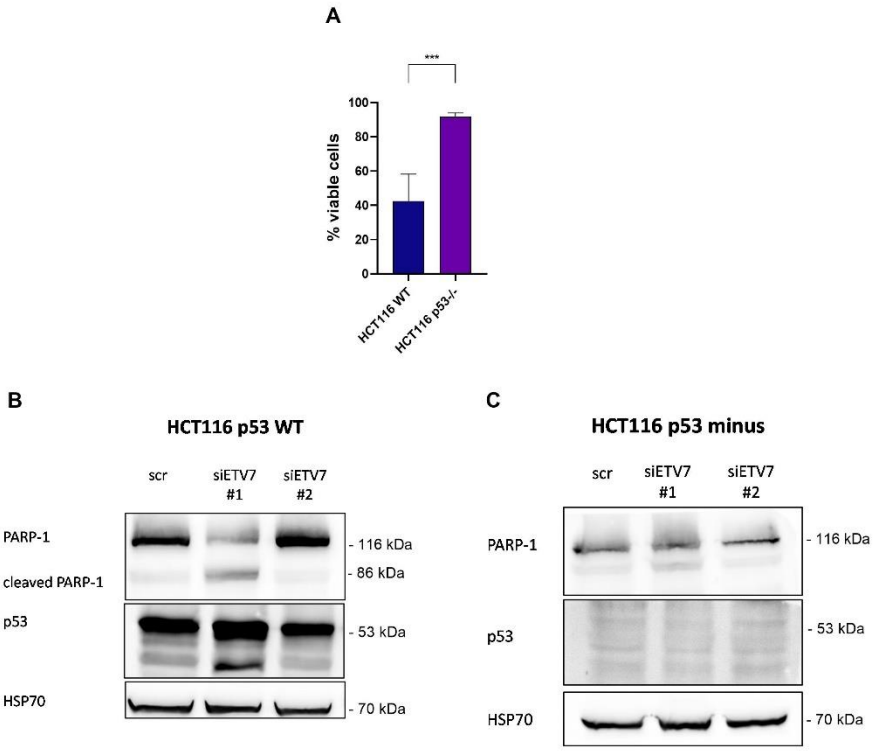

Figure 61. Apoptosis induced upon the silencing of ETV7 is p53-dependent. A) MTT cell viability assay in HCT116 p53 wild-type and HCT116 $p53^{-/-}$ cells upon the silencing of ETV7. *** $p \leq 0.001$. B-C) Western blot analysis of PARP-1 cleavage and p53 accumulation in HCT116 p53 wild-type (B) and HCT116 $p53^{-/-}$ (C) cells upon the silencing with ETV7 targeting siRNAs.

In this chapter, we were able to demonstrate that the silencing of ETV7 can induce apoptosis in the p53-wild-type context, possibly by the p53/PUMA axis.

3.5. Pro-tumorigenic potential of ETV7 *in vivo*

To validate the pro-tumorigenic potential of ETV7 *in vivo*, we decided to inject subcutaneously mouse mammary cancer cells, overexpressing ETV7 or its empty control in BALB/c mice. The choice to use the syngeneic approach instead of xenograft was dependent by the fact that ETV7 is not conserved in rodents, and performing a xenograft experiment would not be optimal due to the lack of immune component in immunodeficient mice and the much higher cost of animals. We chose to use the BALB/c mouse model as it is a simple, cost- and time-efficient model with high tumor growth rates[257] and because it was compatible with the injection of the 4T1 cell line. Firstly, we generated clones of the 4T1 mammary gland tumor cell line stably overexpressing ETV7

or its empty control. We validated the clones by Western blot analysis and could confirm the overexpression of ETV7 (Fig.62).

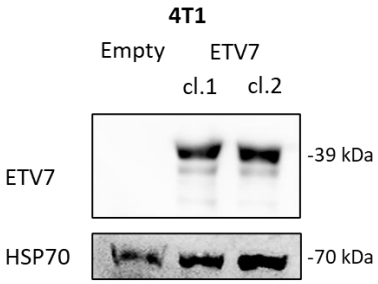

Figure 62. Western blot analysis of ETV7 in 4T1 cells overexpressing ETV7 or harboring Empty vector. HSP70 was used as a loading control.

Moreover, before starting the *in vivo* experiments, we tested if mouse cancer cell lines overexpressing ETV7 have similar characteristics to human breast cancer cells, overexpressing ETV7. Firstly, we tested the colony formation potential of ETV7 overexpressing cells in an anchorage-independent system using a soft agar assay. After three weeks of growth, we could appreciate that 4T1 ETV7 overexpressing cells formed more colonies than 4T1 Empty cells. As the anchorage-independent growth is commonly considered a pro-tumorigenic characteristic, these results suggest than 4T1 cells overexpressing ETV7 are more aggressive that 4T1 cells harboring an Empty vector (Fig. 63).

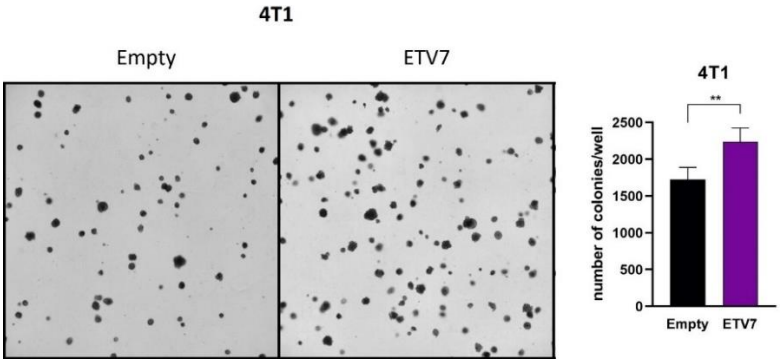

Figure 63. Overexpression of ETV7 increases proliferation potential in 4T1 cells. Soft agar colony formation assay of 4T1 Empty and 4T1 ETV7 cells after 3 weeks of growth. On the left, a representative image and on the right the average of number of colonies/ well. ** $p \leq 0.01$.

Moreover, we were also interested to confirm the role of ETV7 in the development of drug resistance. Hence, we tested the sensitivity of 4T1 Empty and 4T1 ETV7 cells to Doxorubicin and 5-fluorouracil. To analyse the viability of the cells in response to Doxorubicin and 5-FU, we measured the percentage of viable cells in response to different doses of Doxorubicin and

5-FU by performing an MTT assay. After performing these analyses, we confirmed that also in the case of 4T1, the cells overexpressing ETV7 were less sensitive to the treatment with doxorubicin and 5-FU (Fig. 64).

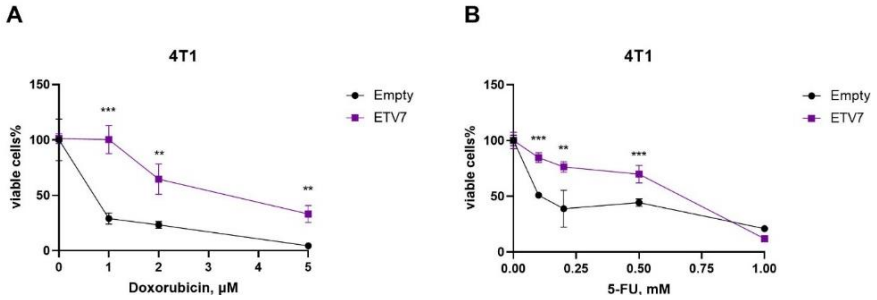

Figure 64. ETV7 affects the sensitivity of 4T1 cells to chemotherapeutic drugs. MTT assay for survival analysis upon Doxorubicin (A) and 5-FU (B) treatment in 4T1 Empty and 4T1 ETV7 cells. ** $p \leq 0.01$; *** $p \leq 0.001$.

After confirming the pro-tumorigenic features in 4T1 cells overexpressing ETV7, we progress to *in vivo* experiment. We subcutaneously injected 4T1 ETV7 or 4T1 Empty cells to five mice in each group and observed the growth of the tumor (Fig. 65A). Tumors in the ETV7 group were detected earlier. Already at day 8 from the injection, there was a palpable tumor, unfortunately, it was too small to be measured with a caliper. The growth of the tumor in both experimental groups from day 18 (when the tumor became measurable with a caliper) till day 22 is shown in figure 65B. The tumors formed from 4T1 ETV7 had significantly bigger volume at day 18, and they were approximately 1.6 times bigger than 4T1 Empty tumors. The tendency to form bigger tumors was maintained until mice were sacrificed, even though the statistical significance was not reached (Fig. 65B). After scarifying mice, tumors from both groups were dissected and weighted. Similar to the tumor size, we could observe the tendency of ETV7 overexpressing 4T1 cells to form a heavier tumor, however, the statistical significance was not reached (Fig. 65C).

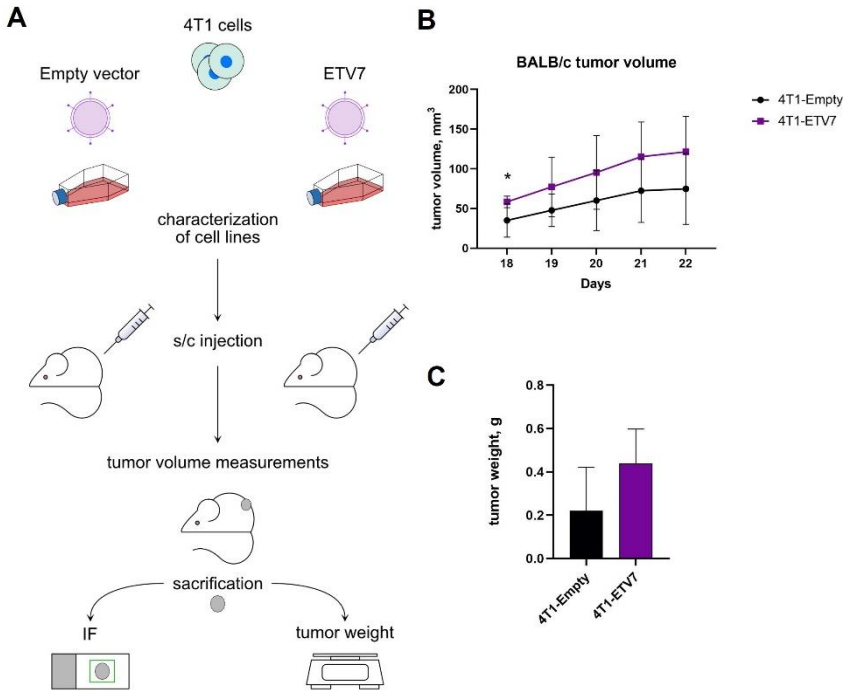

Figure 65. ETV7 enhances the pro-tumorigenic potential of 4T1 cells *in vivo*. A) Experimental flow of in vivo experiment. B) The average tumor volume in each experimental group, measured with a caliper at different time points. * $p \leq 0.05$. C) The average tumor weight in each experimental group at the end of the experiment (23rd day). One mouse in each group did not form the tumor and thus was excluded from the data analysis.

To evaluate if the overexpression of ETV7 affected the architecture of the formed tumor we stained tumors from both groups with hematoxylin and eosin. Unfortunately, we did not detect any significant changes in the architecture of the tumor (Fig.66).

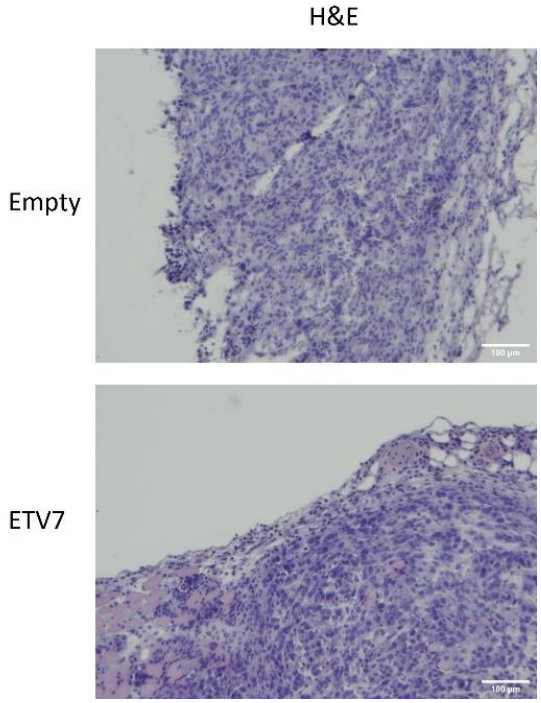

Figure 66. Histological assessments with hematoxylin and eosin (H&E) staining of tumors overexpressing ETV7 or Empty vector. Magnification 13.5X.

Moreover, we wanted to verify if the overexpression of ETV7 affected stemness, EMT, fibroblast infiltration and proliferation. We used specific markers for each of these processes: stemness – CD44, EMT – vimentin, fibroblast infiltration – α-SMA and proliferation – Ki67. After performing immunofluorescence on frozen tissues, we observed a solid increase in Ki67 in ETV7-bearing tumors, confirming higher proliferation rates upon the overexpression of ETV7 (Fig. 67).

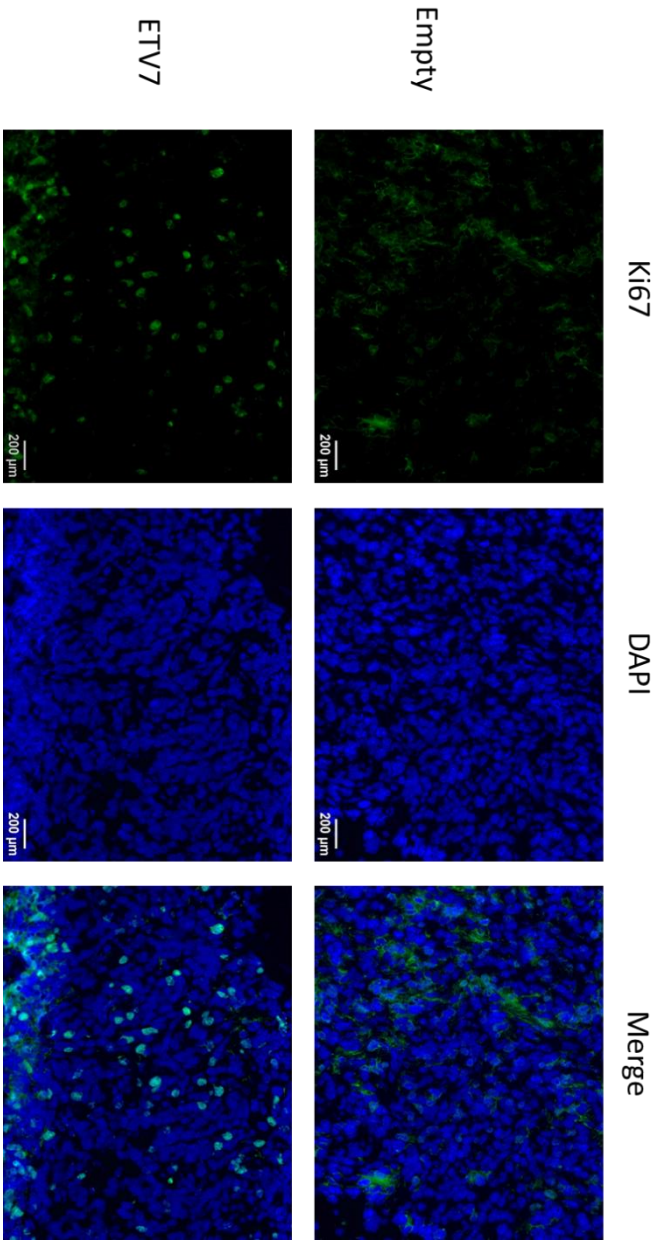

Figure 67. ETV7 increases proliferation in 4T1 tumors in mice. Immunofluorescence analysis of Ki67 on frozen tissue sections. Nuclei were counterstained with DAPI. Magnification 20X.

Furthermore, we also detected higher levels of CD44 and VIM, which are in line with our previous data, demonstrating, that ETV7 regulates stemness and cell plasticity (Fig. 68).

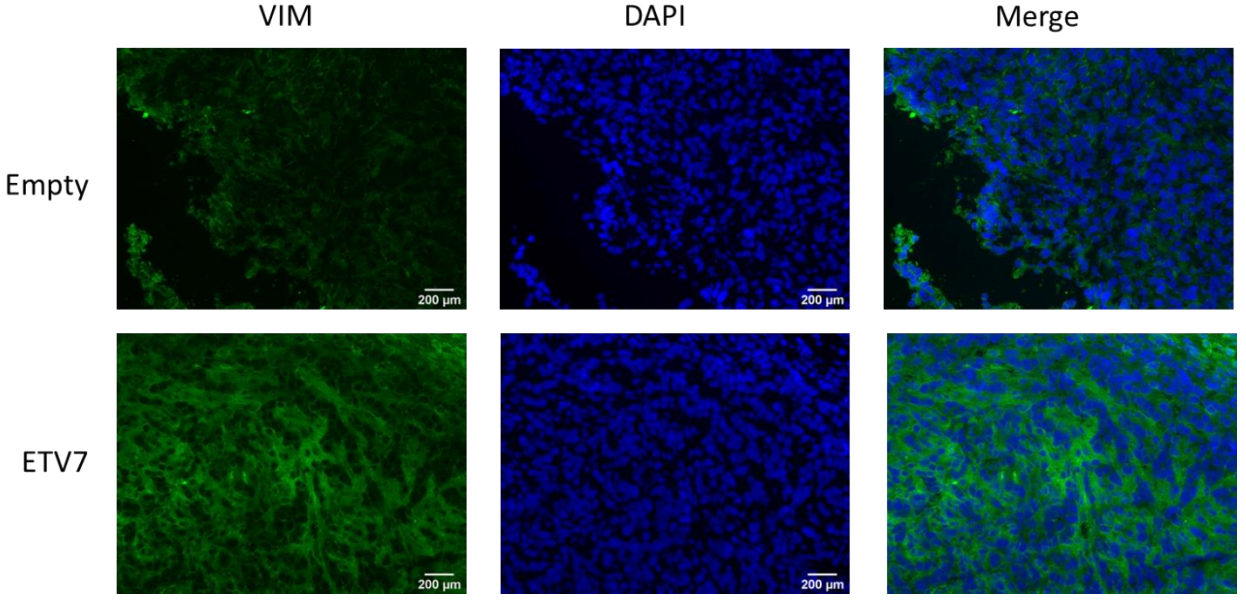
VIM
DAPI
Merge
Empty
ETV7
200 µm
200 µm
200 µm
200 µm

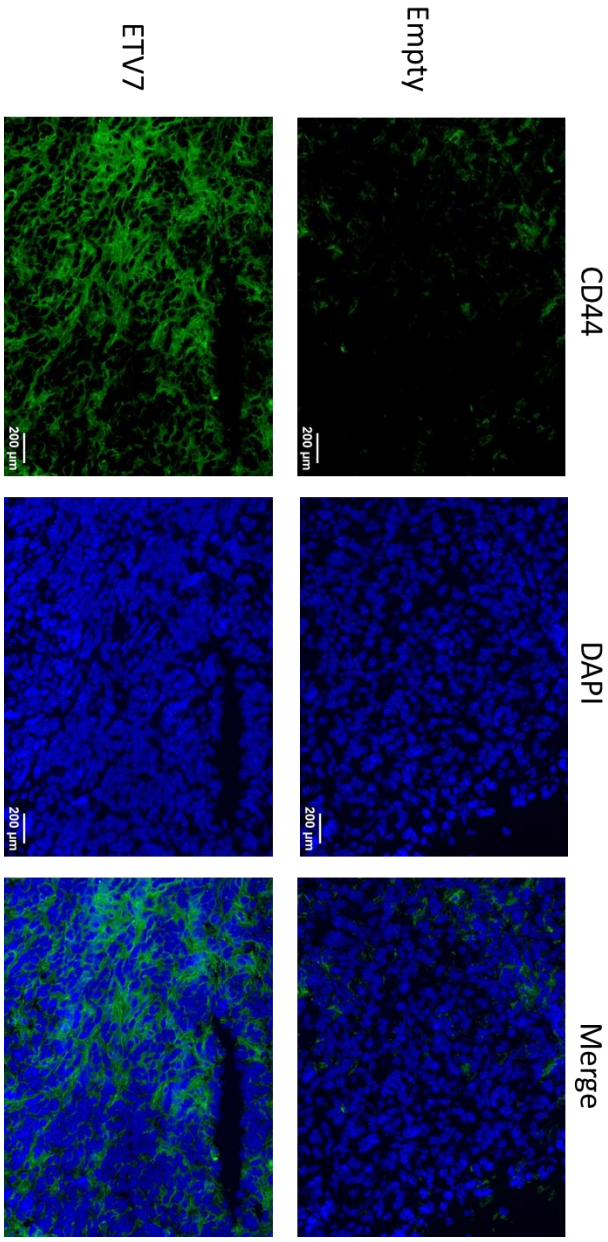

Figure 68. ETV7 increases stemness and EMT in 4T1 tumors in mice. Immunofluorescence analysis of VIM (above) and CD44 (below) on frozen tissue sections. Nuclei were counterstained with DAPI. Magnification 20X.

Finally, we could observe also a slight increase in α-SMA, suggesting that ETV7 could also affect the infiltration of fibroblast (Fig. 69).

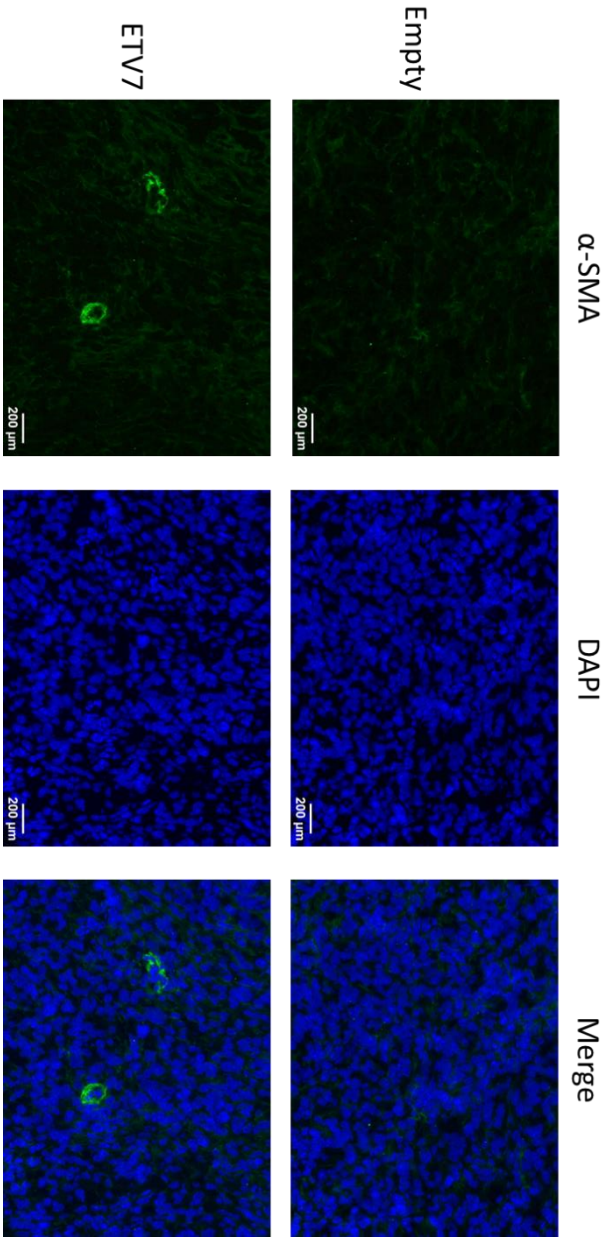

Figure 69. ETV7 increases fibroblast infiltration in 4T1 tumors in mice. Immunofluorescence analysis of α-SMA on frozen tissue sections. Nuclei were counterstained with DAPI. Magnification 20X.

Summarizing, the analysis of ETV7 pro-tumorigenic potential in mice models demonstrated, that tumors with ETV7 grew faster and bigger. Moreover, immunofluorescence analysis on frozen tissues demonstrated that ETV7 overexpressing tumors had higher levels of markers, related to tumor

aggressiveness, confirming the pro-tumorigenic potential of ETV7 also *in vivo*.

4. DISCUSSION

ETV7 is a poorly described transcriptional repressor known to be up-regulated in different types of cancer, such as breast cancer, hepatocellular carcinoma, and medulloblastoma[4,6–8,215]. In breast cancer, increased expression of ETV7 correlates with the aggressiveness of cancer[8]. Previously we demonstrated that in breast cancer cells ETV7 is upregulated upon the treatment with various DNA-damaging drugs and that this increased expression promotes resistance to chemotherapy[9,224].

Given the fact that ETV7 is associated with various types of cancer and previous data regarding its involvement in the development of chemoresistance, in this work, we studied the role of ETV7 in breast cancer aggressiveness.

In the first part of this project, we discovered that the decreased sensitivity to chemotherapeutic drugs in breast cancer cells overexpressing ETV7 is not limited to Doxorubicin[9], but is also valid for 5-fluorouracil treatment both in 2D and 3D breast cancer cellular models (Fig.14C-F, Fig.15 and Fig. 16A). Nevertheless, in further studies, the development of the resistance to 5-FU treatment should be confirmed also *in vivo*. Furthermore, from the previous studies we knew that cancer cells overexpressing ETV7 had higher levels of ABC transporters[9], additionally we observed the increase in the levels of anti-apoptotic proteins BCL-2 and Survivin, upon the overexpression of ETV7 in MCF7 cells (Fig.18). Even though the increased expression of ABC transporters, and high levels of anti-apoptotic proteins are often responsible for drug resistance[258–262], they could only partially explain why cells overexpressing ETV7 were less sensitive to the treatment with 5-FU (Fig.17 and Fig.18).

Given the fact that ETV7 showed some anti-differentiation-roles[233] and the results that demonstrated its involvement in resistance to cancer drugs, upregulation of ABC transporters and anti-apoptotic proteins are known traits of cancer stem cells[53,56,65], we decided to investigate the role of ETV7 in the regulation of cancer stem cell plasticity. We analyzed the presence of some commonly accepted markers for the identification of breast cancer stem cells, that are represented by $CD44^{+}/CD24^{-(low)}$ population and higher levels of EpCAM[82,263]. Interestingly, we observed that the overexpression of ETV7 had a remarkable effect on the breast cancer stem cell population, which increased from 1-5% in cells transduced with an empty vector to more than 30% in cells overexpressing ETV7 (Fig.19). The increase of cancer stem cells was confirmed also by the high levels of EpCAM in MCF7 and T47D overexpressing ETV7 (Fig.21). Significantly, we confirmed that the ETV7-mediated regulation of cancer stem cell population is bi-directional, as

$CD44^{+}/CD24^{low/-}$ cancer stem cell population decreases in SK-BR-3 ETV7 KO cells (Fig.20). In the future, this study could benefit from the further characteristics of ETV7 KO cells, for example by analyzing mammosphere formation efficiency or the effect of ETV7 KO on the treatment with DNA-damaging drugs. Moreover, as the analysis of markers may not be sufficient to confirm the self-renewal characteristics of cancer stem cells[89,263], we also performed mammosphere formation assay and confirmed that ETV7 overexpressing cells can successfully grow in non-adherent and non-differentiating conditions (Fig.22). Nonetheless, in the future, the acquisition of stem-like characteristics upon the overexpression of ETV7 in breast cancer cells should be confirmed also *in vivo*. The self-renewal potential of ETV7 overexpressing breast cancer cells could be validated by performing a limited dilution experiment in immunocompromised mice. Moreover, to further confirm our hypothesis limited dilution experiments *in vivo* should be also performed with ETV7 KO cells.

Furthermore, we observed a significant repression of a set of Interferon-stimulated genes (ISGs) in cells overexpressing ETV7 (Fig. 23). The repressed interferon signaling could explain the increase in the cancer stem cell population upon the overexpression of ETV7, as previous studies have demonstrated that immune-repressed triple-negative breast tumors, lacking endogenous interferon/STATs signaling are resistant to chemotherapy, highly recurrent and are enriched in cancer stem cells[264,265]. Moreover, the prolonged treatment with IFN-β could reduce the ETV7-mediated increase in the BCSC population [247]. Hence, future investigation of the molecular mechanism by which ETV7 regulates ISGs is needed. There are several potential mechanisms for how ETV7 might regulate the expression of ISGs. As a transcriptional repressor ETV7 could directly downregulate these genes by acting on their regulatory regions, on the other hand, during this study we also observed that ETV7 represses several other pathways, such as STAT or NF-κb and hence indirectly repress interferon response. Moreover, it would be particularly interesting to confirm our findings, relative to the development of 5-FU resistance due to the repression of ISGs and increase in BCSCs, *in vivo*. This could be achieved by performing experiments in mice, where control or ETV7-overexpressing cells are injected into mice and after the formation of the tumors, mice would be treated with 5-FU or combination with 5-FU and interferons. The results acquired during this experiment could be beneficial for the more translational application of our findings.

The involvement of ETV7 in the regulation of interferon-stimulates genes and the previously published data showing that ETV7 has a role in the viral immune response by suppressing a subset of ISGs that are important in controlling Influenza viruses[11,12], suggest that ETV7 is an important novel player in the regulation of immune response. However, the role of ETV7 in BC immune processes is still to be studied. Hence, in the second and third parts of this project, we studied the role of ETV7 in breast cancer

inflammatory and immune responses. The RNA-seq analysis previously performed on the breast cancer-derived cells MCF7 and T47D over-expressing ETV7 or its empty control demonstrated the involvement of ETV7 in inflammation and immune responses (Fig. 25). After validating several putative targets - *TLR2, TNFRSF1A, IL1R1, IL10RB*, which are involved in inflammatory and immune processes[266–268] – and confirming their downregulation in ETV7 overexpressing cells (Fig. 26), we focused on the regulation of the *TNFRSF1A* gene expression (Fig. 27).

In this part of the study, we demonstrated that the *TNFRSF1A* gene was significantly down-regulated by ETV7 at mRNA and protein levels both in MCF7 and T47D cell lines (Fig. 27). We also confirmed the transcriptional repression of *TNFRSF1A* in other breast cancer-derived cell lines, such as MDA-MB-231 and SK-BR-3 upon transient over-expression of ETV7 (Fig. 27). Furthermore, were able to demonstrate that the regulation of *TNFRSF1A* is bi-directional and that the silencing of ETV7 restored the expression of *TNFRSF1A* in several breast cancer-derived cellular models (Fig. 28). Moreover, we confirmed the lower *TNFRSF1A* expression in breast cancer tissue compared to normal breast tissues (from TCGA; Fig. 30) and this reduced expression of *TNFRSF1A* correlated with a worse prognosis (Fig. 30), which suggests the potential translational relevance of our observations. We also demonstrated that *TNFRSF1A* repression involves the direct binding of ETV7 to the Intron of *TNFRSF1A*, and we identified three ETV7 binding sites in this region (Fig. 31). Furthermore, we showed that ETV7 not only binds to the regulatory region of *TNFRSF1A* but also recruits chromatin remodelers responsible for heterochromatin - less accessible chromatin (i.e., HDACs and specific histone methyltransferases) (Fig. 32). This observation is consistent with the previously known information about ETV7 and chromatin remodelers, published by Boccuni and colleagues[269]. They demonstrated that ETV7 can interact with H-L(3)MBT, a component of the Polycomb repressive complex, confirming the role of ETV7 in the modulation of chromatin status[269].

TNFRSF1A encodes for Tumor Necrosis Factor Receptor 1 (TNFR1), one of the most important transmembrane receptors for TNF-α[153]. By binding to the TNFR1 receptor, TNF-α activates NF-κB signaling, a group of transcription factors including RelA/p65, RelB, c-Rel, p50, and p52[153,270–272]. NF-κB is involved in the regulation of several key cellular processes, such as proliferation, cell death, survival, and cellular homeostasis[271]. Furthermore, an essential function of NF-κB is the control of the immune response. Indeed, NF-κB regulates the expression of different genes involved in both innate and adaptive immune responses, as well as inflammation[272,273].

According to the literature, TNFR1 is crucial for the activation of the NF-κB signaling pathway[153]; therefore, we aimed to understand if the ETV7-mediated repression of *TNFRSF1A* also affects the activation of NF-κB. We demonstrated that in breast cancer cells over-expressing ETV7, the repression

of *TNFRSF1A* reduced the activation of NF-κB both in the basal state and upon the stimulation with TNF-α (Fig. 33). The ETV7-mediated reduction in NF-κB signaling was stronger in MCF7 cells compared with T47D cells, as T47D cells were globally less responsive to TNF-α. We hypothesize that this reduced responsiveness to TNF-α is due to already high endogenous NF-κB activity in T47D cells. The reduced activity of NF-κB was also confirmed by lower levels of phosphorylated IκBα, which is important for releasing NF-κB members from the inactive complex in cytoplasm[274] (Fig. 36) and following diminished nuclear translocation of p65 (Fig. 37, Fig. 38 and Suppl. Fig. 1D) in cells over-expressing ETV7. Moreover, the reduced activation of NF-κB led to the downregulation of several NF-κB target genes IL-8, IL-6, A20, and TNF-α, which are well-known to be involved in the inflammatory processes, indicating reduced inflammatory and immune processes (Fig. 34)[248,275,276]. Importantly, this regulation was bi-directional, as the expression of these NF-κB targets was restored upon the silencing of ETV7 (Fig.35). Clearly, the reduced inflammatory and immune responses could be confirmed only after the validation of the secretion of pro-inflammatory cytokines or chemokines. With ELISA assay on the supernatant of cells overexpressing ETV7, we confirmed the reduced release of IL-6 and IL-8 pro-inflammatory cytokines even in response to TNF-α stimulation (Fig.39 and Fig.40), confirming that ETV7 can reduce the inflammatory response. Furthermore, we demonstrated that the introduction of ectopic TNFR1 into our cellular systems, could at least partially restore the NF-κB activity in cells overexpressing ETV7 (Fig. 41). This partial rescue could be due to the fact that ETV7 also downregulates other elements, such as Toll-like receptor 2 or IL-1 receptor 1 (Fig. 26), that are also involved in the activation of NF-κB[272,277].

Interestingly, STAT3, another master regulator of inflammatory and immune responses, induces NF-κB activation via up-regulation of *TNFRSF1A*, specifically by directly binding to its first intron, the same regulatory region, we demonstrated to be bound by ETV7 (Fig.31)[248]. However, in our breast cancer cell lines overexpressing ETV7, we could not observe this STAT3-mediated regulation of *TNFRSF1A*, even upon the activation of STAT3 (Fig.45), indicating that there is a potential competitive relationship between ETV7 and STAT3 in the regulation of *TNFRSF1A*.

Given that the DNA-binding motifs of STAT3 and ETV7 are similar (i.e., TTCCCGGAA and CA/CGGAAGT, respectively[203,214,216,252,278], we looked for possible binding sites for ETV7 in the first intron of the *TNFRSF1A* gene that could also be used by STAT3 (Fig.43). By performing chromatin immunoprecipitation, we demonstrated that ETV7 can reduce the binding of STAT3 to the Intron 1 of TNFRSF1A, confirming our hypothesis that ETV7 competes with STAT3 when the binding sites are close to each other (Fig.46 and Fig. 49). To confirm further the competition between ETV7 and STAT3 in the regulation of the *TNFRSF1A* gene, a reporter assay could be performed in cancer cells over-expressing ETV7 using a reporter vector containing the

first intron of the *TNFRSF1A* gene. Based on our data, we propose a novel regulatory mechanism for *TNFRSF1A* (Fig.51*)*. In the context of high ETV7, e.g. upon the treatment with DNA-damaging drugs, ETV7 represses *TNFRSF1A* through the displacement of STAT3 (a positive regulator) from *TNFRSF1A* Intron 1, rendering chromatin less accessible; this repression leads to the significant reduction of NF-κB activity, hence reduced inflammatory and immune responses.

Our findings discussed in the first and second chapters strongly suggest that ETV7 represses several pathways related to immune response, such as interferon or inflammatory responses. Logically, arises the question, why the downregulation of these pathways is beneficial for cancer cells. It is known that the role of NF-κB in tumor cells and tumor microenvironment is double-edged and depends on the tumor context[279,280]. It is widely reported that NF-κB target genes control several pro-tumorigenic processes such as proliferation, cell survival, angiogenesis, and invasion. Additionally, NF-κB sustains tumor-associated chronic inflammation by producing chemokines and cytokines[281]. However, more and more studies show the role of NF-κB as a tumor suppressor, particularly important in regulating the anti-tumor immune response. Hence, we hypothesize that the ETV7-mediated reduced activation of NF-κB could help cancer cells evade the host immune response, as proper stimulation is essential for both innate and adaptive immune responses[281]. It is known that NF-κB controls the mRNA expression and protein stability of PD-L1 in tumor cells, thereby inhibiting the activity of cytotoxic CD8+ T cells[282,283]. Besides, a study in the pancreatic ductal carcinoma mouse model shows that TNF and TNFR1 are required for an optimal functioning of cytotoxic CD8+ T and tumor rejection[279,283]. Furthermore, reduced activation of NF-κB leads to the loss of MHC-I expression, which is one of the most important mechanisms of immune evasion in cancer[136,181]. The loss of MHC-I results not only in immune evasion but also in reduced sensitivity to immunotherapy[284]. Interestingly, also the repression of the interferon signaling leads to impaired antigen presentation via MHC class I[136,181]. ETV7-mediated repression of two important transcriptional regulators of antigen presentation, suggested that ETV7 could be a novel player in cancer immune evasion.

We confirmed that ETV7 downregulated both at mRNA and protein levels elements involved in antigen presentation (Fig.52, Fig.53, and Suppl. Fig. 1E). Moreover, the same result was also confirmed upon the stimulation of IFN-γ, which induces the antigen presentation via MHC I[256], suggesting that the ETV7-mediated impairment of antigen presentation cannot be simply restored by the stimulation with interferon-gamma (Fig. 55). Importantly, the downregulation of antigen presentation machinery was also confirmed in mammospheres, that have an enriched population of cancer stem cells (Fig. 54). These results can provide a bigger picture of ETV7-mediated effects to breast cancer aggressiveness, suggesting that the overexpression of ETV7

leads to an increase in cancer stem cell population, which are not only more resistant to chemotherapeutic treatment but also have an enhanced immune evasion. Moreover, as the downregulation of antigen-presenting elements not only affect cancer cell clearance by T cell, but also reduces the effectiveness of immunotherapies, the role of ETV7 in modulating response to the immunotherapy should be further investigated. For example, breast cancer cell lines overexpressing ETV7 could be co-cultured with PBMCs-derived T cells using 3D models and then treated with known checkpoint inhibitors (e.g. atezolizumab, ipilimumb etc.) and observed changes (e.g. spheroid size, viability) evaluated.

Furthermore, as ETV7 regulates the expression of various soluble molecules (such as chemokines, cytokines, etc.) it would be interesting to understand the role of ETV7 in orchestrating tumor microenvironment. Exploring the impact of ETV7-overexpressing breast cancer cells on tumor-associated macrophages could be a promising novel direction for this study. For example, we could co-culture ETV7-overexpressing breast cancer cells with resting macrophages and observe if overexpression of ETV7 could affect the polarization of macrophages towards pro-inflammatory (M1) or anti-inflammatory (M2) status.

Our results indicate that ETV7 is an important player in breast cancer aggressiveness, suggesting that it could be a potential target for the treatment of breast cancer. After validating the effects of ETV7-silencing in a panel of cancer cell lines, we observed that the silencing of ETV7 can induce apoptosis in wild-type p53 context, suggesting that ETV7 is fundamental for the survival in p53 wild-type cancer cells, however, is less crucial when p53 is mutated (Fig.56, Fig.57, Fig.58 and Fig.59). Since p53 is frequently mutated in breast cancer patients (*TP53* is mutated in 30% of breast cancer patients)[285], it is not clear if direct targeting of ETV7 may be the best option for the treatment of these patients. However, it could be still beneficial for tumor with wild-type p53. Moreover, silencing of ETV7 in p53-mutated breast cancer lines, even if not killing them, almost always reverted the ETV7-dependent phenotypes (Fig.24, Fig. 28, and Fig.35), suggesting that ETV7 targeting could be useful for cancer patients. It is important to mention, that the direct targeting of ETV7 can be challenging, due to the similarity to another member of the ETS family, ETV6, which works insead as tumor suppressor[215].

Finally, we tested a pro-tumorigenic potential of ETV7 also *in vivo.* We generated a mouse mammary gland tumor cell line (4T1) overexpressing ETV7 or control vector and injected them subcutaneously into BALB/c mice (Fig.62 and Fig.65). By observing tumor growth dynamics, we could appreciate that the tumor formed from ETV7 overexpressing 4T1 cells were bigger. Even though the statistical significance was reached only at the beginning of tumor formation, the tendency to form bigger tumors was maintained throughout the whole experiment (Fig.67). The slight difference and not statistically significant differences could be explained by the fact that

4T1 is already very aggressive cancer cell line[286], hence it is more difficult to observe further increase in the aggressiveness. Immunofluorescence analyses on the frozen tumor sections, confirmed that ETV7 overexpressing tumors were more aggressive, as we observed higher levels of the proliferation marker Ki67[287] (Fig.67), increased stemness and EMT markers – CD44 and VIM, respectively[288,289] (Fig.68) and elevated levels of fibroblast infiltration marker α-SMA[290,291](Fig.69). In summary, *in vivo* experiments performed in this study are still very preliminary, however acquired results suggest that ETV7 has a pro-tumorigenic potential *in vivo*. Clearly, in the future, a deep further in vivo study should be performed to be able to confirm these finds. There are different aspects that should be further validated using mouse models. As ETV7 seems to play an important role in the regulation of immune response, evaluation of immune cell infiltration in control tumors and tumor formed by ETV7-overexpressing cells should be performed. Moreover, further understanding of ETV7's role in breast cancer progression and metastasis formation should be investigated. For example, using the syngeneic mouse model, tumors formed by control or ETV7-overexpressing cells can be surgically removed and metastasis growth observed over a period of time, mimicking the situation in human patients.

Taken collectively, the data acquired during this project confirm the role of ETV7 as an important regulator of breast cancer aggressiveness both *in vitro* and *in vivo*, and propose ETV7, as a novel player in breast cancer immunity, opening a new research direction and giving useful insights for more effective therapeutic strategies.

CONCLUSIONS

1. ETV7 represses a large panel of interferon response genes and increases cancer stem-like cell plasticity, leading to resistance to 5-fluorouracil.
2. ETV7 displaces STAT3 from the regulatory region of *TNFRSF1A* and represses TNFR1/NF-κB axis, suggesting that ETV7 could reduce pro-inflammatory responses.
3. ETV7 downregulates genes involved in the antigen-presenting pathway, which could potentially lead to cancer immune evasion.
4. The silencing of ETV7 in cancer cells induces p53-dependent apoptosis.
5. Preliminary data suggest, that ETV7 could enhance breast cancer aggressiveness also *in vivo*.

SANTRAUKA

Įvadas

2020 metais krūties vėžys buvo dažniausiai pasaulyje diagnozuotas vėžio tipas (11.7% visų atvejų, iš viso 2,3 naujų atvejų 2020 metais). Moterų tarpe krūties vėžys yra dažniausiai diagnozuojamas vėžys, kurio mirtingumas išlieka aukštas[1]. Nepaisant progreso ankstyvojoje diagnostikoje ir gydyme bei pakankamai didelio išgyvenamumo, krūties vėžio gydymas išlieka sudėtingu, nes vėžinės ląstelės dažnai tampa atsparios gydymui ir metastazuoja, kas dažniausiai lemia paciento mirtį. Dėl to yra ypatingai svarbu nuolatos gilintis į krūties vėžio biologiją ir ieškoti naujų galimų taikinių krūties vėžio gydymui[2,3]. Šio tyrimo centre yra ETV7, prastai chrakterizuotas transkripcijos slopiklis, kurio raiška yra padidėjusi daugelyje vėžio tipų[4–8]. Krūties vėžio atveju, ETV7 raiška teigiamai koreliuoja su naviko agresyvumu[8]. Literatūroje yra aprašyta, kad krūties vėžio ląstelėse, ETV7 raiška padidėja jas veikiant įvairiais DNR pažaidas sukeliančiais vaistas ir ši padidėjusi ETV7 raiška lemia atsparumo chemoterapijai išsivystymą[9,10]. Svarbu paminėti, kad interferonai taip pat stimuliuoja ETV7 raišką[11]. Be to, neseniai buvo pademonstruota, kad ląstelėse užkrėstose gripo virusu, ETV7 slopina su interferonų atsaku susijusiu genų raišką ir tokiu būdu padeda virusu užkrėstoms ląstelėms išvengti šeimininko imuninio atsako[12]. Interferoninis atsakas yra taip pat labai svarbus naviko ir imuninės sistemos sąveikos reguliatorius[13,14]. Šie literatūroje pateikti duomenys bei mūsų laboratorijoje gauti preliminarūs duomenys sufleruoja, kad ETV7 skatina krūties vėžio agresyvumą ir kad ETV7 galėtų būti naujas krūties vėžio imuniteto reguliatorius.

Tikslas ir uždaviniai

Šio darbo tikslas yra identifikuoti ETV7 transkripcijos veiksnio vaidmenį krūties vėžio agresyvume ir vėžio imunitete.

Šio darbo uždaviniai:

1. Identifikuoti, ETV7 įtaką atsparumo 5-fluorouracilo vystumuisi bei krūties vėžio ląstelių plastiškumo reguliacijai.
2. Ištirti, ETV7 vaidmenį krūties vėžio uždegiminiuose procesuose.
3. Tirti, kokią įtaką ETV7 turi krūties vėžio imunitetui.
4. Įvertinti, ETV7 nutildymo poveikį vėžinėms ląstelėms.
5. Patvirtinti, ETV7 poveikį navimų formavimuisi *in vivo* modeliuose.

Aktualumas ir naujumas

Nors padidėjusi ETV7 raiška yra aptinkama daugelyje vėžio tipų, tikslios ETV7 funkcijos vėžio agresyvumo vystymesi nėra detaliai charakterizuotos. Šis tyrimas yra pirmas tyrimas, kuris tiria ETV7 vaidmenį krūties vėžio

kamieninių ląstelių populiacijos reguliacijoje. Be to, iki šios nėra atlika tyrimų, kurie vertintų ETV7 poveikį vėžio imunitetui, dėl to šis tyrimas yra pirmasis tyrimas, kuris tiria, kaip ETV7 padeda vėžiui išvengti šeimininko imuninio atsako. Svarbu paminėti, kad graužikai neturi *ETV7* geno, dėl to praktiškai nėra atlikta su ETV7 susijusių *in vivo* tyrimų. Šiame tyrime pirmą kartą bus tiriamas ETV7 potencialas formuoti pieno liaukos navikus pelės.

Medžiagos ir metodai

Ląstelių linijos

In vitro tyrimamas buvo naudotos įvairios žmogaus krūties vėžio bei kitų tipų vėžio ląstelių linijos, tuo tarpu *in vivo* tyrimui buvo panaudota pelės pieno liaukos naviko ląstelių linija 4T1. MCF7, T47D, SK-BR-3, ir HUH-7 ląstelės buvo kultivuojamos DMEM terpėje, papildytoje 10% jaučio embriono serumu, 2mM L-glutamino bei 100 U/ml penicilino ir 100 µg/ml streptamicino mišiniu. MDA-MB-231 ląstelės buvo kultivuojamos toje pačioj terpėje, į kurią papildomai buvo pridėta 1% nebūtinųjų amino rūgščių. 4T1, A549, HCT166, HCC70, HCT116 p53 KO, H460, SJSA1, U2OS, H1975, H1299, BT-549 ir ZR-75-1 ląstelės buvo auginamos RPMI terpėje, papildytoje 10% jaučio embriono serumu, 2mM L-glutamino bei 100 U/ml penicilino ir 100 µg/ml streptamicino mišiniu. BT-549 ląstelių terpė taip pat buvo papildyta 1% insulino-transferino-selenio mišiniu, o ZR-75-1 ląstelių terpė buvo papildyta 1% natrio piruvatu. Ląstelės buvo kultivuojamos 37°C temperatūroje, 5% CO_2, drėkinamoje aplinkoje. Ląstelėms buvo reguliariai atliekamas mikoplazmų tyrimas.

Stimuliacija ir poveikis vaistais

Priklausomai nuo eksperimento, ląstelės buvo paveikiamos įvairiomis 5-fluorouracilo ir doksirubicino koncentracijomis, įvairias laiko tarpais. MCF7 ir T47D ląstelės buvo paveikiamos 20 ng/ml IL-6 ir atitinkamai 10 ng/ml arba 20 ng/ml TNF-α. Stimuliacijos trukmė priklausė nuo eksperimento tipo: baltymų išskyrimui – 1 valanda, RNR analizei, genų-reporterių tyrimui ir chromatino imunoprecipitacijai – 4 valandos, o ELISA tyrimui – 24 valandos. Ląstelių stimuliacijos trukmė 20 ng/ml rekombinantiniu žmogaus IFN-γ priklausė nuo eksperimento tipo.

ETV7 nutildymas

ETV7 buvo nutildytas naudojant dvi prieš ETV7 nukreiptas siRNR bei transfekcijos reagentą INTERFERin®. 24 valandas prieš prieš transfekciją ląstelės buvo išsėtos į 6 arba 96 šulinėlių plokšteles. Po to, kiekviename šulinėlyje esančios ląstelės buvo transfekuotos 20 nM siRNR ir 7 µl (arba 0.75 µl, priklausomai nuo plokštelės) INTERFERin reagentu. Transfekcijos mišinys buvo atskiedžiamas 200 µl (arba 50 µl) OptiMEM terpės, gerai

sumaišomas ir inkubuojamas 15 min kambario temperatūroje ir lėtai užpilamas ant ląstelių. Transfekuotų ląstelių analizė buvo atliekama praėjus 72 valandoms po transfekcijos.

Western blot analizė

Baltymai iš ląstelių buvo išskirti naudojant RIPA buferinį tirpalą (150mM natrio chloridas, 1,0% NP-40, 0,5% natrio deoksicholatas, 0,1% SDS ir 50mM Tris-HCl pH 8,0) papildytą proteazių inhibitoriais. Baltymų koncentracija buvo įvertinta naudojant BCA metodą. Į 8%, 10% ir 12 % poliakrilamido gelio šulinėlius buvo suleista po 25-50 µg baltymų lizato ir baltymai buvo atskirti pasitelkiant dodecil sulfato-poliakrilamido gelių eletroforezę (SDS-PAGE). Po atskyrimo, baltymai buvo perkelti ant nitroceliuliozinės membranos ir membranos buvo inkubuojamos per naktį 4°C temperatūroje su specifiniais pirminiais antikūnais, atskiestais naudojant 1-3% nugriebto pieno-PBS-0.1% Tween tirpalą. Naudoti pirminiai antikūnai: TNFR1 (H-5, Santa Cruz Biotechnologies, DBA, Milan, Italy), STAT3 (124H6, Cell Signaling Technologies, Euroclone, Milan, Italy), pSTAT3 (Y705, Cell Signaling Technologies), HSP70 (C92F3A-5, Santa Cruz Biotechnologies), TEL2 (E-1, Santa Cruz Biotechnologies), GAPDH (6C5, Santa Cruz Biotechnologies), pIKBα (Ser32/36, Santa Cruz Biotechnologies), p53 (DO-I, sc-126, Santa Cruz Biotechnologies), α-actinin (H2, sc-17829, Santa Cruz Biotechnologiesm), BCL-2 (100, sc-509, Santa Cruz Biotechnologies), Survivin (D-8, sc-17779, Santa Cruz Biotechnologies), EpCAM (ab71916, Abcam, Cambridge, UK), β-Tubulin (3F3-G2, sc-53140, Santa Cruz Biotechnologies), H3 (ab18521, Abcam), B2M (BBM.1, sc-13565, Santa Cruz Biotechnologies), PARP-1 (46D11, Cell Signaling Technologies), LMP-2 (G-3, sc-373996, Santa Cruz Biotechnologies), LMP-7 (A-12, sc-365699, Santa Cruz Biotechnologies), IRF-1 (E-4, sc-514544, Santa Cruz Biotechnologies). Po to, membranos buvo plaunamos ir inkubuojamos su antriniais antikūnais. Signalas buvo nustatomas pasitelkiant ECL Select reagentą ir naudojant ChemiDoc XRS+ (BioRad) arba UVITec Alliance LD2 vizualizacijos sistemą.

RNA išskyrimas ir kiekybinė tikro-laiko polimerazės grandininė reakcija (RT-qPCR)

RNA buvo išskirta naudojant RNeasy® Mini, RNeasy® Mini Plus arba NucleoSpin RNA rinkinius. Atvirkštinė transkripcija buvo atlikta naudojant PrimeScriptTM RT rinkinį. RT-qPCR buvo atlikta naudojant qPCRBIO SyGreen 2X mišinį, CFX384 Biorad arba QuantStudio™ 5 tikro-laiko PGR termocikleryje. *YWHAZ*, *ACTB ir GAPDH* buvo panaudoti kaip endogeninė kontrolė, genų raiško skirtumas buvo įvertintas taikant ΔΔCt metodą[238].

Chromatino immunoprecipitacija (ChIP)

Chromatino imunoprecipitacijai ląstelė buvo kultivuojamos įprastomis sąlygomis. Atlikus visas reikiamas stimuliacijas, ląstelės buvo fiksuojamos 8 min, naudojat 1% formaldehidą. Pasibaigus inkubacijai, formaldehido veikimas buvo inhibuojamas 125 mM glicino tirpalu. Po to ląstelės buvo gerai nuplaunamos lediniu PBS tirpalu ir surenkamos į 1 ml PBS tirpalo, papildytą proteazių inhibitoriais. Po to ląstelės buvo lizuotos ir surinkti ląstelių banduoliai, kurie buvo paveikti ultragarsu, kad būtų gaunami 200-700 bp ilgio DNR fragmentai. Taip paruoštas mėginys buvo atskiedžiamas, sumaišomas su 2 µg atitinkamo antikūno (ETV7 (Santa Cruz, TEL2, E-1), pSTAT3 (Cell Signaling Technologies, 124H6), H3K9me3 (Cell Signaling Technologies, 13969P), H3K4me3 (Abcam, ab8580), H3ac (Abcam, ab47919)) arba IgG (pelės arba triušio, priklausomai nuo naudoto antikūno) ir Dynabeads magnetinėmis dalelėmis sujungtomis su G arba A baltymu. Šis mišinys buvo inkubuotas per naktį, 4°C temperatūroje, rotuojant. Kitą dieną mėginiai buvo gerai nuplauti atliekant įvairius plovimus ir DNR buvo išskirta naudojant išskyrimo tirpalą. Kiekybinė PGR buvo atlikta naudojant GoTaq® qPCR Master mišinį ir BioRad CFX384 qPCR sistemą.

Reporterinio vektoriaus tyrimas

Ląstelės buvo pasėtos į 24 šulinėlių plokštelę ir po 24 valandų transfekuojamos su Lipofectamine LTX ir Plus transfekcijos reagentais bei atitinkamomis plazmidžių kombinacijomis. Priklausomai nuo eksperimento: 50 ng normalizacijos vektoriaus pRL-SV40, 200 ng raiškos vektoriaus (pcDNA3.1-Empty/pcDNA3.1-TNFR1) ir reporterinio vektoriaus - 350 ng 4xM67 pTATA TK-Luc arba 300 ng pGL3-NF-κB. Praėjus dvidešimt keturioms valandoms po transfekcijos, jeigu reikėjo, ląstelės buvo stimuliuojamos įvairias citokinais. Po to, ląstelės buvo nuplaunamos su PBS tirpalu ir lizuojamos naudojant Promega PBL (pasyvios lizės) tirpalą. Luciferazės aktyvumas buvo išmatuotas naudojant Dual-Luciferase Reporter Assay sistemą, laikantis gamintojo nurodymų. Chemiliuminescencija buvo nustatoma naudojant Varioskan LUX multimode plokštelių skaitytuvą. *Renilla* luciferazės aktyvumas buvo naudojamas kaip transfekcijos efektyvumo indikatorius.

Sferoidų formavimas

Tam, kad ląstelės formuotu daugialąstelinius sferoidus, 96 šulinėlių plokštelės buvo padengtos 1,5% agaroze. Siekiant po 72 valandų užauginti suformuotus sferoidus, į šulinėlius buvo sėjama po 5000 T47D ląstelių. Suformuoti sferoidai buvo veikiami vaistais ir vaistų poveikis buvo vertinamas praėjus 72 valandoms. Nuotraukos buvo daromos su 10X padidinimu, o duomenys buvo analizuojami naudojant ImageJ programą.

Mamosferų kultivavimas

Mamosferos buvo formuojamos pasitelkiant anksčiau publikuotą protokolą[88]. Tam, kad suformuotų pirmines mamosferas, ląstelės buvo atkeliamos, suskaičiuoamos ir perkeliamos į mamosferoms tinkamą terpę (DMEM/F12 papildytą 20 ng/ml rekombinantiniu žmogaus augimo faktoriumi (EGF), 10ng/ml rekombinantiniu žmogaus baziniu fibroblastų augimo faktoriumi (bFGF), 1X B27 papildu, 2mM L-glutaminu ir 100U/ml penicilinu ir 100µg/ml streptomicinu) Tam, kad būtų gauta pavienių ląstelių suspencija, ląstelės buvo sumaišomos naudojant 25G adatą ir sėjamos į mažo prikibimo plokšteles. Mamosferos buvo auginamos inkubatoriuje vieną savaitę, jų nejudinant. Mamosferų formavimo efektyvumas buvo įvertintas pagal šią formulę: MFE(%) = (# mamosferų skaičius šulinėlyje) / (# sėtų ląstelių skaičius) x 100.

Ląstelių gyvybingumo analizė

Ląstelių gyvybingumas buvo vertinamas pasitelkiant MTT arba Cell Titer Glo metodus. Abiejų tipų analizės buvo atliekamos pagal gamintojo protokolą. Absorbcija buvo matuojama naudojant Varioskan LUX multimode plokštelių skaitytuvą. Kiekvienos eksperimentinės grupės absorbcijos vertė buvo pateikta procentine išraiška, lyginant su kontroline grupe.

Apotozės vertinimas tėkmės citometru, naudojant Aneksino V antikūną ir propidžio jodidą

Apotozė buvo vertinama naudojant BD FITC Annexin V Apoptosis Detection rinkinį. Atlikus reikiamas manipuliacijas, ląstelės buvo nuplaunamos, surenkamos ir suspenduojamos naudojant Annexin V surišimo buferinį tirpalą taip, kad ląstelių koncentracija būtų $1,5 \times 10^6$ ląstelių/ml. Tada, 100 µl ląstelių suspencijos buvo inkubuojama su 2,5 µl FITC-Annexin V antikūno ir 5 µl propidžio jodido 15 minučių, kambario temperatūroje, tamsoje. Po to mėginiai buvo atskiedžiami pridedant 400 µl Annexin V surišimo buferinio tirpalo ir analizuojami. Tėkmės citometrijos analizė buvo atlikta CIBIO Cell Analysis and Separation Core Facility, naudojant FACS Canto A prietaisą.

CD44/CD24 žymenų nustatymas tėkmės citometru

CD44 ir CD24 žymenys, esantys ląstelės paviršiuje buvo nustatomi atliekant dvigubą žymėjimą, su fluoroforais pažymėtais antikūnais ir atliekant tėkmės citometriją. Ląstelės buvo sėjamos į plokšteles su 6 šulinėliais, atlikus visas reikiamas manipuliacijas, ląstelės buvo surenkamos ir nuplaunamos su PBS tirpalu. 3×10^5 ląstelių buvo suspenduojamos 30 µl PBS + 0,1% BSA tirpalo ir inkubuojamos su CD44-APC ir CD24-FITC antikūnais arba jų izotipų kontrolėmis (FITC pelės IgG2a, k izotipas, o APC pelės IgG2b, k izotipas) 30 min, lede. Po inkubacijos ląstelės buvo tris kartus nuplaunamos su PBS tirpalu ir suspenduojamos 300 µl PBS. Tėkmės citometrijos analizė

buvo atlikta CIBIO Cell Analysis and Separation Core Facility, naudojant FACS Canto A prietaisą.

Imunofluorescencija

Norit atlikti imunfluorescenciją, ląstelės buvo paveikiamos įvairiomis medžiagomis ir fiksuojamos naudojant 4% PFA, 10 min, kambario temperatūroje. Po to ląstelės buvo nuplaunamos su PBS tirpalu ir blokuojamos bei permeabilizuojamos, naudojant 3%BSA-0,3%Trinton-X-100 PBS tirpalą, 30 kambario temperatūroje. Pirminis antikūnas prieš p65 (NF-κB p65 (D14E12) XP) buvo atskiestas santykiu 1:400 su 1% BSA tirpalu ir pridedamas į šulinėlius. Ląstelės su pirminiu antikūnu buvo inkubuojamos 60 min kambario temperatūroje. Po to šulinėliai buvo plaunami naudojant 3% BSA tirpalą. Antrinis antikūnas Alexa Fluor® 488 buvo atskiestas santykiu 1:500 su 1% BSA tirpalu ir pridedamas į šulinėlius. Ląstelės su antriniu antikūnu buvo inkubuojamos 60 min, kambario temperatūroje, tamsoje. Po to šulinėliai buvo plaunami naudojant 3% BSA tirpalą. Branduoliai buvo nudažyti naudojant Hoechst 33342 (1:5000) dažus. Nuotraukos buvo gautos pasitelkus IMAGEXPRESS MD Micro Confocal High-Content Imaging sistemą.

Vėžinių ląstelių išeikvotos terpės surinkimas ir paruošimas

Ląstelės buvo sėjamos į 10 cm lėkšteles. Praėjus 24 valandoms ląstelės buvo nuplaunamos su PBS tirpalu. Ląstelėms buvo pridedama naujos terpės, su mažesniu FBS kiekiu (2,5%). Šioje terpėje ląstelės buvo kultivuojamos 48 valandas, po to terpė buvo surenkama ir filtruojama per 0,45 μm filtrą. Prieš panaudojant eksperimentui, nufiltruota terpė buvo laikoma -20°C ilgiausiai 2 savaites.

Fermentinis imunosorbentinis tyrimas (ELISA)

ELISA buvo atlikta naudojant AuthentiKineTM rinkinius, skirtus TNF-α, IL-8 ir IL-6, pagal gamintojo instrukcijas. Tyrimui buvo naudota 100 μl išeikvotos vėžinių ląstelių terpės arba standartinio tirpalo. Absorbcija buvo išmatuota naudojant, Varioskan LUX multimode plokštelių skaitytuvą.

In vivo tyrimai

BALB/c pelės (, n=10; 4 savaičių amžiaus) buvo įsigytos iš Vilniaus universiteto, Gyvybės mokslų centro, Biochemijos instituto, Biologinių modelių skyriaus. Gyvūnai buvo laikomi po penkis plastikiniuose narvuose, su pakankamu vandens ir maisto kiekiu. Pelėms po oda, kaklo srityje buvo sušvirkšta po $12x10^5$ 4T1 Empty arba 4T1 ETV7 ląstelių. Naviko ilgis (L) ir plotis (W) buvo matuojami kasdien, naudojant slankmatį, naviko tūris (V) buvo apskaičiuotas naudojant formulę [$V=(LxW^2)/2$]. Gyvūnai buvo nužudyti su CO_2 dujomis ir atliekant kaklo slankstelio dislokaciją.

Imunofluorescencija su šaldytais naviko pjūviais (IF-F)

Išpreparuoti navikai buvo nuplaunami su PBS tirpalu, įliejami į OCT terpę ir iš karto užšaldomi skystame azote. Kriostato pagalba, navikai buvo supjaustyti į 4 μm storio sekcijas. Mėginiai buvo fiksuojami su lediniu 4% PFA tirpalu, 10 min. Po to mėginiai buvo plaunami 1% ožkos serum PBS-T (PBS with 0.4% Triton X-100) tirpalu 10 min. Nespecifinio signalo tikimybė buvo sumažinama blokuojant mėginius su 5% FBS PBS-T tirpalu, 30 min. Po to mėginiai buvo inkubuojami su pirminiais antikūnais (VIM (RV202, 550513, BD Biosciences), α-SMA (1A4, MA1-06110, Thermo Fischer Scientific), CD44 (OX-49, MA5-17519, Thermo Fischer Scientific), Ki67 (NB110-89717SS, NovusBio) atskiestais su 1% ožkos serumo PBS-T tirpalu, 2 valandas, kambario temperatūroje. Po inkubacijos su pirminiais antikūnais, mėgniai buvo nuplauti su 1% FBS PBS-T tirpalu ir po to inkubuojami su antriniais Alexa Fluor™ 488 (A-11001, Thermo Fischer Scientific) antikūnais 1 valandą, kambario temperatūroje, tamsoje. Po inkubacijos su antriniais antikūnais, mėgniai buvo nuplauti su 1% FBS PBS-T tirpalu. Branduoliai buvo nudažyti su DAPI (1:2000) dažais. Nuotraukos darytos su fluorescenciniu mikroskopu, o duomenų analizė atlikta su ImageJ programa.

Statistinė analizė

Jeigu nenurodyta kitaip, statistinė analizė buvo atlikta naudojant GraphPad Prism (9 versija) programą. Statistinis reikšmingumas tarp dviejų grupių buvo vertinamas taikant nesuporuotą t-testą. Grafinės iliustracijos buvo nupieštos naudojant Affinity designer įrankį.

Rezultatai

ETV7 reguliuoja krūties vėžio ląstelių plastiškumą ir padeda joms įgyti atsparumą 5-fluorouracilui.

Iš literatūros duomenų yra žinoma, kad ETV7 raiška vėžinėse ląstelėse padidėja, kai jos yra veikiamos DNR pažaidas sukeliamais vaistais ir kad ši padidėjusi ETV7 raiška yra susijusi su atsparumo doksorubicinui ir rapamicinui išsivystymu vėžinėse ląstelėse[9,10], todėl mes nusprendėme ištirti, ar padidėjusi ETV7 taip pat gali sumažinti krūties vėžinių ląstelių jautrumą gydymui su 5-fluorouracilu (5-FU). Pirmiausiai, pasitelkę Cell Titer Glo tyrimą, įvertinome ląstelių gyvybingumo pokyčius MCF7 ir T47D kontrolinėse ląstelėse (Empty) ir ląstelėse su padidinta ETV7 raiška, jas veikiant įvairiomis 5-fluorouracilo koncentracijomis ir pastebėjome, kad ląstelės su padidinta ETV7 raiška yra atsparesnės gydymui su 5-FU. Norint patvirtinti, kad ląstelės su padidinta ETV7 raiška yra atsparesnės gydymui 5-FU, pasitelkę tėkmės citometrijos analizę, naudojant aneksino V ir propidžio jodido regentus, mes taip pat įvertinome 5-FU sukeliamą apoptozę T47D kontrolinėse ląstelėse (Empty) bei ląstelėse su padidinta ETV7 raiška ir

nustatėme, kad padidinta ETV7 raiška sumažina ląstelių mirtingumą apoptozės būdu (1 pav.).

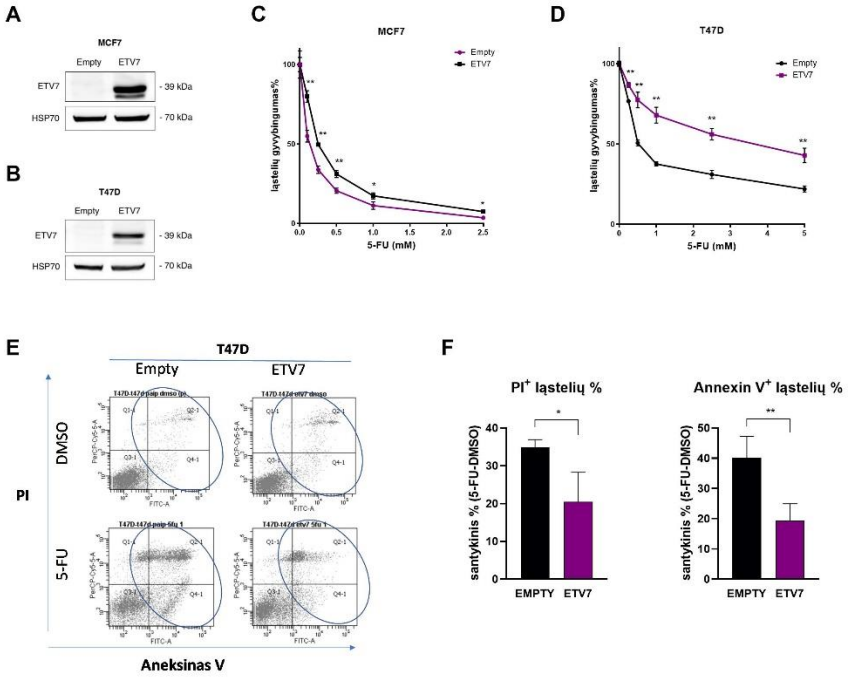

1 pav. Krūties vėžio ląstelėse su padidinta ETV7 raiška yra atsparesnės gydymui su 5-fluorouracilu. A-B) ETV7 baltymo analizė, Western blot metodu, MCF7 ir T47D ląstelėse su padidinta ETV7 raiška. C-D) Cell Titer Glo ląstelių gyvybingumo tyrimas MCF7 ir T47D ląstelėse (Empty arba ETV7), veikiant įvairiomis 5-FU koncentracijomis. E-F) Tėkmės citometrijos rezultatai dažant T47D ląsteles su aneksino V ir propidžio jodido reagentais, po poveikio su 5-FU. * $p < 0,05$; ** $p < 0,01$.

Pasitelkę daugialąstelinius sferoidus, mes taip pat įvertinome, ar ETV7 padeda vėžinėms ląstelėms išsivystyti atsparumą 5-FU gydymui ir 3D kultūrose. Stebėdami sferoidų dydžio pokyčius, galėjome patvirtint, kad ir 3D aplinkoje, padidinta ETV7 raiška sumažina vėžinių ląstelių jautrumą 5-FU gydymui (2 pav).

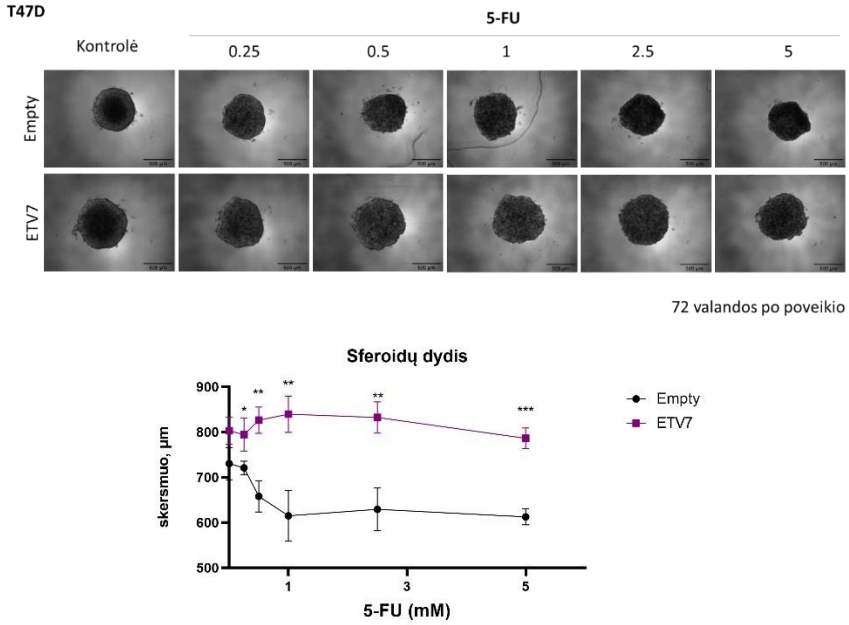

2 pav. Krūties vėžio sferoidai su padidinta ETV7 raiška yra atsparesni gydymui su 5-fluorouracilu. Tipinis sferoidų vaizdas praėjus 72 valandoms po paveikimo įvairiomis 5-FU koncentracijomis. Apačioje pateiktas sferoidų dydžio pokyčio grafikas. * $p < 0,05$; ** $p < 0,01$; *** $p < 0,001$.

Be to, norėdami įsitikinti, kad padidėjusį atsparumą tikrai lemia padidinta ETV7 raiška, mes atlikome atvirkštinį bandymą, t.y. parentalinėse MCF7 ir MDA-MB-231 ląstelių linijose, pasitelkę siRNR, nutildėme ETV7 ir po to paveikėme ląsteles 5-fluorouracilu. Tada įvertinome ląstelių gyvybingumą ir nustatėme, kad ląstelės su nutildytu ETV7 buvo jautresnės gydymui su 5-FU ir patvirtinome, kad ETV7 reguliuoja atsparumo 5-FU vystymąsi krūties vėžinėse ląstelėse (3 pav).

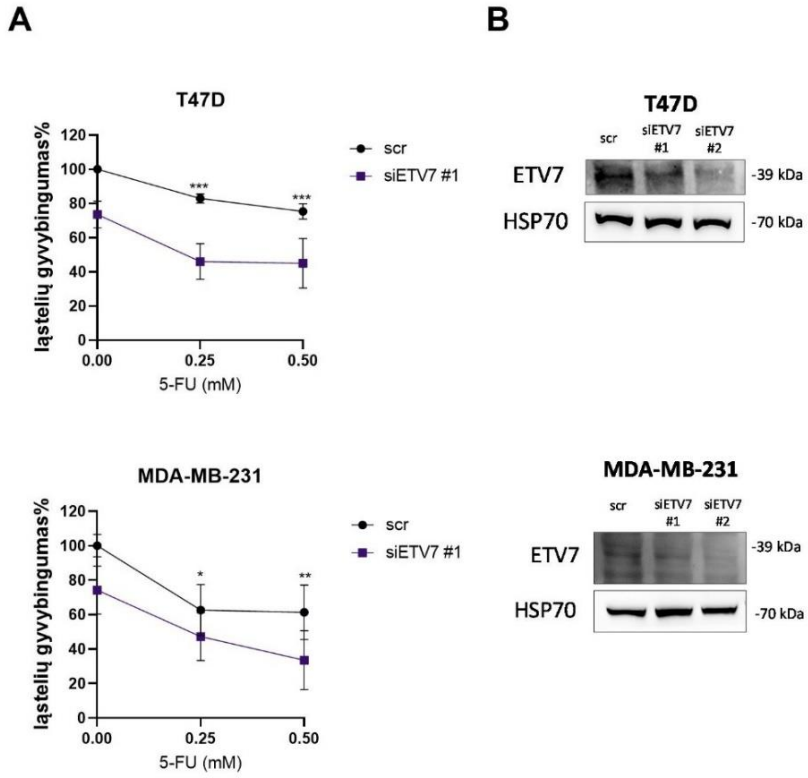

3 pav. ETV7 nutildymas padidina vėžinių ląstelių jautrumą 5-FU gydymui. A) Cell Titer Glo ląstelių gyvybingumo tyrimas T47D ir MDA-MB-231 ląstelėse, po ETV7 nutildymo ir poveikio įvairiomis 5-FU koncentracijomis. B) ETV7 baltymo analizė, Western blot būdu T47D ir MDA-MB-231 ląstelėse po ETV7 nutildymo. * $p < 0,05$; ** $p < 0,01$; *** $p < 0,001$.

Iš literatūros yra žinoma, kad ląstelės su padidinta ETV7 raiška, sintetina didesnį kiekį ABC transporterių[9], be to, mes nustatėme, kad padidinta ETV7 raiška yra taip pat susijusi su padidėjusia priešapototinių baltymų sinteze. Be to, yra žinoma, kad ETV7 yra susijęs su diferencijacijos sutrikdymu[4,233]. Mes taip pat žinome, kad vėžinės kamieninės yra atsparios priešvėžiniams vaistams ir dažnai turi aukščiau paminėtas savybes[56,58]. Atsižvelgiant į visus šiuos faktus, mes išsikėlėm hipotezę, kad ETV7 galėtų būti atsakingas už vėžinių ląstelių plastiškumo reguliaciją. Norėdami patirtinti šią hipotezę, mes pirmiausiai ištyrėme gerai žinomus vėžinių kamieninių ląstelių žymenis. Krūties vėžinių kamieninių ląstelių populiacija yra apibūdinama kaip $CD44^+/CD24^-$ ir $EpCAM^+$. Pirmiausiai pasitelkę tėkmės citometriją, mes ištyrėme ląstelių paviršiuje esančius CD44 ir CD24 žymenis ir nustatėme, labai ryškų vėžinių kamieninių ląstelių populiacijos išaugimą. Kontrolinės

ląstelelės turėjo tik apie 1-5% vėžinių kamieninių ląstelių, tuo tarpu ląstelėse su padidinta ETV7 raiška vėžinių kamieninių ląstelių populiacija išaugo net iki 30-60%. (4 pav. A, B, D, E) Norėdami išsiaiškinti, ar ETV7 tiesiogiai reguliuoja *CD44* ir *CD24* genų raišką, mes atlikome tikro laiko kiekybinę PGR reakciją ir nustatėme, kad MCF7 ir T47D ląstelėse ETV7 reguliuoja tik *CD24* geno traskripciją (4 pav. C ir F).

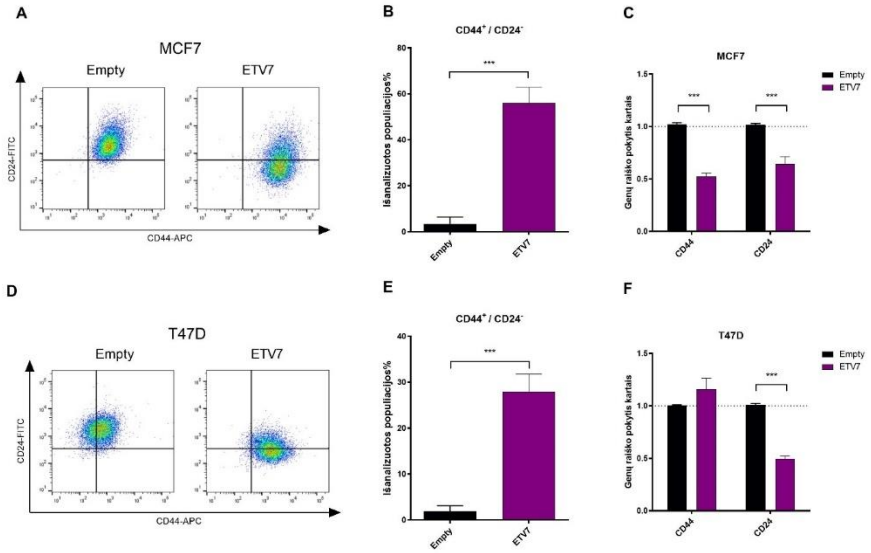

4 pav. ETV7 reguliuoja krūties vėžio ląstelių plastiškumą. A, B, E ir D) CD44 ir CD24 žymenų tyrimas tėkmės citometrijos pagalba MCF7 ir T47D ląstelėse. C ir F) CD44 ir CD24 genų raiškos analizė atlikus tikro laiko kiekybinę PGR reakciją MCF7 ir T47D ląstelėse. * $p < 0,05$; ** $p < 0,01$; *** $p < 0,001$.

Norėdami ištirti, ar ETV7 raiškos moduliacija daro įtaką vėžinių kamieninių ląstelių populiacijai, pasitelkę CRISPR/Cas9 technologiją, SK-BR-3 krūties vėžio ląstelių linijoje, išmušėme ETV7 ir išmatavome CD44 ir CD24 žymenis. Atlikę šį bandymą nustatėme, kad SK-BR-3 ląstelėse, su išmuštu ETV7, vėžinių kamieninių ląstelių populiacija sumažėjo ir tokiu būdu patvirtinome, ETV7 vaidmenį vėžinių kamieninių ląstelių reguliacijoje (5 pav.).

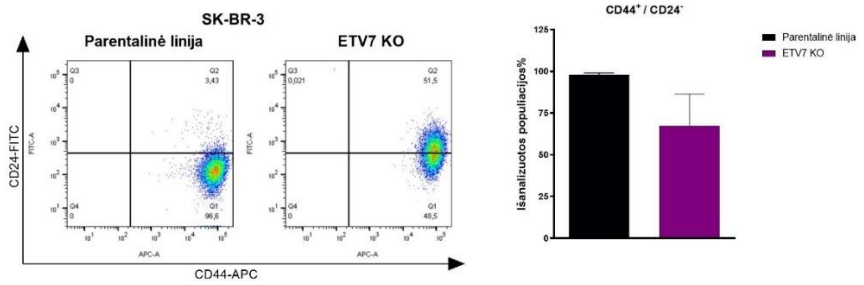

5 pav. ETV7 išmušimas sumažina vėžinių kamieninių ląstelių populiaciją. CD44 ir CD24 žymenų tyrimas tėkmės citometrijos pagalba SK-BR-3 ląstelėse, su išmuštu ETV7.

Pasitelkę Western blot analizę, mes taip pat ištyrėme kitą krūties vėžinių kamieninių ląstelių žymenį – EpCAM ir nustatėme, kad krūties vėžio ląstelės su padidinta ETV7 raiška, sintetina didesnį šio baltymo kiekį t.y. pasižymi didesniu kamieniškumu (6 pav.).

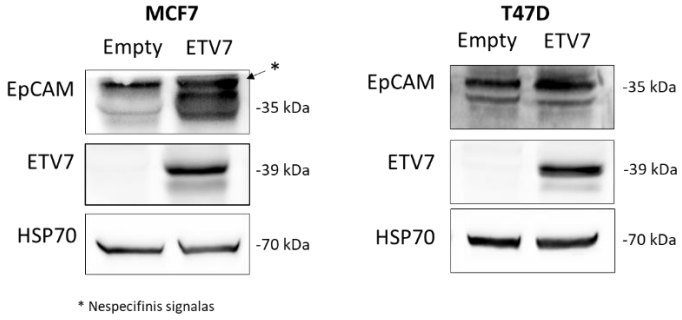

6 pav. ETV7 padidina EpCAM sintezę krūties vėžio ląstelėse. EpCAM baltymo analizė, Western blot metodu MCF7 ir T47D ląstelėse su padidinta ETV7 raiška.

Kadangi viena iš svarbiausių vėžinių kamieninių ląstelių savybių yra jų gebėjimas atsinaujinti, dėl to norėdami įvertinti, ar ląstelėms su padidinta ETV7 raiška yra būdinga ir ši vėžinių kamieninių ląstelių savybė, mes atlikome mamosferų formavimo tyrimą. Šio tyrimo metu ląstelės yra auginamos nediferencijuojančioje ir prikibti neleidžiančioje aplinkoje ir yra stebimas ląstelių gebėjimas išgyventi ir formuoti sferas. Atlikę šį tyrimą pastebėjome, kad ląstelės su padidinta ETV7 raiška žymiai efektyviau formavo mamosferas nei kontrolinės ląstelės (7 pav.).

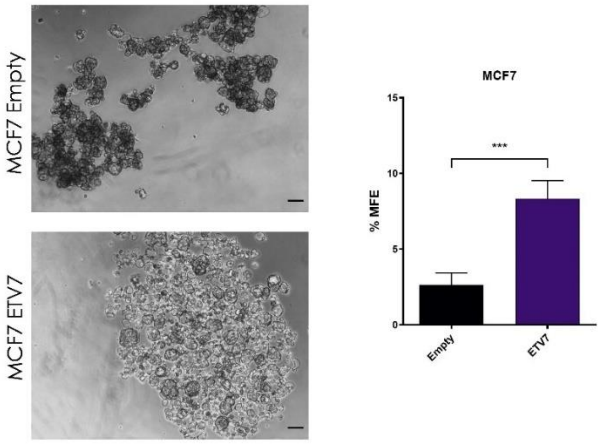

7 pav. ETV7 padidina krūties vėžinių kamieninių ląstelių populiaciją. Tipinė nuotrauka, parodanti mamosferų formavimą MCF7 Empty ir MCF7 ETV7 ląstelėse. Dešinėje esančiame grafike pateiktas mamosferų formavimo efektyvumas. *** $p < 0,001$.

Iš literatūros taip pat yra žinoma, kad vėžinių kamieninių ląstelių populiacijos išaugimą gali lemti nuslopintas interferoninis atsakas vėžinėse ląstelėse[265]. Atsižvelgiant į šį faktą, mes nusprendėme ištirti interferono stimuliuojamų genų raišką MCF7 kontrolinėse (Empty) ir MCF7 ETV7 ląstelėse. Pasitelkę tikro laiko qPGR analizę, mes ištyrėme keleto, su interferonų atsakų susijusių, genų raišką ir nustatėme, kad ETV7 slopina šių genų raišką (8 pav. A). Be to, MCF7 ir kitose krūties vėžio ląstelėse po ETV7 nutildymo, šių genų raiška padidėjo (8 pav. B).

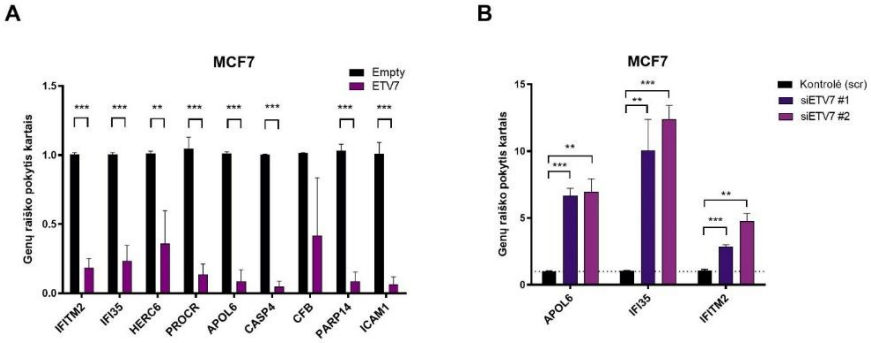

8 pav. ETV7 reguliuoja inferferono stimuliuojamų genų raišką. Interferono stimuliuojamų genų raiškos analizė atlikus tikro laiko kiekybinę PGR MCF7 ląstelėse su padidinta ETV7 raiška (kairėje) arba nutildžius ETV7 (dešinėje). ** $p < 0,01$; *** $p < 0,001$.

ETV7 slopina *TNFRSF1A* geno raišką ir tokiu būdu sumažina uždegiminį atsaką krūties vėžio ląstelių linijose

ETV7 slopina *TNFRSF1A* geno raišką krūties vėžio ląstelių linijose

Analizuojant anksčiau laboratorijoje gautus RNA-seq duomenis (MCF7 ir T47D ląstelių linijos su stabiliai padidinta ETV7 raiška) buvo pastebėta, kad ETV7 galimai dalyvauja signalinių kelių, susijusiu su uždegiminiais procesais ir imuniniu atsaku, reguliacijoje. Kadangi ETV7 yra transkripcijos slopiklis, pirmiausiai buvo įvertinti genai su sumažinta raiška. Naudojant RT-qPCR analizę buvo patvirtinta, kad esant padidintai ETV7 raiškai, MCF7 ir T47D krūties vėžio ląstelių linijose yra žymiai nuslopinta šių, su uždegiminių atsaku susijusių, genų raiška: *IL10Rb, IL1RI, TLR2* ir *TNFRSF1A* (9 pav.). Tolimesni tyrimai buvo sukoncentruoti į ETV7 vaidmenį *TNFRSF1A* geno reguliacijoje.

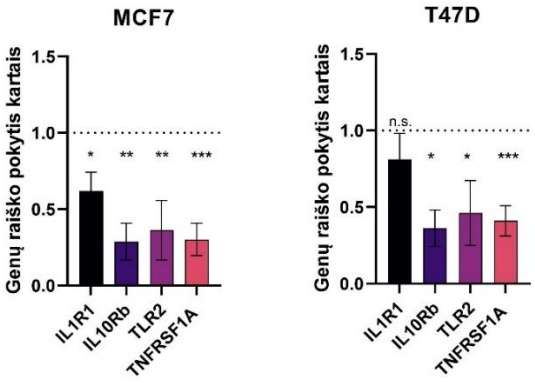

9 pav. ETV7 slopina genų, susijusių su imuniniu ir uždegiminiu atsakais, raišką, krūties vėžio ląstelėse. Su imuniniu ir uždegiminiu atsakais susijusių genų raiškos analizė atlikus tikro laiko kiekybinę PGR reakciją MCF7 ir T47D ląstelėse. * $p < 0,05$; ** $p < 0,01$; *** $p < 0,001$.

Tikro laiko kiekybinės PGR analizės būdu, įvertinome *TNFRSF1A* geno raišką ir kitose krūties vėžio ląstelių linijose su padidinta ETV7 raiška ir patvirtinome, kad ETV7 gali nuslopinti šio geno raišką. Be to, pasitelkę Western blot analizę, parodėme, kad MCF7 ir T47D ląstelėse esant padidintai ETV7 raiškai yra taip pat sumažinama TNFR1 baltymo sintezė (10 pav.).

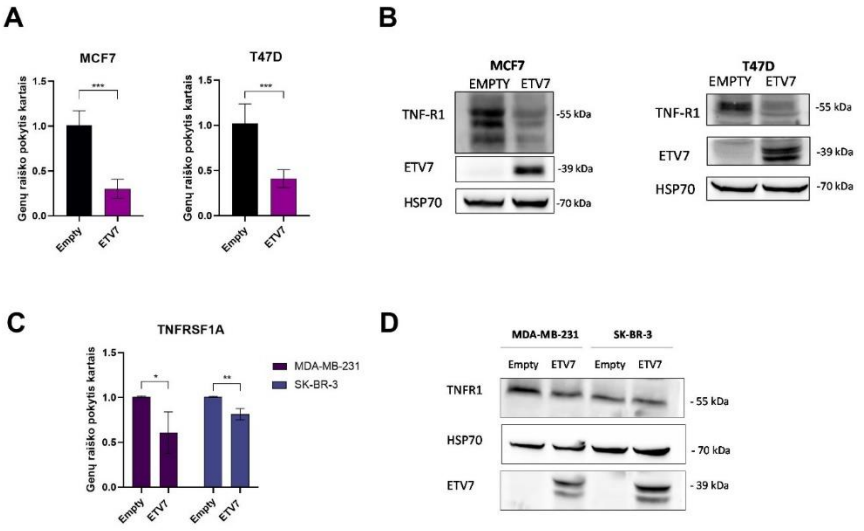

10 pav. ETV7 slopina *TNFRSF1A* raišką ir sumažina TNFR1 baltymo kiekį krūties vėžio ląstelėse. A ir C) *TNFRSF1A* geno raiškos analizė atlikus tikro laiko kiekybinę PGR reakciją krūties vėžio ląstelėse su padidinta ETV7 raiška. B ir D) TNFR-1 baltymo analizė, Western blot metodu, MCF7, T47D, SK-BR-3 ir MDA-MB-231 ląstelėse su padidinta ETV7 raiška. * $p < 0,05$; ** $p < 0,01$; *** $p < 0,001$.

Be to, mes nustatėme, kad nutildžius ETV7, *TNFRSF1A* geno raiška, MCF7 ir kitose krūties vėžio ląstelėse, padidėja (11 pav.).

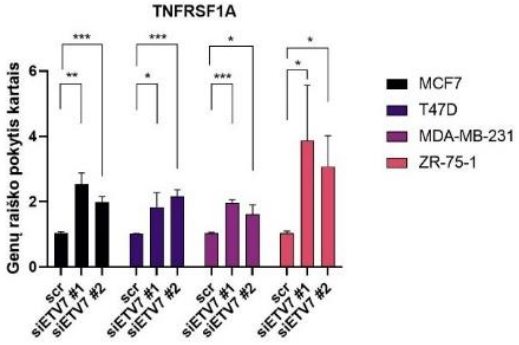

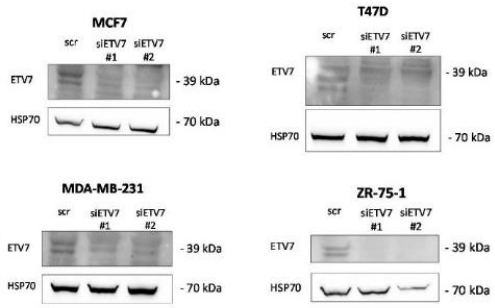

11 pav. Nutildžius ETV7 *TNFRSF1A* raiška yra atstatoma. Viršuje, *TNFRSF1A* geno raiškos analizė atlikus tikro laiko kiekybinę PGR reakciją krūties vėžio ląstelėse su nutildytu ETV7. Apačioje, ETV7 baltymo analizė, Western blot metodu, MCF7, T47D, SK-BR-3 ir MDA-MB-231 ląstelėse su nutildytu ETV7. * $p < 0,05$; ** $p < 0,01$; *** $p < 0,001$.

Kadangi žinome, kad ETV7 yra transkripcijos slopiklis, nusprendėme ištirti, ar ETV7 gali tiesiogiai slopinti *TNFRSF1A* geno raišką. Išanalizavę *TNFRSF1A* geno reguliacinį elementą, nustatėme kelias potencialias ETV7 rišimosi su DNR vietas ir atlikome chromatino precipitaciją. Atlikę chromatino precipitaciją, nustatėme, kad ETV7 tiesiogiai slopina *TNFRSF1A* geno raišką (12 pav.).

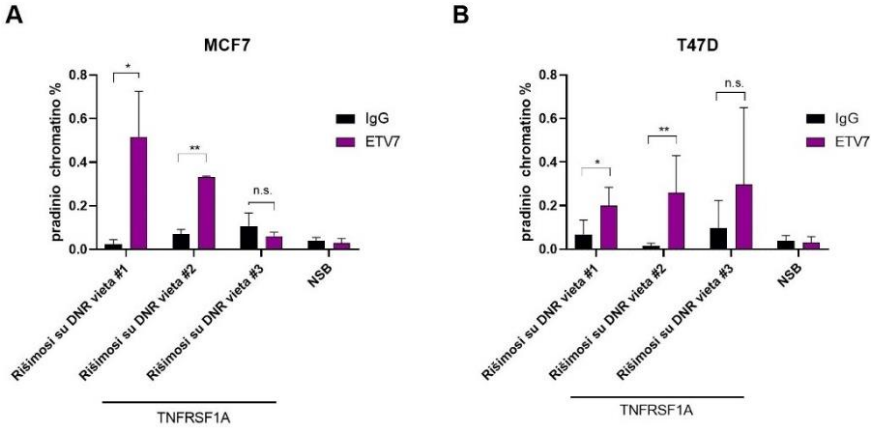

12 pav. ETV7 tiesiogiai slopina *TNFRSF1A* geno raišką. Chromatino imunoprecitacija atlikta MCF7 ir T47D ląstelėse su padidinta ETV7 raiška. * $p < 0,05$; ** $p < 0,01$.

Papildomai norėjome įsigilinti, į ETV7 reguliuojamą slopinimo mechanismą ir ištirti, kaip ETV7 gali moduliuoti prieinamumą prie chromatino. Išsirinkę kelias pagrindines su hetero- ir euchromatinu susijusias modifikacijas, atlikome chromatino imunoprecipitacijos tyrimą ir nustatėme, kad ETV7 gali moduliuoti chromatino būseną ties *TNFRSF1A* geno

reguliaciniu elementu ir paversti chromatiną mažiau prieinamu kitiems transkripcijos veiksniams (13 pav.).

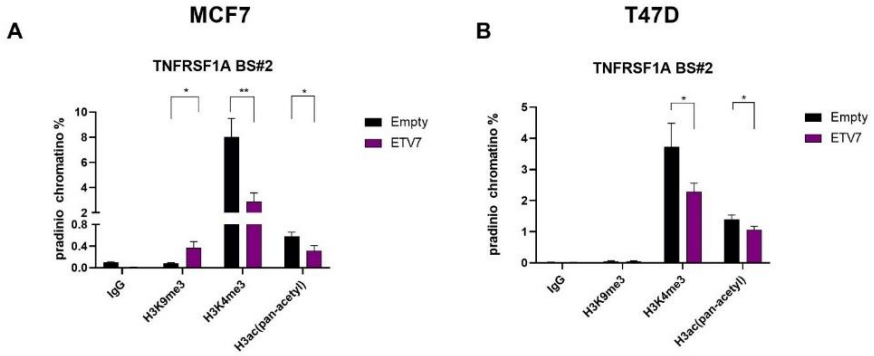

13 pav. ETV7 modeliuoja chromatiną ir padaro jį mažiau prieinamą kitiems transkripcijos faktoriams. Chromatino imunoprecitacija atlikta MCF7 ir T47D ląstelėse su padidinta ETV7 raiška, norint įvertinti įvairias chromatino modifikacijas. * $p < 0,05$; ** $p < 0,01$.

Literatūroje yra aprašyta, kad TNF-α aktyvuoja NF-κB signalinį kelią prisijungdamas prie TNFR1 receptoriaus[153]. Dėl to mes nusprendėme ištirti, ar ETV7 tiesiogiai slopindamas *TNFRSF1A* geno raišką, nuslopina ir NF-κB signalinio kelio aktyvaciją. Pirmiausiai atlikome geno-reporterio tyrimą ir nustatėme, kad MCF7 ir T47D ląstelėsesu padidinta ETV7 raiška NF-κB signalinis kelias yra nuslopintas ir nėra aktyvuojamas, net ir stimuliuojant ląsteles su TNF- α (14 pav.).

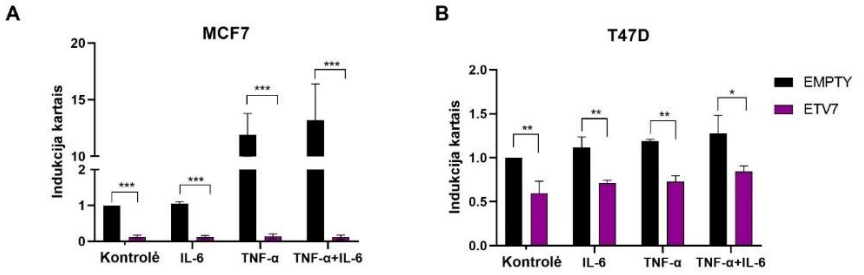

14 pav. ETV7 slopina NF-κB signalinio kelio aktyvaciją. Geno-reporterio analizė MCF7 ir T47D ląstelėse su padidinta ETV7 raišką, stimuliuojant su įvairiais citokinais ir interleukinais. * $p < 0,05$; ** $p < 0,01$; *** $p < 0,001$.

NF-κB signalinio kelio nuslopinimas taip pat buvo įvertintas atliktus NF-κB genų taikinių analizę (RT-qPCR) MCF7 ir T47D ląstelėse. Atlikus RT-qPCR, buvo nustatyta, kad IL-6, IL-8, A20 ir TNF- α raiška buvo nuslopinta krūties vėžio ląstelėse su padidinta ETV7 raiška (15 pav. A-D). Tuo tarpu minėtų genų raiška buvo atkurta nutildžius ETV7 įvairiose krūties vėžio ląstelių linijose (15 pav. E).

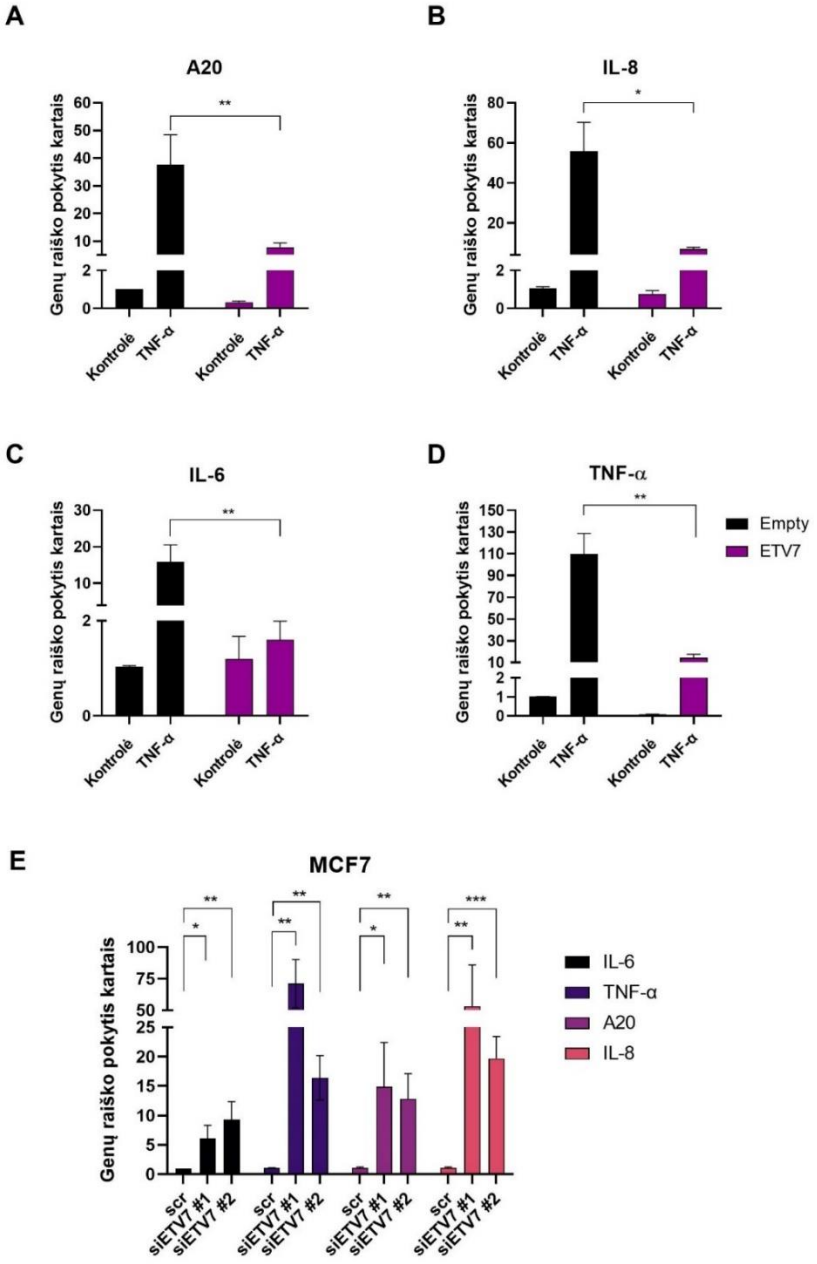

15 pav. ETV7 reguliuoja NF-κB genų-taikinių raišką krūties vėžio ląstelėse. NF-κB genų-taikinių raiškos analizė atlikus tikro laiko kiekybinę PGR MCF7 ląstelėse su padidinta ETV7 raiška arba su nutildytu ETV7. * $p < 0,05$; ** $p < 0,01$; *** $p < 0,001$.

NF-κB signalinio kelio nuslopinimas taip pat buvo nustatytas atlikus fosforilinto IκB-α analizę, Western blot būdu bei įvertinus p65 translokaciją į branduolį, imunofluorescencijos metodu (16 pav.).

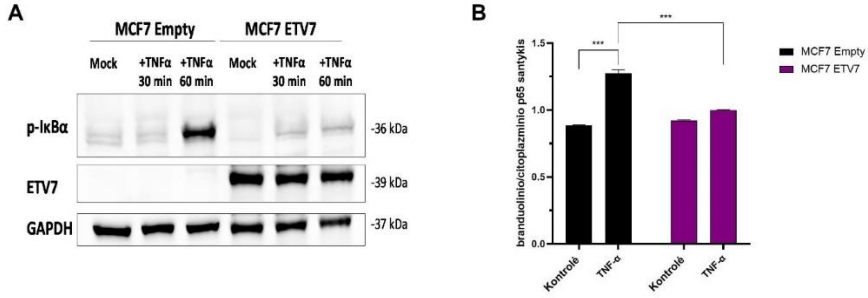

16 pav. ETV7 slopina NF-κB signalinį kelią krūties vėžio ląstelėse. A) Western blot analizė MCF7 ląstelėse su padidinta ETV7 raiška. B) Kiekybinis p65 translokacijos į branduolį įvertinimas MCF7 ląstelėse su padidinta ETV7 raiška (imunofluorescencija). *** $p < 0,001$.

Tam, kad įrodytume, kad NF-κB signalinio kelio nuslopinimas lemia mažesnį uždegiminį atsaką, išanalizavome IL-6, IL-8 ir TNF-α sekreciją. Pasitelkę ELISA, ištyrėme IL-6, IL-8 ir TNF-α koncentraciją MCF7 ir T47D kultivavimo terpėje, ir nustatėme, kad ląstelės su padidinta ETV7 raiška sekretavo žymiai mažiau IL-6, IL-8 ir TNF-α ir patvirtinome, kad ETV7 nuslopindamas NF-κB signalinį kelią, taip pat sumažina uždegiminį atsaką (17 pav.).

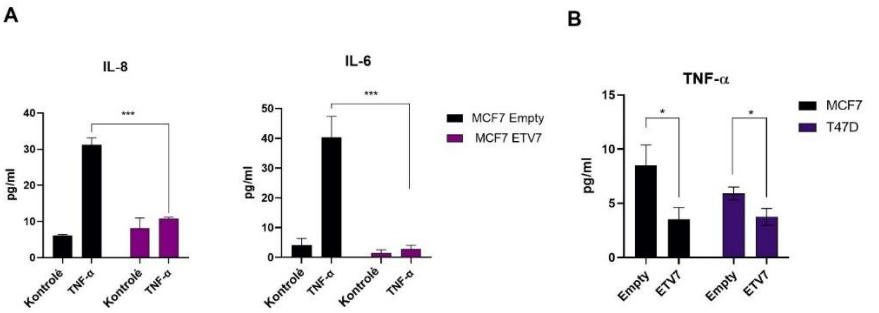

17 pav. ETV7 sumažina sekretuojamų uždegiminių citokinų ir interleukinų kiekį. IL-8, IL6 ir TNF-α ELISA tyrimas krūties vėžio ląstelių su padidinta ETV7 raiška terpėse. * $p < 0,05$; *** $p < 0,001$.

Iš literatūros duomenų yra žinoma, kad STAT3, vienas iš svarbiausių uždegiminių procesų reguliatorių, taip pat reguliuoja *TNFRSF1A* geno raišką, tačiau priešingai nei ETV7, STAT3 yra transkripcijos aktyvatorius. Be to, STAT3 ir ETV7 susiriša su panašiomis DNR sekomis[203,216,252,278]. Dėl šių priežasčių mes iškėlėme hipotezę, kas šie du transkripcijos veiksniai galėtų

tarpusavyje konkuruoti dėl *TNFRSF1A* geno reguliacijos. Norėdami ištirti, kaip vyksta *TNFRSF1A* geno reguliacija ląstelėse su padidinta ETV7, kai yra aktyvuojamas STAT3 (stimuliacija IL-6), atlikome RT-qPCR analizę ir nustatėme, kad ląstelėse su padidinta ETV7 raiška, *TNFRSF1A* geno raiška yra slopinama, net kai yra aktyvuojamas STAT3 (18 pav.). Šie duomenys patvirtino galimą konkurenciją tarp ETV7 ir STAT3.

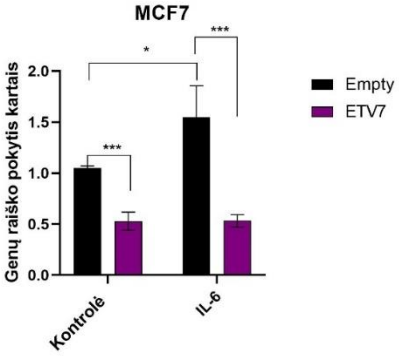

18 pav. ETV7 konkuruoja su STAT3 dėl *TNFRSF1A* geno reguliacijos. *TNFRSF1A* geno raiškos analizė atlikus tikro laiko kiekybinę PGR reakciją MCF7 ląstelėse su padidinta ETV7 raiška bei aktyvuotu STAT3. * $p < 0,05$; *** $p < 0,001$.

Tam, kad pažvelgtume giliau, kas vyksta *TNFRSF1A* geno reguliaciniame elemente, kai vėžinėse ląstelse yra padidinta ETV7 raiška ir yra aktyvus STAT3, mes atlikome chromatino imunoprecipitaciją su stimuliuotomis ir nestimuliuotomis, kontrolinėmis arba su padidinta ETV7 raiška ląstelėmis ir nustatėme, kad esant padidintai ETV7 raiškai, STAT3 gebėjimas reguliuoti *TNFRSF1A* geno raišką sumažėja (19 pav.).

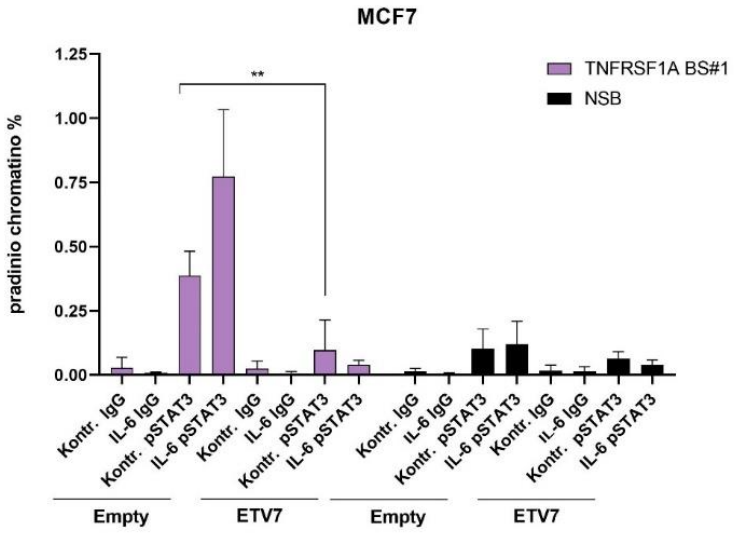

19 pav. Padidinta ETV7 raiška sumažina STAT3 galimybę susirišti su *TNFRSF1A* geno reguliaciniu elementu. Chromatino imunoprecitacija atlikta MCF7 ląstelėse su padidinta ETV7 raiška ir aktyvuotu STAT3. ** $p < 0,01$.

Apibendrinant šiame skyriuje pateiktus duomenis, mes siūlome naują *TNFRSF1A* geno reguliacinį mechanizmą. Kai ląstelėse padaugėja ETV7, šis sugeba konkuruoti su STAT3 dėl susirišimo su *TNFRSF1A* geno reguliaciniu elementu bei paversti chromatiną mažiau prieinamu ir taip slopinti *TNFRSF1A* geno raišką, Nuslopinta *TNFRSF1A* geno lemia mažesnį TNFR1 kiekį ląstelės paviršiuje ir dėl to yra mažiau aktyvuojamas NF-κB signalinis kelias. Mažesnė NF-κB signalinio kelio aktyvacija lemia mažesnį uždegiminį atsaką.

ETV7 slopina antigentų pristatymo signalinį kelią krūties vėžio ląstelėse

Kaip aptarėme ankstesniuose skyriuose, ETV7 slopina du labai svarbius su imuniniu ir uždegiminiu atsaku susijusius - interferonų ir NF-κB - signalinius kelius. Šių kelių slopinimas gali padėti vėžinėms ląstelėms išvengti šeimininko imuninio atsako, nes abu šie keliai yra svarbūs teisingam antigenų pristatymui, kuris lemia efektyvų citotoksinių T ląstelių atsaką[136,187]. Antigenai dažnai yra pristatomi pasitelkiant MHC I klasės molekules[177,186]. Atsižvelgiant į šią informaciją, mes nusprendėme ištirti, ar ETV7 daro įtaką antigenų apdorojimui ir pristatymui. Atlikę RT-qPCR analizę įvertinome įvairių su antigenų pristatymu susijusių genų raišką, ir nustatėme, kad šių genų raišką buvo nuslopinta krūties vėžio ląstelėse su padidinta ETV7 raišką (20 pav. A). Be to, šis faktas buvo patvirtintas ir atlikus imunoproteosomos

baltymų (LMP2 ir LMP7) ir B2M baltymo analizę Western blot būdu kontrolinėse ląstelėse arba ląstelėse su padidinta ETV7 (20 pav. B).

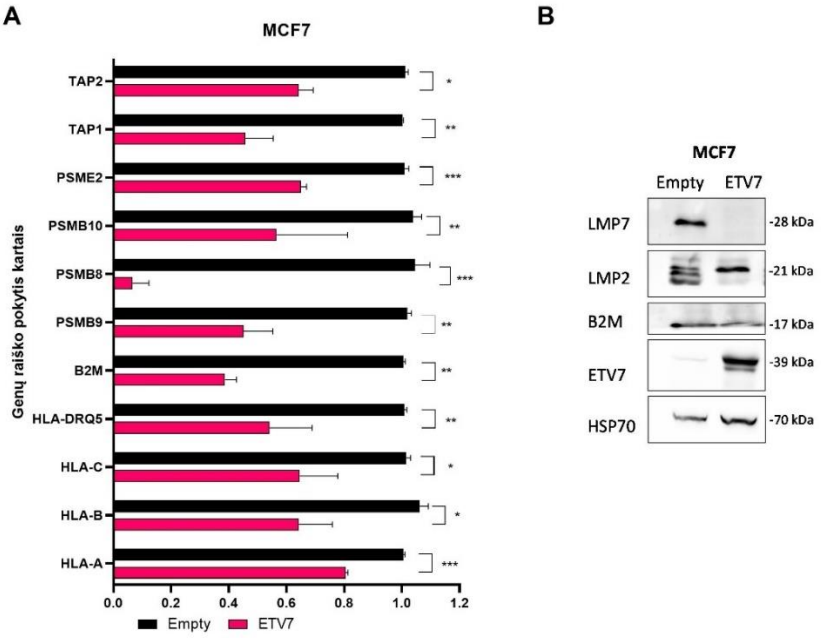

20 pav. ETV7 slopina antigenų pristatymo signalinį kelią. A) Su antigenų pristatymu susijusių genų raiškos analizė atlikus tikro laiko kiekybinę PGR reakciją MCF7 ląstelėse su padidinta ETV7 raiška. B) Su antigenų pristatymu susijusių baltymų analizė, Western blot metodu MCF7 ląstelėse su padidinta ETV7 raiška. * $p < 0,05$; ** $p < 0,01$, *** $p < 0,001$.

Yra žinoma, kad IFN-γ stimuliuoja antigenų apdorojimą ir pristatymą[256], dėl to mes nusprendėme ištirti, ar stimuliacija IFN-γ gali atkurti su antigenų pristatymu susijusių genų raišką ląstelėse su padidinta ETV7. Atlikę tikro laiko qPGR ir Western blot analizes, nustatėme, kad ląstelėse su padidinta ETV7 raiška, antigenų pristatymas nėra atkuriamas net ir po stimuliacijos su IFN-γ (21 pav.). Šis rezultatas parodo, kad ETV7 galėtų būti naujas reguliatorius, padedantis krūties vėžio ląstelėms išvengti šeimininko imuninio atsako ir sėkmingai plisti žmogaus organizme.

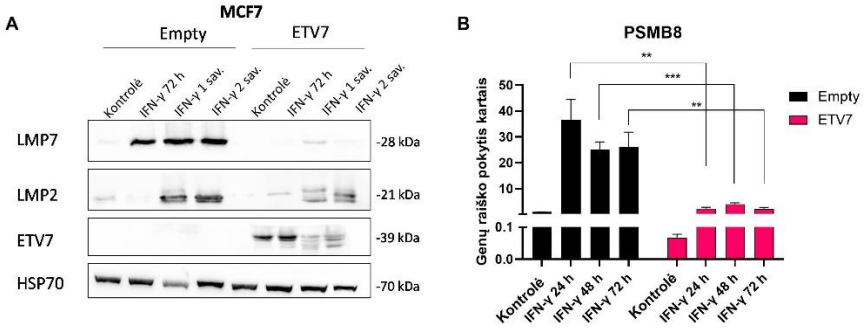

21 pav. Stimuliacija su IFN-γ negali atkurti tinkamo antigenų pristatymo ląstelėse su padidinta ETV7 raiška. A) Su antigenų pristatymu susijusių baltymų Western blot analizė MCF7 ląstelėse su padidinta ETV7 raiška, po stimuliacijos su IFN-γ. B) *PSMB8* geno raiškos analizė atlikus tikro laiko kiekybinę PGR MCF7 ląstelėse su padidinta ETV7 raiška, po stimuliacijos su IFN-γ. ** $p < 0,01$, *** $p < 0,001$.

ETV7 nutildymas sukelia apoptozę vėžinėse ląstelėse, su laukinio tipo p53.

Šiame tyrime pateikėme daug rezultatų, kurie parodė, kad ETV7 nutildymas turi priešingą efektą nei padidinta ETV7 raiška, dėl to ETV7 galėtų būti potencialiu nauju taikiniu krūties vėžio gydymui. Norėdami įvertinti, ar ETV7 galėtų būti geru taikiniu, pirmiausiai ištyrėme, kokį poveikį ląstelių gyvybingumui daro ETV7 nutildymas. Nutildžius ETV7 13-oje vėžinių ląstelių linijų ir įvertinus ląstelių gyvybingumą, atliekant Cell Titer Glo tyrimą, 8 ląstelių linijose pamatėme žymiai sumažėjusį ląstelių gyvybingumą (22 pav.).

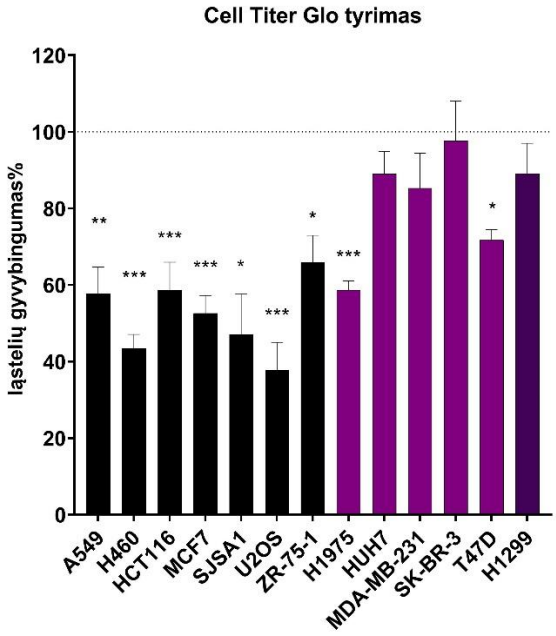

22 pav. ETV7 nutildymas sumažina ląstelių gyvybingumą, dalyje vėžinių ląstelių linijų. Cell Titer Glo ląstelių gyvybingumo tyrimas trylikoje vėžinių ląstelių linijų, po ETV7 nutildymo. * $p < 0,05$; ** $p < 0,01$, *** $p < 0,001$.

Norėdami įsitikinti, kad sumažėjęs ląstelių gyvybingumas yra dėl ląstelių žūties, pasitelkę Western blot metodą, paveiktose ir nepaveiktose vėžinėse ląstelėse įvertinome PARP-1 skilimą, kuris parodo ląstelių žūti apoptozės keliu, ir nustatėme, kad vėžinių ląstelių gyvybingumo sumažėjimą, po ETV7 nutildymo, lėmė ląstelių žūtis (23 pav.).

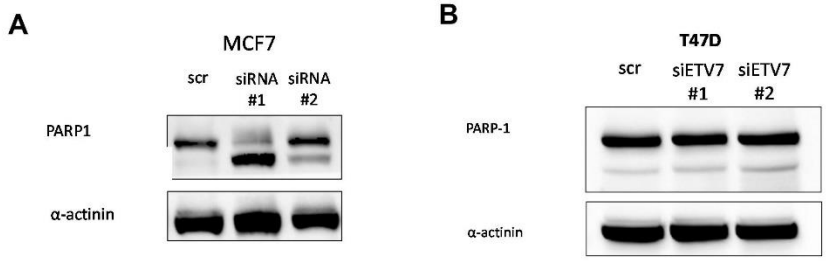

23 pav. ETV7 nutildymas MCF7 ląstelėse sukelia apoptozę. PARP-1 baltymo analizė Western blot metodu MCF7 ir T47D ląstelėse su nutildytu ETV7.

Mums buvo įdomu suprasti, kodėl kai kuriose vėžinėse ląstelių linijose ląstelių gyvybingumas, po ETV7 nutildymo, sumažėjo, o kitose šis efektas nebuvo pastebėtas arba buvo žymiai mažesnis. Mes išanalizavome tirtų ląstelių linijų molekulinius skirtumus ir nustatėme, kad vėžinės ląstelės, kurios žuvo po ETV7 nutildymo, turėjo laukinio tipo p53 (24 pav.).

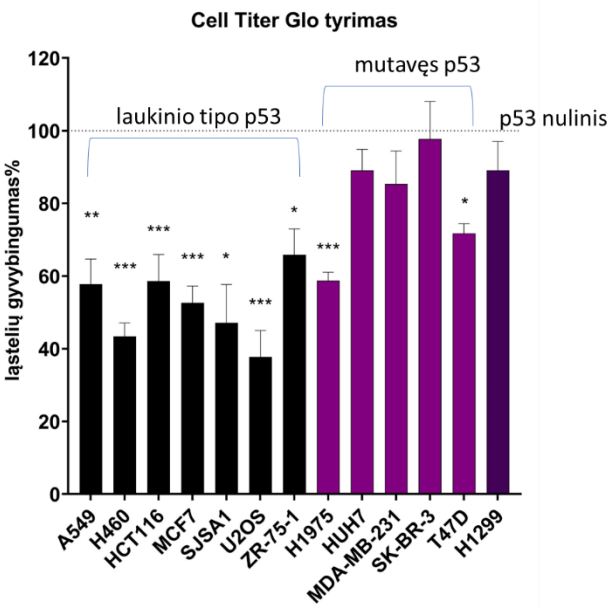

24 pav. ETV7 nutildymas sumažina ląstelių gyvybingumą, vėžinėse ląstelėse su laukinio tipo p53. Cell Titer Glo ląstelių gyvybingumo tyrimas trylikoje vėžinių ląstelių linijų, po ETV7 nutildymo. * $p < 0,05$; ** $p < 0,01$, *** $p < 0,001$.

Dėl to mes nusprendėme ištirti, ar ETV7 nutildymas, sukelia p53 susikaupimą ir tokiu būdu indukuoja apoptozę. Pasitelkę Western blot analizę ištyrėme p53 susikaupimą, ETV7 nutildymo paveiktose ląstelėse ir nustatėme, kad ETV7 nutildymas lemia p53 kiekio padidėjimą (25 pav.).

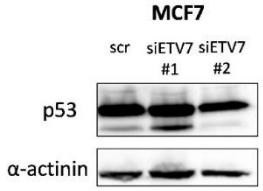

25 pav. ETV7 nutildymas lemia p53 susikaupimą vėžinėse ląstelėse. p53 baltymo analizė Western blot būdu MCF7 ląstelėse su nutildytu ETV7.

Be to, naudodami RT-qPCR, mes ištyrėme kai kurių p53 genų-taikinių raišką ir nustatėme, kad po ETV7 nutildymo, MCF7, A549 ir ZR-75-1 ląstelėse padidėjo *PUMA* geno raiška (26 pav.).

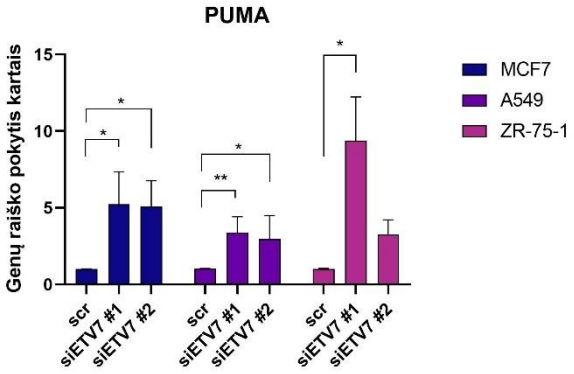

26 pav. ETV7 nutildymas padidina PUMA geno raišką vėžinėse ląstelėse su laukinio tipo p53. *PUMA* geno raiškos analizė atlikus tikro laiko kiekybinę PGR reakciją vėžinėse ląstelėse su nutildytu ETV7. *p<0,05; ** p < 0,01.

Norėdami įsitikinti, kad būtent p53 yra atsakingas už sukeliamą ląstelių žūtį, mes nutildėme ETV7 parentalinėje HCT116 ląstelių linijoje (laukinio tipo p53) ir HCT116 ląstelių linijoje su išmuštu p53. Gauti rezultatai patvirtino prieš tai nustatytus duomenis, HCT116, su laukinio tipo p53, po ETV7 nutildymo žuvo apotozės keliu, tuo tarpu ląstelėse, su išmuštu p53, ETV7 nutildymo poveikis nebuvo matomas (27 pav.).

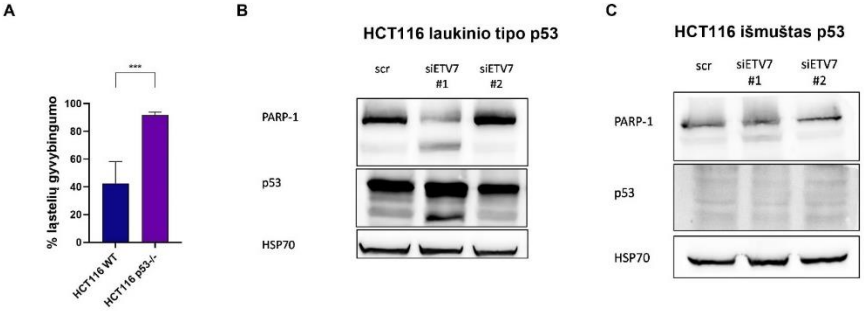

27 pav. ETV7 nutildymas sukelia nuo p53 priklausomą apoptozę vėžinėse ląstelėse. A) MTT ląstelių gyvybingumo tyrimas HCT116 parentalinėje linijoje ir HCT116 ląstelių linijoje su išmuštu p53. *** p < 0,001. B ir C) PARP-1 ir p53 baltymų analizė Western blot būdu HCT116 parentalinėje linijoje ir HCT116 ląstelių linijoje su išmuštu p53.

Apibendrinant galima teigti, kad ETV7 nutildymas sukelia apoptozę vėžinėse ląstelėse, pasitelkiant p53/PUMA ašį.

ETV7 skatina naviko formavimąsi *in vivo* modeliuose

Galiausiai norėjome įvertinti, ar *in vitro* tyrimuose pastebėtos ETV7 savybės, didiančios krūties vėžio agresyvumą, yra matomos ir *in vivo* modeliuose. Pirmiausiai sukūrėme pelės pieno liaukos naviko ląstelių liniją su stabiliai padidinta ETV7 raiška ir įvertinome šių ląstelių proliferacijos

potencialą, augindami jas minkštame agare. Nustatėme, kad ląstelės su padidinta ETV7 raišką formavo daugiau ir didesnes kolonijas (28 pav.).

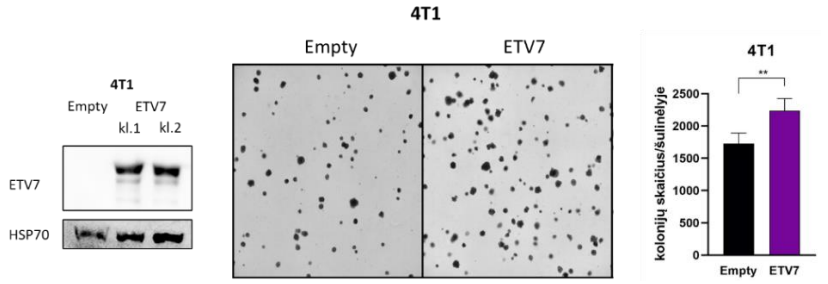

28 pav. Padidinta ETV7 raiška lemia didesnį proliferacinį aktyvumą pelės pieno liaukos naviko ląstelėse (4T1). Kairėje, ETV7 baltymo analizė Western blot būdu 4T1 kontrolinėse ląstelėse ir ląstelėse su padidinta ETV7 raiška. Dešinėje, 4T1 ląstelių su padidinta ETV7 augimo minkštame agare analize – pateikta reprezentatyvi nuotrauka ir grafikas, su kiekybiniu kolonijų skaičiaus įvertinimu. ** $p < 0,01$.

Patvirtinę kai kurias su vėžio agresyvumu susijusias savybes 4T1 ląstelėse su padidinta ETV7 raišką, BALB/c pelėms suleidome 4T1 kontrolines ir 4T1 ETV7 ląsteles ir stebėjome naviko formavimo procesą. Pelėse, kurioms buvo suleista ląstelių linija su ETV7, navikai susiformavo greičiau. Statistiškai reikšmingas naviko dydžio skirtumas buvo pastebėtas tik 18-tą dieną, tačiau tendencija, kad navikai su ETV7 buvo didesni išliko visą tyrimo laikotarpį (29 pav.).

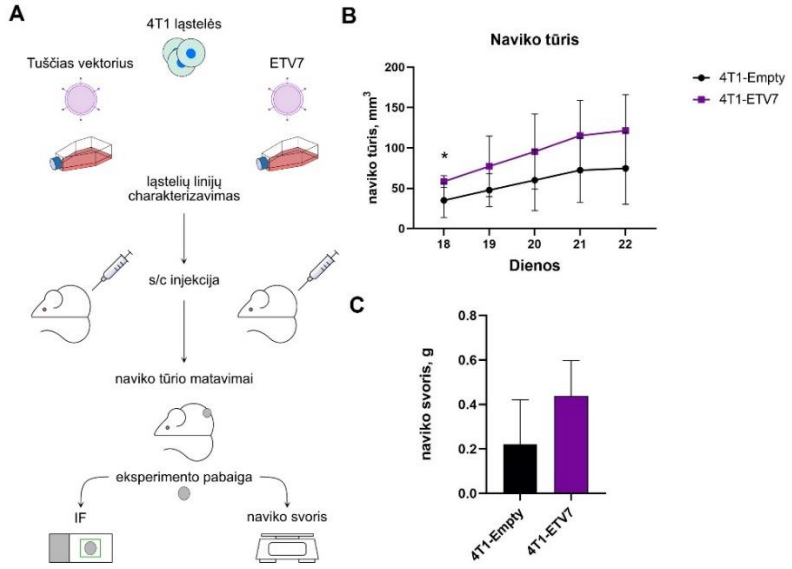

29 pav. ETV7 skatina didesnių navikų formavimąsi *in vivo* modeliuose. A) *In vivo* eksperimento schema B) Naviko augimo dinamika

kontrolinėje grupėje ir grupėje su ETV7, matuojant naviko tūrį slankmačiu. *p<0,05
C) Navikų svoris skirtingose eksperimentinėse grupėse ekspeirmento pabaigoje.

Norint įvertinti ETV7 poveikį vėžinių ląstelių kamieniškumui, EMT, proliferacijai ir fibroblastų infiltracijai buvo panaudoti atitinkami žymenys. Imunofluorescencija atlikta su užšaldytais naviko pjūviais, parodė, kad navikai, suformuoti iš ląstelių su ETV7 pasižymėjo didesniu proliferaciniu potencialu (Ki67 žymuo) (30 pav.).

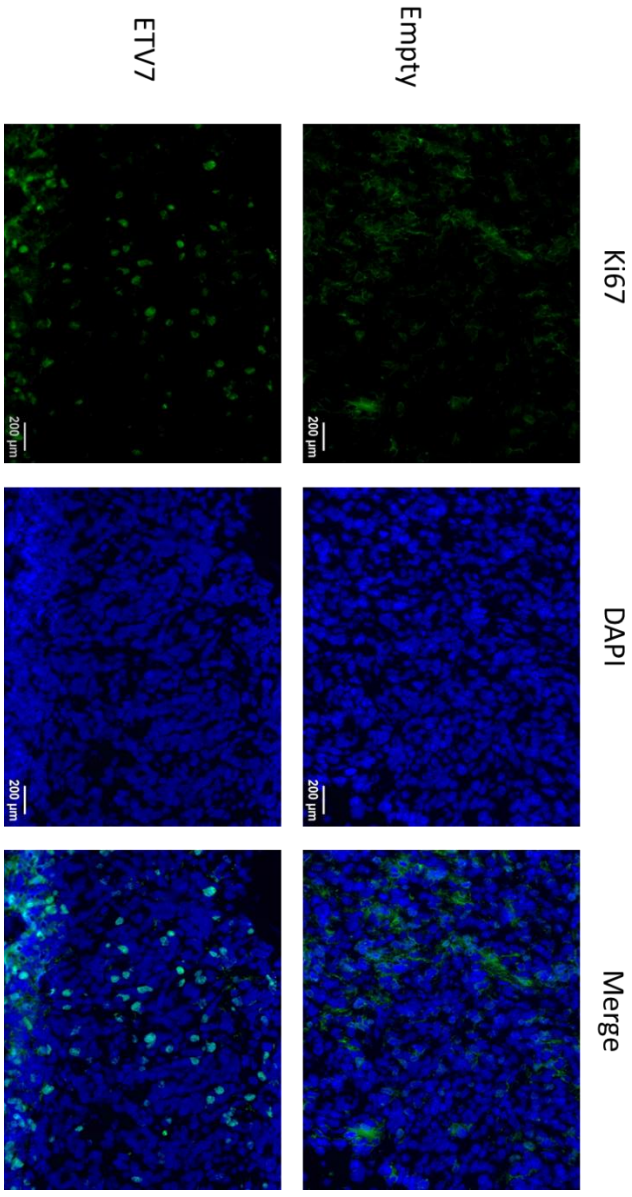

30 pav. Navikai su ETV7 pasižymėjo didesniu proliferaciniu potencialu. Ki67 proliferacijos žymens įvertinimas imunofluorescencijos būdu.

Navikai su ETV7, taip pat pasižymėjo didesniu kamieniškumu (CD44) ir epiteline-mezenchimine tranzicija (VIM) (31 pav.).

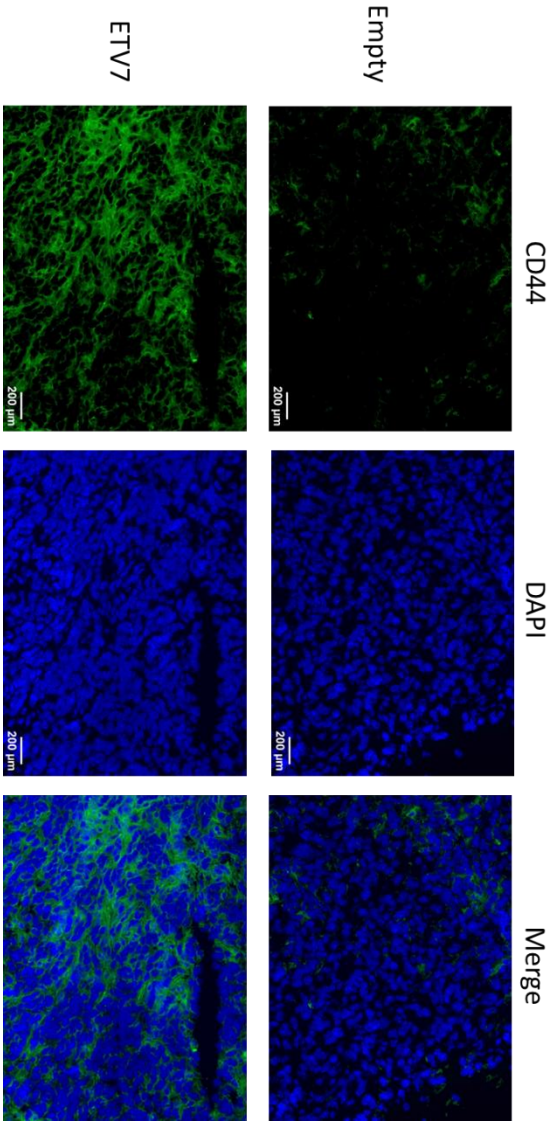

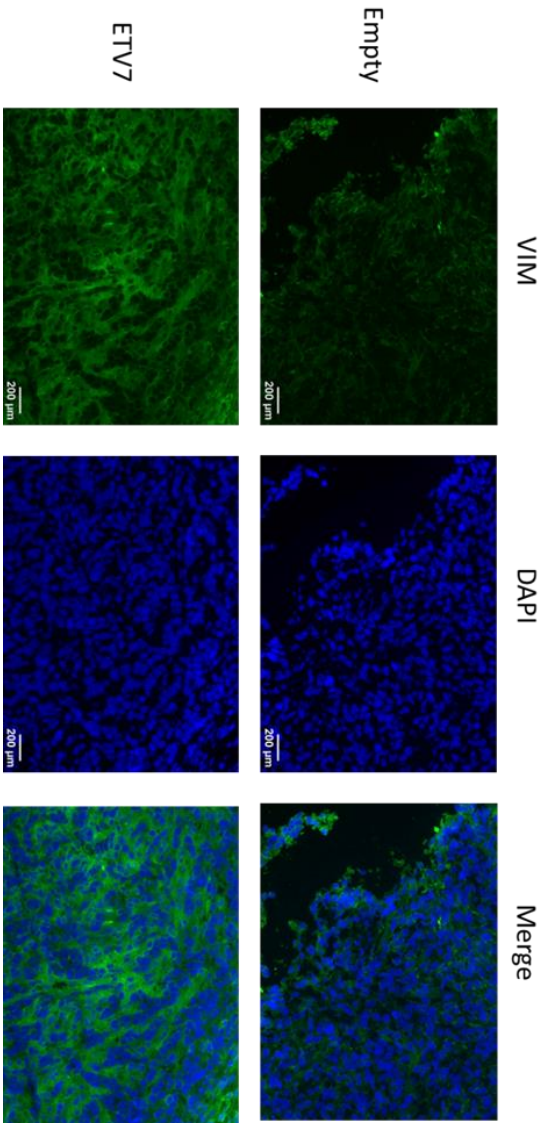

31 pav. Navikams su ETV7 buvo būdingas kamieniškumas ir EMT. CD44 ir VIM žymenų įvertinimas imunofluorescencijos būdu.

Be to, navikams suformuotiems iš ląstelių su padidinta ETV7 raiška taip pat buvo būdinga didesnė fibrolastų infiltracija (α-SMA) (32 pav.).

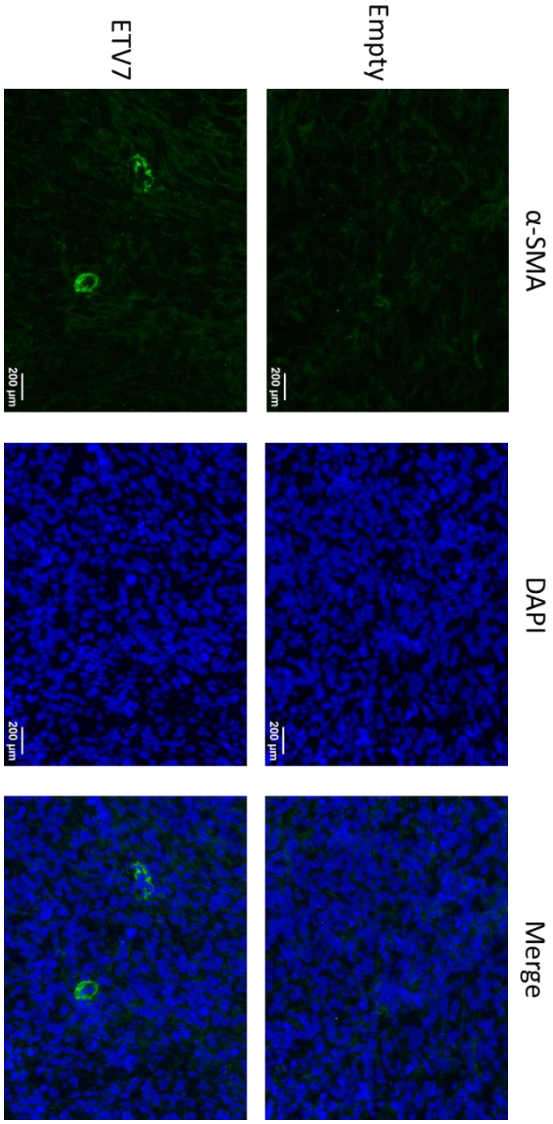

32 pav. Navikai su ETV7 pasižymėjo didesne fibrolastų infiltracija. α-SMA žymens įvertinimas imunofluorescencijos būdu.

Apibendrinant *in vivo* tyrimų metu gautus rezultatus, galime teigti, kad ETV7 skatina navikų formavimąsi ir didina jų agresyvumą ne tik *in vitro*, bet ir *in vivo* modeliuose.

Rezultatų aptarimas

ETV7 yra prastai charakterizuotas transkripcijos slopiklis, kurios raiška yra padidėjusi daugelyje vėžio tipų, tame tarpe ir krūties vėžio atvejais[4,6–8,233].

Įdomu, kad krūties vėžio atveju, ETV7 raiška koreliuoja su vėžio agresyvumu[8]. Prieš tai atliktuose tyrimuose, buvo parodyta, kad ETV7 raiška padidėje ląsteles paveikus DNR pažaidas sukeliančiais vaistas ir kad padidėjusi ETV7 lemia padidėjusį atsparumą priešvėžiniams vaistams[9,10].

Pirmoje šio tyrimo dalyje, mes parodėme, kad ETV7 sumažina krūties vėžio ląstelių jautrumą 5-FU tiek ląstelių monosluoksnuose, tiek ir naudojant 3D modelius (1 pav., 2 pav. ir 3 pav.). Be to, mes pademonstravome, kad šis sumažėjęs jautrumas gydymui 5-fluorouracilu atsiranda dėl to, kad ETV7 slopina interferono stimuliuojamų genų raišką (8 pav.) ir tokių būdu reguliuoja vėžinių ląstelių plastiškumą ir padidina vėžinių kamieninių ląstelių populiaciją (4-7 pav.).

Literatūroje pateikti duomenys, rodantys ETV7 vaidmenį virusinėse infekcijose[11,12] ir mūsų laboraotrijoje gauti preliminarūs duomenys sufleravo, kad ETV7 galėtų būti naujas svarbus vėžio imuninio atsako reguliatorius, todėl antroje ir trečioje šio projekto dalyse mes susikoncentravom ties šių signalinių kelių analize. Įvertinę keletos su uždegiminiaisi ir imuniniais procesais susijusių genų raišką, ląstelėse su padidinta ETV7 raišką, nustatėme, kad ETV7 slopina *TNFRSF1A* geną, kuris koduoja TNFR1 baltymą (10-11 pav.). Mes patvirtinome, kad ETV7 gali tiesiogiai slopinti šį geną santykiaudamas su jo reguliaciniu elementu ir modifikuodamas chromatino prieinamumą kitiems transkripcijos faktoriams (12-13 pav.).

Iš literatūros yra žinoma, kad TNFR1 yra vienas svarbiausių receptorių, aktyvuojančių NF-κB signalinį kelią[149,153,158], dėl to mes ištyrėme, ar ETV7 slopindamas *TNFRSF1A* geną, taip pat nuslopina ir NF-κB signalinį kelią. Mūsų gauti duomenys patvirtino, kad ETV7 sumažina NF-κB signalinio kelio aktyvaciją, kas nulemia mažesnį uždegiminį atsaką krūties vėžinėse ląstelėse (14-17 pav.).

Be to, mes atradome, kad ETV7 konkuruoja su STAT3 dėl *TNFRSF1A* geno reguliacijos (18-19 pav.) ir pasiūlėme naują *TNFRSF1A* geno reguliacijos mechanizmą. Kai ląstelėse padaugėja ETV7, šis sugeba konkuruoti su STAT3 dėl susirišimo su *TNFRSF1A* geno reguliaciniu elementu bei paversti chromatiną mažiau prieinamu ir taip slopinti *TNFRSF1A* geno raišką, Nuslopinta *TNFRSF1A* geno lemia mažesnį TNFR1 kiekį ląstelės paviršiuje ir dėl to yra mažiau aktyvuojamas NF-κB signalinis kelias. Mažesnė NF-κB signalinio kelio reguliacija lemia mažesnį uždegiminį atsaką.

Svarbu paminėti, kad tiek inferferonų, tiek ir NF-κB signaliniai keliai yra labai glaudžiai susijęs su įgimtu ir įgytu imuniniais atsakais[13,273,279]. Mūsų atliktų tyrimu metu, mes parodėme, kad ETV7 slopina abiejų šių kelių aktyvaciją. Inferferonų ir NF-κB signalinių kelių nuslopinimas galima padėti

vėžinėms ląstelėms išvengti šeimininko imuninės sistemos atsako. Iš literatūros yra žinoma, kad abu šie signaliniai keliai dalyvauja antigenų paruošime ir pristatyme, kuris leidžia citotoksinėms T ląstelėms atpažinti vėžines ląsteles ir jas nužudyti[136,161,284]. Šio tyrimo metu mes nustatėme, kad ETV7 slopina antigenų pristatymą vėžinėse ląstelėse ir kad nuslopintas antigenų pristatymas nėra atkuriamas net ir po stimuliacijos su IFN-γ, kuris turėtų indukuoti antigenų pristatymą ant MHC I klasės molekulių[256] (20-21 pav.).

Bendrai įvertinus mūsų rezultatai parodė, kad ETV7 skatina krūties vėžio agresyvumą ir padeda vėžinėms ląstelėms išvengti imuninio atsako. Dėl to mes nusprendėme įvertinti, ar ETV7 galėtų būti potencialus naujas taikinys, krūties vėžio gydymui. Įvertinę ląstelių gyvybingumą po ETV7 nutildymo trylikoje vėžinių ląstelių linijų, pastebėjome, kad ląstelių linijose, kuriose p53 yra laukinio tipo, ETV7 nutildymas lėmė ląstelių žūtį apoptozės būdu (22-27 pav.). Kadangi net 30% krūties vėžio pacientų turi mutavusį p53[285], akivaizdu, kad prieš ETV7 nukreiptas gydymas nepadėtų visiems pacientams, tačiau vis tiek galėtų būti naudingas daliai pacientų.

Galiausiai įvertinome ETV7 poveikį navikų formavimuisi *in vivo* modeliuose. Stebint navikų augimo dinamiką patvirtinome, kad navikai su ETV7 turi didesnį proliferacinį aktyvumą ir formavo didesniu navikus (29 pav.). Be to, ETV7 įtaka navikų agresyvumui buvo patvirtinta ir atlikus imunofluorescencijos analizę su įvairiais žymenimis. Buvo nustatyta, kad ETV7 didina naviko proliferacijos potencialą, kamieniškumą, epitelinę-mezenchiminę tranziciją ir fibrolastų infiltraciją (30-32 pav.).

Apibendrinat visus gautus duomenis, galime teigti, kad ETV7 didina krūties vėžio agresyvumą tiek *in vitro*, tiek *in vivo* modeliuose, be to, mes teigiame, kad ETV7 yra naujas svarbus vėžio imuniteto reguliatorius. Šio tyrimo metu gauti duomenys ne tik padeda geriau suprasti krūties vėžio biologiją, bet ir suteikia svarbios informacijos efektyvesniam vėžio gydymo pritaikymui.

Išvados

1. ETV7 slopina su interferonų atsaku susijusių genų raišką ir tokiu būdu padidina vėžio kamieninių ląstelių populiaciją, kas lemia atsparumo gydymui su 5-fluorouracilu išsivystymą.
2. ETV7 konkuruoja su STAT3 dėl *TNFRSF1A* geno reguliacijos ir slopina TNFR1/NF-κB ašį, tai lemia mažesnį uždegiminį atsaką krūties vėžio ląstelėse.
3. ETV7 slopina su antigenų pristatymu susijusių genų raišką ir tokiu būdu padeda ląstelėms išvengti šeimininko imuninio atsako ir galimai sumažina krūties vėžio ląstelių jautrumą imunoterapijai.

4. ETV7 nutildymas vėžinėse ląstelėse sukelia nuo p53 priklausomą apoptozę.
5. ETV7 skatina krūties vėžio agresyvumą *in vivo* modeliuose.

SOMMARIO

Nel 2020, il cancro al seno è stato il cancro maggiormente diagnosticato nelle donne a livello mondiale (11,7% dei casi totali, 2.3 milioni di nuovi casi nel 2020). Nonostante i progressi nella diagnosi precoce e nel trattamento e i tassi di sopravvivenza relativamente elevati, le metastasi e le recidive dovute alla chemioresistenza rappresentano le principali difficoltà per i medici e le pazienti affette da cancro al seno. In questo studio ci concentriamo su ETV7, un repressore trascrizionale poco studiato, noto per essere up-regolato in diversi tipi di cancro, compreso il cancro al seno. Nella prima parte di questo studio, è stato dimostrato un nuovo ruolo di ETV7 nel promuovere la plasticità delle cellule staminali tumorali (CSCs) mammarie e la resistenza alla chemioterapia nelle cellule di tumore al seno. Abbiamo osservato che le cellule MCF7 e T47D derivate da tumore al seno che sovraesprimono ETV7 mostrano una ridotta sensibilità al farmaco chemioterapico 5-fluorouracile, sia in ambiente 2D che 3D. Abbiamo inoltre osservato che alterazioni nell'espressione di ETV7 possono influenzare significativamente la popolazione delle CSCs mammarie, misurata in base alla popolazione di cellule $CD44^{+}/CD24^{low}$ e all'efficienza di formazione delle mammosfere. Inoltre, abbiamo identificato un gruppo di geni responsivi all'interferone significativamente repressi nelle cellule che sovraesprimono ETV7, a cui potrebbe essere imputato l'aumento della popolazione di CSCs mammarie. Nella seconda e terza parte di questo studio, è stato analizzato il ruolo di ETV7 nelle risposte infiammatorie e immunitarie nelle cellule di cancro al seno. Uno dei geni repressi da ETV7 che abbiamo identificato è *TNFRSF1A*, che codifica per TNFR1, il principale recettore di TNF-α. Abbiamo dimostrato che ETV7 si lega direttamente all'introne I di questo gene e che la down-regolazione di *TNFRSF1A* mediata da ETV7 riduce l'attivazione del signaling di NF-κB. Inoltre, in questo studio abbiamo osservato un potenziale crosstalk tra ETV7 e STAT3, un altro regolatore principale dei processi infiammatori. Sebbene sia noto che STAT3 up-regoli direttamente l'espressione di *TNFRSF1A*, abbiamo qui dimostrato che ETV7 riduce la capacità di STAT3 di legarsi al gene *TNFRSF1A* attraverso un meccanismo competitivo, reclutando rimodellatori della cromatina repressivi, con conseguente repressione della sua trascrizione. Questi risultati suggeriscono che ETV7 possa ridurre le risposte infiammatorie nel cancro al seno attraverso la repressione di *TNFRSF1A*. Inoltre, abbiamo analizzato il coinvolgimento di ETV7 nella regolazione della presentazione dell'antigene, uno dei meccanismi di evasione immunitaria conosciuti, e abbiamo confermato che ETV7 reprime la presentazione dell'antigene nelle cellule di tumore al seno, anche in seguito alla stimolazione con IFN-γ. Nella quarta fase di questo studio, è stato analizzato se il silenziamento di ETV7 possa influire sulla vitalità delle cellule tumorali, ed è stato osservato che il knock-down di ETV7 può indurre l'apoptosi nelle cellule tumorali p53 wild-type. Inoltre, questa apoptosi potrebbe essere mediata dall'asse PUMA/p53. Nell'ultima parte di questa tesi

è stato analizzato il potenziale pro-tumorigenico di ETV7 in modelli *in vivo*. Dopo aver effettuato un'iniezione sottocutanea di cellule di controllo e di cellule che sovraesprimono ETV7, abbiamo osservato che le cellule tumorali della ghiandola mammaria che sovraesprimevano ETV7 formavano tumori più grandi con un potenziale di proliferazione più elevato. Inoltre, in presenza di ETV7, i tumori presentavano livelli più elevati di marcatori legati alla staminalità, alla transizione epitelio-mesenchimale e all'infiltrazione di fibroblasti. Nel complesso, i dati acquisiti nel corso di questo progetto confermano il ruolo di ETV7 come un importante regolatore dell'aggressività del tumore al seno, sia *in vitro* che *in vivo*, e propongono ETV7 come nuovo elemento nell'evasione immunitaria del tumore al seno, aprendo una nuova direzione di ricerca e fornendo utili spunti per strategie terapeutiche più efficaci.

REFERENCES

1. Sung, H. *et al.* Global Cancer Statistics 2020: GLOBOCAN Estimates of Incidence and Mortality Worldwide for 36 Cancers in 185 Countries. *CA: A Cancer Journal for Clinicians* **71**, 209–249 (2021).
2. Masoud, V. & Pagès, G. Targeted therapies in breast cancer: New challenges to fight against resistance. *World J Clin Oncol* **8**, 120–134 (2017).
3. Oliva, D., Andersson, B.-Å., Nilsson, M., Lewin, N. & Lewin, F. Risk for relapse and death after adjuvant chemotherapy associated with SNPs in patients with breast cancer - A retrospective study. *Cancer Treatment and Research Communications* **30**, 100505 (2022).
4. Carella, C. *et al.* The ETS factor TEL2 is a hematopoietic oncoprotein. *Blood* **107**, 1124–1132 (2006).
5. Li, H., Zhang, Y. & Zheng, S. Comprehensive Analysis Identified ETV7 as a Potential Prognostic Biomarker in Bladder Cancer. *Biomed Res Int* **2021**, 8530186 (2021).
6. Matos, J. M., Witzmann, F. A., Cummings, O. W. & Schmidt, C. M. A pilot study of proteomic profiles of human hepatocellular carcinoma in the United States. *J Surg Res* **155**, 237–243 (2009).
7. Thompson, M. C. *et al.* Genomics identifies medulloblastoma subgroups that are enriched for specific genetic alterations. *J Clin Oncol* **24**, 1924–1931 (2006).
8. Piggin, C. L. *et al.* ELF5 isoform expression is tissue-specific and significantly altered in cancer. *Breast Cancer Res* **18**, (2016).
9. Alessandrini, F., Pezzè, L., Menendez, D., Resnick, M. A. & Ciribilli, Y. ETV7-Mediated DNAJC15 Repression Leads to Doxorubicin Resistance in Breast Cancer Cells. *Neoplasia* **20**, 857–870 (2018).
10. Harwood, F. C. *et al.* ETV7 is an essential component of a rapamycin-insensitive mTOR complex in cancer. *Sci Adv* **4**, (2018).
11. Matz, M. *et al.* The regulation of interferon type I pathway-related genes RSAD2 and ETV7 specifically indicates antibody-mediated rejection after kidney transplantation. *Clin Transplant* **32**, e13429 (2018).
12. Froggatt, H. M., Harding, A. T., Chaparian, R. R. & Heaton, N. S. ETV7 limits antiviral gene expression and control of influenza viruses. *Sci Signal* **14**, eabe1194 (2021).
13. Duluc, D. *et al.* Interferon-gamma reverses the immunosuppressive and protumoral properties and prevents the generation of human tumor-associated macrophages. *Int J Cancer* **125**, 367–373 (2009).
14. Kim, S. K. & Cho, S. W. The Evasion Mechanisms of Cancer Immunity and Drug Intervention in the Tumor Microenvironment. *Frontiers in Pharmacology* **13**, (2022).
15. Koren, S. & Bentires-Alj, M. Breast Tumor Heterogeneity: Source of Fitness, Hurdle for Therapy. *Mol Cell* **60**, 537–546 (2015).

16. Lüönd, F., Tiede, S. & Christofori, G. Breast cancer as an example of tumour heterogeneity and tumour cell plasticity during malignant progression. *Br J Cancer* **125**, 164–175 (2021).
17. Polyak, K. Breast cancer: origins and evolution. *J Clin Invest* **117**, 3155–3163 (2007).
18. Coleman, M. P. *et al.* Cancer survival in five continents: a worldwide population-based study (CONCORD). *Lancet Oncol* **9**, 730–756 (2008).
19. Hassiotou, F. & Geddes, D. Anatomy of the human mammary gland: Current status of knowledge. *Clin Anat* **26**, 29–48 (2013).
20. Hennighausen, L. & Robinson, G. W. Information networks in the mammary gland. *Nat Rev Mol Cell Biol* **6**, 715–725 (2005).
21. Shehata, M. *et al.* Phenotypic and functional characterisation of the luminal cell hierarchy of the mammary gland. *Breast Cancer Research* **14**, R134 (2012).
22. Biswas, S. K., Banerjee, S., Baker, G. W., Kuo, C.-Y. & Chowdhury, I. The Mammary Gland: Basic Structure and Molecular Signaling during Development. *International Journal of Molecular Sciences* **23**, 3883 (2022).
23. Akram, M., Iqbal, M., Daniyal, M. & Khan, A. U. Awareness and current knowledge of breast cancer. *Biol Res* **50**, 33 (2017).
24. Colleluori, G., Perugini, J., Barbatelli, G. & Cinti, S. Mammary gland adipocytes in lactation cycle, obesity and breast cancer. *Rev Endocr Metab Disord* **22**, 241–255 (2021).
25. Place, A. E., Jin Huh, S. & Polyak, K. The microenvironment in breast cancer progression: biology and implications for treatment. *Breast Cancer Research* **13**, 227 (2011).
26. Ince, T. A. *et al.* Transformation of different human breast epithelial cell types leads to distinct tumor phenotypes. *Cancer Cell* **12**, 160–170 (2007).
27. Lim, E. *et al.* Aberrant luminal progenitors as the candidate target population for basal tumor development in BRCA1 mutation carriers. *Nat Med* **15**, 907–913 (2009).
28. Keller, P. J. *et al.* Mapping the cellular and molecular heterogeneity of normal and malignant breast tissues and cultured cell lines. *Breast Cancer Res* **12**, R87 (2010).
29. Keller, P. J. *et al.* Defining the cellular precursors to human breast cancer. *Proceedings of the National Academy of Sciences* **109**, 2772–2777 (2012).
30. Nguyen, Q. H. *et al.* Profiling human breast epithelial cells using single cell RNA sequencing identifies cell diversity. *Nat Commun* **9**, 2028 (2018).
31. Langille, E. *et al.* Loss of Epigenetic Regulation Disrupts Lineage Integrity, Induces Aberrant Alveogenesis, and Promotes Breast Cancer. *Cancer Discov* **12**, 2930–2953 (2022).

32. Lin, S., Margueron, R., Charafe-Jauffret, E. & Ginestier, C. Disruption of lineage integrity as a precursor to breast tumor initiation. *Trends in Cell Biology* (2023) doi:10.1016/j.tcb.2023.03.010.
33. Vinuesa-Pitarch, E., Ortega-Álvarez, D. & Rodilla, V. How Lineage Tracing Studies Can Unveil Tumor Heterogeneity in Breast Cancer. *Biomedicines* **10**, 3 (2021).
34. Szymiczek, A., Lone, A. & Akbari, M. R. Molecular intrinsic versus clinical subtyping in breast cancer: A comprehensive review. *Clin Genet* **99**, 613–637 (2021).
35. Feng, Y. *et al.* Breast cancer development and progression: Risk factors, cancer stem cells, signaling pathways, genomics, and molecular pathogenesis. *Genes Dis* **5**, 77–106 (2018).
36. Malhotra, G. K., Zhao, X., Band, H. & Band, V. Histological, molecular and functional subtypes of breast cancers. *Cancer Biol Ther* **10**, 955–960 (2010).
37. Makki, J. Diversity of Breast Carcinoma: Histological Subtypes and Clinical Relevance. *Clin Med Insights Pathol* **8**, 23–31 (2015).
38. Molecular portraits of human breast tumours | Nature. https://www.nature.com/articles/35021093.
39. Comprehensive molecular portraits of human breast tumours | Nature. https://www.nature.com/articles/nature11412.
40. Prat, A. *et al.* Phenotypic and molecular characterization of the claudin-low intrinsic subtype of breast cancer. *Breast Cancer Res* **12**, R68 (2010).
41. Dai, X. *et al.* Breast cancer intrinsic subtype classification, clinical use and future trends. *Am J Cancer Res* **5**, 2929–2943 (2015).
42. Baldassarre, G. & Belletti, B. Molecular biology of breast tumors and prognosis. *F1000Res* **5**, F1000 Faculty Rev-711 (2016).
43. Godoy-Ortiz, A. *et al.* Deciphering HER2 Breast Cancer Disease: Biological and Clinical Implications. *Frontiers in Oncology* **9**, (2019).
44. Charan, M. *et al.* Molecular and Cellular Factors Associated with Racial Disparity in Breast Cancer. *International Journal of Molecular Sciences* **21**, 5936 (2020).
45. Toft, D. J. & Cryns, V. L. Minireview: Basal-Like Breast Cancer: From Molecular Profiles to Targeted Therapies. *Mol Endocrinol* **25**, 199–211 (2011).
46. Badve, S. *et al.* Basal-like and triple-negative breast cancers: a critical review with an emphasis on the implications for pathologists and oncologists. *Mod Pathol* **24**, 157–167 (2011).
47. Conte, F. *et al.* In silico recognition of a prognostic signature in basal-like breast cancer patients. *PLOS ONE* **17**, e0264024 (2022).
48. Wang, W. *et al.* MAPK4 promotes triple negative breast cancer growth and reduces tumor sensitivity to PI3K blockade. *Nat Commun* **13**, 245 (2022).

49. Zong, Y. & Pegram, M. Research advances and new challenges in overcoming triple-negative breast cancer. *Cancer Drug Resistance* **4**, 517–542 (2021).
50. Fougner, C., Bergholtz, H., Norum, J. H. & Sørlie, T. Re-definition of claudin-low as a breast cancer phenotype. *Nat Commun* **11**, 1787 (2020).
51. Pommier, R. M. *et al.* Comprehensive characterization of claudin-low breast tumors reflects the impact of the cell-of-origin on cancer evolution. *Nat Commun* **11**, 3431 (2020).
52. Visvader, J. E. Keeping abreast of the mammary epithelial hierarchy and breast tumorigenesis. *Genes Dev* **23**, 2563–2577 (2009).
53. Arnold, C. R., Mangesius, J., Skvortsova, I.-I. & Ganswindt, U. The Role of Cancer Stem Cells in Radiation Resistance. *Frontiers in Oncology* **10**, (2020).
54. Wang, T. *et al.* Cancer stem cell targeted therapy: progress amid controversies. *Oncotarget* **6**, 44191–44206 (2015).
55. Lei, M. M. L. & Lee, T. K. W. Cancer Stem Cells: Emerging Key Players in Immune Evasion of Cancers. *Front Cell Dev Biol* **9**, 692940 (2021).
56. Atashzar, M. R. *et al.* Cancer stem cells: A review from origin to therapeutic implications. *J Cell Physiol* **235**, 790–803 (2020).
57. Tomasetti, C. & Vogelstein, B. Variation in cancer risk among tissues can be explained by the number of stem cell divisions. *Science* **347**, 78–81 (2015).
58. Ayob, A. Z. & Ramasamy, T. S. Cancer stem cells as key drivers of tumour progression. *Journal of Biomedical Science* **25**, 20 (2018).
59. Joshua, B. *et al.* Frequency of cells expressing CD44, a Head and Neck cancer stem cell marker: Correlation with tumor aggressiveness. *Head & Neck* **34**, 42–49 (2012).
60. O'Brien, C. A., Pollett, A., Gallinger, S. & Dick, J. E. A human colon cancer cell capable of initiating tumour growth in immunodeficient mice. *Nature* **445**, 106–110 (2007).
61. Singh, S. K. *et al.* Identification of human brain tumour initiating cells. *Nature* **432**, 396–401 (2004).
62. Quintana, E. *et al.* Efficient tumour formation by single human melanoma cells. *Nature* **456**, 593–598 (2008).
63. Yu, Z., Pestell, T. G., Lisanti, M. P. & Pestell, R. G. Cancer Stem Cells. *Int J Biochem Cell Biol* **44**, 2144–2151 (2012).
64. Beck, B. & Blanpain, C. Unravelling cancer stem cell potential. *Nat Rev Cancer* **13**, 727–738 (2013).
65. Zhou, H.-M., Zhang, J.-G., Zhang, X. & Li, Q. Targeting cancer stem cells for reversing therapy resistance: mechanism, signaling, and prospective agents. *Sig Transduct Target Ther* **6**, 1–17 (2021).
66. Munz, M., Baeuerle, P. A. & Gires, O. The Emerging Role of EpCAM in Cancer and Stem Cell Signaling. *Cancer Research* **69**, 5627–5629 (2009).

67. Phi, L. T. H. *et al.* Cancer Stem Cells (CSCs) in Drug Resistance and their Therapeutic Implications in Cancer Treatment. *Stem Cells Int* **2018**, 5416923 (2018).
68. Yadav, A. K. & Desai, N. S. Cancer Stem Cells: Acquisition, Characteristics, Therapeutic Implications, Targeting Strategies and Future Prospects. *Stem Cell Rev and Rep* **15**, 331–355 (2019).
69. Bozorgi, A., Khazaei, M. & Khazaei, M. R. New Findings on Breast Cancer Stem Cells: A Review. *J Breast Cancer* **18**, 303 (2015).
70. Mani, S. A. *et al.* The epithelial-mesenchymal transition generates cells with properties of stem cells. *Cell* **133**, 704–715 (2008).
71. da Silva-Diz, V., Lorenzo-Sanz, L., Bernat-Peguera, A., Lopez-Cerda, M. & Muñoz, P. Cancer cell plasticity: Impact on tumor progression and therapy response. *Seminars in Cancer Biology* **53**, 48–58 (2018).
72. Warrier, N. M. *et al.* Understanding cancer stem cells and plasticity: Towards better therapeutics. *European Journal of Cell Biology* **102**, 151321 (2023).
73. Cabrera, M. C., Hollingsworth, R. E. & Hurt, E. M. Cancer stem cell plasticity and tumor hierarchy. *World J Stem Cells* **7**, 27–36 (2015).
74. Aramini, B. *et al.* Cancer stem cells and macrophages: molecular connections and future perspectives against cancer. *Oncotarget* **12**, 230–250 (2021).
75. Thankamony, A. P., Saxena, K., Murali, R., Jolly, M. K. & Nair, R. Cancer Stem Cell Plasticity – A Deadly Deal. *Front Mol Biosci* **7**, 79 (2020).
76. Al-Hajj, M., Wicha, M. S., Benito-Hernandez, A., Morrison, S. J. & Clarke, M. F. Prospective identification of tumorigenic breast cancer cells. *Proc Natl Acad Sci U S A* **100**, 3983–3988 (2003).
77. Zheng, Q., Zhang, M., Zhou, F., Zhang, L. & Meng, X. The Breast Cancer Stem Cells Traits and Drug Resistance. *Frontiers in Pharmacology* **11**, (2021).
78. Zhang, X., Powell, K. & Li, L. Breast Cancer Stem Cells: Biomarkers, Identification and Isolation Methods, Regulating Mechanisms, Cellular Origin, and Beyond. *Cancers (Basel)* **12**, 3765 (2020).
79. Thapa, R. & Wilson, G. D. The Importance of CD44 as a Stem Cell Biomarker and Therapeutic Target in Cancer. *Stem Cells Int* **2016**, 2087204 (2016).
80. Senbanjo, L. T. & Chellaiah, M. A. CD44: A Multifunctional Cell Surface Adhesion Receptor Is a Regulator of Progression and Metastasis of Cancer Cells. *Frontiers in Cell and Developmental Biology* **5**, (2017).
81. Chen, C., Zhao, S., Karnad, A. & Freeman, J. W. The biology and role of CD44 in cancer progression: therapeutic implications. *Journal of Hematology & Oncology* **11**, 64 (2018).
82. Hiraga, T., Ito, S. & Nakamura, H. EpCAM expression in breast cancer cells is associated with enhanced bone metastasis formation. *Int J Cancer* **138**, 1698–1708 (2016).

83. Panigoro, S. S., Kurnia, D., Kurnia, A., Haryono, S. J. & Albar, Z. A. ALDH1 Cancer Stem Cell Marker as a Prognostic Factor in Triple-Negative Breast Cancer. *International Journal of Surgical Oncology* **2020**, e7863243 (2020).
84. Khoury, T. *et al.* Aldehyde dehydrogenase 1A1 expression in breast cancer is associated with stage, triple negativity, and outcome to neoadjuvant chemotherapy. *Mod Pathol* **25**, 388–397 (2012).
85. Liu, X. & Fan, D. The epithelial-mesenchymal transition and cancer stem cells: functional and mechanistic links. *Curr Pharm Des* **21**, 1279–1291 (2015).
86. Liu, S. *et al.* Breast cancer stem cells transition between epithelial and mesenchymal states reflective of their normal counterparts. *Stem Cell Reports* **2**, 78–91 (2014).
87. Khan, M. I. *et al.* Current approaches in identification and isolation of human renal cell carcinoma cancer stem cells. *Stem Cell Res Ther* **6**, 178 (2015).
88. Lombardo, Y., de Giorgio, A., Coombes, C. R., Stebbing, J. & Castellano, L. Mammosphere Formation Assay from Human Breast Cancer Tissues and Cell Lines. *J Vis Exp* 52671 (2015) doi:10.3791/52671.
89. Li, W. *et al.* Unraveling the roles of CD44/CD24 and ALDH1 as cancer stem cell markers in tumorigenesis and metastasis. *Sci Rep* **7**, 13856 (2017).
90. Aiken, C. & Werbowetski-Ogilvie, T. Animal Models of Cancer Stem Cells: What are They Really Telling Us? *Curr Pathobiol Rep* **1**, 91–99 (2013).
91. Luo, M. *et al.* Breast cancer stem cells: current advances and clinical implications. *Methods Mol Biol* **1293**, 1–49 (2015).
92. Nounou, M. I. *et al.* Breast Cancer: Conventional Diagnosis and Treatment Modalities and Recent Patents and Technologies. *Breast Cancer (Auckl)* **9**, 17–34 (2015).
93. Harbeck, N. *et al.* Breast cancer. *Nat Rev Dis Primers* **5**, 1–31 (2019).
94. El Sayed, R. *et al.* Endocrine and Targeted Therapy for Hormone-Receptor-Positive, HER2-Negative Advanced Breast Cancer: Insights to Sequencing Treatment and Overcoming Resistance Based on Clinical Trials. *Frontiers in Oncology* **9**, (2019).
95. Frontiers | Progress in the Understanding of the Mechanism of Tamoxifen Resistance in Breast Cancer. https://www.frontiersin.org/articles/10.3389/fphar.2020.592912/full.
96. Nathan, M. R. & Schmid, P. A Review of Fulvestrant in Breast Cancer. *Oncol Ther* **5**, 17–29 (2017).
97. Bradley, R. *et al.* Trastuzumab for early-stage, HER2-positive breast cancer: a meta-analysis of 13 864 women in seven randomised trials. *The Lancet Oncology* **22**, 1139–1150 (2021).

98. Tong, C. W. S., Wu, M., Cho, W. C. S. & To, K. K. W. Recent Advances in the Treatment of Breast Cancer. *Frontiers in Oncology* **8**, (2018).
99. Shepherd, G. M. Hypersensitivity reactions to chemotherapeutic drugs. *Clin Rev Allergy Immunol* **24**, 253–262 (2003).
100. Amjad, M. T., Chidharla, A. & Kasi, A. *Cancer Chemotherapy*. *StatPearls [Internet]* (StatPearls Publishing, 2022).
101. Akkın, S., Varan, G. & Bilensoy, E. A Review on Cancer Immunotherapy and Applications of Nanotechnology to Chemoimmunotherapy of Different Cancers. *Molecules* **26**, 3382 (2021).
102. Ponce-Cusi, R. & Calaf, G. M. Apoptotic activity of 5-fluorouracil in breast cancer cells transformed by low doses of ionizing α-particle radiation. *International Journal of Oncology* **48**, 774–782 (2016).
103. Christensen, S. *et al.* 5-Fluorouracil treatment induces characteristic T>G mutations in human cancer. *Nat Commun* **10**, 4571 (2019).
104. Longley, D. B., Harkin, D. P. & Johnston, P. G. 5-Fluorouracil: mechanisms of action and clinical strategies. *Nat Rev Cancer* **3**, 330–338 (2003).
105. Zhang, N., Yin, Y., Xu, S.-J. & Chen, W.-S. 5-Fluorouracil: Mechanisms of Resistance and Reversal Strategies. *Molecules* **13**, 1551–1569 (2008).
106. Ghafouri-Fard, S. *et al.* 5-Fluorouracil: A Narrative Review on the Role of Regulatory Mechanisms in Driving Resistance to This Chemotherapeutic Agent. *Frontiers in Oncology* **11**, (2021).
107. Henriques, B., Mendes, F. & Martins, D. Immunotherapy in Breast Cancer: When, How, and What Challenges? *Biomedicines* **9**, 1687 (2021).
108. Debien, V. *et al.* Immunotherapy in breast cancer: an overview of current strategies and perspectives. *npj Breast Cancer* **9**, 1–10 (2023).
109. Galván Morales, M. A., Barrera Rodríguez, R., Santiago Cruz, J. R. & Teran, L. M. Overview of New Treatments with Immunotherapy for Breast Cancer and a Proposal of a Combination Therapy. *Molecules* **25**, 5686 (2020).
110. Waldman, A. D., Fritz, J. M. & Lenardo, M. J. A guide to cancer immunotherapy: from T cell basic science to clinical practice. *Nat Rev Immunol* **20**, 651–668 (2020).
111. Ling, S. P. *et al.* Role of Immunotherapy in the Treatment of Cancer: A Systematic Review. *Cancers* **14**, 5205 (2022).
112. Salemme, V., Centonze, G., Cavallo, F., Defilippi, P. & Conti, L. The Crosstalk Between Tumor Cells and the Immune Microenvironment in Breast Cancer: Implications for Immunotherapy. *Frontiers in Oncology* **11**, (2021).
113. Mehraj, U., Dar, A. H., Wani, N. A. & Mir, M. A. Tumor microenvironment promotes breast cancer chemoresistance. *Cancer Chemother Pharmacol* **87**, 147–158 (2021).

114. Sadeghi Rad, H. *et al.* Understanding the tumor microenvironment for effective immunotherapy. *Med Res Rev* **41**, 1474–1498 (2021).
115. Tang, H., Qiao, J. & Fu, Y.-X. Immunotherapy and tumor microenvironment. *Cancer Lett* **370**, 85–90 (2016).
116. Negishi, H., Taniguchi, T. & Yanai, H. The Interferon (IFN) Class of Cytokines and the IFN Regulatory Factor (IRF) Transcription Factor Family. *Cold Spring Harb Perspect Biol* **10**, a028423 (2018).
117. Wack, A., Terczyńska-Dyla, E. & Hartmann, R. Guarding the frontiers: the biology of type III interferons. *Nat Immunol* **16**, 802–809 (2015).
118. Lee, A. J. & Ashkar, A. A. The Dual Nature of Type I and Type II Interferons. *Frontiers in Immunology* **9**, (2018).
119. Borden, E. C. *et al.* Interferons at age 50: past, current and future impact on biomedicine. *Nat Rev Drug Discov* **6**, 975–990 (2007).
120. Jorgovanovic, D., Song, M., Wang, L. & Zhang, Y. Roles of IFN-γ in tumor progression and regression: a review. *Biomarker Research* **8**, 49 (2020).
121. Mendoza, J. L. *et al.* Structure of the IFNγ receptor complex guides design of biased agonists. *Nature* **567**, 56–60 (2019).
122. Stanifer, M. L., Guo, C., Doldan, P. & Boulant, S. Importance of Type I and III Interferons at Respiratory and Intestinal Barrier Surfaces. *Frontiers in Immunology* **11**, (2020).
123. Schneider, W. M., Chevillotte, M. D. & Rice, C. M. Interferon-Stimulated Genes: A Complex Web of Host Defenses. *Annu Rev Immunol* **32**, 513–545 (2014).
124. Xin, P. *et al.* The role of JAK/STAT signaling pathway and its inhibitors in diseases. *International Immunopharmacology* **80**, 106210 (2020).
125. Hu, X., Li, J., Fu, M., Zhao, X. & Wang, W. The JAK/STAT signaling pathway: from bench to clinic. *Sig Transduct Target Ther* **6**, 1–33 (2021).
126. Ivashkiv, L. B. & Donlin, L. T. Regulation of type I interferon responses. *Nat Rev Immunol* **14**, 36–49 (2014).
127. Deng, S., Graham, M. L. & Chen, X.-M. The Complexity of Interferon Signaling in Host Defense against Protozoan Parasite Infection. *Pathogens* **12**, 319 (2023).
128. Iwasaki, A. A virological view of innate immune recognition. *Annu Rev Microbiol* **66**, 177–196 (2012).
129. Martin-Hijano, L. & Sainz, B. The Interactions Between Cancer Stem Cells and the Innate Interferon Signaling Pathway. *Frontiers in Immunology* **11**, (2020).
130. Zhou, L. *et al.* A Dual Role of Type I Interferons in Antitumor Immunity. *Advanced Biosystems* **4**, 1900237 (2020).
131. Einat, M., Resnitzky, D. & Kimchi, A. Close link between reduction of c-myc expression by interferon and, G0/G1 arrest. *Nature* **313**, 597–600 (1985).

132. Porta, C. *et al.* Interferons α and γ induce p53-dependent and p53-independent apoptosis, respectively. *Oncogene* **24**, 605–615 (2005).
133. Chawla-Sarkar, M., Leaman, D. W. & Borden, E. C. Preferential Induction of Apoptosis by Interferon (IFN)-β Compared with IFN-α2: Correlation with TRAIL/Apo2L Induction in Melanoma Cell Lines. *Clinical Cancer Research* **7**, 1821–1831 (2001).
134. Cheriyath, V. *et al.* G1P3, an IFN-induced survival factor, antagonizes TRAIL-induced apoptosis in human myeloma cells. *J Clin Invest* **117**, 3107–3117 (2007).
135. Bernassola, F. *et al.* Induction of apoptosis by IFNgamma in human neuroblastoma cell lines through the CD95/CD95L autocrine circuit. *Cell Death Differ* **6**, 652–660 (1999).
136. Dhatchinamoorthy, K., Colbert, J. D. & Rock, K. L. Cancer Immune Evasion Through Loss of MHC Class I Antigen Presentation. *Frontiers in Immunology* **12**, (2021).
137. Alavi, S. *et al.* Interferon Signaling Is Frequently Downregulated in Melanoma. *Frontiers in Immunology* **9**, (2018).
138. Schiavoni, G., Mattei, F. & Gabriele, L. Type I Interferons as Stimulators of DC-Mediated Cross-Priming: Impact on Anti-Tumor Response. *Frontiers in Immunology* **4**, (2013).
139. Fuertes, M. B. *et al.* Host type I IFN signals are required for antitumor CD8+ T cell responses through CD8{alpha}+ dendritic cells. *J Exp Med* **208**, 2005–2016 (2011).
140. Weichselbaum, R. R. *et al.* An interferon-related gene signature for DNA damage resistance is a predictive marker for chemotherapy and radiation for breast cancer. *Proc Natl Acad Sci U S A* **105**, 18490–18495 (2008).
141. Balkwill, F. & Mantovani, A. Inflammation and cancer: back to Virchow? *Lancet* **357**, 539–545 (2001).
142. Colotta, F., Allavena, P., Sica, A., Garlanda, C. & Mantovani, A. Cancer-related inflammation, the seventh hallmark of cancer: links to genetic instability. *Carcinogenesis* **30**, 1073–1081 (2009).
143. Mantovani, A., Allavena, P., Sica, A. & Balkwill, F. Cancer-related inflammation. **454**, 9 (2008).
144. Prete, A. D. *et al.* Molecular pathways in cancer-related inflammation. *Biochem Med* **21**, 264–275 (2011).
145. Ferrone, C. & Dranoff, G. Dual Roles for Immunity in Gastrointestinal Cancers. *J Clin Oncol* **28**, 4045–4051 (2010).
146. Schmitt, M. & Greten, F. R. The inflammatory pathogenesis of colorectal cancer. *Nat Rev Immunol* **21**, 653–667 (2021).
147. Tan, Z. *et al.* The Role of Tumor Inflammatory Microenvironment in Lung Cancer. *Frontiers in Pharmacology* **12**, (2021).
148. Gough, P. & Myles, I. A. Tumor Necrosis Factor Receptors: Pleiotropic Signaling Complexes and Their Differential Effects. *Frontiers in Immunology* **11**, (2020).

149. Kalliolias, G. D. & Ivashkiv, L. B. TNF biology, pathogenic mechanisms and emerging therapeutic strategies. *Nat Rev Rheumatol* **12**, 49–62 (2016).
150. Vanamee, É. S. & Faustman, D. L. Structural principles of tumor necrosis factor superfamily signaling. *Sci Signal* **11**, eaao4910 (2018).
151. Brenner, D., Blaser, H. & Mak, T. W. Regulation of tumour necrosis factor signalling: live or let die. *Nat Rev Immunol* **15**, 362–374 (2015).
152. Jang, D. *et al.* The Role of Tumor Necrosis Factor Alpha (TNF-α) in Autoimmune Disease and Current TNF-α Inhibitors in Therapeutics. *Int J Mol Sci* **22**, 2719 (2021).
153. Wajant, H. & Scheurich, P. TNFR1-induced activation of the classical NF-κB pathway. *The FEBS Journal* **278**, 862–876 (2011).
154. Van Quickelberghe, E., De Sutter, D., van Loo, G., Eyckerman, S. & Gevaert, K. A protein-protein interaction map of the TNF-induced NF-κB signal transduction pathway. *Sci Data* **5**, 180289 (2018).
155. Zinatizadeh, M. R. *et al.* The Nuclear Factor Kappa B (NF-kB) signaling in cancer development and immune diseases. *Genes Dis* **8**, 287–297 (2021).
156. Hoesel, B. & Schmid, J. A. The complexity of NF-κB signaling in inflammation and cancer. *Molecular Cancer* **12**, 86 (2013).
157. Peng, C., Ouyang, Y., Lu, N. & Li, N. The NF-κB Signaling Pathway, the Microbiota, and Gastrointestinal Tumorigenesis: Recent Advances. *Frontiers in Immunology* **11**, (2020).
158. Ting, A. T. & Bertrand, M. J. M. More to life than NF-κB in TNFR1 signaling. *Trends Immunol* **37**, 535–545 (2016).
159. Mercogliano, M. F., Bruni, S., Elizalde, P. V. & Schillaci, R. Tumor Necrosis Factor α Blockade: An Opportunity to Tackle Breast Cancer. *Front Oncol* **10**, 584 (2020).
160. O'Reilly, L. A. *et al.* Loss of NF-κB1 Causes Gastric Cancer with Aberrant Inflammation and Expression of Immune Checkpoint Regulators in a STAT-1-Dependent Manner. *Immunity* **48**, 570-583.e8 (2018).
161. Cornel, A. M., Mimpen, I. L. & Nierkens, S. MHC Class I Downregulation in Cancer: Underlying Mechanisms and Potential Targets for Cancer Immunotherapy. *Cancers (Basel)* **12**, E1760 (2020).
162. Bates, J. P., Derakhshandeh, R., Jones, L. & Webb, T. J. Mechanisms of immune evasion in breast cancer. *BMC Cancer* **18**, 556 (2018).
163. Vesely, M. D. & Schreiber, R. D. Cancer Immunoediting: antigens, mechanisms and implications to cancer immunotherapy. *Ann N Y Acad Sci* **1284**, 1–5 (2013).
164. Dunn, G. P., Bruce, A. T., Ikeda, H., Old, L. J. & Schreiber, R. D. Cancer immunoediting: from immunosurveillance to tumor escape. *Nat Immunol* **3**, 991–998 (2002).
165. Mortezaee, K. Immune escape: A critical hallmark in solid tumors. *Life Sci* **258**, 118110 (2020).

166. Suresh, S. & O'Donnell, K. A. Translational Control of Immune Evasion in Cancer. *Trends in Cancer* **7**, 580–582 (2021).
167. Davies, M. New modalities of cancer treatment for NSCLC: focus on immunotherapy. *CMAR* **6**, 63–75 (2014).
168. Hazini, A., Fisher, K. & Seymour, L. Deregulation of HLA-I in cancer and its central importance for immunotherapy. *J Immunother Cancer* **9**, e002899 (2021).
169. Drake, C. G., Jaffee, E. & Pardoll, D. M. Mechanisms of immune evasion by tumors. *Adv Immunol* **90**, 51–81 (2006).
170. Leone, P. *et al.* MHC Class I Antigen Processing and Presenting Machinery: Organization, Function, and Defects in Tumor Cells. *JNCI: Journal of the National Cancer Institute* **105**, 1172–1187 (2013).
171. Yoshihama, S., Vijayan, S., Sidiq, T. & Kobayashi, K. S. NLRC5/CITA: A Key Player in Cancer Immune Surveillance. *Trends Cancer* **3**, 28–38 (2017).
172. Watanabe, A., Yashiroda, H., Ishihara, S., Lo, M. & Murata, S. The Molecular Mechanisms Governing the Assembly of the Immuno- and Thymoproteasomes in the Presence of Constitutive Proteasomes. *Cells* **11**, 1580 (2022).
173. Kincaid, E. Z. *et al.* Mice completely lacking immunoproteasomes show major changes in antigen presentation. *Nat Immunol* **13**, 129–135 (2011).
174. Tripathi, S. C., Vedpathak, D. & Ostrin, E. J. The Functional and Mechanistic Roles of Immunoproteasome Subunits in Cancer. *Cells* **10**, 3587 (2021).
175. Leister, H., Krause, F. F., Mahdavi, R., Steinhoff, U. & Visekruna, A. The Role of Immunoproteasomes in Tumor-Immune Cell Interactions in Melanoma and Colon Cancer. *Arch. Immunol. Ther. Exp.* **70**, 5 (2022).
176. Kalaora, S. *et al.* Immunoproteasome expression is associated with better prognosis and response to checkpoint therapies in melanoma. *Nat Commun* **11**, 896 (2020).
177. Lee, M. Y., Jeon, J. W., Sievers, C. & Allen, C. T. Antigen processing and presentation in cancer immunotherapy. *J Immunother Cancer* **8**, e001111 (2020).
178. Vijayan, S., Sidiq, T., Yousuf, S., van den Elsen, P. J. & Kobayashi, K. S. Class I transactivator, NLRC5: a central player in the MHC class I pathway and cancer immune surveillance. *Immunogenetics* **71**, 273–282 (2019).
179. de Charette, M., Marabelle, A. & Houot, R. Turning tumour cells into antigen presenting cells: The next step to improve cancer immunotherapy? *European Journal of Cancer* **68**, 134–147 (2016).
180. Paschen, A. *et al.* Complete loss of HLA class I antigen expression on melanoma cells: A result of successive mutational events. *International Journal of Cancer* **103**, 759–767 (2003).

181. Jongsma, M. L. M., Guarda, G. & Spaapen, R. M. The regulatory network behind MHC class I expression. *Molecular Immunology* **113**, 16–21 (2019).
182. Wells, K. *et al.* Abstract 5002: Investigating the role of NF- κB signaling and immune checkpoint blockade therapy in melanoma. *Cancer Research* **79**, 5002 (2019).
183. Reyal, F. *et al.* Molecular profiling of patient-derived breast cancer xenografts. *Breast Cancer Research* **14**, R11 (2012).
184. Grasso, C. S. *et al.* Conserved Interferon-γ Signaling Drives Clinical Response to Immune Checkpoint Blockade Therapy in Melanoma. *Cancer Cell* **38**, 500-515.e3 (2020).
185. Gao, J. *et al.* Loss of IFN-γ Pathway Genes in Tumor Cells as a Mechanism of Resistance to Anti-CTLA-4 Therapy. *Cell* **167**, 397-404.e9 (2016).
186. Gettinger, S. *et al.* Impaired HLA Class I Antigen Processing and Presentation as a Mechanism of Acquired Resistance to Immune Checkpoint Inhibitors in Lung Cancer. *Cancer Discov* **7**, 1420–1435 (2017).
187. Meissner, T. B. *et al.* NLR family member NLRC5 is a transcriptional regulator of MHC class I genes. *Proc Natl Acad Sci U S A* **107**, 13794–13799 (2010).
188. Ozcan, M., Janikovits, J., von Knebel Doeberitz, M. & Kloor, M. Complex pattern of immune evasion in MSI colorectal cancer. *Oncoimmunology* **7**, e1445453 (2018).
189. Yoshihama, S. *et al.* NLRC5/MHC class I transactivator is a target for immune evasion in cancer. *Proc Natl Acad Sci U S A* **113**, 5999–6004 (2016).
190. Chandrasekaran, S. *et al.* Phosphoinositide 3-Kinase Signaling Can Modulate MHC Class I and II Expression. *Mol Cancer Res* **17**, 2395–2409 (2019).
191. Herrmann, F. *et al.* HER-2/neu-mediated regulation of components of the MHC class I antigen-processing pathway. *Cancer Res* **64**, 215–220 (2004).
192. Brea, E. J. *et al.* Kinase Regulation of Human MHC Class I Molecule Expression on Cancer Cells. *Cancer Immunol Res* **4**, 936–947 (2016).
193. Khan, A. N. H., Gregorie, C. J. & Tomasi, T. B. Histone deacetylase inhibitors induce TAP, LMP, Tapasin genes and MHC class I antigen presentation by melanoma cells. *Cancer Immunol Immunother* **57**, 647–654 (2008).
194. Mora-García, M. de L. *et al.* Up-regulation of HLA class-I antigen expression and antigen-specific CTL response in cervical cancer cells by the demethylating agent hydralazine and the histone deacetylase inhibitor valproic acid. *J Transl Med* **4**, 55 (2006).
195. Yang, W., Li, Y., Gao, R., Xiu, Z. & Sun, T. MHC class I dysfunction of glioma stem cells escapes from CTL-mediated immune response via

activation of Wnt/β-catenin signaling pathway. *Oncogene* **39**, 1098–1111 (2020).
196. Luo, N. *et al.* DNA methyltransferase inhibition upregulates MHC-I to potentiate cytotoxic T lymphocyte responses in breast cancer. *Nat Commun* **9**, 248 (2018).
197. Qiu, Y. *et al.* Next frontier in tumor immunotherapy: macrophage-mediated immune evasion. *Biomarker Research* **9**, 72 (2021).
198. Petty, A. J. & Yang, Y. Tumor-associated macrophages: implications in cancer immunotherapy. *Immunotherapy* **9**, 289–302 (2017).
199. van Ravenswaay Claasen, H. H., Kluin, P. M. & Fleuren, G. J. Tumor infiltrating cells in human cancer. On the possible role of CD16+ macrophages in antitumor cytotoxicity. *Lab Invest* **67**, 166–174 (1992).
200. Pinto, M. L. *et al.* The Two Faces of Tumor-Associated Macrophages and Their Clinical Significance in Colorectal Cancer. *Front Immunol* **10**, 1875 (2019).
201. Pollard, J. W. Macrophages define the invasive microenvironment in breast cancer. *Journal of Leukocyte Biology* **84**, 623–630 (2008).
202. Sawa-Wejksza, K., Dudek, A., Lemieszek, M., Kaławaj, K. & Kandefer-Szerszeń, M. Colon cancer–derived conditioned medium induces differentiation of THP-1 monocytes into a mixed population of M1/M2 cells. *Tumour Biol.* **40**, 1010428318797880 (2018).
203. Potter, M. D., Buijs, A., Kreider, B., van Rompaey, L. & Grosveld, G. C. Identification and characterization of a new human ETS-family transcription factor, TEL2, that is expressed in hematopoietic tissues and can associate with TEL1/ETV6. *Blood* **95**, 3341–3348 (2000).
204. Hsu, T., Trojanowska, M. & Watson, D. K. Ets Proteins in Biological Control and Cancer. *J Cell Biochem* **91**, 896–903 (2004).
205. Sizemore, G. M., Pitarresi, J. R., Balakrishnan, S. & Ostrowski, M. C. The ETS family of oncogenic transcription factors in solid tumours. *Nat Rev Cancer* **17**, 337–351 (2017).
206. Findlay, V. J., LaRue, A. C., Turner, D. P., Watson, P. M. & Watson, D. K. Understanding the Role of ETS-Mediated Gene Regulation in Complex Biological Processes. *Adv Cancer Res* **119**, 1–61 (2013).
207. Kim, G.-C. *et al.* ETS1 Suppresses Tumorigenesis of Human Breast Cancer via Trans-Activation of Canonical Tumor Suppressor Genes. *Frontiers in Oncology* **10**, (2020).
208. Sang, Y. *et al.* TEL2 suppresses metastasis by down-regulating SERPINE1 in nasopharyngeal carcinoma. *Oncotarget* **6**, 29240–29253 (2015).
209. Kar, A. & Gutierrez-Hartmann, A. Molecular mechanisms of ETS transcription factor mediated tumorigenesis. *Crit Rev Biochem Mol Biol* **48**, 522–543 (2013).
210. Tomlins, S. A. *et al.* Recurrent Fusion of TMPRSS2 and ETS Transcription Factor Genes in Prostate Cancer. *Science* **310**, 644–648 (2005).

211. Seth, A. & Watson, D. K. ETS transcription factors and their emerging roles in human cancer. *European Journal of Cancer* **41**, 2462–2478 (2005).
212. Prescott, J. D., Poczobutt, J. M., Tentler, J. J., Walker, D. M. & Gutierrez-Hartmann, A. Mapping of ESE-1 subdomains required to initiate mammary epithelial cell transformation via a cytoplasmic mechanism. *Molecular Cancer* **10**, 103 (2011).
213. Gutierrez-Hartmann, A., Duval, D. L. & Bradford, A. P. ETS transcription factors in endocrine systems. *Trends Endocrinol Metab* **18**, 150–158 (2007).
214. Wei, G.-H. *et al.* Genome-wide analysis of ETS-family DNA-binding in vitro and in vivo. *EMBO J* **29**, 2147–2160 (2010).
215. Rasighaemi, P. & Ward, A. C. ETV6 and ETV7: Siblings in hematopoiesis and its disruption in disease. *Critical Reviews in Oncology/Hematology* **116**, 106–115 (2017).
216. Gu, X. *et al.* Tel-2 Is a Novel Transcriptional Repressor Related to the Ets Factor Tel/ETV-6*. *Journal of Biological Chemistry* **276**, 9421–9436 (2001).
217. Hock, H. & Shimamura, A. ETV6 in Hematopoiesis and Leukemia Predisposition. *Semin Hematol* **54**, 98–104 (2017).
218. Poirel, H. *et al.* Characterization of a novel ETS gene, TELB, encoding a protein structurally and functionally related to TEL. *Oncogene* **19**, 4802–4806 (2000).
219. Numata, M., Geltink, R. K. & Grosveld, G. The ETS Transcription Factor ETV7 Exhausts Hematopoietic Stem Cells By Enhancing The Cell Cycle Entry and Cell Proliferation. *Blood* **122**, 733 (2013).
220. Quintana, A. M., Picchione, F., Klein Geltink, R. I., Taylor, M. R. & Grosveld, G. C. Zebrafish ETV7 regulates red blood cell development through the cholesterol synthesis pathway. *Dis Model Mech* **7**, 265–270 (2014).
221. Kawagoe, H., Potter, M., Ellis, J. & Grosveld, G. C. TEL2, an ETS Factor Expressed in Human Leukemia, Regulates Monocytic Differentiation of U937 Cells and Blocks the Inhibitory Effect of TEL1 on Ras-Induced Cellular Transformation. *Cancer Research* **64**, 6091–6100 (2004).
222. Lopez, R. G., Carron, C. & Ghysdael, J. v-SRC Specifically Regulates the Nucleo-cytoplasmic Delocalization of the Major Isoform of TEL (ETV6) *. *Journal of Biological Chemistry* **278**, 41316–41325 (2003).
223. Park, H., Seo, Y., Kim, J. I., Kim, W. & Choe, S. Y. Identification of the nuclear localization motif in the ETV6 (TEL) protein. *Cancer Genet Cytogenet* **167**, 117–121 (2006).
224. Bisio, A. *et al.* Cooperative interactions between p53 and NFκB enhance cell plasticity. *Oncotarget* **5**, 12111–12125 (2014).
225. Minutti, C. M. *et al.* Surfactant Protein A Prevents IFN-γ/IFN-γ Receptor Interaction and Attenuates Classical Activation of Human

Alveolar Macrophages. *The Journal of Immunology* **197**, 590–598 (2016).
226. Qiao, Y., Kang, K., Giannopoulou, E., Fang, C. & Ivashkiv, L. B. IFN-γ Induces Histone 3 Lysine 27 Trimethylation in a Small Subset of Promoters to Stably Silence Gene Expression in Human Macrophages. *Cell Rep* **16**, 3121–3129 (2016).
227. Pervolaraki, K. *et al.* Differential induction of interferon stimulated genes between type I and type III interferons is independent of interferon receptor abundance. *PLoS Pathog* **14**, e1007420 (2018).
228. Froggatt, H. M., Harding, A. T., Heaton, B. E. & Heaton, N. S. *ETV7 limits antiviral gene expression and control of SARS-CoV-2 and influenza viruses*. 851543 https://www.biorxiv.org/content/10.1101/851543v3 (2020) doi:10.1101/851543.
229. Irudayam, J. I. *et al.* Characterization of type I interferon pathway during hepatic differentiation of human pluripotent stem cells and hepatitis C virus infection. *Stem Cell Res* **15**, 354–364 (2015).
230. Santos, G. C., Zielenska, M., Prasad, M. & Squire, J. A. Chromosome 6p amplification and cancer progression. *J Clin Pathol* **60**, 1–7 (2007).
231. Numata, M., Klein Geltink, R. I. & Grosveld, G. C. Establishment of a transgenic mouse to model ETV7 expressing human tumors. *Transgenic Res* **28**, 115–128 (2019).
232. Neale, G. *et al.* Molecular characterization of the pediatric preclinical testing panel. *Clin Cancer Res* **14**, 4572–4583 (2008).
233. Cardone, M. *et al.* The Novel ETS Factor TEL2 Cooperates with Myc in B Lymphomagenesis. *Molecular and Cellular Biology* **25**, 2395–2405 (2005).
234. Maeda, O. *et al.* Alteration of gene expression and DNA methylation in drug-resistant gastric cancer. *Oncology Reports* **31**, 1883–1890 (2014).
235. Jiang, G. *et al.* Comprehensive comparison of molecular portraits between cell lines and tumors in breast cancer. *BMC Genomics* **17**, 525 (2016).
236. D'Alessio, A. *et al.* Targeting of tumor necrosis factor receptor 1 to low density plasma membrane domains in human endothelial cells. *J Biol Chem* **285**, 23868–23879 (2010).
237. Tadijan, A. *et al.* Altered Expression of Shorter p53 Family Isoforms Can Impact Melanoma Aggressiveness. *Cancers (Basel)* **13**, 5231 (2021).
238. Monti, P. *et al.* ΔN-P63α and TA-P63α exhibit intrinsic differences in transactivation specificities that depend on distinct features of DNA target sites. *Oncotarget* **5**, 2116–2130 (2014).
239. Concordet, J.-P. & Haeussler, M. CRISPOR: intuitive guide selection for CRISPR/Cas9 genome editing experiments and screens. *Nucleic Acids Res* **46**, W242–W245 (2018).

240. Brinkman, E. K., Chen, T., Amendola, M. & van Steensel, B. Easy quantitative assessment of genome editing by sequence trace decomposition. *Nucleic Acids Res* **42**, e168 (2014).
241. Adorno, M. *et al.* A Mutant-p53/Smad Complex Opposes p63 to Empower TGFβ-Induced Metastasis. *Cell* **137**, 87–98 (2009).
242. Győrffy, B. Survival analysis across the entire transcriptome identifies biomarkers with the highest prognostic power in breast cancer. *Computational and Structural Biotechnology Journal* **19**, 4101–4109 (2021).
243. Kao, J. *et al.* Molecular Profiling of Breast Cancer Cell Lines Defines Relevant Tumor Models and Provides a Resource for Cancer Gene Discovery. *PLOS ONE* **4**, e6146 (2009).
244. Riaz, M. *et al.* Low-risk susceptibility alleles in 40 human breast cancer cell lines. *BMC Cancer* **9**, 236 (2009).
245. Filipiak-Duliban, A., Brodaczewska, K., Kajdasz, A. & Kieda, C. Spheroid Culture Differentially Affects Cancer Cell Sensitivity to Drugs in Melanoma and RCC Models. *Int J Mol Sci* **23**, 1166 (2022).
246. Azharuddin, M. *et al.* Multicellular tumor spheroids- an effective in vitro model for understanding drug resistance in head and neck cancer. 702316 Preprint at https://doi.org/10.1101/702316 (2019).
247. Pezzè, L. *et al.* ETV7 regulates breast cancer stem-like cell features by repressing IFN-response genes. *Cell Death Dis* **12**, 742 (2021).
248. Egusquiaguirre, S. P., Yeh, J. E., Walker, S. R., Liu, S. & Frank, D. A. The STAT3 Target Gene TNFRSF1A Modulates the NF-κB Pathway in Breast Cancer Cells. *Neoplasia* **20**, 489–498 (2018).
249. Shrum, C. K., DeFrancisco, D. & Meffert, M. K. Stimulated nuclear translocation of NF-κB and shuttling differentially depend on dynein and the dynactin complex. *Proceedings of the National Academy of Sciences* **106**, 2647–2652 (2009).
250. Maguire, O., O'Loughlin, K. & Minderman, H. Simultaneous assessment of NF-κB/p65 phosphorylation and nuclear localization using imaging flow cytometry. *J Immunol Methods* **423**, 3–11 (2015).
251. Kanzaki, H. *et al.* Disabling the Nuclear Translocalization of RelA/NF-κB by a Small Molecule Inhibits Triple-Negative Breast Cancer Growth. *Breast Cancer (Dove Med Press)* **13**, 419–430 (2021).
252. Tripathi, S. K. *et al.* Genome-wide Analysis of STAT3-Mediated Transcription during Early Human Th17 Cell Differentiation. *Cell Rep* **19**, 1888–1901 (2017).
253. Reim, F. *et al.* Immunoselection of Breast and Ovarian Cancer Cells with Trastuzumab and Natural Killer Cells: Selective Escape of CD44high/CD24low/HER2low Breast Cancer Stem Cells. *Cancer Research* **69**, 8058–8066 (2009).
254. Schatton, T. *et al.* Modulation of T-Cell Activation by Malignant Melanoma Initiating Cells. *Cancer Research* **70**, 697–708 (2010).

255. Dianat-Moghadam, H. *et al.* Immune evader cancer stem cells direct the perspective approaches to cancer immunotherapy. *Stem Cell Research & Therapy* **13**, 150 (2022).
256. Zhou, F. Molecular mechanisms of IFN-gamma to up-regulate MHC class I antigen processing and presentation. *Int Rev Immunol* **28**, 239–260 (2009).
257. Ireson, C. R., Alavijeh, M. S., Palmer, A. M., Fowler, E. R. & Jones, H. J. The role of mouse tumour models in the discovery and development of anticancer drugs. *Br J Cancer* **121**, 101–108 (2019).
258. Fletcher, J. I., Williams, R. T., Henderson, M. J., Norris, M. D. & Haber, M. ABC transporters as mediators of drug resistance and contributors to cancer cell biology. *Drug Resistance Updates* **26**, 1–9 (2016).
259. Sun, Y.-L., Patel, A., Kumar, P. & Chen, Z.-S. Role of ABC transporters in cancer chemotherapy. *Chin J Cancer* **31**, 51–57 (2012).
260. Zheng, Y., Ma, L. & Sun, Q. Clinically-Relevant ABC Transporter for Anti-Cancer Drug Resistance. *Frontiers in Pharmacology* **12**, (2021).
261. Guo, W. *et al.* Discovering and Characterizing of Survivin Dominant Negative Mutants With Stronger Pro-apoptotic Activity on Cancer Cells and CSCs. *Frontiers in Oncology* **11**, (2021).
262. García-Aranda, M., Pérez-Ruiz, E. & Redondo, M. Bcl-2 Inhibition to Overcome Resistance to Chemo- and Immunotherapy. *Int J Mol Sci* **19**, 3950 (2018).
263. Jaggupilli, A. & Elkord, E. Significance of CD44 and CD24 as cancer stem cell markers: an enduring ambiguity. *Clin Dev Immunol* **2012**, 708036 (2012).
264. Huang, J.-L., Chen, S.-Y. & Lin, C.-S. Targeting Cancer Stem Cells through Epigenetic Modulation of Interferon Response. *Journal of Personalized Medicine* **12**, 556 (2022).
265. Doherty, M. R. *et al.* Interferon-beta represses cancer stem cell properties in triple-negative breast cancer. *Proc Natl Acad Sci U S A* **114**, 13792–13797 (2017).
266. Mantovani, A., Barajon, I. & Garlanda, C. IL-1 and IL-1 Regulatory Pathways in Cancer Progression and Therapy. *Immunol Rev* **281**, 57–61 (2018).
267. Hanna, B. S. *et al.* Interleukin-10 receptor signaling promotes the maintenance of a PD-1int TCF-1+ CD8+ T cell population that sustains anti-tumor immunity. *Immunity* **54**, 2825-2841.e10 (2021).
268. Mokhtari, Y. *et al.* Toll-like receptors (TLRs): An old family of immune receptors with a new face in cancer pathogenesis. *Journal of Cellular and Molecular Medicine* **25**, 639–651 (2021).
269. Boccuni, P., MacGrogan, D., Scandura, J. M. & Nimer, S. D. The human L(3)MBT polycomb group protein is a transcriptional repressor and interacts physically and functionally with TEL (ETV6). *J Biol Chem* **278**, 15412–15420 (2003).

270. Jackson-Bernitsas, D. G. *et al.* Evidence that TNF-TNFR1-TRADD-TRAF2-RIP-TAK1-IKK pathway mediates constitutive NF-kappaB activation and proliferation in human head and neck squamous cell carcinoma. *Oncogene* **26**, 1385–1397 (2007).
271. Soleimani, A. *et al.* Role of the NF-κB signaling pathway in the pathogenesis of colorectal cancer. *Gene* **726**, 144132 (2020).
272. Bonizzi, G. & Karin, M. The two NF-κB activation pathways and their role in innate and adaptive immunity. *Trends in Immunology* **25**, 280–288 (2004).
273. Taniguchi, K. & Karin, M. NF-κB, inflammation, immunity and cancer: coming of age. *Nat Rev Immunol* **18**, 309–324 (2018).
274. Viatour, P., Merville, M.-P., Bours, V. & Chariot, A. Phosphorylation of NF-kappaB and IkappaB proteins: implications in cancer and inflammation. *Trends Biochem Sci* **30**, 43–52 (2005).
275. Koelman, L., Pivovarova-Ramich, O., Pfeiffer, A. F. H., Grune, T. & Aleksandrova, K. Cytokines for evaluation of chronic inflammatory status in ageing research: reliability and phenotypic characterisation. *Immunity & Ageing* **16**, 11 (2019).
276. Tanaka, T., Narazaki, M. & Kishimoto, T. IL-6 in Inflammation, Immunity, and Disease. *Cold Spring Harb Perspect Biol* **6**, a016295 (2014).
277. Yu, H., Lin, L., Zhang, Z., Zhang, H. & Hu, H. Targeting NF-κB pathway for the therapy of diseases: mechanism and clinical study. *Sig Transduct Target Ther* **5**, 1–23 (2020).
278. Vallania, F. *et al.* Genome-wide discovery of functional transcription factor binding sites by comparative genomics: The case of Stat3. *Proceedings of the National Academy of Sciences* **106**, 5117–5122 (2009).
279. Chopra, M. *et al.* Tumor Necrosis Factor Induces Tumor Promoting and Anti-Tumoral Effects on Pancreatic Cancer via TNFR1. *PLOS ONE* **8**, e75737 (2013).
280. Lalle, G., Twardowski, J. & Grinberg-Bleyer, Y. NF-κB in Cancer Immunity: Friend or Foe? *Cells* **10**, 355 (2021).
281. Pfeffer, L. M. The Role of Nuclear Factor κB in the Interferon Response. *J Interferon Cytokine Res* **31**, 553–559 (2011).
282. Manguso, R. T. *et al.* In vivo CRISPR screening identifies Ptpn2 as a cancer immunotherapy target. *Nature* **547**, 413–418 (2017).
283. Pan, D. *et al.* A major chromatin regulator determines resistance of tumor cells to T cell–mediated killing. *Science* **359**, 770–775 (2018).
284. Taylor, B. C. & Balko, J. M. Mechanisms of MHC-I Downregulation and Role in Immunotherapy Response. *Front Immunol* **13**, 844866 (2022).
285. Shahbandi, A., Nguyen, H. D. & Jackson, J. G. TP53 Mutations and Outcomes in Breast Cancer: Reading beyond the Headlines. *Trends in Cancer* **6**, 98–110 (2020).

286. Pulaski, B. A. & Ostrand-Rosenberg, S. Mouse 4T1 Breast Tumor Model. *Current Protocols in Immunology* **39**, 20.2.1-20.2.16 (2000).
287. Bahaddin, M. M. A comparative study between Ki67 positive versus Ki67 negative females with breast cancer: Cross sectional study. *Annals of Medicine and Surgery* **60**, 232–235 (2020).
288. Winter, M. *et al.* Vimentin Promotes the Aggressiveness of Triple Negative Breast Cancer Cells Surviving Chemotherapeutic Treatment. *Cells* **10**, 1504 (2021).
289. Xu, H., Niu, M., Yuan, X., Wu, K. & Liu, A. CD44 as a tumor biomarker and therapeutic target. *Experimental Hematology & Oncology* **9**, 36 (2020).
290. Muchlińska, A. *et al.* Alpha-smooth muscle actin-positive cancer-associated fibroblasts secreting osteopontin promote growth of luminal breast cancer. *Cell Mol Biol Lett* **27**, 45 (2022).
291. Han, C., Liu, T. & Yin, R. Biomarkers for cancer-associated fibroblasts. *Biomark Res* **8**, 64 (2020).

SUPPLEMENTARY MATERIAL

Supplementary table 1. Primer sequences

RT-qPCR Primer	**Sequence 5'→3'**
ETV7 Fw	CAAGATCTTCCGAGTTGTGGA
ETV7 Rv	GTTCACCCGGTTCTTGTGAT
IL1R1 Fw	CTGAGAAGCTGGACCCCTTG
IL1R1 Rv	GCATTTATCAGCCTCCAGAGA
IL10RB Fw	GTGAGCCTGTCTGTGAGCAA
IL10RB Rv	TGAGGATGGCCCAAAAACTCTT
ACT B Fw	AAGAATTCATACCGCCGAGACCGCGTCCGC
ACT B Rv	AACATATGGGTGAGCTGGCGGCGGGTGT'
YWHAZ Fw	CAACACATCCTATCAGACTGGG
YWHAZ Rv	AATGTATCAAGTTCAGCAATGGC
IL-6 Fw	GAAAGCAGCAAAGAGGCACT
IL-6 Rv	TTTCACCAGGCAAGTCTCCT
IL-8 Fw	CTCTCTTGGCAGCCTTCCT
IL-8 Rv	GGGTGGAAAGGTTTGGAGTA
A20 (TNFAIP3) Fw	AAAGCCCTCATCGACAGAAA
A20 (TNFAIP3) Rv	AGAAGTGGCATGCATGAGG
TNF-α Fw	GGGACCTCTCTCTAATCAGC
TNF-α Rv	TCAGCTTGAGGGTTTGCTAC
TLR2 Fw	GCCTCTCCAAGGAAGAATCC
TLR2 Rv	TCCTGTTGTTGGACAGGTCA
STAT3 Fw	GAAACAGTTGGGACCCCTGA
STAT3 Rv	AGGTACCGTGTGTCAAGCTG
TNFRSF1A Fw	ATTGGACTGGTCCCTCACCT
TNFRSF1A Rv	AGTAGGTTCCTTTGTGGCACTT
IFITM2 Fw	CGCGTACTCCGTGAAGTCTA
IFITM2 Rv	ACGACCAACACTGGGATGAT
IFI35 Fw	TGAGAGAGACCACAGCCCTT
IFI35 Rv	GGAGGGCGGCATCCAGT
HERC6 Fw	GGAGCTGCCAGAACCAATTC
HERC6 Rv	AAGACCCTTCCTTTGTGGCA
PROCR Fw	CTCGGTATGAACTGCGGGAA
PROCR Rv	TTGTTTGGCTCCCTTTCGTG
APOL6 Fw	TTTCTCCAGCCCAGACACTC
APOL6 Rv	TCAAATGATTTTCTTCTCTCCACGG

CASP4 Fw	CTGTTCCCTATGGCAGAAGGC
CASP4 Rv	TCTGCCATGACCCGAACTTT
CFB Fw	GACACGAGAGCTGTATGGGG
CFB Rv	CTTCTCCCCTCCTACGCTGA
PARP14 Fw	TGCCAAGAATGGCCAGACAA
PARP14 Rv	TATGCCACAGCATTCTTTCCG
ICAM1 Fw	ATGGCAACGACTCCTTCTCG
ICAM1 Rv	GCCGGAAAGCTGTAGATGGT
HLA-A Fw	AGATACACCTGCCATGTGCAGC
HLA-A Rv	GATCACAGCTCCAAGGAGAACC
TAP2 Fw	CCCTGGCCGAGCGTA
TAP2 Rv	CCAGCAGCCCTCTTAGCTTTA
IRF1 Fw	GGCCCTGACTCCAGCTACAA
IRF1 Rv	TACCCCTTCCCATCCACGTT
PSMB8 (LMP7) Fw	CCTTACCTGCTTGGCACCATGT
PSMB8 (LMP7) Rv	GAGAGCCGAGTCCCATGTTC
PSMB9 (LMP2) Fw	TGCTGACTCGACAGCCTTTT
PSMB9 (LMP2) Rv	TGCCCAAGATGACTCGATGG
PSMB10 Fw	ATACGCGAGCCACTAACGAT
PSMB10 Rv	AGCCCCACAGCAGTAGATTTT
PSME2 Fw	GGATCCAACACCTGATCCCC
PSME2 Rv	TCTTGACGGCATTCACCCTC
IRF2 Fw	GTCCCATCTGGACAGCAACA
IRF2 Rv	ATTCCTCTTCCGCCAGTGTG
HLA-B Fw	GATGGCGAGGACCAAACTCA
HLA-B Rv	CTCCGATGACCACAACTGCT
HLA-C Fw	CCACCCGGACTCACATTCTC
HLA-C Rv	TCATGGAGTGGGAGCAGGC
NLRC5 Fw	GTGAGCATCTCGGACCTCTT
NLRC5 Rv	GACAGTGTCGTGGTCCGATT
ChIP primer	**Sequence 5'→3'**
ACTB (NSB) Fw	TCTCCCTCCTCCCTTCTTCAAT
ACTB (NSB) Rv	TCGCGCCGCTGGGTTTTATA
TNFRSF1A BS#1Fw	CACAGACCCTTGTCCCACTT
TNFRSF1A BS#1 Rv	GGGAGACTTCCCTTCGGGA

TNFRSF1A BS#2 Fw	GCCACGTGTTCCCTTCTCTT
TNFRSF1A BS#2 Rv	CTAGTTCCCTCTCCCCTCCC
TNFRSF1A BS#3 Fw	GGGGAAAGGAACCACACTTT
TNFRSF1A BS#3 Rv	TCTGCTGAGAACAGGACTGG
MED16 Fw	GAAAGTGCTCGTTGTTCTACC
MED16 Rv	TTGCATACGACCATTTCCAG

Supplementary figure 1.

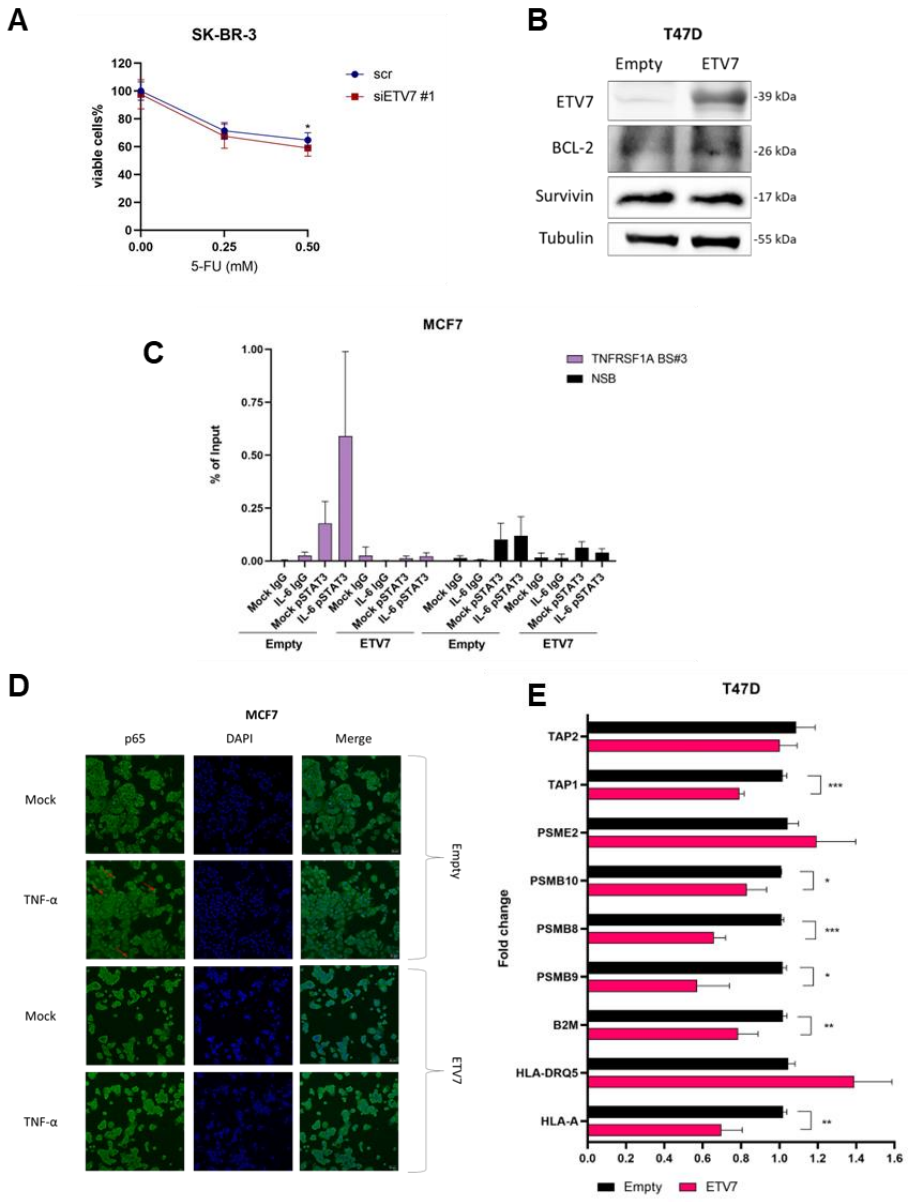

A) Cell Titer Glo assay for survival analysis upon treatment with 5-FU in SK-BR-3 cells transfected with siETV7 #1 or the scrambled control. Bars represent the averages and standard deviations of at least three independent experiments. * p≤0.05. B) Western blot analysis of BCL-2 and Survivin proteins in T47D Empty and T47D ETV7 cells C) ChIP-qPCR of TNSFRSF1A Intron 1 Binding site #3 in MCF7 cells over-expressing ETV7 untreated or treated with IL-6 (20 ng/ml) for 4 hours. The percentage of the enrichment of pSTAT3 or control (normal rabbit IgG) bound to TNFRSF1A Intron 1 with respect to Input DNA is shown. NSB=non-specific binding,

a region within the ACTB promoter. BS = binding site. Bars represent the averages and standard deviations of at least three biological replicates.D) Immunofluorescence analysis for the p65 (green signal) nuclear translocation in MCF7 Empty and MCF7 ETV7 cells. Nuclei are stained in blue. MCF7 cells were untreated or treated with 15 ng/ml TNF-α for 60 min. Representative data for at least three biological replicates. 20X magnification. E) RT-qPCR analysis of antigen-presenting in T47D cells over-expressing ETV7 or its Empty counterpart. * p≤0.05; ** p≤0.01; *** p≤0.01.

Raw Western blot data

Figure 13

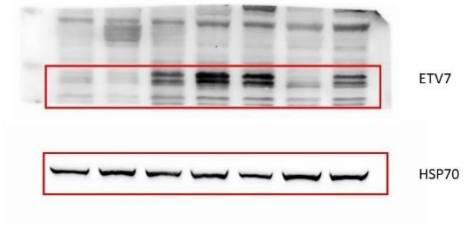

Figure 14

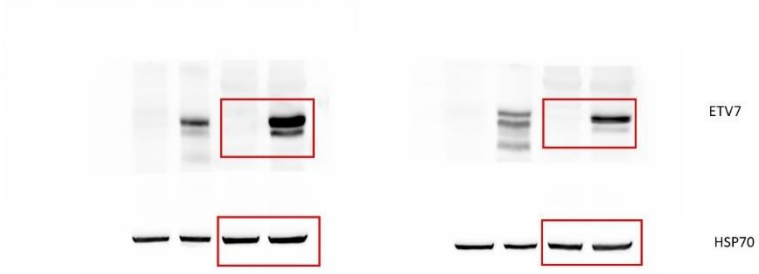

Figure 16

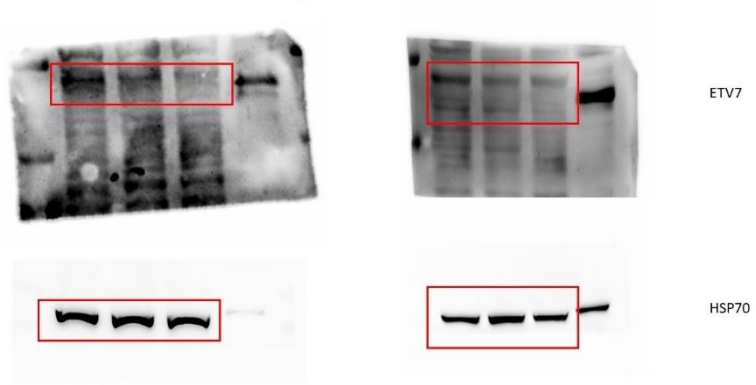

Figure 21

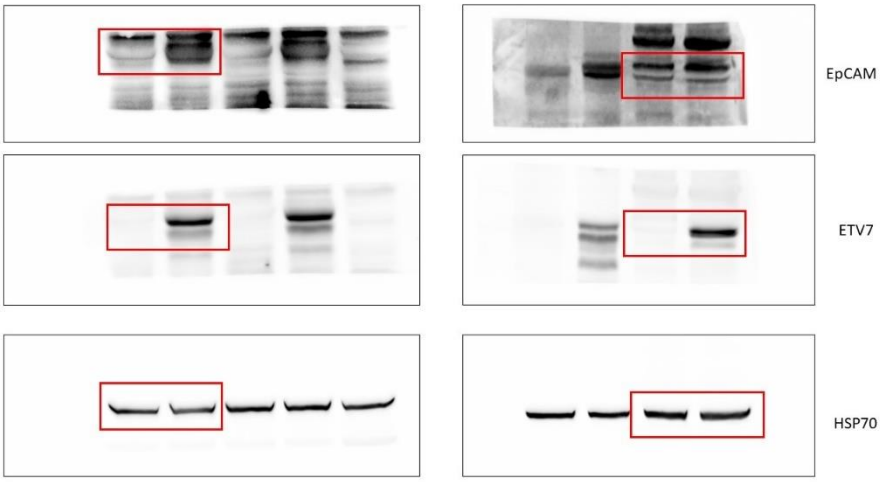

Figure 27

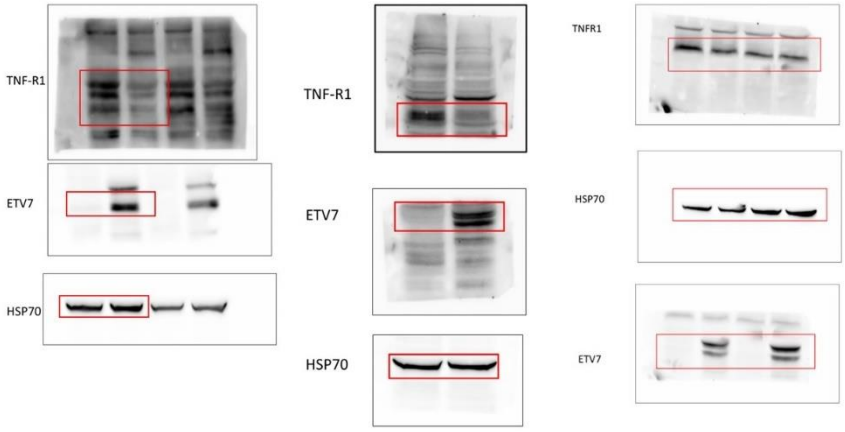

Figure 28

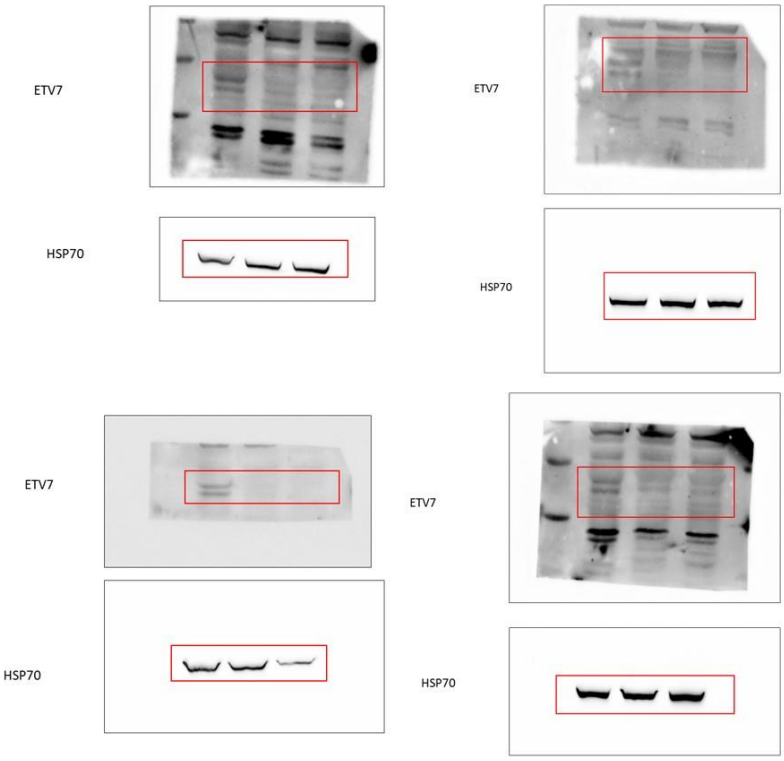

Figure 36

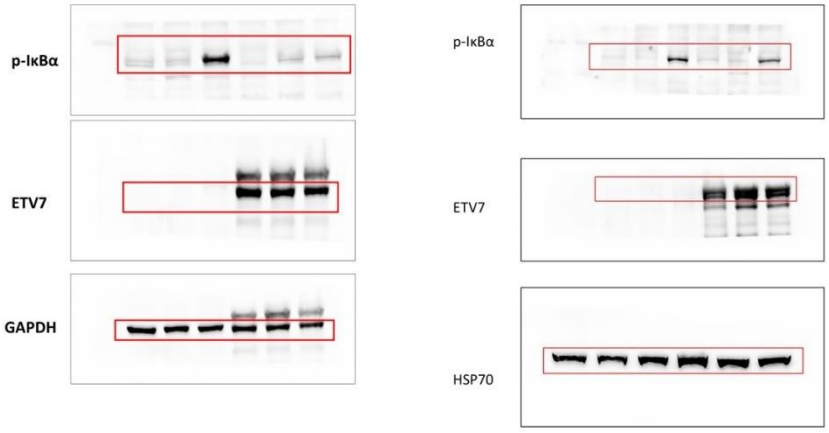

Figure 41

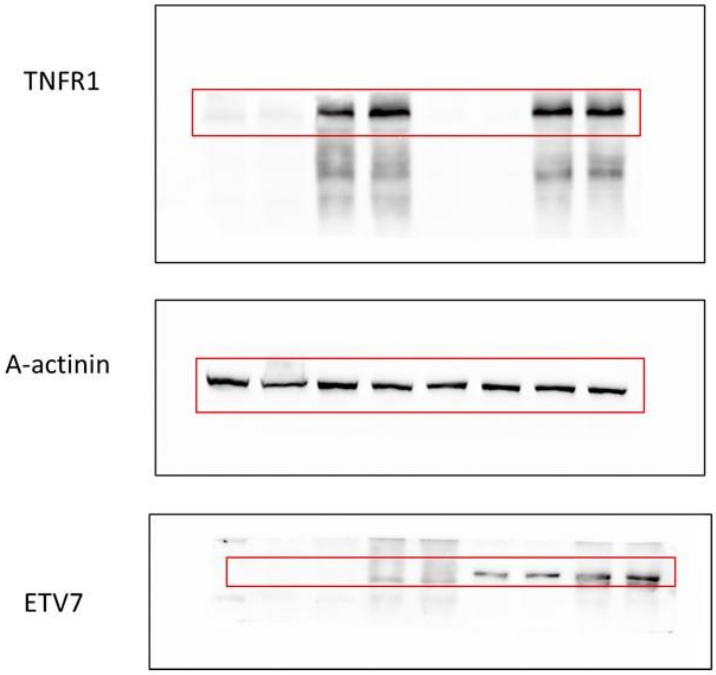

Figure 44

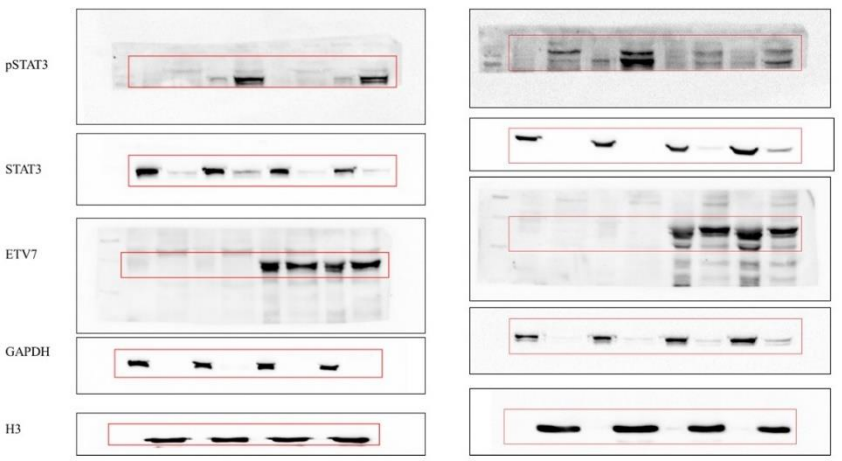

Figure 46

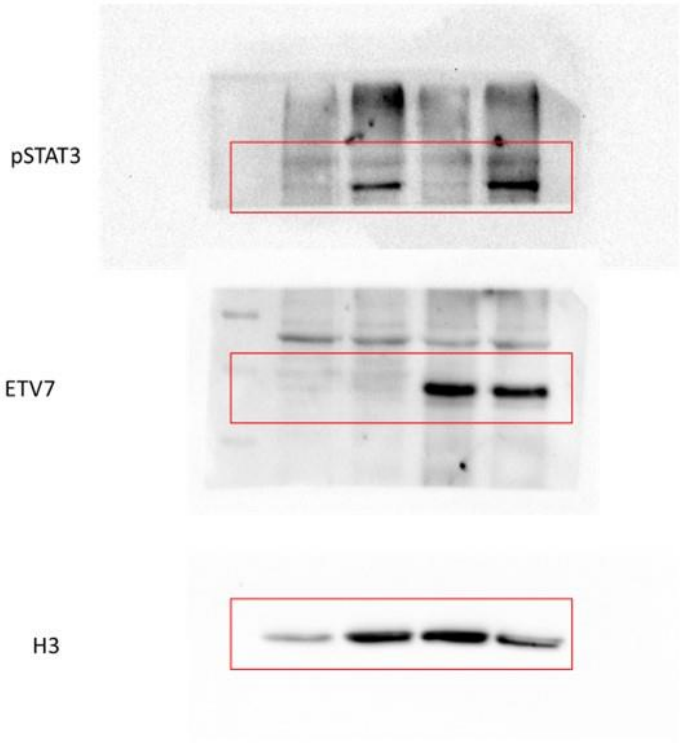

Figure 50

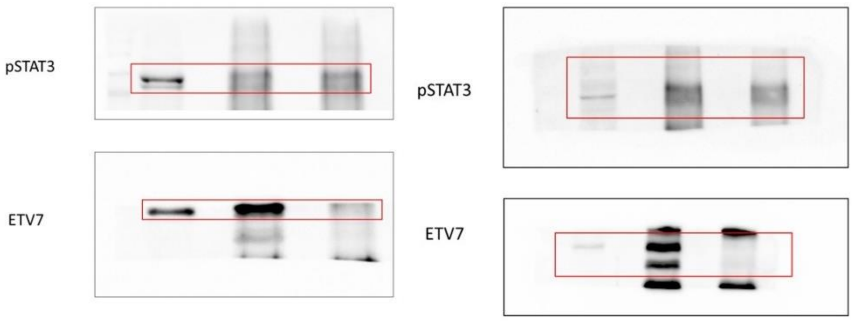

Figure 52

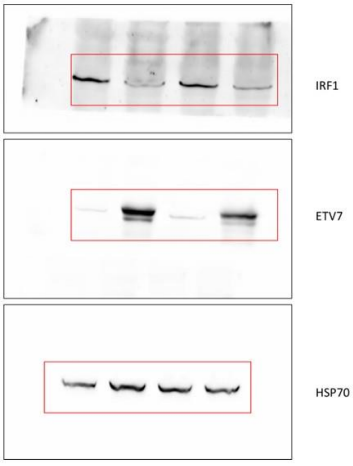

Figure 53

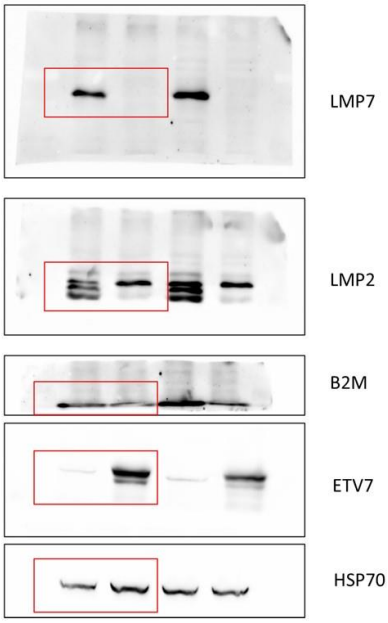

Figure 55

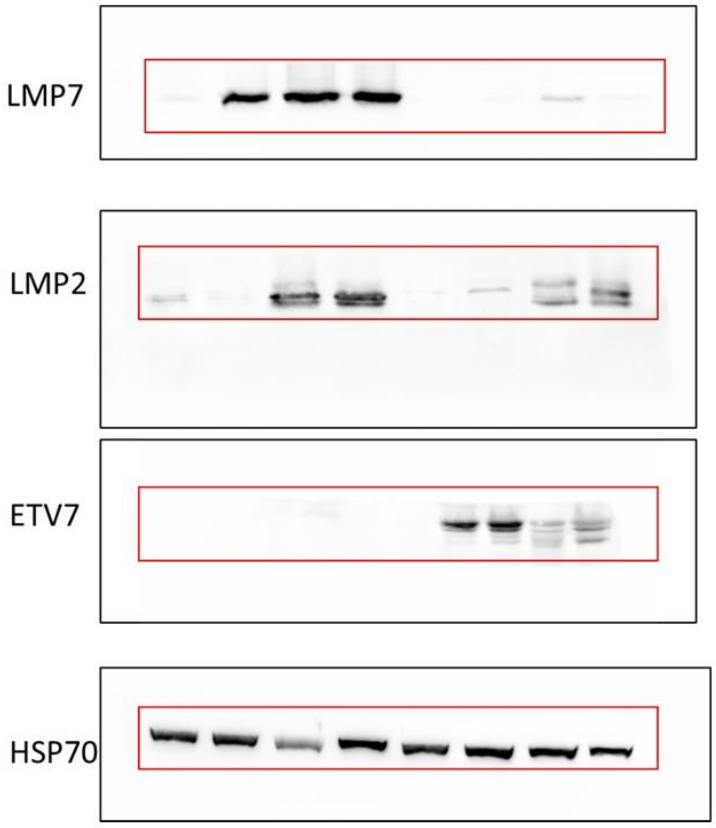

Figure 57

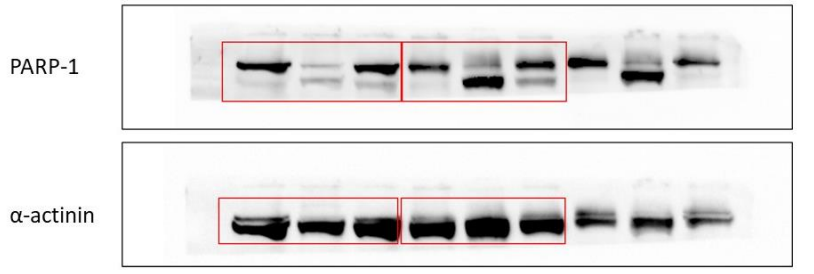

Figure 57

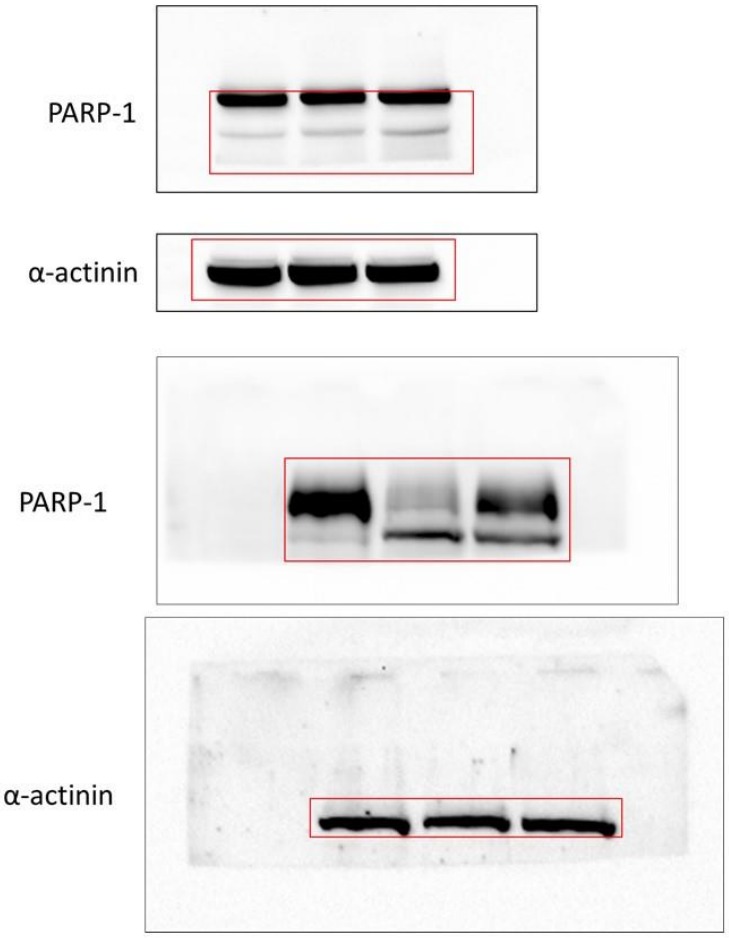

Figure 59

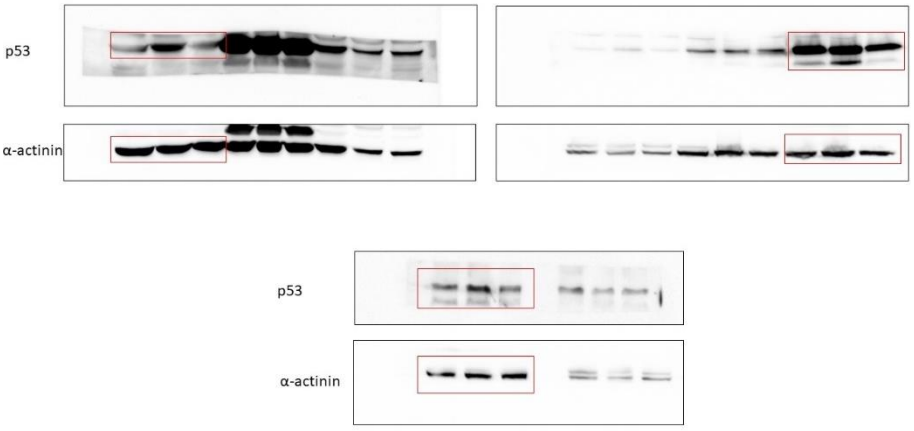

Figure 61

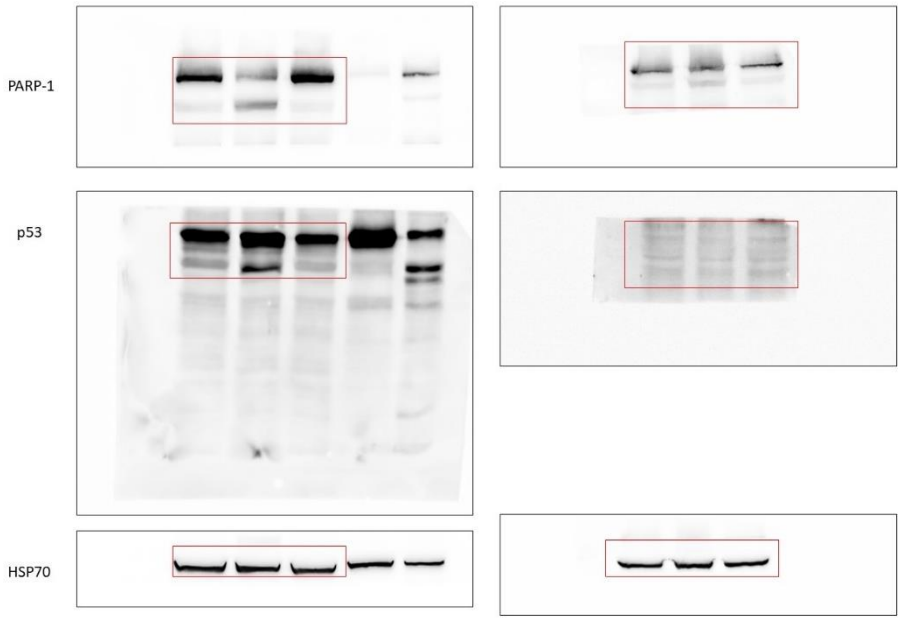

Figure 62

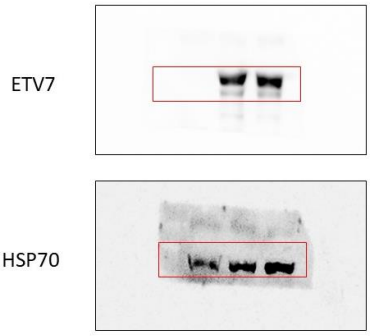

Suppl. Fig. 1

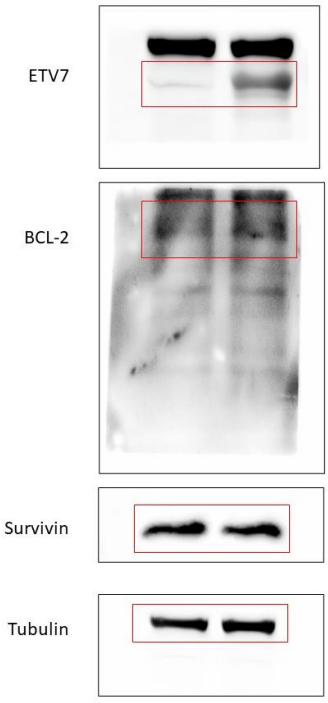

ACKNOWLEDGMENTS

First of all, I would like to thank my supervisors Dr. Daiva Baltriukienė and Dr. Yari Ciribilli for allowing me to be a part of their laboratories and for their willingness to participate in this sometimes challenging collaboration between the two Universties. I am very grateful for the possibility to learn and grow as a scientist, in particular, I am grateful for the trust that I felt from both of my supervisors. Additionally, I would like to thank Prof. Virginija Bukelskienė who took me under her wing from the very start of my scientific carrier and always made me feel welcome in the Laboratory of Biological Models.

I would also like to express my gratitude to all the facility members, collaborators, students, and colleagues for their support, technical help, and company. In particular, I would like to thank Prof. Alberto Inga and Dr. Alessandra Bisio for sharing reagents, knowledge, and enthusiasm for science. I would also like to thank Dr. Mattia Forcato and Prof. Silvio Bicciato for the RNA-seq data and patient data analyses.

I am sincerely grateful for the wonderful and stimulating environment that I encountered at both Vilnius and Trento Universities. I have met so many inspiring and interesting people who have affected both my scientific and personal life in various ways. In particular, I would like to thank all present and past people in Green 7, who made my everyday lab life bearable even at the worst moments. I would like to thank Giulia for all love, tears, and hugs that we shared during our Ph.D. period, Orsetta for caring and being my "bear" pal, and Francesca for spreading calmness and being a role model. I thank Dario for the interesting companionship inside and outside of the lab and for introducing me to the lunch "family" – it changed my life. I would like to thank Laura for so many things: for all the scientific, technical, and emotional support that she gave me and for being one of the most inspiring scientists and friends, Sally – for the positiveness, enthusiasm, and companionship during our adventures, Francesca – for caring, listening, understanding and for being a very good friend, Michele – for always having time for "big" talks about world, life and the future, especially when I was experiencing little crises, Nicolò – for having this great passion for science and becoming like a younger brother to me.

Last but not least, I would like to thank my family. I am very grateful to have a father who thought me to be curious and to explore nature from my early childhood and who showed me that being a scientist is not a work, but a lifestyle, a mission. I am so proud to have my father as my greatest scientific role model. I want to thank my mother, who sacrificed so much to allow me to become who I am now. She was the one holding the rest of the world in place while I was focusing on my studies. And also for teaching me how to

load electrophoresis gel. I am also grateful for my big sister, who always supported, and loved me and who is one of the strongest people that I have ever met. I am also very thankful for having Beatričė and Uršulė in my life, who gives me strenght when I need it and inspires me to change this world for the better.

Lastly, I would like to thank my husband for his never-ending support, patience, and love. I am grateful for his being here for me during all ups and downs of Ph.D. studies, for being understanding, when I needed to sacrifice my time with him for the experiments, and for giving sense to my life.

LIST OF PUBLICATIONS

Publications, related to the doctoral project:

- Pezzè L, **Meškytė EM**, Forcato M, et al. ETV7 regulates breast cancer stem-like cell features by repressing IFN-response genes. Cell Death Dis. 2021;12(8):742. doi:10.1038/s41419-021-04005-y.

- **Meškytė EM,** Pezzè L, Bartolomei L, Forcato M, Bocci IA, Bertalot G, Barbareschi M, Oliveira-Ferrer L, Bisio A, Bicciato S, Baltriukienė D, Ciribilli Y. ETV7 reduces inflammatory responses in breast cancer cells by repressing the TNFR1/NF-κB axis. Cell Death Dis. 2023;14(4):263. doi: 10.1038/s41419-023-05718-y.

Other publications

- **Meškytė E.M.**, Keskas S, Ciribilli Y. MYC as a Multifaceted Regulator of Tumor Microenvironment Leading to Metastasis. International Journal of Molecular Sciences. 21(20):7710; 2020.

- Nassiri I, Inga A, **Meškytė E.M.,** Alessandrini F, Ciribilli Y, Priami C. Regulatory Crosstalk of Doxorubicin, Estradiol and TNFα Combined Treatment in Breast Cancer-derived Cell Lines. Sci Rep. 9(1):15172; 2019.

Conferences

- EORTC Pathobiology Group Autumn Meeting, 23-25/10/2022, Badalona, Spain, **Oral presentation** "ETV7 – a novel regulator of breast cancer immunity ".

- European Association of Cancer Research 2022 congress, 20-23/06/2022, Seville, Spain. **Poster** "ETV7 – a novel regulator of breast cancer immunity ".

- 33rd Pezcoller Symposium, 13-14/06/2022, Trento, Italy. **Poster** „ETV7 – a novel regulator of breast cancer immunity".

- EORTC Pathobiology Group Spring Meeting, 28/04/2022, Virtual event. **Oral presentation** "ETV7 reduces inflammatory responses in breast cancer through the down-regulation of the TNFRSF1A gene".

- European Association of Cancer Research, Virtual Congress 2021, 2021/06/09-12. **Virtual poster** - "ETV7 reduces inflammatory responses in breast cancer through the down-regulation of the TNFRSF1A gene".

CURRICULUM VITAE

Work and research experience

04.11.2022- 30.03.2023	**Junior researcher** Laboratory of Biological Models, Biochemistry Institute, Life Sciences Center, Vilnius University (Sauletekio al. 7, Vilnius 10223, Lithuania)
01.10.2018-present	**PhD student (University of Trento - Vilnius University bilateral agreement)** **PROJECT: The role of ETV7 in breast cancer aggressiveness** Supervisors: Dr. Yari Ciribilli & Dr. Daiva Baltrukiene Laboratory of Molecular Cancer Genetics, CIBIO, University of Trento (Via Sommarive 9, 38123 Povo (TN), Italy) Laboratory of Biological Models, Biochemistry Institute, Life Sciences Center, Vilnius University (Sauletekio al. 7, Vilnius 10223, Lithuania)
11.01.2018- 01.02.2019	**Veterinarian** Ospedale Veterinario Cles (di Ghirardini Alessandra & C.S.a.S.) (Via C. A. Martini 18, 38023 Cles (TN), Italy)
14.07.2013- 15.07.2015	**Vet Assistant** Private Veterinary Practice (Aukstaiciu g. 54, Kaunas 44163, Lithuania)

Education and training

09.2011- 28.02.2017	**Master of Veterinary Medicine (cum laude)** **Thesis: Diversity of fimbrillin A of *Porphyromonas spp*. in the dental plaque of Lithuanian dogs** Supervisor: Prof. Dr. Ilona Teodora Miceikiene Lithuanian University of Health Sciences, Veterinary Academy (Tilzes g. 18, Kaunas 47181, Lithuania)
10.2015 - 08.2016	**Erasmus exchange period** University of Veterinary Medicine Hanover (Bünteweg 9, 30559 Hannover, Germany)
25.07.2016- 06.09.2016 30.11.2015- 21.02.2016	**Internship** Small Animal Clinic, University of Veterinary Medicine Hanover (Bünteweg 9, 30559 Hannover, Germany)

Certificates/Courses/travel grants:

- CellFit Training School "**Add a new dimension to cell culture**", 10-14th February 2019, Ponte di Legno, Italy.
- **Basics to Work With Extracellular Vesicles**, Institute of Biomedicine and Translational Medicine, University of Tartu, Estonia, 21-24/05/2019, 20 hours.
- **PreCanMed summer school on Tumour organoids**, Consorzio Interuniversitario per le Biotechnologie, Laboratorio Nazionale, University of Trieste, Italy, 11-14/06/2019, 20 hours.
- **Certificate to work with laboratory animals.**

Lithuanian	Mother tongue
English	C1 (IELTS overall band score 7.5 - 2017)
Italian	C1
German	B2

Vilniaus universiteto leidykla
Saulėtekio al. 9, III rūmai, LT-10222 Vilnius
El. p. info@leidykla.vu.lt, www.leidykla.vu.lt
bookshop.vu.lt, journals.vu.lt
Tiražas 15 egz.